Study and Analysis of Spectrally Efficient Modulation Formats in High Speed DWDM Optical Systems

THESIS

Submitted in partial fulfillment
of the requirements for the degree of

DOCTOR OF PHILOSOPHY

by

LUCKY SHARAN

ID No. 2009PHXF041P

Under the Supervision of

Dr. V. K. CHAUBEY

BITS Pilani
Pilani | Dubai | Goa | Hyderabad

BIRLA INSTITUTE OF TECHNOLOGY AND SCIENCE, PILANI
PILANI - 333031 (RAJASTHAN) INDIA
2017

Study and Analysis of Spectrally Efficient Modulation Formats in High Speed DWDM Optical Systems

THESIS

Submitted in partial fulfillment
of the requirements for the degree of

DOCTOR OF PHILOSOPHY

by

LUCKY SHARAN

ID No. 2009PHXF041P

Under the Supervision of

Dr. V. K. Chaubey

BITS Pilani
Pilani | Dubai | Goa | Hyderabad

BIRLA INSTITUTE OF TECHNOLOGY AND SCIENCE, PILANI
PILANI - 333031 (RAJASTHAN) INDIA

2017

BIRLA INSTITUTE OF TECHNOLOGY AND SCIENCE, PILANI

CERTIFICATE

This is to certify that the thesis entitled **"Study and Analysis of Spectrally Efficient Modulation Formats in High Speed DWDM Optical Systems"** submitted by Mrs. Lucky Sharan, ID. No. 2009PHXF041P, for the award of Ph.D. degree of the Institute, embodies the original work done by her under my supervision to the best of our knowledge.

Signature of the Supervisor:

Name: Dr. V. K. Chaubey

Designation: Professor

Department of Electrical and Electronics Engineering

BITS-Pilani, Pilani Campus

Date: April 21, 2017

To my beloved family,

for your continued support and encouragement

Acknowledgments

I believe that an atmosphere supporting free spirit of investigation is required for researchers to develop a thorough understanding about a particular field, and make subsequent contributions. I was fortunate to have Prof. V. K Chaubey as my advisor and guide. He granted me the freedom to explore while ensuring that I progressed in the right direction, encouraged abstract thought, was patient and motivated me with his insight as I struggled to understand fiber optic systems and the field of research, and worked relentlessly to improve the quality of my research. I sincerely thank him for all his endeavors in shaping my academic career, and am indebted to him for the tireless efforts to improve this dissertation.

I take this opportunity to thank Prof. Souvik Bhattacharyya, Vice-Chancellor BITS, Pilani and Prof A. K. Sarkar, Director, BITS, Pilani (Pilani Campus) for providing me the necessary infrastructure, facilities and constant inspiration. I also acknowledge the kind support from R. N. Saha (Director, Dubai campus), Prof. G. Sundar (Director, Hyderabad Campus), Prof. G. Raghurama (Director, Goa Campus) and Prof. S. K. Verma Dean (Academic Research and Development). I am also thankful to Dr. Navneet Gupta (HOD, Department of Electrical and Electronics Engineering. I would also like to express my sincere gratitude to Prof. Surekha Bhanot for constantly supporting and motivating me in a special way, sharing views and her experience in both work and life. I also thank my DAC members Prof. R. R. Misra and Dr. Rahul Singhal for carefully going through my thesis drafts, correcting my presentations, and helping me learn the various skills of academic research. I also thank DRC convener, Dr. Abhijeet Asati and other DRC committee members for their time and insightful comments. A big thanks to the rest of the people that are or have been with BITS-Pilani during my time here so far, you all make this a great place to work at.

My Ph.D experience was made enjoyable by the numerous discussions, often illuminating and profound, sometimes confusing and trite, but always fun, that I had with my colleagues and friends. I thank Vinita for the technical, Silky and Anie for the non-technical, Radhika, Priyanka and Anjali for the motivational, and Ashish my hubby for all this and everything else.

I would like to thank my parents Dr. V.B Sharan and Mrs. Usha Sharan, for the love they have always given me and bringing me up with a respect for knowledge and a desire to pursue it to the best of my abilities. Their undying faith in me, the values they have instilled in me, the lessons of humility and hard work that they have taught kept me grounded and motivated to finish this dissertation. I owe my sincere thanks to Manish Sharan, my brother and Ankita my sister-in-law, Manisha Sharan, my sister and Rajat her husband and my father-in-law Mr. Hari Mohan Mishra for being a constant pillar of support. This dissertation may be far from perfect and may not measure to their sacrifices that enabled me to pursue my dreams; nevertheless, I humbly dedicate this work to them.

A special thanks goes to my superhero son Adyut for being the light of my eyes and the joy of my heart. Without his sweet distractions I would not have been able to get through the tiring research work. I am grateful to you for bearing with my absence at times when you needed me, handling my irritation when I had a tough day, showing a lot of patience and making each day brighter with your charming smile.

Finally, to Ashish for being the best and for all your love. I cannot begin to express my unfailing gratitude and love to him for supporting me throughout this process and constantly encouraging me when the tasks seemed arduous and insurmountable. You have been patient with me when I'm frustrated, you celebrate with me when even the littlest things go right, and you are there whenever I need you to just listen. Thank you for the little things you've done like taking care of Adyut when I worked late nights. Without you this thesis would never have been possible. Above all, I owe it all to Almighty God for granting me the wisdom, health and strength to undertake this research task and enabling me to its completion.

Date: Signature:

Place: Name: Lucky Sharan

Abstract

The exponentially increasing demand for the channel capacity in long haul high speed transmission systems has pushed the fiber-optic communication technology to adopt dense wavelength division multiplexing (DWDM) system as a viable solution. To maximize the performance of such optical networks, suitable system design strategies to optimize the parameters related to data transmission within the channel characteristics becomes a critical area of research. Usually the optical channel capacity is influenced by signal shape, dispersive and non-linear characteristics of the guiding medium and the interference from various sources. These impairments appear to be much detrimental in a multi-channel optical guiding medium especially at a higher data rate in the presence of fiber nonlinearities. Thus, in order to exploit the best system transmission capacity with the least performance degradation, a thorough understanding, modeling and characterization of optical channel behavior under various operating environments becomes an important problem.

The main objective of this thesis is to analyze different approaches to mitigate the channel impairments influencing the capacity limitations in optical fiber communication. Changes in optical transmitters, receivers and transmission medium are not a preferred solution owing to relatively higher cost and complex hardware setup requirements. However, efficient optical modulation approach emerges as a promising technique with cost effective solution in the current scenario. In fact, signal spectral bandwidth, tolerance to dispersion, resistance to nonlinear crosstalk, susceptibility to accumulated noise, and other system performance measures are directly related to the optical modulation format. Incorporation of certain modulation scheme in optical transmitter with appropriate receiver helps to improve the capacity crisis of the transmission system quite effectively. Recent research in advanced optical modulation formats confirms the improved data transmission with an acceptable system reliability under optimum operating conditions.

The transmission quality of the optical signals is subject to optical signal-to-noise ratio (OSNR) degradation, intra-channel nonlinearities, residual chromatic dispersion (CD), first-order polarization mode dispersion (PMD) and optical filtering at the add/drop sites. High speed long haul optical communication links consist of multi-span optically amplified systems accumulating amplified spontaneous emission (ASE) noise adding system power penalty and the receiver performance. To ensure an acceptable signal-to-noise-ratio (SNR), a higher optical signal power is required but it generates signal crosstalk through such power dependent fiber nonlinear effect. Similarly, the higher

data rate increases the optical spectral width of the signal to make it more susceptible to chromatic dispersion. Further, these systems also require a larger receiver electrical bandwidth to add complexity in receiver design. Although there does not exists a perfect modulation format that is immune to all such sources of performance degradations, yet the proper selection of an appropriate optical modulation format does improve the system performance to some extent. Until not a long time ago, non-return-to-zero (NRZ) had been the dominant optical modulation format in intensity-modulation, direct-detection (IM-DD) fiber-optic systems. Only recently some commercial systems based on differential phase modulation have surfaced and thus opened a scope of further exploration and innovation in related technology. New research in this domain has led to propose some spectrally efficient modulation formats to overcome the problems associated with bandwidth limitations in DWDM optical systems. Multilevel modulation formats being spectrally efficient, enhance the transmission capacity by transmitting more information in the amplitude, phase, polarization or a combination of all.

This thesis investigates the influence of spectrally efficient modulated systems in optical communication links to manage the linear and non-linear impairments arising in high data rate transmission. Such stringent restrictions over optical channel characteristics require an efficient DWDM optical communication system incorporating judicious choice of modulation format and pulse shape. Modulation formats such as intensity and phase modulation formats have emerged as an acceptable technology that enables the design of such networks to perform satisfactorily. This dissertation discusses the theoretical aspects of different models used in the analysis and simulation of high speed optical communication links to gain an understanding of how different system components and applied modulation format affects the performance of the complete system. Five modulation formats viz., Carrier Suppressed Return to Zero (CSRZ) Duobinary, Modified Duobinary which are intensity modulation formats along with Differential Phase Shift Keying (DPSK) and Differential Quadrature Phase Shift Keying (DQPSK) have been considered in the present analysis focusing on theoretical considerations, mathematical modeling and computer simulations.

The major focus is to analyze, evaluate and characterize different types of optimal encoding schemes to infer the system design parameters in order to achieve an optimum data rate for a possible longest optical link. This broad objective set leads inevitably to investigate theoretical and numerical models in order to establish suitable simulation set ups to carry out several link parameter analysis evaluating eye opening, BER, electrical and optical filtering, propagation distance, and limitations for each non-linear process and their combination. The attempted simulation configurations closely reflect practical conditions of existing terrestrial fiber link infrastructures. In contrast with laboratory transmission

experiments which often use non-zero dispersion shifted fiber (NZDSF) links, the proposed investigations are based on standard single mode fiber (SSMF) link, which is the most largely deployed fiber on terrestrial transmission networks with Erbium-doped fiber amplifiers (EDFA). During the analysis different test are run, the results are analyzed and the design is optimized in order to dimension the network in terms of fiber reach, number of users, power budget, bandwidth capacity, etc. Further to gain physical signal propagation understanding in an optical link, a single channel DQPSK link is developed using Matlab Simulink based model designing transmitter, receiver and fiber sections. A systematic study regarding the impact of optimal filtering in such developed model has been done.

Conventional binary modulation formats are rather inapplicable and incompetent for high speed networks owing to their lower spectral efficiency and OSNR degradation. However, phase modulation exhibits higher noise sensitivity than intensity modulation, and is more tolerant to the effects of fiber nonlinearity. The present study shows superior tolerance of DQPSK format in nonlinear fiber propagation and thus makes this strategy as an effective solution. Thus, DQPSK emerges as an attractive scheme amongst the available modulation schemes in terms of low error rate, reduced symbol rate and bandwidth efficiency. The analysis and findings of the work indicates a superior choice of multilevel modulation scheme to achieve increased capacity in optical communication link. So it can be established that there is a benefit to be gained in terms of system performance and tolerance to improvements by adopting a more sophisticated modulation format rather than convention binary intensity modulation. The selection of parameters for a particular system must be carefully effectuated taking account of a wide range of factors based on the detailed findings and limitations established here. These researches in both modeling and numerical methods give us an insight view of advanced modulation formats and provide a foundation for future research. This work emphasizes the anticipated capacity dilemma and required challenges to be faced by presenting an optimal solution to compete with the traffic growth in the next decade.

TABLE OF CONTENTS

List of Acronyms

ASE	Amplified Spontaneous Emission
BER	Bit-Error Rate
BPF	Band Pass Filter
CD	Chromatic Dispersion
CSRZ	Carrier-Suppressed Return-to-Zero
CW	Continuous Wave
DCF	Dispersion Compensating Fiber
DGD	Differential Group Delay
DPSK	Differential Phase-Shift Keying
DQPSK	Differential Quadrature Phase-Shift Keying
DRZ	Duobinary Return-to-Zero
DSP	Digital Signal Processing
DWDM	Dense Wavelength-Division Multiplexing
EDC	Electronic Dispersion Compensation
EDFA	Erbium-Doped Fiber Amplifier
ER	Extinction Ratio
FSR	Free Spectral Range
FWHM	Full Width at Half Maximum
FWM	Four-Wave Mixing
GVD	Group Velocity Dispersion
IM-DD	Intensity Modulation Direct Detection
ITU	International Telecommunications Union
MDRZ	Modified Duobinary Return-to-Zero
MZM	Mach-Zehnder Modulator
MZIM	Mach-Zehnder Interferometer
MZDI	Mach-Zehnder Delay Interferometer

NLSE	Non Linear Schrödinger Equation
NRZ	Non-Return-to-Zero
OOK	On-Off Keying
OSNR	Optical Signal-to-Noise Ratio
PMD	Polarization Mode Dispersion
PRBS	Pseudo-Random Bit Sequence
PLL	Phase Locked Loop
RZ	Return-to-Zero
RZ-DPSK	Return-to-Zero Differential Phase-Shift Keying
SOA	Semiconductor Optical Amplifier
SOP	State of Polarization
SMF	Single Mode Fiber
SPM	Self-Phase Modulation
SSFM	Split Step Fourier Method
UDWDM	Ultra Dense Wavelength-Division Multiplexing
WDM	Dense Wavelength-Division Multiplexing
XPM	Cross-Phase Modulation

LIST OF FIGURES

LIST OF TABLES

Chapter 1

Introduction

The phenomenal increase in the ever-growing internet traffic has led to an aggressive demand for higher transmission bandwidth, and thereby resulting in a dramatic growth of broadband networks. The drive for higher capacity, better flexibility and enhanced functionality has been further expedited due to the emergence of real-time interactive multimedia applications involving enormous data exchange. The data volume is ever growing and such crucial messages need to be transmitted over global distances in the fraction of a second. This calls for a responsive, secure and bandwidth efficient supporting network to facilitate end-to-end transmission of data/messages of any conceivable size encountered in real-life communication.

The internet, or more broadly any communication network, consists of various interconnected nodes, which exchange information through an underlying backbone, consisting of a transmitter, a channel and a receiver. Depending on the channel utilized for transmission of information, different technologies can be deployed to transmit and receive bits of information. Optical communication system forms the core of high speed transport infrastructure by offering its potentially unlimited capabilities [1, 2] such as enormous bandwidth, low signal attenuation, minimum signal distortion, lesser material usage, smaller power requirement and lesser effective cost. Currently, virtually almost all the telephonic/cellular conversations, voice/data messages, and internet packets pass through an optical fiber communication network between the source and destination at some instances. Optical communication systems, use light as the carrier of information and optical fiber as the information transmission medium with a capability to transmit high data rates over long distance [3]. However, the main challenge is to increase the bandwidth-distance product of fiber link by researching the mitigation approaches to resolve the intrinsic impairments of fiber channel, i.e., attenuation, dispersion and non-linearities [4, 5].

1.1. Literature Background

The era of modern fiber-optic communications started in around 1970s with the advent of GaAs semiconductor laser and the reduction of fiber losses to 20 dB/km near the 1 μm wavelength region.

Since then, optical communication has radically impacted the development of data communication technology by resolving the bottleneck of high speed network access to the end users at a minimum bandwidth cost [6] with an extremely high channel capacity [7]. The tremendous growth of lightwave systems can be grouped into several generations each distinguished by bit rate-distance product (BL), as a figure of merit, where B is the bit rate and L is the repeater spacing. Fig. 1.1 shows the growth rate of bit rate-distance product with the development of lightwave systems in the initial years.

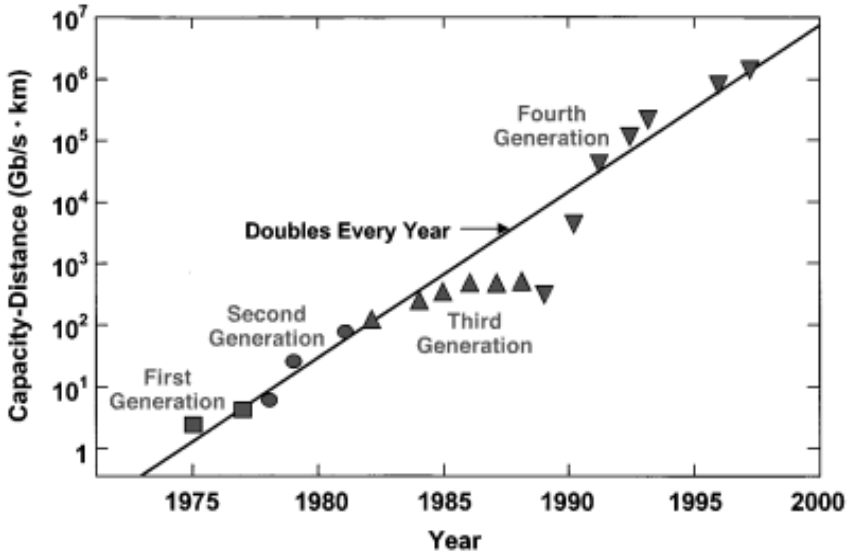

Fig. 1.1: Increase in the BL product through several generations of lightwave systems [Source: 1]

The first generation of lightwave systems became commercially available in 1980 and operated near 0.8 μm window at a bit rate of 45 Mbps allowing repeater spacing of up to 10 Km using GaAs based semiconductor lasers. The second generation optical communication systems were deployed commercially in 1987 and operated near 1.3 μm wavelength regime at which fiber loss is less than 1 dB/km and dispersion is minimum. This was enabled by the rapid development of InGaAsP semiconductor lasers and detectors operating near 1.3 μm and the use of single-mode fibers (SMF) thereby allowing 1.7 Gbps data rate and 50 Km repeater spacing. The third-generation lightwave systems came into existence in 1990, enabling 2.5 Gbps data rate in silica fibers having minimum loss (0.2-dB/km) at 1.55 μm wavelength. However, operation was severely limited by large fiber dispersion encountered near 1.55 μm and was overcome by the development of usage of dispersion-shifted fiber (DSF) and narrow linewidth single-longitudinal-mode lasers. Moreover, the signal needed to be electronically regenerated periodically with the repeater spacing of typically from 60 to 70 Km to meet the requirement of high data rate optical link design.

Fourth-generation lightwave systems led to a revolution in optical channel capacity with the advent of erbium-doped fiber amplifiers (EDFAs) and wavelength-division multiplexing (WDM) which resulted in capacity enhancement by simply an increase in the number of channels without deploying more fibers. Wide band optical amplification provided by low-noise and high-gain EDFAs made long haul transmission possible without using electronic regenerator and stimulated the development of WDM systems by transmitting the information using multiple carriers simultaneously. These systems working upto 10 Gbps data rate were commercially available in 2001 but were largely limited by dispersion [8, 9]. To solve this bottleneck, considerable research has been done for the development of fifth-generation systems which focus on increasing the number of WDM channels, by extending the wavelength range to L-band (1570 nm–1610 nm) and S-band (1485 nm–520 nm) over the conventional wavelength window, known as C-band, covering 1530 nm to 1565 nm. Another driving force is to increase the data rate of each channel. Also optical soliton pulses were extensively studied to counteract the dispersion effects through fiber non-linearities [10], thereby preserving their shape over a lossless fiber. Recent efforts have been directed towards realizing greater capacity by multiplexing an even larger number of wavelengths. These systems referred as Dense Wavelength Division Multiplexing (DWDM) systems aim at reducing the current wavelength separation of 0.8 nm to less than 0.5 nm. Controlling the wavelength stability and the development of wavelength de-multiplexing devices is a critical issue [11- 13] in such systems.

Stupendous advances in optical communication technology has made it possible to develop systems which can combine DWDM, optical time-division multiplexing (OTDM) and optical code-division multiple access (OCDMA) systems. Moreover, coherent fiber optic communication systems are realizable with the introduction of homodyne or heterodyne detection schemes at the receiver end. The high receiver sensitivity offered by these systems initiated a huge surge in their demand. These systems faced a tough route of commercialization due to costly and complex components required including precise optical phase locked loops (PLLs). More recently, coherent optical systems are re-emerging as interesting domain of research due to development of phase stabilized sub-megahertz line width lasers. Further, high-speed digital signal processing (DSP) techniques have also enabled the implementation of critical operations like phase locking, frequency synchronization and polarization control in the electronic domain through digital means leading to realization of cost effective and stable coherent receiver design. These possibilities are still appearing as a topic of further research and opens a future scope of this thesis [14, 15].

1.2. WDM Optical Systems

Though the optical fiber networks were initially deployed for mainly long-haul or submarine transmission, now their presence in strongly seen virtually in all metro networks. This is primarily possible due to successful implementation of WDM technology which allows the data in separate parallel channels operating at their corresponding wavelengths and thereby fully exploits the bandwidth of optical fiber [16-19]. International Telecommunication Union (ITU) standards propose two variations of WDM,: i) Coarse wavelength division multiplexing (CWDM) which supports a relatively small number of channels (four or eight) with single channel bit rate between 1 and 3.125 Gbps, and a large channel spacing of about 20 nm with nominal wavelengths ranging between 1310 nm to 1610 nm , ii) Dense wavelength division multiplexing (DWDM) on the other hand is capable of supporting a greater number of channels (40, 80, or 160) at a conventional channel spacing of 50 GHz (0.4 nm) but can even support smaller channel spacing such as 12.5 GHz (0.1 nm) and 25 GHz (0.2 nm) commonly referred as Ultra DWDM (UDWDM) systems. The reference frequency is 193.10 THz (1552.5 nm) for all optical channels and can easily handle single-channel bit rates of 10 Gbps, 20 Gbps, 40 Gbps and up to 100 Gbps [20]. Fig. 1.2 shows a schematic of an optically amplified DWDM communication system.

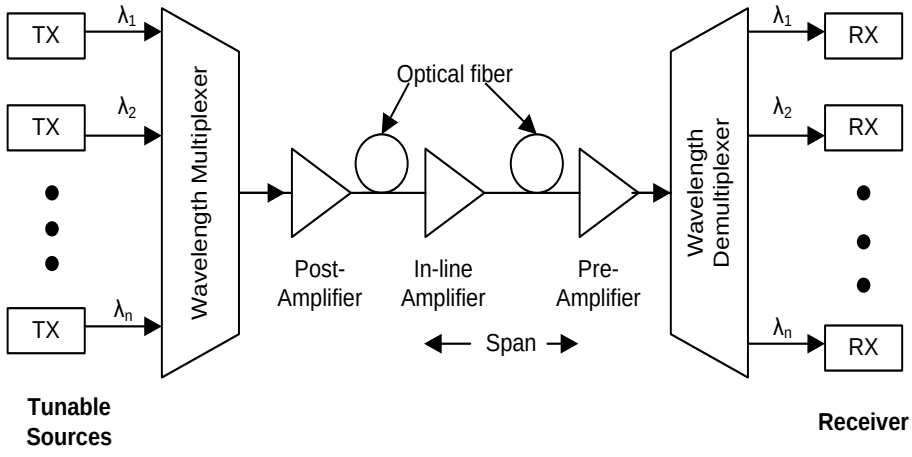

Fig. 1.2: Implementation of a typical DWDM link

The link or the optical transmission path is usually formed by a cascade of identically equipped sections comprising of appropriate optical signal conditioning blocks. At the transmitter side, laser source generates the light and modulates the electrical signal into the optical data stream. Several such

modulated optical signals at different wavelengths from individual transmitters are multiplexed together and launched over a link consisting of fibers and optical amplifiers. The post-amplifier negates the insertion loss of the multiplexer at the transmitter side and the pre-amplifier enhances the receiver sensitivity. It is also customary to include an in-line amplifier to cater for the attenuation in the fiber. This combined optical signal is de-multiplexed before it propagates to each individual receiver, which recovers the original electrical data by detecting and demodulating the optical signal.

1.3. Challenges and Solutions

The exponential rise in the transmission capacity has triggered an era of faster and reliable optical data transfer techniques resulting in the exploration of spectrally efficient systems suitable at extremely high data rate. This in turn led to the migration from the existing 10 Gbps to 40 Gbps systems. As the transmission capacity of the optical network increases, the optical signal power required at the transmitter end to ensure acceptable bit error rate (BER) at the receiver also increases. This increased power level leads to signal distortions due to fiber Kerr nonlinearity induced impairments which results in loss, interference and distortion in the transmitted signals. These limitations impose an upper bound on the maximum effective SNR of a link, and limit the achievable transmission performance. On the other hand, linear impairments such as chromatic dispersion (CD), optical-signal-to-noise-ratio (OSNR) degradation, filter concatenation, amplified spontaneous emission (ASE) noise and the crosstalk introduced by transmission over long concatenated fiber links also become dominant factors in deciding the system performance [21-24].

The optical bandwidth of the amplifiers and the frequency separation between adjacent channels are the two factors which limit the number of channels supported on a link. Though the ITU grid specifications use 100 GHz channel separation, but currently systems with even smaller channel spacing such as 50 GHz (DWDM) to 25 GHz (UDWDM) are being explored. These modified systems invite increased non-linearity in the form of both intra and inter-channel crosstalk and thus present a challenge to the researchers. While high capacity DWDM systems keep heading to closer channel spacing and broader bandwidth of optical amplifiers fully exploits the fiber bandwidth, on the other hand, upgrading the embedded systems presents a crucial challenge. Unfortunately, most of the embedded fibers are conventional single mode fibers (SMF) which suffer from a large dispersion at the 1.55 μm window. Changing the existing fiber bed is an economical challenge and hence upgrading

these systems calls for effective techniques based on specific requirements to optimize system performance in terms of mitigation of linear and non-linear impairments [25-27].

Despite the introduction of several advanced modulation formats, the spectral efficiency is limited by linear and non-linear impairments encountered during signal propagation such as self-phase modulation (SPM), cross phase modulation (XPM), cross polarization modulation (XPolM) and four wave mixing (FWM). [28] These linear and non-linear impairments not only impact the core junction networks but also affect the fiber optic access networks and limit the transmission capacity and the distance reach of DWDM systems. The dominant constraints in optical access networks are insertion losses in passive optical devices, linear crosstalk in multiplexing and de-multiplexing devices [29] and attenuation in the fiber optic cables. These effects have been discussed in detail in chapter 2. Thus, in the design of a high speed multi-channel optical transmission system, limitations of dispersive influences and management of non-linear impairments have attracted much attention for research work to explore viable solutions.

While several methods have been proposed to curtail linear impairments, but the induced non-linear impairments impose a limit on the overall fiber channel capacity especially for long haul WDM transmission links. Transmission capacity can be significantly exalted by mitigation or compensation of non-linear effects and has driven considerable research efforts in this domain over the past decade. There can be two approaches to handle this aggravating problem, (i) design a robust system resilient to non-linear effects and (ii) remove the non-linear impairments. From the view point of system design, the non-linear tolerance can be enhanced by optimizing the pulse shape [30], receiver filter [31] or fiber dispersion maps [32, 33], using pre-distorted signals [34, 35] or discovering novel modulation formats which are more robust towards fiber nonlinearities [36-38]. Besides, polarization interleaving [39, 40] and advanced amplification methods [41] can also decrease the nonlinear transmission penalty. On the other hand, nonlinear post processing [42, 43] and optical phase conjugation [44, 45] dealing with the optical signal phase are used for nonlinear compensation. However, these mentioned optical methods appear less flexible and costly for implementation.

DWDM offers a manifold increase in the capacity of long-haul optical transmission systems or in other words a substantial lowering of the cost per transmitted bit. However, in a conventional DWDM network, the intensity of the optical carrier is modulated by the electrical information signal and uses direct detection at the receiver, enabled by a photo-diode which acts as square law detector and converts the optical signal to electrical domain. The implementation of intensity modulation (IM) on the

transmitter side and direct detection (DD) at the receiver end is known as intensity modulation-direct detection (IM-DD) scheme and has been extensively used till now. However, the phase information of the transmitted signal is lost due to the power law of a photo diode, preventing the employment of phase-modulated schemes, thus resulting in low spectral efficiency [46, 47]. Moreover, the input signal power cannot be arbitrary large due to the accumulation of non-linear effects in fiber leading to low power efficiency. This necessitates the use of high sensitivity optical receivers in a noise limited system. Therefore, both spectral efficiency and power efficiency are limited in a fiber-optic system using direct detection.

To improve the transmission performance and spectral efficiency of DWDM systems, a wide variety of techniques have been proposed such as: effective bandwidth management (by increasing the bit rate per channel or increasing the number of channels or decreasing the channel spacing); channel noise mitigation (by use of advanced modulation formats to trade off noise resilience and fiber propagating characteristics by manipulating the spectrum of signal, using different fiber types to reduce nonlinear signal distortions, effective management of nonlinear impairments and dispersion) and optimum system design (accurate analytical modeling and simulation of optical link and the various components and use of advanced DSP based signal conditioning algorithms such as signal equalization, forward error correction (FEC), Digital back propagation [48-52]). The power efficiency can be improved by minimizing the required average signal power or OSNR at a given level of BER. The signal spectral efficiency is measure in bit/s/Hz, and can be increased using various spectrally efficient modulation schemes [53-55] and the same has been the focus of this thesis. The study in the thesis attempts to combine the above methods to achieve a robust long haul transmission link using spectrally efficient modulation schemes.

1.4. Advanced Modulation Formats

The dramatic development in fiber optic communication is fueled primarily by two reasons: lowering the cost of the transmitted bandwidth and meeting the insatiable demand of increased bandwidth. To cope with the expected bandwidth demand in the near future, new technologies have to be researched, developed and subsequently deployed in long-haul transmission systems. This has led to tremendous research efforts and consequently spectrally efficient advanced modulation formats received special attention as they offer narrow bandwidth and high immunity to non-linear distortion. These spectrally efficient modulation schemes could be deployed selectively in the upcoming optical networks

depending on the operating bit rate, system requirements and network reach. In general, different data formats lead to different signal quality at the receiver end for a given transmission link, because they exhibit different waveforms and spectra [56]. At the same time, links with different system parameters (reach, channel spacing, fiber type, amplification schemes, etc.) may also require different optimal data formats. The ideal modulation format for long-haul, high-speed WDM transmission links would be one that has a compact spectrum, low susceptibility to fiber non-linear effects, large dispersion tolerance, simple and cost-effective configurations for generation and detection [57, 58].

In order to facilitate the 40 Gbps system to fit into the existing 50 GHz spaced DWDM infrastructure, research in advanced modulation formats for optical transmission received a strong emphasis [59] as they provide a cost effective solution to manage various transmission impairments. Several new modulation schemes were investigated which along with carrying information in their amplitude also modulate their phase information to augment the tolerance against dispersion, optical filtering and non-linearities, leading to a robust optical link. Modulation formats such as chirped return-to-zero (CRZ), single sideband band RZ (SSB-RZ), carrier suppressed return-to-zero (CSRZ), Duobinary return-to-zero (DRZ), Modified Duobinary return-to-zero (MDRZ) and Alternate Mark Inversion (AMI) belong to this advanced group [60-64]. Another category of modulation schemes carry the information modulated in their own optical phase and are known as Phase Shift Keying (PSK) formats. One of the most promising format for long haul networks is Differential Phase Shift Keying (DPSK) [65, 66], wherein the difference in phase of the previous bit is used as reference and it uses a balanced receiver in place of direct detection to gain the 3 dB sensitivity benefit. Recently, several multi-bit per symbol optical modulation schemes have also been proposed as a competitive method to achieve higher spectral efficiency with relaxed dispersion management and improved PMD tolerance [67, 68]. This thesis also focuses on multi-level modulation formats, in particular the Differential Quadrature Phase Shift Keying (DQPSK) format, which has attracted a considerable interest as it offers 3 dB improvement in receiver sensitivity and has the best spectral efficiency compared to the other modulation formats discussed above.

However, as each modulation format exhibits specific features (e.g. receiver sensitivity, implementation cost/complexity, tolerance to impairments, it becomes a crucial task to characterize an optimal modulation scheme for a particular application. Innumerable factors are to be considered to select an appropriate modulation format, such as (i) tolerance to chromatic dispersion; (ii) improvement attained in spectral efficiency; (iii) ease of implementation; (iv) span reach and (v) maximum allowable

DWDM channels without the need to apply error correction coding, making the proper selection a major challenge.

1.5. Methods for Signal Quality Assessment

Numerical simulations are widely used for investigating fiber-optic communication systems. Not only accurate physical models of individual devices are important but reliable estimation of system performance is essential for enhancing simulation accuracy. Unlike practical systems, direct error counting becomes unrealistic in numerical simulations due to the required large number of simulated bits. Based on the knowledge of noise statistic property or deterministic propagation or filtering effects, incorporating some analytical solutions has been proven to be a reliable way and the simulation time for signal quality evaluation at receiver can be thus saved, especially for error-free systems [69]. Appropriate analytical models are needed according to the implemented modulation formats as the noise behavior may appear differently for intensity and phase modulated signals [70]. In this section, some common methods employed in numerical simulations for system performance characterization are discussed.

1.5.1. Monte-Carlo Error Counting Method

The fluctuating optical signal caused by various kinds of impairments in fiber link is received by receiver, which converts optical signal to electrical signal. The electrical signal is fed into an error detector, which contains a decision circuit to sample the signal and compares to the transmitted data patterns. The most direct way to estimate system performance is to calculate BER by comparing the received bits and the transmitted bits as given by:

$$BER = \frac{number\ of\ error\ bits}{number\ of\ total\ bits} \quad \ldots (1.1)$$

Hence, a BER of 4 x 10^{-6} corresponds to an average 4 errors per million bits. BER can also be defined as the probability of incorrect identification of a bit by the decision circuit of the receiver [10]. The Monte-Carlo method aims to directly counts the number of error bits which is similar to experimental measurement. To ensure reliable estimation, it is necessary to transmit a sufficient number of bits for a certain BER level. In Monte-Carlo simulations, the interaction between optical signal and noise is also considered in performance evaluation which enhances the accuracy for transmission with high fiber non-linearities. Besides, Monte-Carlo error counting method does not depend on the implemented

modulation formats and gives reliable BER estimation for various modulated signals and receiver types. In an optical fiber communication system, BER may often be measured only experimentally as the high quality performance of a conventional optical fiber communication link (BER =$10^{-9)}$ requires an extremely large number of bits to evaluate BER, thus making numerical simulation of BER generally impractical. Therefore, the Monte-Carlo method is less favorable in current research but can still be employed for evaluating high BER or as a good reference for other BER estimation methods.

1.5.2. Eye Diagram and Eye-Opening

In addition to counting error bits, it is also possible to examine the signal quality by analyzing the received pulse shape, i.e., the eye diagram at the receiver. An eye diagram is generated by overlapping the received electrical pulses in individual bit duration into one-bit duration as represented in Fig. 1.3.

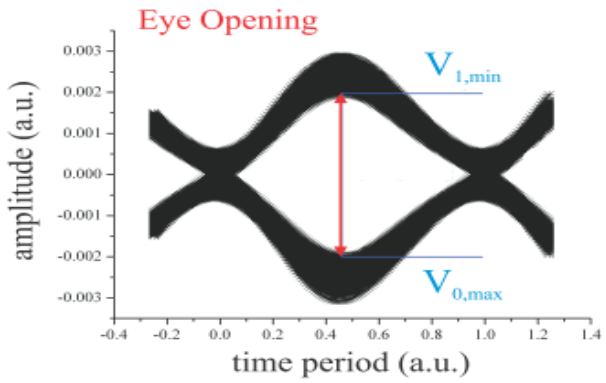

Fig. 1.3: Illustration of a received signal eye diagram and eye-opening definition.

An eye-opening (EO) parameter can be defined from a given eye diagram as the difference between the least upper rail (V_1, min) and the lower rail (V_0, max) of the eye, and is expressed as [71]:

$$Eye\ opening\ (EO) = V_{1,min} - V_{0,max} \quad \ldots (1.2)$$

In general, EO of the received signal can be used to describe the signal evolution in a transmission system and is compared to EO of a reference signal which can be a back-to-back ideal signal or a distorted signal, as depicted by Eq. 1.3:

$$EO\ penalty\ or\ EO\ improvement = 10log_{10}\frac{EO\ of\ the\ received\ signal}{EO\ of\ the\ refernce\ signal} \quad \ldots (1.3)$$

In the absence of noise, relating the received EO to ideal EO normally represents a penalty due to signal distortion in fiber propagation, denoted as eye-opening penalty. If a distorted signal is taken as a reference for the received EO which is distortion compensated, an eye-opening improvement can be obtained to assess the ability of the employed compensation technique.

1.5.3. Q-factor and Error Vector Magnitude

With assistance of a known statistic process, the direct error counting of the Monte-Carlo method can be replaced with a simple analytical model to estimate system performance. Assuming the received current at the decision instant in any received bits has a distribution of Gaussian shape, BER can be approximated by a quality factor (Q-factor):

$$BER = \frac{1}{2} erfc\left(\frac{Q}{\sqrt{2}}\right), \qquad where\ Q = \frac{I_1 - I_0}{\sigma_0 + \sigma_1} \qquad \ldots (1.4)$$

The performance criterion of a receiver is governed by the BER, defined as the probability of incorrect identification of a bit by the decision circuit of the receiver. A receiver is said to be more sensitive if it achieves the same performance with less required incident power. The common receiver sensitivity is defined as the minimum average received power for a receiver to achieve a BER of 10^{-9} [72].

The Q-factor can be calculated by the ratio of difference between two mean values to the total standard deviation of the two rails in a received eye diagram. I_0 and I_1 denote the mean values, and σ_0 and σ_1 denote the standard deviations of probability density function (PDF) for bit 0 and bit 1 respectively. Q becomes small for poor signal quality that corresponds to higher BER. Note that this approach can provide sufficient accuracy in BER estimation for an On-off keying (OOK) system under the assumption that the noise distribution follows Gaussian approximation. However, for phase-modulation format, Chi-squared approximation is alternatively used.

1.5.4. Spectral Efficiency

The spectral efficiency (SE) of an optical communication system is the net bitrate (useful information rate excluding error-correcting codes) or the maximum throughput divided by the bandwidth in hertz of a communication channel and is given by:

$$SE = \frac{C}{\Delta f} \quad \ldots (1.5)$$

where C is the capacity per channel with unit of bits per second (b/s) and Δf is the channel spacing. Spectral efficiency is very important in fiber optics, since the spectral bandwidth affects the number of channels occupied in a single fiber and must be maximized.

1.6. Motivation

One of the important changes in fiber-optic communication systems brought by EDFAs is the expansion of long haul communication link upto transoceanic distances. However, a new problem results which is the accumulation of fiber nonlinearities along the links through multiple cumulative ASE noise of the line amplifiers. Further, the high optical power levels available from EDFAs makes system performance more vulnerable to various nonlinear effects. In a multi-channel system, the effect of fiber non- electrical signal linearities should be addressed more precisely to understand inter-channel effects along with intra-channel effects. While the other two conventional limiting factors in designing optical communication systems, namely, fiber loss and dispersion, are relatively well understood, and can be easily overcome by optical amplifiers and dispersion compensation, but the fiber nonlinearities have not been fully analyzed and understood despite a rich collection of literature dealing with fiber non-linearities. Therefore, it is crucial to understand fiber nonlinearities and their effects on fiber-optic communication systems, especially for a multi-channel high speed link. In optical communication systems, the input signal to the fiber is usually a composite optical signal modulated with information bit streams. When all the input signal frequencies interact due to fiber nonlinearities, the output bit stream may behave in a complicated way resulting in adverse effects on system performance due to pulse shape and spectrum distortion. This thesis studies and mathematically models nonlinear interactions among channels of modern high bit rate (amplitude/ phase modulated) optical systems along with simulation of such systems to gain intuitive understanding. The key objective of the work is to develop analytical models to characterize fiber nonlinearities and use it to understand signal propagation and enhance transmission reach. Modeling of various optical components such as SMF and dispersion compensating fiber (DCF) is also attempted mathematically and supported with a corresponding Simulink model.

The migration from 2.5 Gbps system to 10 Gbps DWDM systems was achieved by encompassing the improved laser and optical transmitters employing OOK modulation and direct intensity detection at

the receiver. However, for upgradation to 40 Gbps DWDM network, just an improvement in optical devices no longer suffices and needs some modern communication techniques such as advanced modulation formats need to be experimented with. The motivation of the work performed is to study, analyze and implement different advanced modulation formats at 40 Gbps data rate. The modeling and simulation investigations have been performed to measure their performance characteristics regarding their sensitivities, CD tolerance, and spectral bandwidth and compare them with each other. Both Intensity Modulated and Phase Modulated formats have been studied in this thesis viz., CSRZ, DRZ, MDRZ, DPSK and DQPSK. All these modulation formats offer higher spectral efficiency compared to the binary Non-Return-to-Zero amplitude modulation (NRZ).

In the literature, these formats have been studied for WDM systems having 50 GHz channel separation [73-75], but with up to 16 channels or at a lower data rate [76-80]. Moreover, an integrated study of complete link design for distance optimization has not has not been much emphasized in literature. Here, in the present analysis, an attempt has been made to improve the bandwidth efficiency of the channel and find the most suitable format for an optimized transmission distance operating at 40 Gbps for 32 channel DWDM system each having 50 GHz channel spacing as an integrated approach. The study also explores the potentiality of the integration of unequal channel spacing for suppression of FWM in such optical links. Further the applicability of 40 Gbps system in UDWDM is also a crucial design issue to be investigated. An alternate polarized DQPSK modulated UDWDM system to evaluate its resilience to XPM and fiber nonlinearity has also been explored in the later portion of the thesis. The results obtained in this thesis gives the reader or system designer useful information that can be used to choose between different modulation formats to match the requirements of a specific optical transmission system for short to medium reach transmission applications.

1.7. Objectives

1. To understand signal propagation and investigate the various linear and non-linear channel impairments using linear piece-wise models to optimize optical network performance.
2. Investigation of various intensity and phase modulation formats based on application and their influence on non-linear channel impairments.
3. (i) Design and simulate long haul transmission link with various modulation formats to study the performance of each format under various transmission impairments and varying channel spacing using OptiSystem software.

(ii) Develop suitable non-linear mathematical model for optical link analytically using Simulink.

4. Investigate spectrally efficient modulation formats for UDWDM systems and increase the transmission distance in presence of impairments.

1.8. Methodology

To analyze the performance of DWDM systems in the presence of fiber non-linearities various analytical models, based on the solution of the nonlinear Schrodinger equation (NLSE), have been proposed in most of the reported work. In general, it is not possible to solve the equation analytically. Conventional ways of analyzing fiber nonlinearities either rely on pure numerical methods such as the split-step Fourier method (SSFM) or rely on analytical solutions with over simplifications such as the assumption of non-linearity alone. Modeling and theoretical analysis of DWDM system, though interesting is quite complicated, as it involves expertise in physical theory of optical dispersion, laser and photo detector conversion phenomena etc. Unfortunately, these analytical models can not accurately describe the system specifications such as the total transmission distance, the number of WDM channels and spacing between them, allowable power per channel, the amplifier spacing, etc. Alternatively, numerical simulation of such systems can be used to rectify this problem and to approach, experimental and realistic cases with accuracy, thus offering better insight to system design by allowing parameter optimization of the components used in model. So we have used both the approaches to gain a better understanding of optical systems. The analytical models are developed in Simulink using mathematical analysis, and are a bit complex and computationally extensive. The rising complexity of link design demands for more powerful simulation tools and faster algorithms. In this thesis, the OptiSystem 10.0 platform has been used to simulate the dispersion and nonlinear tolerance of a 32-channel fiber optic transmission system. Simulation test beds are developed to study and analyze various modulation formats and infer their characteristics. Firstly, a single channel link is designed for each modulation technique under investigation and then gradually the number of channels, bit-rates and system complexity is increased by using different type of system components. The performance is enhanced by various optimizations in transmitter and receiver architectures, types and order of filters and using various dispersion compensation techniques and results are evaluated in terms of BER, Q value and eye diagrams.

1.9. Thesis organization

This thesis is organized as follows: **Chapter 1** outlines the thesis motivation and describes the development and current state in DWDM systems. The importance of advanced optical modulation formats and the necessity of achieving high spectral efficiency in future all-optical networks is highlighted based on which the objectives are defined.

Chapter 2 introduces the basic concepts of optical fiber communications starting from propagation of light in optical fibers and focuses on the factors that limit the performance of WDM systems. The dispersion and the non-linearities of the fiber are discussed in more detail as they contribute significantly to the factors limiting WDM. A brief discussion of the nature of these phenomena and the modeling of XPM effect is presented. The need for dispersion compensation as a means of improving the utilization of the bandwidth in DWDM systems is presented. The theory behind the operation of the various components used in optical communication systems and their corresponding mathematical modeling is also discussed. The chapter reviews the basic of optical transmitter, receiver, and common transmission impairments as well as compensation techniques in optical networks. The background knowledge in this chapter will help in the understanding of technology proposed in this thesis.

Chapter 3 gives a classification of various intensity modulated advanced modulation formats. In addition to the conventional direct modulated optical transmitter, the operation behind MZM is also explained. The employed transmitter and receiver architectures of CSRZ, DRZ and MDRZ format are described and simulated at 40 Gbps, and, a performance comparison is presented. The effect of FWM suppression using unequal channel spacing in also presented.

In **Chapter 4**, transmitters and receiver architectures for the advanced phase modulation formats such as DPSK and DQPSK are presented, and a 32 channel DWDM system is designed and analyzed by numerical simulations at 40 Gbps. The results highlight the superiority of DQPSK format over the other studied schemes. Further, a Matlab Simulink model of a single channel DQPSK modulated link has been developed to get a better physical intuition of the transmission characteristics of DQPSK signaling in a realistic optical link. The simulation model considers the different optical components used in link design with their behavior as represented initially by theoretical interpretation in Chapter 2. The included transmitter topology, MZM module, propagation model for optical fibers and the receiver block set enables to realize an operational experimental WDM configuration.

In **Chapter 5**, we further explore the suitability of DQPSK format for UDWDM scheme. An UDWDM system based on DQPSK format and supporting 32 channels, each operating at 40 Gbps and spaced at

25 GHz is studied numerically for long-haul optical communication system using OptiSystem simulator to estimate OSNR penalties to mitigate XPM effects. The work discussed in this thesis shows that multi-level modulation formats enable long-haul transmission systems. Proper dispersion management improves the transmission tolerances, simplifies system design and allows these formats to be used on the existing infrastructure of systems optimized for 40 Gbps transmission.

Chapter 6 summarizes and discusses the important finding of this thesis and also gives possible suggestions for the further research with respect to the DSP based techniques for improvement in spectral efficiency and transmission reach.

Chapter 2

Narrow Pulse in Optical Link: System Modeling

When an optical pulse travels inside the fiber, due to its intensity fluctuations and variations in the effective refractive index of the medium along the fiber length, various temporal disturbances are created. These temporal and spatial changes in the pulse lead to various linear and nonlinear impairments. Different wavelength components of the pulse travel at different speeds and result in pulse dispersion, distortion and signal interference at the receiving end. The performance of long-distance optical communication systems is thus limited due to the interactive and accumulative effects of chromatic dispersion and nonlinear phenomena [81]. As the signal propagates over the fiber, the OSNR deteriorates with the increase in signal bandwidth, requiring an increase in the launched power of optical signal, further inviting nonlinear fiber effects [4]. The problem is particularly critical for systems operating at 40 Gbps or higher as it means transmitting pulses are as narrow as 25 ps. Moreover, as the data to be transmitted is encoded in amplitude, frequency or phase of the optical pulse, preserving the pulse shape is of paramount importance especially in long haul transmission systems.

In a single channel system an effective solution is to use solitons which preserve pulse shape by counter balancing SPM and GVD (Group Velocity Dispersion) effects and thereby facilitate to achieve larger distance. However, such multiple propagating pulse trains in a multichannel WDM environment gives rise to a very complex channel dynamics and it becomes too complicated for a system designer to understand. Although the power in each individual channel maybe below the required threshold value to produce nonlinearities, but the accumulative effects of all channels can initiate non-linear complexities significantly [82,83]. As the number of channels is increased and the frequency separation between the channels is reduced, these detrimental effects become quite significant and need to be clearly understood and analyzed to achieve satisfactory system performance. With this aim in this chapter, first an overview of the pulse propagation in an optical fiber and the various impairments an optical fiber is subjected to is discussed. Then a generic system model is presented to provide an in-depth description of various system components used in an optical communication link. The system components and the various impairments that the link is subjected to are mathematically modeled to get an intuitive understanding of the functioning of the link and influence of the interplay between

various propagation effects. It was seen that even modeling of a single channel optical system is quite tedious and needs a huge simulation run time, making it very challenging and time consuming for the case of a DWDM system. So in the present study, a simple mathematical model for a single channel has been attempted to gain insight into pulse propagation in an optical communication link. However, the DWDM link supporting large channels has been studied with suitably designed system models using Optisystem 10.0 simulation package and discussed in detail in chapter 3, 4 and 5.

In its simplest form, an optical fiber consists of a central glass core surrounded by a cladding layer whose refractive index n_2 is slightly lower than the core index n_1 [4] as shown in Fig. 2.1. To gain an insight of the evolution of optical field in the optical fiber, it is necessary to consider the theory of electromagnetic wave propagation in dispersive nonlinear media and use this for channel modeling. Like all electromagnetic phenomena, the propagation of optical fields in fibers is governed by Maxwell's equations [84] under suitable boundary conditions at core cladding interfaces.

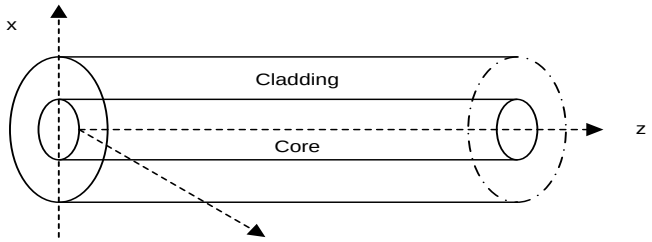

Fig. 2.1: Physical structure of the optical fiber.

2.1. Signal Propagation in Optical Fibers

When the optical intensity inside an optical fiber increases, the refractive index of the fiber gets modified. The wave propagation characteristics then become a function of optical power. Unlike linear fiber optics, where the propagation constant is a function of fiber and the wavelength only, the propagation constant now becomes a function of optical power in addition to the other parameters. Inside a SMF, an optical power of few tens of milliwatts may drive the medium into non-linearity [8, 9]. Since the non-linearity affects the signal propagation as a whole, therefore it becomes important to visualize the related impairments and represent them in mathematical models to explore the signal transmission behavior. The propagation of optical signals in SMF is governed by Maxwell’s equations which lead to the wave equation given as:

$$\nabla^2 \boldsymbol{E} - \frac{1}{c^2}\frac{\partial^2 \boldsymbol{E}}{\partial^2 t} = -\mu_0 \frac{\partial^2 \boldsymbol{P}(\boldsymbol{E})}{\partial^2 t} \quad \ldots (2.1)$$

where $\boldsymbol{E}$ is the electric vector, μ_0 is the vacuum permeability, c is the speed of light, and $\boldsymbol{P}$ is the polarization density field. In very low optical power regime, the induced polarization shows a linear relationship with $\boldsymbol{E}$ as given by

$$\boldsymbol{P}_L(\boldsymbol{r},t) = \varepsilon_0 \int_{-\infty}^{\infty} \chi^{(1)}(t-t').\boldsymbol{E}(\boldsymbol{r},t')\,dt' \quad \ldots (2.2)$$

where ε_0 is the vacuum permittivity, and $\chi^{(1)}$ is the first order susceptibility. Fiber nonlinearities can be accounted for by splitting the polarization in two parts.

$$\boldsymbol{P}_{(\boldsymbol{r},t)} = \boldsymbol{P}_L(\boldsymbol{r},t) + \boldsymbol{P}_{NL}(\boldsymbol{r},t) \quad \ldots (2.3)$$

where $\boldsymbol{P}_{NL}(\boldsymbol{r},t)$ is the nonlinear part of the polarization. In silica fiber, the nonlinear part of the polarization is contributed by the third order susceptibility χ^3 [11] which is a fourth rank tensor, and has up to 81 independent terms, however in an isotropic medium such as SMF, the number of such terms reduces to 1. Certain assumptions are generally made to arrive at a simple solution of Eq. (2.1) such as (i) we treat $\boldsymbol{P}_{NL}$ as a small perturbation of $\boldsymbol{P}_L$, and maintain the field polarization along the fiber length (ii) index difference between core and cladding is very small (weakly guiding approximation), and the center frequency of the wave is assumed to be much greater than the spectral width of the wave (known as quasi-monochromatic assumption) leading to the slowly varying envelope approximation in time domain. Assuming the input electric field to be propagating in the +*z* direction and polarized in the *x* direction, Eq. (2.1) can be written as [4]:

$$\frac{\partial}{\partial z}A(z,t) = -\frac{\alpha}{2}A(z,t) \qquad \text{(linear attenuation)}$$

$$+j\frac{\beta_2}{2}\frac{\partial^2}{\partial^2 t}A(z,t) \qquad \text{(second order dispersion)}$$

$$+\frac{\beta_3}{6}\frac{\partial^3}{\partial^3 t}A(z,t) \qquad \text{(third order dispersion)}$$

$$-j\gamma|A(z,t)|^2 A(z,t) \qquad \text{(Kerr effect)}$$

$$+j\gamma T_R \frac{\partial}{\partial t}\,|A(z,t)|^2 A(z,t) \qquad \text{(SRS)}$$

$$-\frac{\gamma}{\omega_0}\frac{\partial}{\partial t}\,|A(z,t)|^2A(z,t) \qquad \text{(self-steepening effect)} \qquad \ldots (2.4)$$

where $A(z,t)$ is the slowly varying envelope of the electric field, z is the propagation distance, $t = t' - z/v_g$ (t'= physical time, v_g is the group velocity at the center wavelength), α is fiber loss/km, β_2 is the second order propagation constant ([ps^2/km], β_3 is the third order propagation constant ([ps^3/km]), γ is the nonlinear coefficient given by $2\pi n_2/\lambda_0 A_{eff}$, n_2 is the nonlinear index coefficient, A_{eff} is the effective core area of fiber, λ_0 is the center wavelength, ω_0 is the center angular frequency and T_R is the slope of the Raman gain (~ 5 fs). Eq. (2.4) is commonly known as the generalized Non-linear Schrödinger Equation (NLSE), and is applicable for propagation of pulses as short as ~ 50 fs which translates to a spectral width of ~20 THz. For pulses with width greater than 1ps, Eq. (2.4) can further be simplified as the Raman effect term and the self-steepening effect term become negligible compared to the Kerr effect term [11] and is given by:

$$\frac{\partial A}{\partial z} = -\frac{i}{2}\beta_2\frac{\partial^2 A}{\partial t^2} - \frac{\alpha}{2}A + i\gamma|A|^2A \qquad \ldots (2.5)$$

The third order dispersion term is also neglected in Eq. (2.5), as it is inconsequential compared to the second order dispersion term unless we operate near the zero-dispersion wavelength. Though it acts as a propagation equation in contemporary optical communication systems with a fairly good accuracy but being a nonlinear partial differential equation it generally does not have an analytical solution when both the nonlinearity and the dispersion effect are present, except in the very special case of soliton transmission. Thus, a numerical approach/algorithm is vital to perceive various signal impairments during pulse propagation [85, 86]. Most of the simulators use SSFM to replicate optical pulse evolution over fiber as it offers good accuracy and relatively modest computing cost. In standard SSFM method, the fiber span is divided into many short sections and the dispersion operator and the nonlinear operator are treated separately in each section. Considering a fiber of length L, the output envelope *A (z = L, t)* can be calculated by dividing the fiber into small segments of length dz and applying the split-step Fourier algorithm to each one segment as shown in Fig. 2.2. The algorithm is briefly discussed in this section. Here, Eq. (2.5) can be expressed as

$$\frac{\partial A(z,t)}{\partial z} = \left(\hat{L} + \hat{N}\right)A(z,t) \qquad \ldots (2.6)$$

where $\hat{L} = -\frac{\alpha}{2} - \frac{j}{2}\beta_2 \frac{\partial^2}{\partial t^2}$ is the linear operator that accounts for attenuation and absorption, and $\hat{N}$ is the non-linear operator, $\hat{N} = j\gamma|A(z,t)|^2$, and governs the effect of fiber non-linearities.

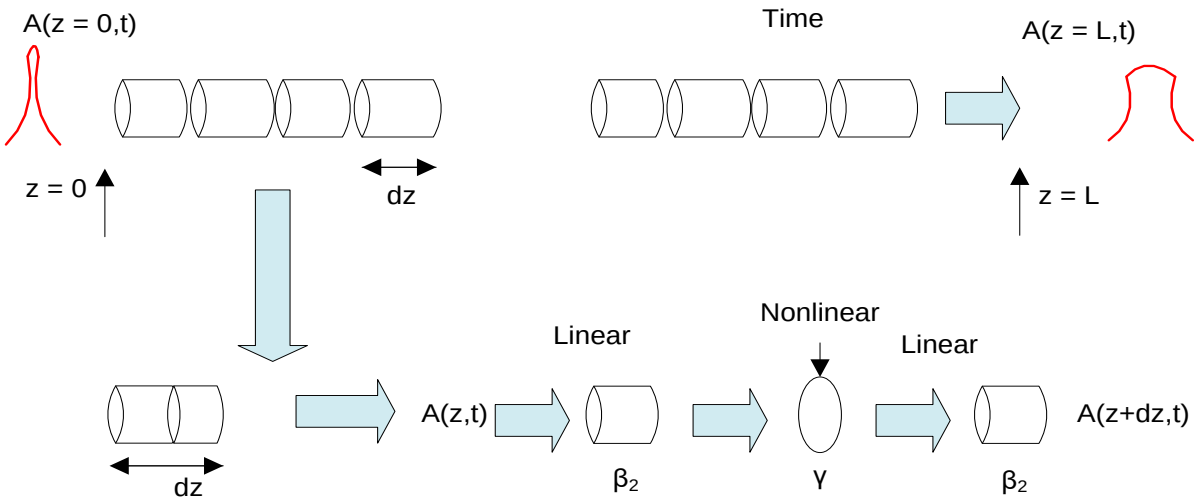

Fig. 2.2: Symmetric split-step Fourier algorithm.

An approximate solution to Eq. (2.6) is obtained by making the following assumptions:

I. The dispersive and non-linear behavior acts independently of each other.

II. A small distance Δz , accurately describes the optical field during propagation.

When the electric field envelope, $A(z,t)$, has propagated from $z + \Delta z$, the analytical solution of Eq. (2.6) is given by:

$$A(z + \Delta z, t) = \exp\left((\Delta z)(\hat{L} + \hat{N})\right) A(z,t) \quad \ldots (2.7)$$

Assuming that the two operators commute with each other we obtain

$$A(z + \Delta z, t) = \exp(\Delta z \hat{L}) \exp(\Delta z \hat{N}) A(z,t) \quad \ldots (2.8)$$

Hence, $A(z + \Delta z, t)$ can be predicted by applying the two operators independently. The simulation time of Eq. (2.8) depends greatly on the size of Δz. If Δz is sufficiently small, Eq. (2.8) gives a fairly good results and hence Δz is usually chosen such that the maximum phase shift $\phi_{max}(\sim \gamma|A_p|\Delta z$, with peak value of $A(z,t)$ as A_p) due to the non-linear operator is negligible (generally $\phi_{max} \leq 0.05$

rad). Simulation time is further reduced by using a more refined algorithm, known as symmetric SSFM [11, 87] which is expressed mathematically as below:

$$A(z+\Delta z,t) \approx \exp\left(\frac{\Delta z}{2}\,\hat{L}\right) exp\left(\int_{z}^{z+\Delta z} \hat{N}\,(z')dz'\right) \exp\left(\frac{\Delta z}{2}\,\hat{L}\right) A(z,t) \quad \ldots (2.9)$$

While Eq. (2.9) assumes that nonlinearities are lumped at every Δz i.e. at the segment boundary, Eq. (2.10) treats nonlinearities to be distributed throughout the segment, which is more realistic. When Δz is sufficiently small, the evaluation of the nonlinear operator is approximated as:

$$\int_{z}^{z+\Delta z} \hat{N}\,(z')dz' \approx \frac{\Delta z}{2}\left[\,\hat{N}(z) + \hat{N}(z+\Delta z)\right] \quad \ldots (2.10)$$

However, Eq. (2.10) requires iterative evaluation because $\hat{N}(z+\Delta z)$ is not known at $z+\Delta z/2$. Initially, $\hat{N}(z+\Delta z)$ will be assumed to be the same as $\hat{N}(z)$. Although the iterative evaluation is time-consuming, the improved numerical algorithm allows us to use larger Δz than that of Eq. (2.8), which results in saving overall computational time.

2.2. Linear Effects

The optical fiber is often seen as a perfect transmission medium with almost limitless bandwidth, but in practice the propagation through optical fiber is beset with several limitations especially as distance is increased to multi-span amplified systems. As the transmission systems evolve to longer distances and higher bit rates, the linear effect of fibers, which is the attenuation and dispersion, becomes the important limiting factor. As for DWDM systems that transmit multiple wavelengths simultaneously at even higher bit rates and distances, the nonlinear effects in the fiber present a serious limitation. The success of high bit rate long haul point-to-point optical transmission networks depends upon how best the linear and nonlinear effects are managed. This section briefly highlights the various fiber induced impairments and their influence in restricting the achievable capacity of the transmission link.

2.2.1. Optical Loss

Attenuation is a result of the various material, structural, and modular impairments in a fiber and severely affects signal propagation and limits the transmission distance in fiber [6]. When the optical

signal propagates over fiber, its power is lost and its amplitude is reduced due to material absorption and Rayleigh scattering. This power reduction is referred as attenuation and can be expressed as:

$$\frac{dP}{dz} = -\alpha P \qquad \ldots (2.11)$$

where α is the attenuation coefficient. The solution of this equation provides P_{out} after a length of propagation of L (km) for a given input optical power P_{in} given as:

$$P_{out} = P_{in} \exp(-\alpha L) \qquad \ldots (2.12)$$

This residual power at length L is due to the accumulative extrinsic and intrinsic linear loss of the channel. Modern telecom fibers exhibit an attenuation constant below 0.2 dB/km near 1.55 μm wavelength band where the attenuation is nearly minimum [2, 88] over a bandwidth of several THz and appropriate attenuation factors have been considered in simulation and modeling evaluations.

2.2.2. Amplified Spontaneous Emission Noise (ASE)

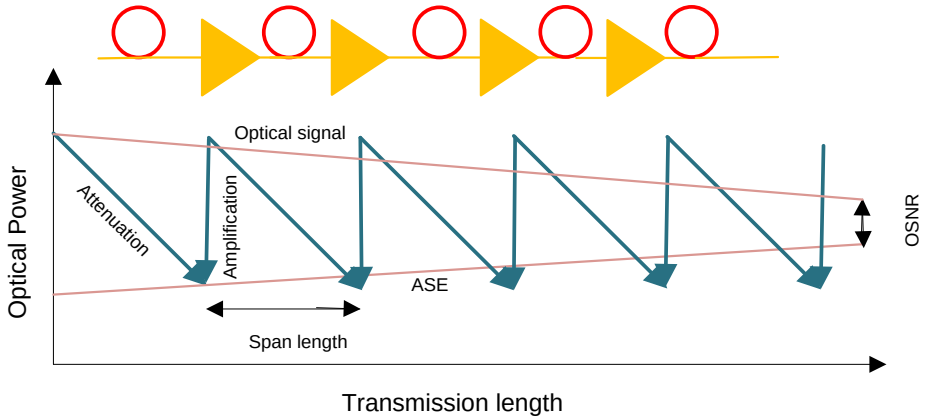

Fig. 2.3: ASE accumulation and OSNR reduction in an amplified transmission system

In a long haul optical communication system cascading of multiple optical amplifier stages plays an important role. ASE is the dominant noise generated in such optical amplifier due to the spontaneous recombination of electrons and holes in the amplifier medium. The nonlinear interaction between the ASE noise from optical amplifiers and the signal, results in amplification of ASE noise during propagation as shown in Fig. 2.3. The amount of noise generated by the amplifier depends on factors

such as the amplifier gain spectrum, noise bandwidth, and the population inversion parameter, which specifies the degree of population inversion that has been achieved between two energy levels.

When multiple optical amplifiers are cascaded to periodically compensate for fiber loss, ASE further builds up in the system. This noise build-up reflects in the form of OSNR, which degrades with every amplifier along the propagation path and such accumulated noise also gets converted into phase noise leading to system degradations. The OSNR is typically defined as the average optical signal power divided by the ASE power, measured in both polarizations and in a 12.5 GHz optical reference bandwidth. Optical amplifiers based on erbium-doped fibers provide higher gain, larger optical bandwidth, and low-noise figure (NF) [3, 8] and have been considered in this study.

2.2.3. Dispersion

Dispersion refers to the broadening of the optical pulse while it traverses along the fiber. Fig. 2.4 shows how dispersion limits the information capacity by causing short pulses to become wider resulting in serious Inter Symbol Interference (ISI), and thus degrades the performance severely.

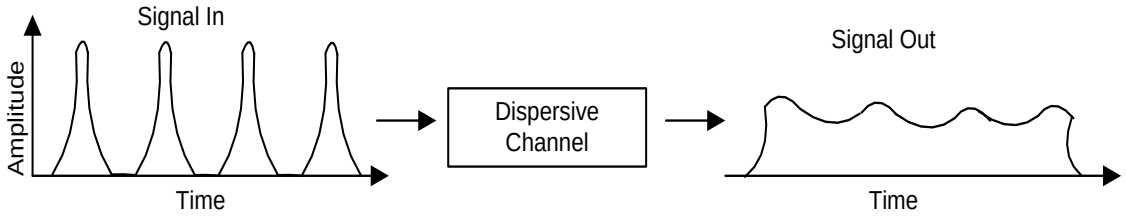

Fig. 2.4: Limitation of dispersion on information capacity

SMFs effectively eliminate inter-modal dispersion by limiting the number of modes to just one through a much smaller core diameter satisfying single mode condition. However, the pulse broadening still occurs in SMFs due to intra-modal dispersion which is described in the next sub-section.

2.2.3.1. Chromatic Dispersion

When an electromagnetic wave interacts with the bound electrons of a dielectric, the medium response, in general, depends on the optical frequency ω. This property manifests through the frequency dependence of the refractive index $n(\omega)$ and causes different spectral components associated with the pulse travel at different speeds resulting in the pulse to broaden in time domain. This phenomenon occurs due to group velocity dispersion or chromatic dispersion and plays a momentous role in pulse

propagation in the optical fiber. Assuming the spectral width of the pulse to be Δω, the pulse broadening at the output of the optical fiber is approximated as [89]

$$\Delta T \sim L\frac{d^2\beta}{d\omega^2}\Delta\omega = L\beta_2\Delta\omega \quad \ldots(2.13)$$

where $\beta_2 = \frac{d^2\beta}{d\omega^2}$ is known as GVD parameter and L is the fiber length. It is evident from Eq. (2.13), that the amount of pulse broadening is determined by the spectral width of pulse, Δω and the value of GVD parameter. This dispersion-induced spectrum broadening is very important even without nonlinearity for high data-rate transmission systems and it limits the maximum error-free transmission distance. Since dispersion depends on β and ω, to account for these effects of dispersion mathematically, the Taylor expansion series of the mode-propagation constant β about the carrier frequency ω_0 is considered to visualize the higher order dispersion coefficient contribution. This expansion is expressed as,

$$\beta(\omega) = \beta_0 + (\omega - \omega_0)\beta_1 + \frac{1}{2}(\omega - \omega_{0)}{}^2\beta_2 + \frac{1}{6}(\omega - \omega_{0)}{}^3\beta_3 + \cdots \quad \ldots(2.14)$$

where,

$$\beta_n = \left[\frac{d^n\beta}{d\omega^n}\right]_{\omega=\omega_0}$$

In this expression β_1 is the inverse group velocity, and β_2 is the second order dispersion coefficient and β_3 term indicates the third order dispersion parameter and represents the dispersion curve slope. The second order propagation constant, β_2 [ps^2/km], accounts for the dispersion effects in fiber-optic communication systems and depending on its sign, we can classify the dispersion into two regions, normal ($\beta_2 > 0$) and anomalous ($\beta_2 < 0$). Qualitatively, in the normal dispersion region, the higher frequency components of an optical signal travel slower than the lower frequency components and the reverse occur in the anomalous dispersion region. Fiber dispersion is often characterized by a parameter, D [ps/(nm.km)], commonly known as dispersion parameter and depends on the fiber and source parameter [2, 56-57] by the following expression:

$$D = D_m + D_w \quad \ldots(2.15)$$

where D_m and D_w correspond to the material and waveguide contributions respectively. If the source is characterized by a spectral width Δλ, then each wavelength component within Δλ travels with a different group velocity resulting in pulse broadening. This broadening is given by

$$\Delta\tau = \frac{d\tau}{d\lambda}\Delta\lambda = -\frac{L}{c}\lambda\frac{d^2n}{d\lambda^2}\Delta\lambda \quad \ldots (2.16)$$

which results in the material contribution to be given by:

$$D_m = \frac{1}{L}\frac{d\tau}{d\lambda} = -\frac{\lambda}{c}\frac{d^2n}{d\lambda^2} \quad \ldots (2.17)$$

while the waveguide contribution for a step-index fiber is given by

$$D_w = -\frac{n_2\Delta}{c\lambda}\left(V\frac{d^2(bV)}{dV^2}\right) \quad \ldots (2.18)$$

where V is the normalized waveguide parameter defined by

$$V = \frac{2\pi}{\lambda}a\sqrt{(n_1^2 - n_2^2)} \quad \ldots (2.19)$$

and b represents the normalized propagation constant of the mode

$$b = \frac{n_{eff}^2 - n_2^2}{n_1^2 - n_2^2} \quad \ldots (2.20)$$

with n_1 and n_2 being the refractive indices of core and cladding and n_{eff} is the effective refractive index.

Waveguide dispersion can be understood from the fact that the effective index of the mode depends on the fraction of power in the core and the cladding at a particular wavelength. As the wavelength changes, this fraction also changes. Thus even if the refractive indices of the core and the cladding are assumed to be independent of wavelength; the effective index will change with wavelength. It is this dependence of $n_{eff}(\lambda_0)$ that leads to waveguide dispersion. Since the sign of material dispersion depends on the operating wavelength region, it is possible that the two effects namely, material and waveguide dispersions cancel each other at a certain wavelength. Such a wavelength, which is a very important parameter of single-mode fibers, is referred to as the zero-dispersion wavelength (λ_{ZD}).

Two signals with a wavelength separation of $\Delta\lambda$ and having dispersion coefficient of D, walk-off by a time of $D\Delta\lambda L$ after a distance of L. In optical communication link, the impact of the group velocity dispersion is conventionally described using the dispersion length ($L_D = \frac{T_0^2}{\beta_2}$) which indicates the pulse broadening by $\sqrt{2}$ times while propagating over L_D. This L_D length provides a scale over which the dispersive effect becomes significant for pulse evolution along a fiber, however in case of insignificant β_3 a limiting length ($L'_D = \frac{T_0^2}{\beta_3}$) plays an important role in signal transmission over fibers. Chromatic dispersion is modeled by considering a phase change in the fiber transfer function [3]:

$$H(f) = \exp[-i\theta(\Delta\omega/\omega_0)^2) \quad \ldots(2.21)$$

where, $\theta = -\frac{\pi}{c}\lambda^2 DL\omega_0^2$

is the phase change due to dispersion. In this study, we consider chromatic dispersion semi-analytically together with self-phase modulation and evaluate an eye closure penalty induced from the combination of the two impairments.

2.2.3.2. Polarization Mode Dispersion (PMD)

For an ideal circularly symmetric fiber, both polarization states of the wave experience identical refractive index and therefore travel at the same speed. Nevertheless, in reality the fiber core may have asymmetric geometry causing slight refractive index difference between two polarizations, known as fiber birefringence. This makes one polarization state propagates faster than the other which leads to differential group delay (DGD) between two orthogonal polarizations [90]. When the propagating signal is split between the two polarizations, it results in pulse dispersion and corresponding time delay $\Delta\tau_{DGD}$ characterized by PMD parameter D_{PMD} to yield the following expression:

$$\Delta\tau_{DGD} = D_{PMD.}\sqrt{L} \quad \ldots(2.22)$$

$\Delta\tau_{DGD}$ is normally measured in ps. D_{PMD} (ps/L) appears more tolerant for longer distance at a symbol rate below 40 Gbaud. However, its stochastic behavior makes compensation difficult and also can become a limiting propagation effect for particular fiber types and higher data-rate systems. Contrary to chromatic dispersion, the PMD changes quickly with time [15]. These influences become important in modeling and simulation of high speed long haul optical links. The PMD introduces dispersion and

during the propagation through the channel results in some power penalty (δ_{PMD}) which can be modeled using [6]:

$$\delta_{PMD}(dB) = 10.2B^2D_{PMD}^2L \quad \ldots(2.23)$$

where L is the fiber length and B is the signal bit rate. This gets worsened for a long haul link and the upper bound on the maximum length of an M-link segment can be defined by

$$\sqrt{\sum_{i=1}^{M}(D_{PMD,l})^2 d_l} \propto \frac{f}{B} \quad \ldots(2.24)$$

where f is a fraction of the bit duration (typically 0.1). These models have been used in our simulation study to investigate the effect of PMD.

2.3. Nonlinear Effects

The optical fiber medium can only be approximated as a linear medium when the launch power is sufficiently low. However, in long-haul fiber optic transmission system using wideband WDM, to combat accumulated noise added by the amplifier chain along the transmission fiber link, the launch power must be increased to keep SNR high enough for the error-free detection at receiver. As the launch power increases, the nonlinearity of fiber becomes significant and leads to severe performance issues. Nonlinear effects in optical fibers are mainly due to two causes. One root cause lies in the fact that the index of refraction of many materials, including glass, is a function of light intensity and the phenomenon is called the Kerr effect. The second root cause is the non-elastic scattering of photons in fibers, which results in stimulated Raman and stimulated Brillouin scattering phenomena. One major difference between scattering effects and the Kerr effect is that stimulated scatterings have threshold power levels at which the nonlinear effects manifest themselves while the Kerr effect doesn't have such a threshold. These non-linear effects play an important role in the system modeling and simulation studies and therefore in the next subsection we present a brief discussion of various non-linear effects.

2.3.1. Stimulated Scattering

The stimulated Brillouin scattering is a single-channel effect caused by the interaction between the optical signal and sound waves in the fiber. The result is that power from the optical signal can be

scattered back towards the transmitter and deplete the forward going power in the link. The SBS effect has a high threshold, which also increases with the signal bandwidth. Therefore, as long as the signal power in the WDM channels does not exceed the threshold, the SBS does not cause significant impact on the system [91] and hence is not considered in this thesis.

Stimulated Raman Scattering (SRS) is the nonlinear parametric interaction between the optical signal and optical phonons of silica molecules present in the optical fiber. This interaction can lead to the transfer of power from shorter wavelength, higher photon energy channels, to longer wavelength, lower photon energy channels. This effect becomes more significant when the WDM signal bandwidth is broad and the power is increased [12] and hence is not studied in much detail in this thesis.

2.3.2. Optical Kerr Effect

The refractive index of silica fiber is weakly dependent on optical intensity, and is given by [14] as,

$$n(\omega, P) = n_0(\omega) + n_2 \frac{P}{A_{eff}} \quad \ldots (2.25)$$

where n_0 is the linear part of the refractive index, n_2 is the Kerr coefficient with typical value of 10^{-20} m^2/W, P is the optical power, and A_{eff} is the effective core area. In spite of the intrinsically small values of the nonlinear coefficients in fused silica, the nonlinear effects in optical fibers can be observed at relatively practical operating power levels. This is possible because of two important characteristics of SMF: (i) a small effective core area and (ii) extremely low loss (< 1 dB/Km). The dependence of the refractive index on the light intensity results in the propagation constant, β, and the same can be written as

$$\beta(\omega, P) = \beta_0(\omega) + \frac{2\pi n_2}{\lambda A_{eff}} P \quad \ldots (2.26)$$

where $\beta_0(\omega)$ is the propagation constant in the absence of nonlinear effects, and

$$\gamma = \frac{2\pi n_2}{\lambda A_{eff}} \quad \ldots (2.27)$$

is known as the fiber nonlinear coefficient. The total nonlinear phase shift (ϕ_{NL}) due to the Kerr effect after the distance L is given by

$$\phi_{NL} = \int_0^L [\beta - \beta_0] dz \quad \ldots (2.28)$$

This ϕ_{NL} can be expressed in fiber with an attenuation coefficient by the following equation

$$\phi_{NL} = \gamma P_0 \int_0^L \exp(-\alpha z)\, dz = \gamma P_0 \frac{1 - \exp(-\alpha L)}{\alpha} = \frac{L_{eff}}{L_{NL}} \quad \ldots (2.29)$$

where,

$$L_{eff} = \frac{1 - \exp(-\alpha L)}{\alpha}$$

is the effective length, and

$$L_{NL} = \frac{1}{\gamma P_0}$$

is the nonlinear length. Physically, the nonlinear length L_{NL} indicates the distance at which the nonlinear phase shift reaches 1 radian, and it provides a length scale over which the nonlinear effects become relevant for optical fibers. It can be seen from Eq. (2.29) that the fiber nonlinear effect enhances when L_{NL} decreases, or equivalently power P_0 increases. There are three types of important fiber nonlinearities due to the Kerr effect (i) SPM) (ii) XPM, and (iii) FWM and have been considered in the thesis.

2.3.2.1. Self-Phase Modulation (SPM)

SPM is a single channel effect and refers to the self-induced power dependent phase shift experienced by an optical field during its propagation in the optical fiber. The power-dependent refractive index causes a nonlinear phase shift proportional to the signal power and the effective length. This nonlinear phase shift modulates the phase of signal itself and therefore is called self-phase modulation. SPM induced phase shift is defined as

$$\emptyset_{SPM}(z, t) = \gamma\, P_0 \quad \ldots (2.30)$$

This time-dependent phase variation leads to a frequency shift given by:

$$\delta f(t) = -\frac{\partial \emptyset}{\partial t} = -\gamma . L_{eff} \frac{\partial}{\partial t} |E|^2 \quad \ldots (2.31)$$

implying the spectral broadening effect where the leading edge of the pulse produces red shift and the trailing edge of the pulse produces blue shift. In the presence of chromatic dispersion SPM causes temporal pulse broadening (in normal dispersion regime ($\beta_2 > 0$), or pulse compression (in anomalous dispersion regime ($\beta_2 < 0$) even in a single channel system. Therefore, in a multichannel DWDM system as this spectrum broadening is significant and leads to crosstalk between neighboring channels. The combined effects of SPM and chromatic dispersion can be approximated analytically, instead of solving the NLSE. We assume that the transmitter has an extra frequency chirping that causes the same amount of distortion as if there was in transmission through a nonlinear optical fiber (causing the same amount of distortion due to chromatic dispersion). The frequency chirping of the transmitter can be modeled as [2]:

$$\alpha_{SPM} = -\frac{k}{B}\sum_{i=1}^{N}\gamma_i\left(\frac{P^i D^i}{\alpha^i}\left\{l^i - \frac{1}{\alpha^i}(1-e^{-a_i l_i})\right\} + \frac{P^i}{\alpha^i}\sum_{k=i+1}^{N} l^k D^k (1-e^{-a_i l_i})\right) \quad \ldots(2.32)$$

where *k* is the chirp parameter, *B* is the total chromatic dispersion of the link, *N* is the number of fiber segments, *P* the input power of each segment, *D* the chromatic dispersion, α the attenuation and *l* the length of the respective segment. These effects have been appropriately modeled and managed using suitable optical components and subsystems in the simulation studies

2.3.2.2. Cross Phase Modulation (XPM)

While SPM is the effect of a pulse on its own phase, XPM is a nonlinear phase shift due to optical pulses in other channels or from other state of polarization. The XPM effects are quite important for WDM lightwave systems since the phase of each optical channel is affected by both the average power and the bit pattern of all other channels. In WDM systems, the nonlinear phase shift in k−th channel can be written as:

$$\phi_{NL} = \gamma L_{eff} P_o^{(k)} + 2\sum_{h=1, h\neq k}^{N} \gamma L_{eff} P_o^{(h)} \quad \ldots(2.33)$$

where $P_o^{(k)}$ denotes the peak power in kth channel. The first term is the SPM and the second term denotes the contribution of XPM. In deriving Eq. (2.33), $P_o^{(k)}$ was assumed to be constant. In practice, time dependence of $P_o^{(k)}$ makes ϕ_{NL} to vary with time. In fact, the nonlinear optical phase shift changes

with time in exactly the same fashion as the optical pulse due to SPM. It can be seen from Eq. (2.33), that the XPM induced phase shift is twice of SPM when the optical power of all the channels is equal. XPM causes asymmetric spectral broadening of optical pulses, timing jitter and amplitude distortion in time domain and induces power penalty at the receiver end. Therefore, proper modeling and management of such impairments becomes an important issue especially in the case of WDM systems and is discussed in detail later.

2.3.2.3. Four Wave Mixing (FWM)

FWM is due to multiple signals causing variations in refractive index at their difference frequencies. The refractive index then modulates the original carriers to produce sidebands at new frequencies. For WDM systems, with carrier frequencies of f_1, f_2, f_3 a signal at new frequency $f_{123}=f_1 + f_2 - f_3$ can be generated by FWM, which leads to serious performance degradation when the newly generate frequency components fall into other WDM channels.

For a single carrier system, when the pulse has a strong broadening due to chromatic dispersion, the nonlinear mixing of overlapped pulses generates ghost pulses in neighboring time slots due to intra-channel four wave mixing (IFWM), which is one of the dominant penalties for high bit rate fiber optic systems [92, 93]. The difference between FWM and IFWM is that echo pulses appear in time domain instead of in frequency domain. When the WDM channels are equally spaced, FWM causes nonlinear crosstalk. One way to manage the FWM is to use unequal channel spacing so that the mixing products do not coincide with signal frequencies and has been used in this work. Another very effective way is fiber dispersion management method. This method is also effective for SPM and XPM [13] and is discussed in detail in the next section.

2.4. Dispersion Compensation Techniques

In fiber optic communication systems, information is transmitted over an optical fiber by using a coded sequence of optical pulses, whose width is set by the bit rate B of the system. Dispersion-induced broadening of pulses is undesirable as it interferes with the detection process, and it leads to errors if the pulse spreads outside its allocated bit slot ($T_B = 1/B$). Clearly, GVD limits the bit rate B for a fixed transmission distance L. The dispersion problem becomes quite serious when optical amplifiers are used to compensate for fiber losses in case of long-haul systems. The implementation of fiber dispersion

compensation can be done at the transmitter, at the receiver or within the fiber link. In this section, several dispersion compensation techniques have been briefly discussed.

An ideal dispersion compensator must have a quite stringent list of characteristics. Regarding the chromatic dispersion, it has to be well matched to the transport fiber, have a smooth dispersion profile (i.e. no dispersion ripples or group delay ripples), be tunable, reliable and provide acceptable characteristics or the range of operating channels. The ideal compensator must also be compact, provide low insertion loss and be capable of handling high optical power. [19, 94]. Obviously, in a practical design of a dispersion compensator suitable trade-offs must be made between the different requirements. The main technologies are dispersion compensating fiber, Fiber Bragg gratings, etalon filter and optical phase conjugation. Furthermore, Electronic Dispersion Compensation (EDC) and advanced modulation formats have also emerged as an attractive solution due to the high dispersion tolerance [95].

All recently deployed optical communication systems employ dispersion management, in which the dispersion varies periodically. Each period consists of a concatenation of several fiber spans with different local fiber dispersions, and the variation of dispersion in one period is referred to as the dispersion map. The dispersion map is characterized by the average map dispersion D_{map}. For a map consisting of two fiber links, D_{map} given by:

$$D_{map} = \frac{D_1 L_1 + D_2 L_2}{L_1 + L_2} \quad \ldots (2.34)$$

where D_1 and D_2 are dispersion of the first and the second sections of the map and L_1 and L_2 are the corresponding fiber lengths. If $D_{map} \neq 0$ then the residual accumulated dispersion is compensated at the terminals by means of extra links of fiber known as pre and post-compensation fibers. It is typically beneficial to operate the system at non-zero average dispersion as has been implemented in this thesis in Chapter 3. Using dispersion pre-compensation results in spreading out the optical pulses initially, which reduces the effects of four-wave mixing and cross-phase modulation. However, excessive spreading leads to intra-channel four-wave mixing [60]. This tradeoff determines the optimal value of D_{map}, which we will discuss further in this section. The amount of both the pre- and post-compensation dispersion must be carefully chosen to avoid intra-channel cross-phase modulation [47], [61-62].

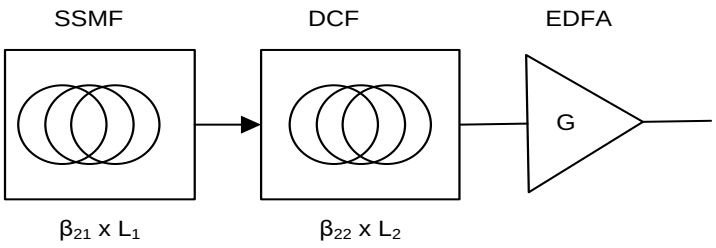

Fig. 2.5: A transmission span with a DCF

Conventional optical systems employ a dispersion management scheme that places a dispersion compensation module (DCM) at the amplifier site to negate the dispersion of the transmission link. A DCM could be a DCF with the reverse sign of GVD parameters as that of the transmission fiber, or an optical filter with inverse transfer function of the fiber channel. A typical transmission fiber (TF) consists of the standard SMF with anomalous dispersion at 1550 nm and the DCF placed at the optical amplifier site within a double stage amplifier and is shown in Fig. 2.5. Here $\beta_{21,}\, L_1, \beta_{22}, L_2$ are the GVD parameter and length for SSMF and DCF, respectively. It can be shown that the total transfer function of SSMF cascaded with a DCF is given by

$$H_{span}(\omega) = exp\left[\frac{j\omega^2}{2}(\beta_{21}L_1 + \beta_{22}L_2)\right]s(t) \qquad \ldots (2.35)$$

It is evident from Eq. (2.35), that the perfect dispersion compensation is realized if

$$\beta_{21}L_1 + \beta_{22}L_2 = 0 \qquad \ldots (2.36)$$

Therefore, the optical pulses at the receiver are not broadened negating the ISI due to dispersion. Since β_{21} is negative (anomalous GVD) for standard fibers, therefore DCF must have normal dispersion β_{22} > 0, such that the accumulated dispersion becomes zero. The DCF with large positive value of GVD have been developed for the sole purpose of dispersion compensation in order to keep L_2 as small as possible. The use of DCFs provides an all-optical technique that is capable of overcoming the detrimental effects of CD in optical fibers at lower average signal power under negligible nonlinear effects and the same has been studied in this thesis [96].

This scheme is quite attractive but suffers from two problems. First, insertion losses of a DCF module typically exceed 5 dB. This insertion loss can be compensated by increasing the amplifier gain but only at the expense of enhanced ASE noise. Second, because of a relatively small mode diameter of DCFs,

the effective mode area is only ~ 20 μm ^{2}. As the optical intensity is large inside a DCF at a given input power, the nonlinear effects are considerably enhanced. These limitations put constraint and challenges on the use of DCF in the long-haul fiber links. Since the early 1990s, there has been great interest in using electronic equalizers as replacements for optical dispersion compensating modules at the receiver. Compared with the optical counterpart, the EDC has the advantages of lower cost and ease of adaption. In a transmitter based dispersion compensation scheme, fiber dispersion can be managed by pre-distorting the input pulses before they are launched into the fiber link. Koch and Alferness presented a technique in 1985 to compensate fiber dispersion using the synthesis of pre-distorted signal [97]. The pre-chirped Gaussian pulse with the chirp parameter $C > 0$ such that $C\beta_2 < 0$ in a single mode optical fiber with typical $\beta_2 = -21$ ps^2/Km enables the dispersion induced chirp to canceled out the intentionally induced chirp in the input pulses. However, with the advances in the performance of high-speed devices since 1990s, the pulse pre-distortion can be done in electrical domain using DSP for the bit rate of 10 Gbps and above to implement the dispersion management in optical transmission systems.

The pre-compensating scheme lacks in exact dispersion compensation even if the transfer function of the fiber link is fully known. The optimum performance of the dispersion compensation is still hard to reach due to linear and nonlinear phase distortions in the channel, interaction with dispersion and change in pulse shape delay response. To avoid prior-knowledge of the fiber link setup requirement and achieve optimum dispersion compensation, the dispersion compensation strategy shifted from the transmitter to the receiver side and these schemes are called dispersion post compensation or receiver based dispersion compensation. There are several receiver-based EDC techniques. A linear equalizer can be used between the receiver and the detector to compensate for the ISI caused by fiber dispersion. A transversal filter (tapped delay line) is often used as a linear equalizer, and the weight coefficients can be adaptively adjust using well known least-mean square (LMS) and zero-forcing (ZF) algorithms [98]. For a conventional fiber-optic communication system with direct detection, due to the power-law detection the linear EDC techniques discussed above can only partially undo the fiber dispersion because linear dispersion-induced distortion in optical domain becomes nonlinear in the electrical domain. Some nonlinear equalization techniques were therefore developed for direct detection [99-100].

For a fiber optic communication system with direct detection, the nonlinearity induced by power law of the photo-detector makes the dispersion compensation scheme more complex and less efficient. With development of powerful DSPs during the 2000s, the difficulty in tracking the received optical

carrier phase in an optical coherent receiver was overcome by using digital carrier phase estimation circuit [101]. Hence, the coherent receiver combined with EDC using DSP has become more practical in past decade. Since the phase information of transmitted signal is preserved in the coherent systems, in the other words the complex valued electrical field is fully detected at the coherent receivers, more options are available in coherent optical systems compare to direct detection. However, due to complexities in the DSP based coherent receiver implementation, we have considered the DCF based pre, post and symmetric compensation schemes to simulate the link performance.

2.5. Optical Link Modeling

In an optical communication link, the information in form of optical pulse propagates through the fiber dispersive media which modifies the pulse both in frequency and time domain in a complex way. Dispersion, a linear phenomenon, is relatively well understood, and various effective dispersion compensation techniques have been devised to cope with dispersion induced performance degradation as discussed in the previous section. Fiber nonlinearities, on the other hand, have not been fully analyzed and understood especially in the presence of dispersion [102]. Their effects on the system performance are usually estimated by numerical simulations or by experiments. Therefore, it is interesting to have analytical tools for the estimation of fiber nonlinearity induced performance degradation which might give us better physical insight in designing and analyzing the optical transmission systems.

Testing and measurement of optical systems has become more complex with the constant evolution of such networks. Although test and measurement requirements were modest for initial systems, however, current systems have to be more intolerant to impairments and demand more rigorous testing. Forecasting the network demand, statistical analysis of cost, planning the layout, engineering the model and deploying the technology is a continuous process and several issues must be considered as shown in Fig. 2.6.

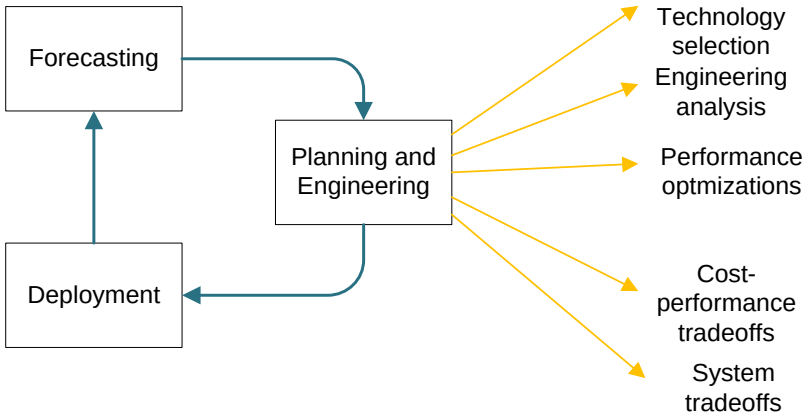

Fig. 2.6: Steps in a network design and issues involved

Various network planning and design tools are required as the design complexity scales with network size and traffic. To meet the demand for spectrally efficient systems operating over longer distances we need more amplifiers, switches etc., faster line rates and several wavelength channels. The first approach is to do a physical modeling of the system under investigation. It requires extensive lab experiments, field trials, tests and measurements and use of system parts which are scaled down version of a system under test. But it has various disadvantages such as it requires sufficient and skilled manpower and high upfront investment in test and measurement equipment and network devices. If the budget is limited only certain number of limited experiments can be performed and full exploration of system cannot be undertaken. Hence, first a mathematical model is developed for the system under test and extensive analytical modeling and simulation of the system is recommended before physical implementation. This has been explained as a flowchart in Fig. 2.7. Accordingly, we have first tried to develop a mathematical model of the single channel optical system and then used analytical modeling and simulation tools to fully exploit and understand the system performance under various conditions.

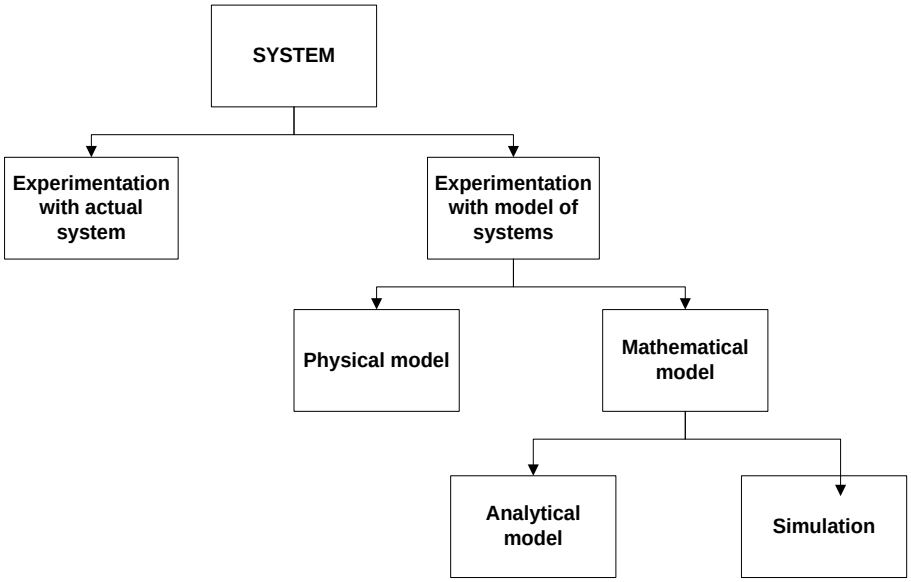

Fig. 2.7: Flowchart depicting modeling strategy and methodologies for studying system behavior

A typical block diagram of an optical link is shown in Fig. 2.8. The input to the optical source is represented by coded output of a data signal generator. The source output is coupled to a transmitting optical components block. These components may be connectors, couplers, or filters. The optical output power is usually directly modulated by varying the drive current, but external optical modulation is also possible. To gain understanding, the system components needed for an optical link design are characterized by their mathematical models, which are mostly differential equations. The realization of an accurate and practical model is a major task, which takes into consideration simultaneously the various linear and nonlinear impairments caused at the different block levels of the optical link along with the interplay among the different phenomena such as source chirping, CD, ASE, crosstalk, etc. Obviously an accurate system model requires complex equations and the algorithms to solve the mathematical linear and non-linear equations governing various components [103].

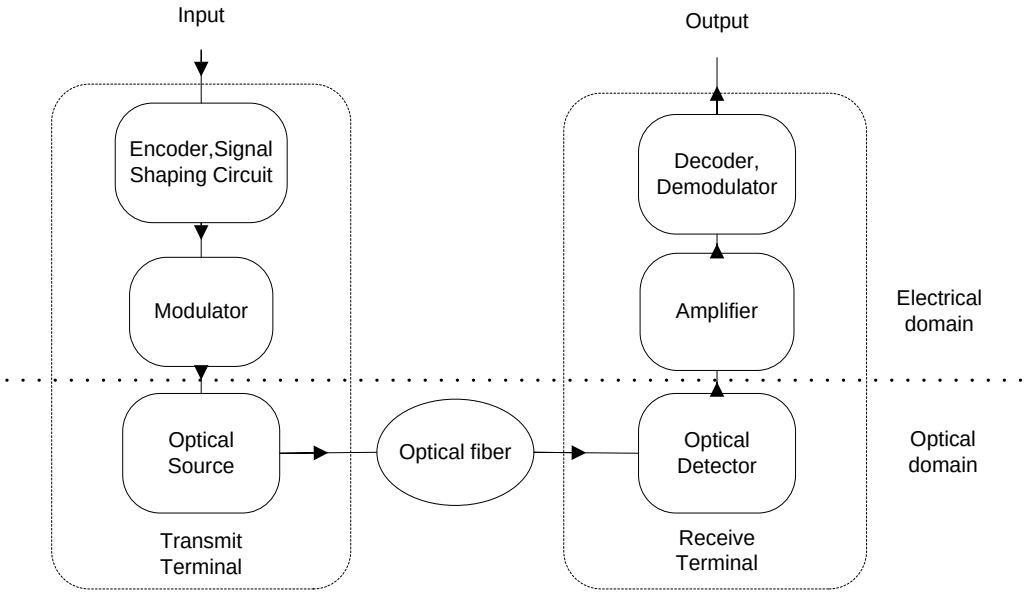

Fig. 2.8: Typical optical link

Evidently nonlinear propagation effects in co-existence with dispersion, polarization, and attenuation generate complex degradations in the pulse spectrum. It is interesting to note that FWM efficiency depends strongly on the CD of the fiber; SPM can support very stable pulse propagation in the presence of the right amount of CD; the impact of PMD can be reduced by nonlinear fiber interactions; the polarization dependence of SRS may introduce PDG on the basis of theoretical and experimental investigations [104]. Thus, to visualize such influences fiber modeling needs to include appropriate nonlinear and linear phenomena to predict detrimental and beneficial interactions between these characteristics. Non-linear effects like SPM, XPM and FWM in optical fiber combined with dispersion induced signal broadening and additive noise, in general, make it impossible to arrive at a simple analytical description of the system transfer function linking the received optical field to the transmitted field. Moreover, modeling of non-linearity is very complicated due to the complex mathematical representation of the various contributions to non-linearity.

To consider the detrimental effects outlined in the previous section, we adopted a semi-analytical model in which signal propagation along the link is evaluated using simulation. The following sub-sections, describe the design and implementation of an optical transmission link mathematically. The various system components used in such an optical link are mathematically modeled. These include optical transmitters consisting of electrical sources, optical lasers, optical carrier generators and modulators, SMF and DCF fibers, optical amplification devices mainly the EDFAs, multiplexing and de-

multiplexing optical devices for DWDM and the optical receivers and demodulators. The first task is to generate the pseudorandom sequences and is modeled next.

2.5.1. Generation of Pseudorandom Sequences

In a digital communication system, the information source can be modeled as a random binary sequence, which is a statistically independent sequence of zeros and ones; each occurring with equal probability. Pseudo-random binary sequences (PRBS) can be generated using linear feedback shift registers (LFSR) [105], as shown in Fig. 2.9. The coefficients g_i represents the tap weights and take the values 1 for taps that are connected (fed back) and 0 otherwise.

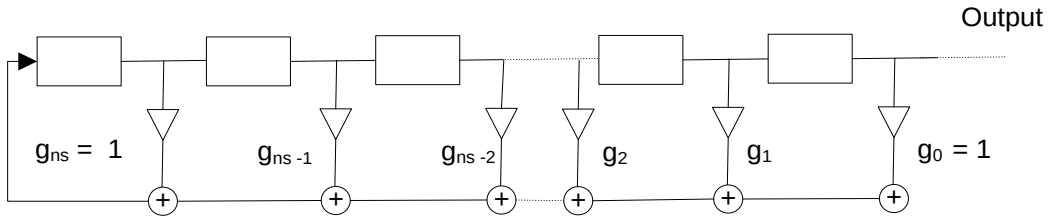

Fig 2.9: Linear Feedback Shift Register, Fibonacci implementation with n_s Shift registers

Any LFSR can be represented as a polynomial of variable X, referred to as the generator polynomial:

$$G(X) = g_{n_s}X^{n_s} + g_{n_{s-1}}X^{n_{s-1}} + g_{n_{s-2}}X^{n_{s-2}} + \cdots + g_2X^2 + g_1X + g_0 \qquad \ldots (2.37)$$

Since there are n_s registers, the maximum period of the output sequence is $N_{seq} = 2^{ns}-1$. Many communication systems use modulation formats, where more than one bit per symbol is transmitted. In this case, the information source outputs a random sequence, where r bits per symbol are transmitted and the elements $\{0, 1, \ldots, 2r-1\}$ occur with equal probability. Pseudo-random maximum length r-ary sequences can be generated by extending the binary case. Fig. 2.10 (a) shows the block diagram of the information source. Each output $a_i(t)$ is a signal with period $(2^r)^{ns}$. Ts, which represents the bit sequence $\tilde{\boldsymbol{a}}_i$ and is given by

$$a_i(t) = \sum_{k=0}^{(2^r)^{n_s}} \tilde{a}_i^k \,.\, \delta(t - k.T_s) \qquad \ldots (2.38)$$

where $\delta(t)$ is the dirac delta function, $\tilde{a}_i^k \in \{0, 1\}$ and T_s is the symbol duration.

2.5.2. Electrical Signal Generation

The information source generates pseudo-random sequences, which are represented as electrical signals. Due to the bandwidth limitation of the components, these signals have non-zero rise and fall time. In order to correctly generate the electrical signal, each bit is modeled as a non-return-to-zero (NRZ) raised cosine pulse given by [106]:

$$h_{RC}(t) = \begin{Bmatrix} 1 \\ \frac{1}{2}\left[1 - sin\left(\frac{\pi}{2}\frac{2|t|-T_s}{T_s\,\alpha_{RC}}\right)\right] \\ 0 \end{Bmatrix} \quad \begin{Bmatrix} |t| < \frac{T_s}{2}(1-\alpha_{RC}) \\ \frac{T_s}{2}(1-\alpha_{RC}) \le |t| < \frac{T_s}{2}(1+\alpha_{RC}) \\ |t| > \frac{T_s}{2}(1+\alpha_{RC}) \end{Bmatrix} \qquad \ldots (2.39)$$

$$H_{RC}(f) = \frac{\sin(\pi f T_s)}{\pi f T_s} \cdot \frac{\cos(\alpha_{RC}\pi f T_s)}{1-(2\alpha_{RC} f T_s)^2} \qquad \ldots (2.40)$$

where $0 \le \alpha_{RC} \le 1$ is the roll-off factor and T_s is the symbol duration.

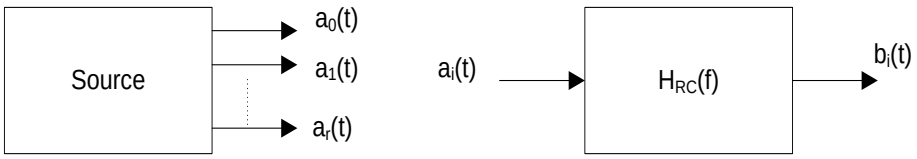

Fig. 2.10: Block diagram of the information source (left) and the electrical signal generation (right).

The pulse has smooth rising and falling edges with well-defined rise and fall times of 0.59 Ts α_{RC}. Note that the raised cosine pulse is defined in time domain, which differs from [107] where the spectrum is limited to a certain bandwidth. Here the pulse is limited in time to avoid ISI. Fig. 2.10 (b) depicts the block diagram of the electrical signal generation.

2.5.3. Laser Modeling

Optical sources generate the optical carrier through two fundamental processes: spontaneous or stimulated emission. An atom can move from the ground state to the excited state (meta-stable state) by absorbing the energy from an externally pumped source to achieve a population inversion. An atom in the excited state can eventually return to the ground state either spontaneously or by stimulation and

emit a photon. These processes are called spontaneous emission and stimulated emission, respectively. Photons generated by spontaneous emission assume frequencies within a certain line width and have random phase and polarization state and cause ASE noise. On the other hand, stimulated emission occurs when an incident photon causes an atom in the excited state to move from the excited state to the ground state. The emitted photon is a copy of the incident photon and the emitted light in this process is coherent.

Despite the mature technology of fiber lasers and amplifiers, most of the optical sources employ semiconductor devices such as light-emitting diodes (LED) or semiconductor lasers to generate the optical carrier. They offer several advantages: easy integration due to their compact size, efficient conversion of electrical into optical power, good reliability, dimensions compatible with the optical fiber core and possibility of direct modulation at relatively high frequencies [1,108]. The main difference between LED's and lasers is the dominant process of light emission. While LED's emit incoherent light through spontaneous emission, lasers generate coherent light through stimulated emission. Therefore, they have different applications in optical communication systems. Due to its relatively wide spectral width (30-60 nm), low cost, low output power and low modulation band-width, LED's are usually used in short reach optical links at data rates lower than 5 Gbps and distances up to few kilometers. Lasers are commonly used in optical communication systems operating at data rates greater than 5 Gbps, such as metro and backbone net-works. At the transmitter, lasers can be found as optical sources and in optical amplifiers as pump devices used to achieve population inversion in a doped fiber.

The laser model expresses the optical power at the output according to the electrical power input or according to the current of polarization [109, 110]. The behavior of a semiconductor laser diode is modeled with a set of three differential equations which describe the mechanism by which electrical current causes stimulated photon emission. Several models have been proposed and the Tucker Model has been used in this study. There are many forms of these equations, but here we use a modified form of Tucker's equations [1] employed by Bjerkan et al. [111] whose coefficients are defined in the Table 2.1.

$$\frac{dN(t)}{dt} = \frac{I(t)}{q.V_0} - g_0 \frac{[N(t) - N_0].S(t)}{1 + \epsilon.S(t)} - \frac{N(t)}{\tau_n} \qquad \dots (2.41)$$

$$\frac{dS(t)}{dt} = \Gamma . g_0 \frac{\left[[N(t) - N_0].S(t\right]}{1 + \epsilon . S(t)} - \frac{S(t)}{\tau_p} + \frac{\Gamma . \beta}{\tau_n} . N(t) \quad \ldots (2.42)$$

$$\frac{d\phi(t)}{dt} = \frac{1}{2}\alpha \left[\Gamma . g_0 [N(t) - N_0] - \frac{1}{\tau_p}\right] \quad \ldots (2.43)$$

Table 2.1: Coefficients of Rate Equations

Symbol	**Value**	**Dimension**	**Description**
I(t)	-	A	Laser current
S(t)	-	m^3	Photon density
Γ	0.44	-	Optical Confinement factor
g_0	3.0 x 10^6	cm^{-3}/s	Gain slope
N(t)	-	m^{-3}	Carrier Density
N_0	1.2 x 10^{12}	cm^{-3}	Carrier Density at transparency
ϵ	3.4 x 10^{17}	cm^{-3}	Gain saturation parameter
τ_p	1 x 10^{12}	s	Photon lifetime
β	4 x 10^4	-	Spontaneous emission factor
τ_n	3 x 10^9	-	Carrier lifetime
V_0	9 x 10^{21}	cm^3	Volume of active region
ϕ	-	-	Phase of the electric field from the laser
α	-	-	Line width enhancement factor
P(t)	-	W	Optical power from laser
q		C	Electronic charge
η	0.1	-	Total quantum efficiency
h	6.624 x 10^{34}	J-s	Plank's Constants
Δv		s^{-1}	Instantaneous optical frequency deviation
D		s/m^2	Fiber dispersion coefficient
L		**m**	**Fiber length**

These equations describe carrier density; photon density and optical phase, respectively. This is a large-signal model that describes laser diode behavior in both the spontaneous emission and stimulated emission regions applicable to linear simulated region. However, nonlinear saturation region due to junction heating is not included in this model. Additionally, the optical power $p(t)$ generated by the diode is:

$$p(t) = \frac{S(t)V_0\eta_0 h\nu}{2\Gamma\tau_p} \quad \ldots (2.44)$$

This model's purpose is to identify the various regions of operation of the laser diode. Building the large signal model is essential in determining operating points within the 'semi' linear lasing region.

The problem with finding a closed form solution to the rate equations lies in the fact that the equations are cross-coupled by the product term containing both the photon and electron density. In order to obtain values to simulate the small signal response, the non-linear rate equations were linearized by taking the partial derivative of each time-dependent term with respect to photon and electron density. It is this new model that allows the results of the large signal response to be used in simulating the small signal response and is used in analysis.

2.5.4. Optical Fiber Modeling

The transfer function of an optical fiber can be modeled in terms of its parameters. The developed model allows us to visualize the effect of change of the fiber parameters over the transmission characteristics of different types of fiber like SMF and DCF. The non-linear feature of the fiber is also modeled to predict and simulate the influence of various types of non-linearity as a function of fiber characteristics. [4, 112].

2.5.4.1 Linear model of single mode fiber

When the fiber loss and nonlinearity are neglected, a single-mode optical fiber can be considered as an all-pass filter with nonlinear phase response, and the corresponding transfer function can be written as:

$$H(\omega) = exp\left\{-jz\left[\beta_0 + (\Delta\omega)\beta_1 + \frac{1}{2}(\Delta\omega)^2\beta_2 + \frac{1}{6}(\Delta\omega)^3\beta_3 + \cdots\right]\right\} \quad \ldots(2.45)$$

It should be noted that Eq. (2.45) is derived under the assumption that $\Delta\omega << \omega_0$, so $\beta(\omega)$ can be expanded about ω_0 by using a Taylor series. In terms of communication theory, the low-pass filter whose transfer function is given by (2.45) would cause waveform distortion due to the nonlinear phase response and this is commonly called dispersion in the fiber optic communication. The model of the transfer function of a SMF assimilates optical fiber to a Low pass filter [113] given by:

$$H(f) = e^{-j\pi D\lambda L f} \quad \ldots(2.46)$$

where D represents dispersion, λ represents the operational wavelength, f is the frequency and L represents the length of fiber.

2.5.4.2. Nonlinear model of single mode fiber

We can approximate the nonlinear model by:

$$H(f) = e^{-j\emptyset_{NL}} \quad \ldots (2.47)$$

where $\emptyset_{NL}$ represents the phase contribution due to several non-linear effects. This parameter acts as a multiplier and it depends on the power injected from the laser and it is defined by the following equation:

$$\emptyset_{NL} = \gamma P_{in} L_{eff} \quad \ldots (2.48)$$

The nonlinear effect is negligible for an injected power lower than the threshold power, but otherwise has to be considered. The propagating pulse consists of different frequency components and propagation modes and its power profile $p(t)$ can be represented as:

$$p(t) = \sum_{i,m} p(t, \lambda_i, m) \quad \ldots (2.49)$$

Here *i* is the index to different frequency components and *m* is the index to different propagation modes. GVD effect manifests as different frequency components of a pulse disperse during propagation due to the frequency dependence of the group velocity which finally results in broadening of the pulse. The root mean square (RMS) pulse width after propagating through the fiber is defined as:

$$\Delta\omega \stackrel{\text{def}}{=} \left[\sum_{i.m} (\tau_{i.m} - \tau)^2 \, p(\lambda_{i,m})\right]^2 \quad \ldots (2.50)$$

where $p(\lambda_{i,m})$ is the percentage power of the pulse $p(t, \lambda_i, m)$ with respect to the total power and τ is the average delay over both i and m. This on solving further gives the expression for $\Delta\omega_{rms}$ for an arbitrary pulse as:

$$\Delta\omega_{rms} = \left[\sum_{m} \left[D^2_{intra,m} p(m) + D^2_{modal}\right]\right]^{1/2} \quad \ldots (2.51)$$

which clearly points out that the total dispersion encountered is sum of both intra-channel dispersion and inter-modal dispersion. In this model, the theoretical values of dispersion in the nonlinear Schrödinger equation are used to account for both β_2 and β_3 for a single mode fiber and have ignored the inter-modal part.

The fiber is modeled as an optical bandpass filter with a flat amplitude response and a linear group delay within the bandwidth of the data sequence that modulates the light wave by computing the dispersion coefficient as a function of wavelength using the following equation:

$$D_{SMF}(\lambda) = \frac{S_0}{4}\lambda\left(1 - \frac{\lambda^4}{\lambda_0}\right) \quad \ldots (2.52)$$

with λ_0 and S_0 being the zero-dispersion wavelength and the dispersion slope at λ_0. The corresponding approximation for DCF is:

$$D_{DCF}(\lambda) = S_c(\lambda - \lambda_c) + D_C \quad \ldots (2.53)$$

where S_c and D_C being the dispersion slope and the dispersion at the wavelength λ_c = 1550 nm.

2.5.5. Mach-Zehnder modulator (MZM) Modeling

MZM is used to modulate the incoming optical signal. Mathematically, the operation of a MZM can be described as follows. For the X-cut MZM, the electro-optic effect is maximum along the z-axis of the crystal. Therefore, the electric field is assumed to be polarized along the z-axis and only the scalar electric fields $E_{in}(t)$ and $E_{out}(t)$are analyzed. When the light propagates through the arms of the MZM, the phase shift in branches 1 and 2 can be approximated linearly according to the Pockels effect [114, 115] with $v_1(t)$ and $v_2(t)$ being the voltages in respective arms as:

$$\varphi_1 = \varphi_0 - \pi\frac{v_1(t)}{2V_\pi} \quad \ldots (2.54)$$

$$\varphi_2 = \varphi_0 - \pi\frac{v_2(t)}{2V_\pi} \quad \ldots (2.55)$$

The output electric field $E_{out}(t)$ can be expressed as

$$E_{out}(t) = \frac{\sqrt{2}}{2}e^{j\omega_0 t}\left(\sqrt{P_1}\,e^{-j\frac{\pi}{2V_\pi}v_1(t)} + \sqrt{P_2}\,e^{-j\frac{\pi}{2V_\pi}v_2(t)}\right) \quad \ldots (2.56)$$

where ω_0 is frequency of the optical carrier, $\sqrt{P}_1$ and $\sqrt{P}_2$ are the amplitudes of the optical field in each arm of the Mach-Zehnder interferometer. This can be further simplified as:

$$E_{out}(t)\frac{\sqrt{2}}{2}e^{j\omega_0 t}\left(\sqrt{P_1}\,e^{j\frac{\pi}{4V_\pi}(v_1(t)-v_2(t))}\sqrt{P_2}\,e^{-j\frac{\pi}{4V_\pi}(v_1(t)-v_2(t))}\right)e^{j\frac{\pi}{4V_\pi}(v_1(t)+v_2(t))} \quad \ldots (2.57)$$

The linear frequency chirp parameter is defined as $\alpha_c(t) = \frac{v_1(t)+v_2(t)}{v_1(t)-v_2(t)}$ and can be set to zero. This requires that both the input ports are driven in a push-pull configuration, i.e. $v_2(t) = -v_1(t)$. The extinction ratio (ξ_{ER}) of the modulator is defined as the ratio between the maximum and minimum output powers and becomes infinite for $P_1 = P_2$. The $E_{out}(t)$ can be expressed for such cases as:

$$E_{out}(t) = \sqrt{P}.\cos\left(\frac{\pi}{2V_\pi}v(t)\right).e^{j\omega_0 t} \quad \ldots (2.58)$$

Note that in this derivation the intrinsic loss of the MZM was neglected. In case of unequal powers, the extinction ratio becomes finite and the electric field at the output of the modulator is given by

$$E_{out}(t) = \sqrt{\frac{P}{2(\xi^2+1)}}.\left(\xi\,e^{j\frac{\pi}{2V_\pi}v(t)} + e^{-j\frac{\pi}{2V_\pi}v(t)}\right).e^{j\omega_0 t} \quad \ldots (2.59)$$

where,

$$\xi = \frac{\sqrt{\xi_{ER}}+1}{\sqrt{\xi_{ER}}-1},\ P_1 = \xi^2.P_2 \text{ and } P = P_1 + P_2 = P_2\,(\xi^2+1)$$

These expressions have been used in the modeling and simulation of MZM operation for the various modulation formats investigated in this thesis.

2.5.6. EDFA Noise Model

Optical amplifiers make use of semiconductor lasers without feedback or active fibers to amplify the incoming signal. Most of the optical amplifiers are developed exploiting the parametric amplification, stimulated Raman scattering, semiconductor optical amplification (SOA) and laser activity in active doped-fibers. Out of these parametric and Raman amplifiers require high pump powers while semiconductor optical amplifiers suffer from polarization sensitivity and inter-channel crosstalk, which severely limit the system performance. However, doped-fiber amplifiers using rare-earth elements (erbium, praseodymium, thulium, neodymium, etc.) offer attractive features such as practical absence of nonlinearities, low coupling losses to the transmission line, very low dependence of gain on light polarization and wide transparency to signal format and bit rate [1, 116] and thus are widely used. The

basic operation of a doped-fiber amplifier consists of amplifying the incident light through stimulated emission. The fundamental parameters defining the performance of an optical fiber amplifier are its gain and noise as a function of the signal wavelength in the amplification band. The spectral gain and the spectral noise figure of the EDFA can be completely described through the propagation and rate equations modeling the interaction of the optical field with erbium ions [117]. A numerical solution of these equations can determine the spectral gain and noise figure for specified amplifier parameters. This approach is very efficient for the design of optical amplifiers, but requires accurate characteristic data for all amplifier components.

The black-box model is another approach which is based upon input-output experimental data obtained in a simple test measurement of a certain amplifier unit and does not require access to internal details of the amplifier construction [118]. The physical background is the same as for most rate-equation based models [109]. The black-box model is especially suitable for WDM systems because the characteristic data of the optical amplifier is not always available. In the case of a single-channel simulation, a very simple model can be used, where the amplifier is characterized by its gain G and noise figure F_n. The amplified spontaneous emission noise (Φ_{ASE}) is modeled as complex additive white Gaussian noise (AWGN), whose single sided power spectral density for each polarization is given by [76] :

$$\Phi_{ASE} = \frac{F_n . h . c . G}{2\lambda_o} \qquad \ldots (2.60)$$

where h is Planck's constant and λ_0 the operating wavelength. Since the noise is a stochastic process and the optical bandpass filter is linear and time-invariant, the noise power can be calculated by integrating in the frequency domain the response of a linear time-invariant system to a random input signal. Therefore, the noise power P_{ASE} is given by

$$P_{ASE} = \int_{-\infty}^{\infty} |H_0(f)|^2 . \Phi_{ASE} . df \qquad \ldots (2.61)$$

where $|H_0(f)|$ is the low-pass equivalent transfer function of the optical filter. This can be evaluated to find the contribution of ASE power (P_{ASE}) of an amplifier with gain G given as :

$$P_{ASE} = 2h\nu B_0 n_{sp} \, (G - 1) \qquad \ldots (2.62)$$

where B_0 is the optical bandwidth, ν is the signal frequency and n_{sp} is the spontaneous emission factor. The spontaneous emission factor n_{sp} is determined by the inversion of the amplifiers Er ions. The contribution of each amplifier's ASE to the accumulated ASE is characterized by the amplifier's noise figure (F_n), which at high gain can be approximated by $F_n \approx 2n_{sp}$. Following the analysis presented by [56] the ASE power (($P_{ase}(k, \lambda_i)$) through the inline amplifiers can be expressed as follows:

$$P_{ase}(k, \lambda_i) = P_{ase}(k-1, \lambda_i) L_f(k-1, \lambda_i) G_{in}(k, \lambda_i) L_{tap} + 2n_{sp} \lceil G_{in}(k, \lambda_i) - 1 \rceil h\nu_i B_0 L_{tap} \quad \ldots (2.63)$$

where $P_{ase}(k, \lambda_i)$ corresponds to the ASE noise power at the kth amplifier and λ_i wavelength and L_x (k, λ_i) and G_x (k, λ_i) are the losses and gain of the various elements through the amplifier chain. The ASE noise variance at the end of the chain is described by:

$$\sigma_{ASE}^2 = 4R_\lambda^2 b_i P_{avg}(N, \lambda_i)\, B_e / B_0 \quad \ldots (2.64)$$

where b_i is zero or two if $i = 0$ or $i = 1$, R_λ is the responsivity of the receiver, P_{avg} is the average signal power and B_e the electrical bandwidth of the receiver. The ASE noise variance will be used to calculate the Q factor degradation due to ASE in the simulation study. Another constraint on the maximum number of optical amplifiers can be set, that is proportional to the average optical power P_{avg} launched at the transmitter and inversely proportional to an acceptable optical $SNR_{min.}$.Thus the maximum number of amplifier stage is limited by P_{ASE} and average optical power P_{avg} and can be expressed using (2.62) to give:

$$N \leq \left\lfloor \frac{P_{avg}}{2h\nu B_0 (G-1) n_{sp} SNR_{min}} \right\rfloor \quad \ldots (2.65)$$

These amplifier parameters have been used in the analysis of simulation setups in this study.

2.5.7. Signal Crosstalk

Crosstalk is introduced in WDM systems due to leakage of optical signals during multiplexing/ de-multiplexing, switching, and other optical signal conditioning and thus imposing some power penalties at the receiver. Therefore, the level of crosstalk introduced through an optical path is closely linked with the node architecture and traffic management strategies. Two types of crosstalk arise in WDM

systems: intra-channel crosstalk and inter-channel crosstalk. The former occurs when the interference is on the same wavelength or sufficiently close with the desired signal so that the difference in wavelengths is within the electrical bandwidth of the receiver. The latter is when the crosstalk (XT) interference is on a sufficiently different wavelength than the desired signal's wavelength, that the difference is larger than the receiver's electrical bandwidth.

In-band crosstalk can be generated upon filtering through multipath interference. Non-perfect filtering implies leaking of the channel energy into other ports than the dedicated. Upon multiplexing a part of the leaking energy propagates back with the useful signal. Intra-channel crosstalk is related to the non-perfect extinction of the neighboring channels at the last de-multiplexer. Both are measured in terms of the ratio of the perturbation to the useful signal. Intra-channel crosstalk is accumulated at each node. They are specified as maximum acceptable crosstalk level at the receiver. We consider only in-band crosstalk as its effect is much more severe compared to out of band crosstalk. We study crosstalk in conjunction with ASE due to their close correlation and dependence on the signal power. The amount of energy that leaks to neighboring wavelengths is described by the signal-to-crosstalk ratio (X_{sw}) and is expressed as [56]:

$$P_{XT}(k,\lambda_i) = \sum_{j=1}^{J_k} X_{sw} p_{in}(j,k,\lambda_i)\, L_{sw}(k) L_{mx}(k) G_{out}(k,\lambda_i) L_{tap} \quad \ldots (2.66)$$

where $p_{in}(j,k,\lambda)$ is the power of the jth co-propagating signal at the switch shared by the desired signal, and J_k is the total number of crosstalk sources at the kth node. Finally, the noise variance of crosstalk is described by [56, 63]:

$$\sigma_{XT}^2 = 2\xi_{pol} R_\lambda^2 b(i) P_{ave} P_{XT} \quad \ldots (2.67)$$

where ξ_{pol} is the polarization mismatch factor between the signal and the crosstalk light waves. The above analysis forms the background of our simulation study.

2.5.8. Filter Concatenation

In an optical network, the light wave signal passes through a number of concatenated components, such as WDM multiplexers (MUXs), de-multiplexers (DEMUXs) and noise limiting optical bandpass filters. WDM MUXs and DEMUXs are the similar physical device, the only difference being what is labeled input and output. Multiplexers take multiple light sources and combine them into a composite optical

signal. De-multiplexers split this composite signal into its respective frequency components or channels. Both devices rely on a frequency selective component which can either be a diffraction grating and a lens or a collection of narrow filters and directional couplers [3]. This makes the system susceptible to filter passband misalignments arising from device imperfections, temperature variations and aging. The emission spectrum of the laser source may also be misaligned with the effective center frequency of the optical filters owing to manufacturing tolerances, aging, or operating conditions. Performance degradation in WDM systems may arise owing to the combined effects of optical filter misalignments, laser misalignments, and laser chirp. The concatenation of such optical components can be modeled as a combination of optical filter and the corresponding system component.

In optically pre-amplified receivers, the best system performance is achieved with an optical matched filter and no post-detection electrical filtering [89, 119]. In this case, signal distortion introduced by filtering and noise are balanced. However, due to practical reasons, most optical systems employ fiber Bragg grating (FBG), Fabry-Perot or arrayed waveguide grating (AWG) filters. The low-pass equivalent transfer function of these filters can be modeled as a Gaussian function of order n_o given by [120].

$$H_o(f) = exp\left[-\ln(\sqrt{2})\left(\frac{2f}{B_0}\right)^{2n_0}\right] \quad \ldots (2.68)$$

where B_o is the 3 dB bandwidth.

The filters have transmission functions that could be fitted using a Butterworth-like filter transfer function. In particular, many filters have characteristics that are well approximated by third-order Butterworth filter transfer functions. The equation describing a complex third-order Butterworth filter is given as [59]:

$$H(f) = \frac{1}{\prod_{k-1}^{3}\left[\frac{jf}{f_{3dB}} - exp\left(\frac{j\pi}{2}\left(1 + \frac{2k-1}{3}\right)\right)\right]} \quad \ldots (2.69)$$

where, f is the frequency assumed to be centered around 0, f_{3dB} is the half bandwidth of the filter at the 3 dB power transmission level.

In optical communication systems operating at data rates greater than 10 Gbps, electrical filtering occurs mainly due to the bandwidth limitation of the electrical components [120]. Therefore, Bessel

filters with high orders can be used in order to properly model the low-pass characteristics of the electrical components. The transfer function of a fifth-order Bessel filter is given by [121]

$$H_e(f) = \frac{945}{jF^5 + 15F^4 - 105jF^3 - 420F^2 + 945jF + 945} \quad \ldots (2.70)$$

where $F = \frac{K.f}{B_e}$, B_e is the 3 dB bandwidth and K = 2.427410702 is the 3 dB normalization constant.

In the present study for a lower data rate third order Butterworth filter performs satisfactorily, however for a data rate of 40 Gbps and beyond high order Bessel filters has been found suitable. The effective spectral transfer function of the cascaded filter set is the multiplication of each of the individual filters, which can, therefore, be much narrower in spectral width than a single filter. Spectral narrowing of the effective transfer function can be further exacerbated by any misalignments in center frequency of the individual filters traversed by the signal. If the transmission laser is offset from the center of the pass band of the effective filter transfer function, then part of the signal spectrum may be attenuated out of proportion to the rest of the spectrum as the signal gets too close to one of the sidewalls of the filter transfer function. This, in turn, can lead to a time-domain distortion and a distortion-induced eye-closure penalty in addition to simple excess signal loss and thus must be considered.

2.5.9. Photodetector

Classical receiver models for pre-amplified optical receivers—that account in the simplest form possible for the detected ASE noise (but do not consider signal filtering or ISI effects)—assume an integrator-type band pass filter impulse response as well as a discrete-type integrator impulse response of the low pass filter [122]. The noise correlation effects have been accounted for in receiver models that are, in principle, based on the classical model for heterodyne receivers by Schwartz et. Al. [123]. This has been used by several authors in order to give a model formulation for band pass filters with Lorentzian transfer function. In [124], an extension of the last receiver model discussed was presented to a realistic WDM transmission system environment including effects of practical optical amplifiers, realistic optical filters including a periodic DEMUX characteristic, and shot and thermal noise. These models do not account for signal amplitude variations over the bit-period (ISI) caused by fiber dispersion and nonlinear effects and only allows a simplistic description of the electrical filtering in the

receiver—assuming a discrete integrator time response of the filter. From a mathematical point of view, the complete fiber propagation of the signal can be considered a separate problem from the receiver modeling. The resulting deterministic signal variation with time and the ASE statistics are simply inputs to the receiver model.

In this thesis, the photodetector consists of an ideal p-i-n photodiode with responsivity (R). The main task of a photodetector is to convert the optical signal into an electrical signal under appropriate operating conditions. The main requirements for a photodetector are: high sensitivity, high speed, large bandwidth, low noise, low cost and high reliability [125]. The output in time and frequency domains by a pin receiver is given by

$$I_{out}(t) = |E_{in}(t)|^2$$

$$\tilde{I}_{out}(f) = \tilde{E}_{in}(f) * \tilde{E}^*_{in}(-f) \quad \ldots (2.71)$$

where the operator $*$ denotes the convolution operation. When a modulated signal of optical power P*(t)* falls on the detector, the primary photocurrent generated is given by:

$$I_{sig} = \frac{\eta q P}{hf} \quad \ldots (2.72)$$

2.5.10. Cross Phase Modulation Modeling

XPM is a critical limiting factor in high speed DWDM systems and depends not only on the power of that particular channel, but also on the total power and the bit pattern of the other channels and results in pulse broadening. The degree of XPM impairment is influenced by various parameters, such as nonlinear fiber coefficient γ, walk-off between the two adjacent channels, individual channel power and the modulation format used [126]. To evaluate the optical system performance under the influence of XPM, an analytical model is proposed which is faster, simple and as accurate as possible. The root of this model lies in the derivation of the analytical time jitter formula. Previous analytical studies involved analyzing only the intensity modulation generated at the end of the fiber only for the NRZ modulation format. This thesis provides a simple and efficient way to model the cross phase modulation involving both intensity distortion and time jitter in a DWDM optical system employing various efficient modulation schemes.

In reference [127], a generalized method is developed to calculate the XPM induced field distortions in multi-span WDM systems. This method does not involve the split-step Fourier transform. The XPM-induced optical phase modulation and the resulted signal power fluctuations are calculated and the accuracy of the model is checked with numerical simulation. They considered only the optical phase modulation and the resulting intensity crosstalk but did not calculate the time jitter at the output of the fiber. A five span system with each span length accounting to 100 Km is considered operating at of 3 dBm power level at 10 Gbps with NRZ modulation. However, the work did not put attention to the delay analysis between the pump and probe channel's bit patterns. Though the delays impose only minor problems, yet the effect of bit shifts must be considered to improve the accuracy of the results. The derived model considers the delays between the data patterns which efficiently simulate the effects of bit shifts in the real system as well as both intensity crosstalk and timing jitter distortions. In the model the SSFM has been used to implement the effect of SPM and dispersion.

Spectral characteristics of XPM in multi-span IM-DD optical systems have been investigated theoretically in [128] by developing an analytical model. In their study, intensity modulated NRZ system was considered to validate the model through experiment even with relatively higher launch powers of the order of 11.5 dBm. It considers only the IM-DD and PM-IM systems mechanisms due to phase modulation distortion and intensity modulation correlation, however the effect of timing jitter has not been taken into account. The present model extends the study to RZ formats along with the influence of the delay between the probe and the pump channel. Thus our model can be used to calculate both the both intensity and timing jitter effects of XPM.

Propagation equation of signals in a two channel optical fiber system is governed by the following Coupled Nonlinear Schrodinger Equations [129]:

$$\frac{\partial A_1}{\partial z} + \frac{i}{2}\beta_{21}\frac{\partial^2 A_1}{\partial t^2} + \frac{\alpha}{2}A_1 = i\gamma(|A_1|^2 + 2|A_2|^2)A_1 \qquad \ldots(2.73)$$

$$\frac{\partial A_2}{\partial z} + d_{walk-off}\frac{\partial A_2}{\partial t} + \frac{i}{2}\beta_{22}\frac{\partial^2 A_2}{\partial t^2} + \frac{\alpha}{2}A_2 = i\gamma(|A_2|^2 + 2|A_1|^2)A_2 \qquad \ldots(2.74)$$

Where A_1 and A_2 are complex amplitudes of electric field envelopes, β_{21} and β_{22} are GVD dispersion parameters at channel 1 and 2, respectively. The walk–off parameter ($d_{walk-off}$) which accounts for group velocity mismatch between the channels is approximated in terms of channel spacing $\Delta\upsilon$ and chromatic dispersion D as follows:

$$d_{walk-off} \approx \frac{D\lambda^2 \Delta v}{c} \quad \ldots (2.75)$$

In this model higher order dispersion is neglected and only XPM and SPM are considered. Walk off length introduces the intensity changes due to the change in the relative alignments of the interacting channels. This relative change accounts for the small time difference between the pulses, which characterizes this intensity changes. When the channel spacing is very large, the walk off length becomes shorter than the effective length of the fiber and is insignificant. In case of very small wavelength separation, walk off length becomes large enough in comparison to the effective length of the fiber. In this case, the XPM distortions are governed by the fiber losses and the walk off length becomes independent of wavelength spacing.

The objective is to model the nonlinear impact of intensity fluctuations of channel 1 on the phase of the signal in channel 2. A multi-segmented, optically amplified system is assumed to arrive at the generalized forms of fiber non linearity-induced distortions. Signal launch power is kept low enough to ensure that the system is not susceptible to SPM induced nonlinearities. Deployment of appropriate DCFs in the fiber link curtails the degradation due to GVD in SMF. The CW probe channel at the input of the fiber is analyzed under the influence of another pumped channel. The phase variation $(d\theta_i)$ in the probe channeled due to Kerr interaction with kth pump channel along the infinitesimal distance from z to $z + dz$ is modeled using [130],

$$d\theta_i(z,\omega) = -2\gamma_i P_k(z,\omega) dz \quad \ldots (2.76)$$

Here γ_i is the non-linear coefficient of the i[th] channel. The pump channel power (P_k) with the assumption made by the small signal analysis in [131] is given by:

$$P_k(z,\omega) = P_k(0,\omega).\cos(q_k z).\exp(-\alpha z - {}^{i\omega z}/_{v_{g,k}}) \quad \ldots (2.77)$$

Further, $q_k = -\beta_{2,k}\omega^2/2$ and $v_{g,k}$ denotes the group velocity for the respective mode. Due to chromatic dispersion, the small phase modulation evolves into an intensity fluctuation through PM-IM conversion and also a phase delay occurs through a PM-PM conversion and the corresponding expression for intensity fluctuated dP_{XPM} and phase fluctuated $d\theta_{XPM}$ is given by:

$$dP_{XPM,i} = -2P_i(z) exp\left[\left(-\alpha - i\,\omega/v_{g,i}\right)(L-z)\right].\sin[q_i(L-z)]\, d\theta_i(z,\omega) \quad \ldots (2.78)$$

$$d\theta_{XPM,i} = exp\left[\left(-\alpha - i\,\omega/v_{g,i}\right)(L-z)\right].\cos[q_i(L-z)]\,d\theta_i(z,\omega) \quad \ldots(2.79)$$

Here the attenuation and propagation delay of the channel i is given by

$$exp\left[\left(-\alpha - i\,\omega/v_{g,i}\right)\right] \quad \ldots(2.80)$$

and $P_i(z)$ is the average power of the channel i at a distance z from the beginning of the fiber. Since the major focus of this work is to derive analytical equations to calculate XPM-induced time jitter, the presented analytical model considers the phase fluctuation given by equation (2.80) and is analyzed and used in chapter 4 of the thesis. The present study considers XPM separately from other linear distortions with an assumption that the intensity modulated pumps affects the phase modulated probes through Kerr nonlinearity without PM-IM conversion. This assumption allows us to consider chromatic dispersion as a lumped distortion at the end of each span which can be compensated by using DCF as done in the simulation analysis.

2.5.11. Four Wave Mixing Modeling

In the FWM models mentioned thus far GVD is taken into account only with respect to the phase mismatch and the inter-channel pulse walk-off due to GVD is not accounted for [132]. Due to the GVD of the fiber, channels at different wavelengths have different group velocities. This means that the data pulse train on different channels will experience different delay as the pulses travel down the fiber. This relative delay between the data pulses on neighboring channels is called inter-channel pulse walk-off. In itself the inter-channel walk-off poses no impairment to the transmission quality but it does play an important role when evaluating the interaction of the neighboring channels through fiber nonlinearity. It is seen that inter-channel walk-off plays a very important role for the other inter-channel nonlinearities mentioned above XPM and SRS [133]. In [62, 63] an initial version of a finite-band noise model including walk-off was presented for degenerate FWM. Inside fiber, the nonlinear polarization causes three signals at frequencies f_i, f_j and f_k to interact and produce signals at frequencies, $\pm f_i \pm f_j \pm f_k$. Among these signals, the most troublesome are the frequencies corresponding to case when $f_{ijk} = f_i + f_j - f_k$ due to its energy and momentum conservation.

The basic model [134] that is further used to find the power of FWM components denoted as P_{ijk} on a link is given below:

$$P_{ijk}(L) = \frac{\eta_{ijk}}{9} D_{ijk}^2 \left(\frac{2\pi n_2}{\lambda_c A_{eff}}\right)^2 P_i P_j P_k e^{-\alpha L} L_{eff}^2 \quad \ldots (2.81)$$

where *Pijk* is the FWM power at frequency $f_{ijk} = f_i + f_j + f_k$. P_i; P_j and P_k are input light power correspond to f_i, f_j, and f_k frequencies, L is the instantaneous system length, n_{ijk} represents FWM efficiency, D_{ijk} is the degeneracy factor whose values are D =1 if $i = j = k$, D = 3 if $i = j \neq k$ or D=6 if $i \neq j \neq k$. The FWM efficiency is given as:

$$\eta_{ijk} = \frac{\alpha^2}{\alpha^2 + \Delta\beta_{ijk}^2} \quad \ldots (2.82)$$

This expression of efficiency is valid if L is much longer than $1/\alpha$. According to [135], the phase-matching factor is given as:

$$\Delta\beta_{ijk} = \left(\frac{2\pi\lambda_0^2}{c}\right)(f_i - f_k)(f_j - f_k)\left(\left[D_C + \left(\frac{\lambda_0^2}{2c}\right)\left(\frac{dD_c}{d\lambda}\right)(f_i - f_o)(f_j - f_0)\right]\right) \quad \ldots (2.83)$$

In a multichannel transmission system an analytical expression for the noise-variance due to FWM is derived as:

$$\sigma_{FWM}^2 = 2K^2 P_s \left\{\frac{1}{8}\sum_{I} P_{pqr} + \frac{1}{4}\sum_{II} P_{pqs} + \frac{1}{4}\sum_{III} P_{ppr}\right\} \quad \ldots (2.84)$$

where P_s is the peak power of the selected signal light, $K = ne/hf$, P_{pqr} is the power of the FWM light generated from a channel combination of p, q and rth channels that satisfy p + q - r = s, and n is the quantum efficiency of the detector. The channel combinations are classified into three categories. These may be either all different or in some cases two or more may be same.

2.6. Summary

In this chapter, the non-linear properties of optical fibers in the presence of dispersive behavior have been discussed to infer its deleterious effects in the channel propagation characteristics. Although residual local dispersion is desirable in order to suppress nonlinear effects, yet the accumulated dispersion necessitates the need for dispersion compensation necessary. This dispersion compensation introduces additional loss and thus requires various system configurations of the deployed fibers to ensure an optimum transmission performance. The system component modeling of single-channel

optical long-haul systems has been presented with a view to use them for simulation study in detail in the following chapters. The generation of the information carrying electrical signal was modeled using pseudo-random sequences with pulse shaping. In order to efficiently modulate the electrical signal into the optical carrier, the theory and operation of MZM is described in detail with appropriate mathematical models. Propagation losses are compensated by optical amplifiers, where different amplifier strategies were discussed, but only the EDFA, which is commonly used in WDM networks, was treated in detail. The mathematical model of each component has been discussed and is used in Chapter 4 to develop a Matlab Simulink Model for optical link using DQPSK format. The system configuration is not the only key factor that improves the overall optical communication link performance. The transmitting signal bandwidth corresponding to various encoding formats plays an important role in maximizing the overall system performance and is the subject of the remainder of this dissertation.

Chapter 3

Non-Linearity Mitigation through Intensity Modulation

In a conventional optical communication link the impairments caused by nonlinearity, such as XPM and FWM, can be managed through residual local dispersion of the fiber or by adjusting the channel spacing to a sufficiently large value. Obviously as dispersion is a linear process, the dispersion accumulated along the transmission fiber can be equalized by performing dispersion compensation either periodically along the link or at the receiver end. This, however, increases the complexity when compared with systems employing optical fibers with relatively smaller dispersion values to avoid dispersion compensation. The other alternative of larger channel spacing deteriorates the bandwidth utilization leading to poor spectrum efficiency [136, 137]. The main purpose of spacing channels sufficiently far apart or employing fibers with adequate dispersion is to suppress the inter channel impairments. However, some intra channel interaction between dispersion and nonlinearity still exists and causes performance degradation on a given channel. Although the dispersion can be compensated upto some desirable level but fiber nonlinearity management becomes a challenging issue for the researchers. The interaction between dispersion and nonlinearity along the main transmission fiber causes local phase degradation of the waveform even in a dispersion compensated link. It was observed from the literature survey that intra channel performance degradation can be minimized if the transmitted signal possesses some special characteristic [138]. This leads to an interesting option to explore the choice of some novel optical modulation formats towards the mitigation of non-linearities in the fiber.

One of the important issue in system design is to understand the encoded pulse response in the channel having some specific patterns. In fact, signal optical spectral bandwidth, tolerance to chromatic dispersion, resistance to nonlinear crosstalk, susceptibility to accumulated noise, and other system performance measures are directly related to the optical modulation format. To minimize both the linear and the nonlinear impairments over the transmission fiber, an optimal modulation format is needed. A modulation format with a narrow optical spectrum can enhance spectral efficiency and tolerate more CD distortion. A modulation format with constant optical power can be less susceptible to SPM and XPM; modulation format with multiple signal levels will carry more information than binary signals and its longer symbol duration will reduce the distortion induced by CD and PMD. In addition, in long-

haul networks, ASE noise produced by EDFAs is another factor that requires modulation formats more tolerant to additive ASE noise. These advanced modulation schemes combined with other key technologies, like low noise optical amplifiers, new advanced optical fibers and forward error correction techniques, are crucial to realize spectrally efficient, high-capacity optical transport networks [139-142].

Many optical modulation formats have been considered in the scope of this research. Carrier Suppressed RZ [143] is a pseudo-multilevel modulation format and is characterized by reversing the sign of the optical field at each bit transition. It reduces the non-linear impairments in a channel and improves the spectral efficiency in high bit rate systems. The optical duobinary and modified duobinary modulation formats also turn out to be the leading choices as they have high tolerance to CD, better non-linear tolerance and can go through narrowband optical filtering to put more channels close to each other to improve spectral efficiency. Furthermore, it is easy to implement, since there is a minor change in the transmitter and uses photo-diode at the receiver side for DD. The overall system setup is simpler compared to other competing formats, like DPSK, and DQPSK, which require modifications at the transmitter and at the receiver, further increasing system cost and complexity. On the other hand, these phase modulation formats have an inherent 3-dB receiver sensitivity improvement by using balanced detection. They also reduce the effects of SPM and XPM resulting in reduction of signal distortion that accumulates in the optical signal over the fiber link and have proved to be strong candidates for high data-rate and spectral efficient DWDM systems [143 - 145].

The purpose of this thesis is to investigate the influence of different optical modulation formats in terms of signal characteristics, system implementation, and power spectrum to evaluate and establish performance enhancement of optical communication links for several multiplexed channels. Different modulation formats have different characteristics, which lead to unique performance improvements. As it is not possible to cover all the modulation formats in one thesis, so here a few important ones such as CSRZ, Duobinary, Modified Duobinary, DPSK and DQPSK have been modeled, simulated and implemented in standard simulation tools and MATLAB environment. It may be interesting to note that different fiber types and different modulation formats could affect the system performance. Therefore, there is a need to develop simulation test beds based on OptiSystem 10.0 [146] tool to study and analyze various modulation formats and infer their characteristics and applicability in designing of high speed optical communication link. The proposed analysis also focuses on the study of optical linear and nonlinear effects for system performance evaluation in terms of minimal BER.

This chapter focusses on intensity modulated formats particularly RZ, CSRZ, Duobinary and Modified Duobinary to test their characteristics. In the following parts, basic waveform generation/detection and major characteristics of the above modulation formats will be discussed. The phase modulated formats DPSK and DQPSK are investigated in chapter 4. Although this does covers a complete screening of the advanced optical modulation formats arena, but the results in this thesis and the mechanism under each modulation format are still valuable and can be extended for the future research. This chapter begins with a discussion of the various modulator technologies employed for DWDM systems.

3.1. Modulator Technologies

Optical modulation is the conversion of a signal from the electrical into the optical domain. Three basic technologies to modulate the light are commonly used today: directly modulated lasers (DML), electro-absorption modulators (EAM) and MZM. A new and innovative way to use these existing modulator technologies usually gives rise to a novel optical modulation format. These modulator technologies can be used with modulation formats to find a novel and cost effective modulation technique in order to resolve the future needs of high spectral efficient and high bit-rate optical DWDM networks. In order to realize high-speed modulation an optical modulator should have (i) a high electro-optical bandwidth, (ii) low optical insertion loss, (iii) not induce undesired frequency chirp in the signal and (iv) have a high enough extinction ratio. The extinction ratio is defined as the ratio of the energy in the ’0’ compared to the energy in the ’1’s [147].

3.1.1. Directly Modulated Lasers

Direct modulation of lasers is the easiest way to impose data on an optical carrier. The transmitted data is modulated onto the laser drive current, which then switches on and off the light emerging from the laser. This resulting modulation format is binary intensity modulation [2]. Directly Modulated Lasers are widely available up to modulation rates of 2.5 Gbps but with some limited availability up to 40 Gb/s. The main limitation of DMLs for high data-rate transmission systems is their inherent, highly component-specific chirp which broadens the optical spectrum and interact with fiber chromatic dispersion to cause increased signal distortions [148].

3.1.2. Electro absorption Modulators

An electro absorption modulator is a semiconductor device which controls the intensity of a laser beam via an electric voltage. Its operation principle is based on the Franz-Keldysh effect, i.e., a change of

the absorption spectrum caused by an applied electric field, which usually does not involve the excitation of carriers by the electric field. EAMs typically feature relatively low drive voltages and are cost-effective in volume production. They are available for high-speed modulation rates up to 40 Gbps today, with some research demonstrations up to 100 Gbps [149]. However, similar to DMLs, they also exhibit some residual chirp and impose limitation at relatively high data rates. They have wavelength dependent absorption characteristics, dynamic extinction ratios typically not exceeding 10 dB, and limited optical power handling capabilities. Their fiber-to-fiber insertion loss is about 10 dB which can be eliminated by integration with semiconductor optical amplifiers (SOAs) [1,3]. On-chip integration with laser diodes avoids the high loss at the input fiber-to-chip interface, and leads to compact transmitter packages.

3.1.3. Mach–Zehnder Modulators

Unlike electro absorption modulators, Mach-Zehnder modulators work on the principle of interference. Incoming light is divided into two paths at an input coupler. One path has a phase modulator that lets the two optical fields acquire some phase difference relative to each other, controlled by the applied voltages $V_{1,2}$. This applied electrical voltage creates destructive or constructive interference depending on the phase difference introduced and thereby results in intensity modulation. Due to their better modulation performance and the possibility of independently modulating intensity and phase of the optical field, many advanced optical modulation formats use MZMs popularly implemented in $LiNbO_3$ substrate [150]. Fig. 3.1 shows the structure of such a MZM. The incoming light is split into two arms when entering the modulator and travels under the influence of applied voltages $v_1(t)$ and $v_2(t)$. At the output of the MZM, the light waves of the two arms couple and interfere with each other based on the phase difference and cause the desired modulation.

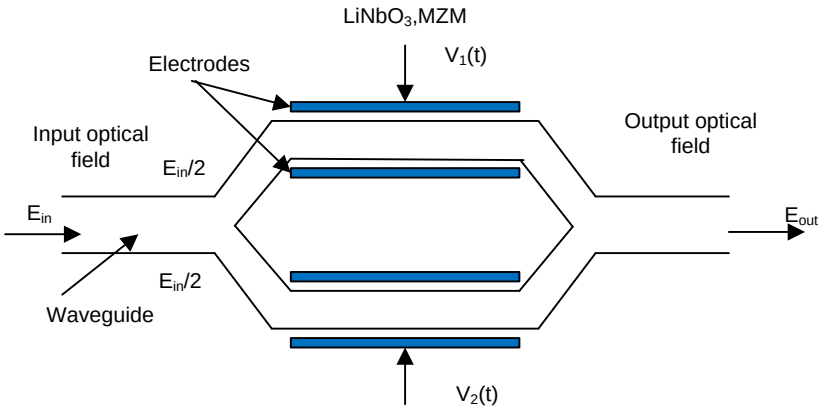

Fig. 3.1: Optical intensity modulator based on Mach- Zehnder interferometric structure [15]

This modulation describes how the data is coded onto the optical signal. The amplitude, phase, frequency and state of polarization (SOP) of optical signal can be modulated resulting in various formats as discussed in the next subsection.

3.2. Modulation Formats under investigation

Numerous factors that should be considered for the right choice of modulation format include: spectral efficiency, power margin, and tolerance against GVD and against fiber nonlinear effects like SPM, XPM, FWM, and SRS. The most basic format which has been deployed extensively so far in IMDD systems is the NRZ format, as it is easy to generate, detect and process. In the recent years, as optical systems are advancing to higher data rates with the integration of DWDM and optical amplifiers, NRZ modulation format may not be the best choice for high capacity optical systems [151,152]. However, as it has been widely deployed in field and due to its simplicity, and its historic dominance, NRZ would be a good reference for the comparison.

3.2.1. Non Return to Zero (NRZ) Format

The NRZ format has the simplest configuration and is widely used in commercial products so far because of several reasons: First, it requires a low electrical bandwidth for the transmitters and receivers (compared to return-to-zero); second, it is not sensitive to laser phase noise (compared to phase shift keying); and last, it has the simplest configuration for the transmitter and receiver. Fig. 3.2 shows the representation of NRZ code.

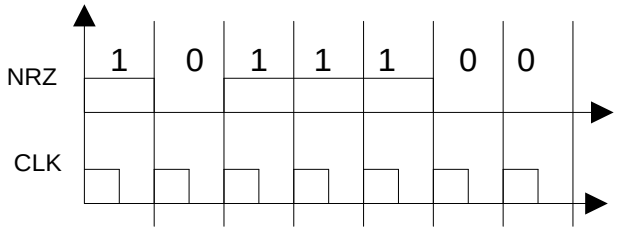

Fig. 3.2: Representation of the NRZ code.

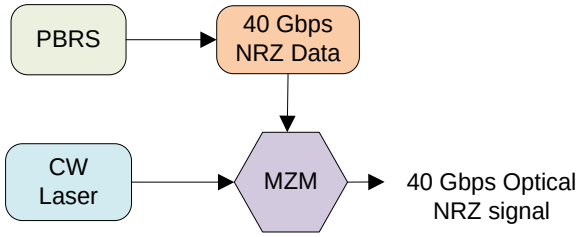

Fig. 3.3: Block diagram of NRZ transmitter

A schematic block diagram of the 40 Gbps NRZ transmitter is shown in Fig. 3.3. An optical signal generated by the continuous-wave (CW) laser source is ON–OFF keyed by the MZM driven by 40-GHz NRZ data signal. The intensity of the carrier light wave is modulated by the applied electric field whose voltage varies with a determined function. The MZM is driven at the quadrature point of the modulator power transfer function with an electrical NRZ signal. To detect a NRZ optical signal, a simple photodiode is used at the receiver, which converts optical power of signal into electrical current. This is called direct detection. If there is no mention, same direct detection scheme is used for other modulation formats in this thesis.

The NRZ pulses possess a narrow optical spectrum due to the lower on-off transitions. The reduced spectral width improves the dispersion tolerance and enables higher spectral efficiency, but on the other hand it leads to ISI between the pulses. NRZ modulated optical signal is less resistive to fiber nonlinear effect compared to its RZ counterpart [153] and hence RZ format is investigated further.

3.2.2. Return-to-Zero (RZ) Format

At higher bit rates such as 40 Gbps, the effect of non-linearity also becomes more important, and the RZ signal format proves to be superior to NRZ. In RZ format, for the logical 1 bit the power level returns to 0 after half of the period, whereas for the 0 bit, the power level is 0 continuously as shown in Fig. 3.4.

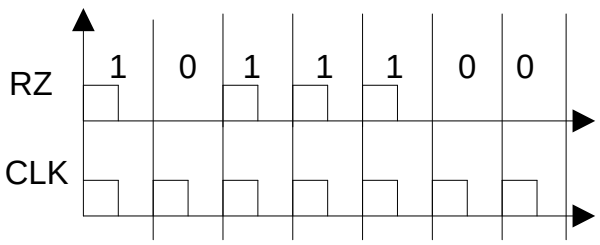

Fig. 3.4: Representation of the RZ code.

The advantages of the RZ signal format over the NRZ are discussed below. Due to the fact that the RZ signal format has larger bandwidth than the NRZ, the RZ pulses are broadened more rapidly by dispersion. However, this turns out to be beneficial because as a pulse is broadened, its peak decreases. The severe pulse broadening in the case of RZ signals makes it more robust to the effect of nonlinearity [154] due to the fact that the non-linear effect is proportional to the signal intensity. This is very important in high-bit-rate systems in which high launched power is required to provide adequate SNR at the receiver. The effect of accumulated dispersion can be removed by employing dispersion compensation, which in effect recovers the waveform back to its original form.

Since the pulse width of the RZ signal is narrower than that of the NRZ signal, the RZ pulse has higher peak power than the NRZ for a given average power. Thus, the eye opening of the RZ signal format is wider than that of the NRZ, resulting in better receiver sensitivity than the NRZ for a given average power [155]. This implies that for required receiver sensitivity, the transmitted power can be lowered by employing the RZ signal format rather than the NRZ. The better receiver sensitivity in the case of the RZ signal also suggests that the transmission distance can be increased compared with the NRZ signal for the same transmitted power. When SPM is considered, its interaction with dispersion depends strongly on the pulse width. In the case of the NRZ signal format, the transmitted signal consists of pulses having different pulse widths depending on the data pattern. Thus, the effect of SPM depends on the data pattern. On the other hand, the transmitted RZ signal consists of a sequence of identical pulses corresponding to the data pattern; hence, the pattern-dependence of SPM-induced waveform distortion can be avoided. In addition, the interaction between the SPM and dispersion in the anomalous dispersion regime can be exploited effectively in the case of the RZ signal, resulting in uniform pulse compression.

The advantages of the RZ signal over the NRZ are not limited to reducing the intra channel nonlinear effect. In fact, the RZ signal format is significantly superior to NRZ when the inter channel nonlinear effects are considered. As discussed in Chapter 2, the XPM and FWM are strongest when pulses at different wavelengths completely overlap one another in the time domain. This condition can be easily satisfied in the case of the NRZ signal format. Generally, the pulse width of the RZ signal is shorter than that of the NRZ signal. Thus, the NRZ pulses at different wavelengths take longer time than the

RZ pulses to walk off from one another. This in effect favors the generation of FWM and XPM. Therefore, NRZ systems are more susceptible to inter channel nonlinear effects than RZ systems.

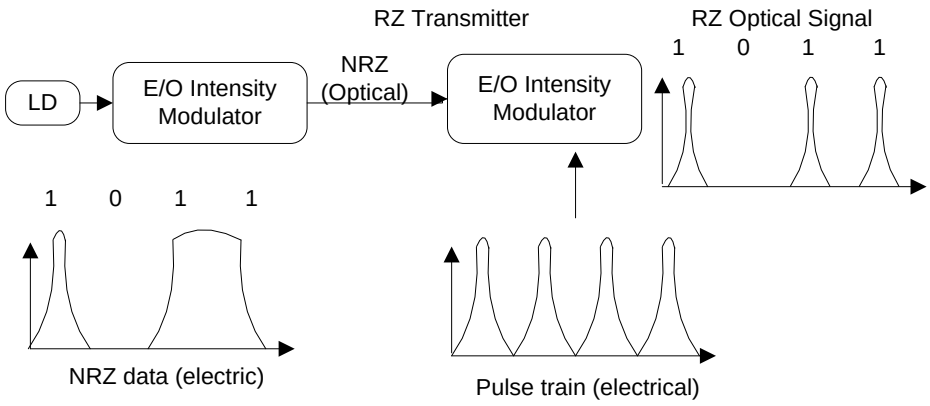

Fig. 3.5: Block diagram of RZ transmitter

It should be noted that NRZ systems are more robust to linear cross talk among channels than the RZ systems due to the fact that the NRZ signal has narrower bandwidth than RZ signal. However, with proper spectral filtering or pulse shaping at the transmitter to remove unwanted high-frequency components, the linear cross talk among channels in RZ systems can be minimized, causing RZ systems to further outperform NRZ systems [66]. A schematic diagram of the 40 Gbps RZ transmitter is shown in Fig. 3.5. RZ transmitters can be implemented either by electronically generating RZ waveforms, which are then modulated onto an optical carrier, or by carving pulses out of an NRZ signal using an additional modulator, called pulse carver. Firstly, NRZ optical signal is generated by an external intensity modulator. Then, it is modulated by a synchronized pulse train with the same data rate as the electrical signal using another intensity modulator. RZ modulation format is mostly preferred in submarine systems where costlier transmitters and receivers are used and forms the base of different formats discussed in this thesis. Carrier Suppressed RZ (CSRZ) is a variation of RZ formation and is discussed next.

3.2.3. Transmitter Design for Carrier Suppressed Return-to-Zero (CSRZ) Format

CSRZ format is a modification of RZ format and a number of transmission experiments have employed this format as it is highly tolerant to the mixed effect of SPM and GVD, and has a narrower pedestal shape of the optical spectrum than the conventional RZ format [153]. The difference between CSRZ and conventional RZ is that the CSRZ signal has π phase shift between adjacent bits. In contrast to the

correlative coding formats like duobinary, the sign reversals occur at every bit transition, and are completely independent of the information-carrying part of the signal. This phase alternation, in the optical domain, produces no carrier component for CSRZ [27, 156], and the alternating phase between adjacent bit slots reduces the fundamental frequency components to half of the data rate.

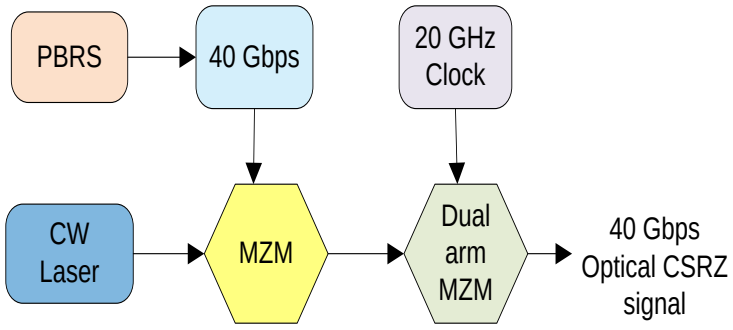

Fig. 3.6: Block diagram of CSRZ transmitter

CSRZ has better tolerance to chromatic dispersion due to its lower optical power, allowing for more channels multiplexed in transmission. In addition, carrier suppression reduces the efficiency of FWM in WDM systems [28]. Fig. 3.6 shows the CSRZ transmitter setup designed for analysis. The generation of a CSRZ optical signal exploits two concatenated MZMs. The first MZM modulates the intensity of the light from a CW laser source with a 40 Gbps NRZ data. Then the generated NRZ optical signal is modulated by the second MZ modulator that is driven by a clock at the half bit-rate, 20 GHz in this case, to generate a CSRZ optical signal.

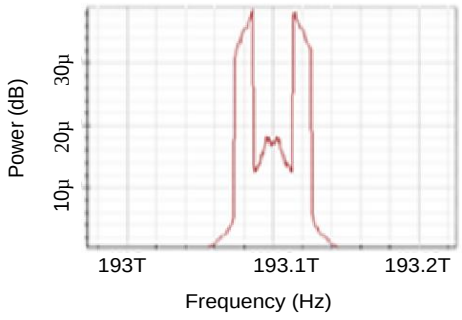

Fig. 3.7: Spectrum of CSRZ signal

Phase inversions between adjacent bits are achieved because optical field transfer function of the MZM changes its sign at the transmission minimum. This introduces a pi phase shift between any two adjacent

bits and the spectrum gets modified such that the central peak at the carrier frequency is suppressed as shown in the diagram in Fig. 3.7.

3.2.4. Transmitter Design for Duobinary (DRZ) Format

Optical duobinary scheme belongs to a class of correlative coding formats and is also known as phase shaped binary transmission (PSBT) [157]. Duobinary format is very attractive because of its low spectral occupancy and high tolerance (~3.5) to residual CD [158–160] than NRZ. This feature is particularly important as it alleviates the requirement of tunable dispersion compensation module into the receiver, which is mandatory when NRZ or CSRZ are implemented. Furthermore, its compact spectrum makes duobinary compliant with 50 GHz ITU grid thus ensuring the compliance of 40 Gbps transport with existing 10 Gbps WDM long-haul transmission infrastructures [161, 27]. It permits easy up-gradation by simply replacing a 10 Gbps transmitter by a 40 Gbps one without major changes in the design of the receiver and transmission line. DB signal being highly tolerant to CD facilitates to achieve longer transmission distances and is one of the most spectrally-efficient modulation schemes. Moreover, the DB signal can be demodulated into a binary signal easily using a conventional direct detection optical receiver making the receiver design simpler.

Duobinary modulation is a 3-level format that is generated by using differential precoding and electrical or optical filtering. Conventional DB transmitters use a differential precoder at the input. An exclusive-or gate with a delayed feedback path constitutes the duobinary precoder. Fig. 3.8 shows a typical duobinary precoder and encoder.

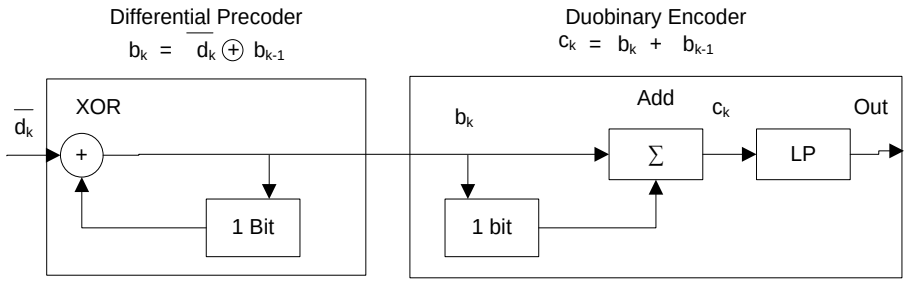

Fig. 3.8: Duobinary Precoder and Encoder

Although it is possible to use decoder at the receiver but precoding at the transmitter is used in order to avoid error propagation. Pre-coded sequence is converted to three-level electrical signals by using low pass electrical filter. This LPF can also be implemented by a delay-and-add circuit, which typically

results into a better back-to-back sensitivity while carefully selected low-pass filter enhances CD tolerance at the expense of this sensitivity [162,163]. Compared to NRZ, duobinary format has a phase modulation in addition to amplitude modulation which reduces the pulse spreading thereby making it less sensitive to chromatic dispersion and intra-channel nonlinear effects.

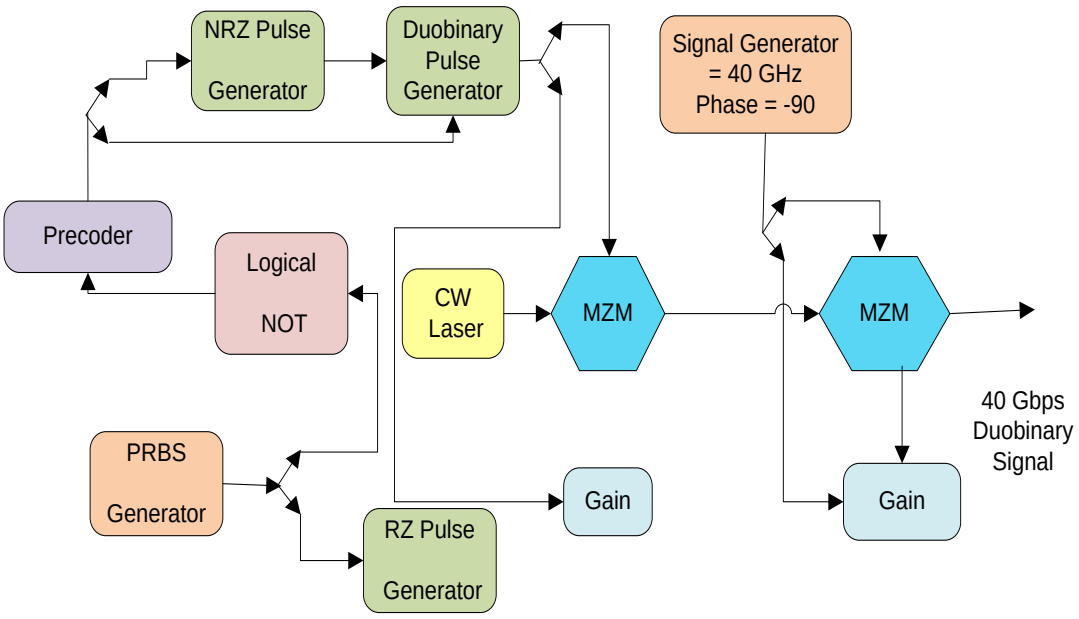

Fig. 3.9: Block diagram of Duobinary transmitter

Typically, in duobinary, a π phase shift takes place between two groups of "1" s when the number of "0" s in-between is odd. Fig. 3.9 shows the configuration of a 40 Gbps duobinary transmitter. The duobinary signal is generated by first creating a NRZ duobinary signal using a duobinary precoder, NRZ generator and a duobinary pulse generator [164]. The generator drives the first MZM, whose output is concatenated with a second MZM that is driven by an electrical sinusoidal signal with a frequency of 40 GHz, phase = - 90^{o}. The optical modulation bandwidth of DRZ format is B i.e. half of the bandwidth of NRZ format as shown in Fig. 3.10. Here we use MZM biased at its null point. With '0' input no light is transmitted but +1 and -1 are transmitted as +E and –E electrical field respectively. Thus three level electrical signals are converted to two level optical signal.

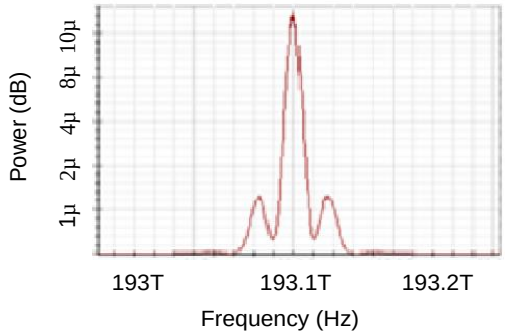

Fig. 3.10: Spectrum of DRZ signal

3.2.5. Transmitter Design for Modified Duo-binary Return-to-Zero (MDRZ) Format

MDRZ format has a much narrower optical bandwidth over the DRZ leading to greater dispersion tolerance and higher fiber non linearity tolerance [165-168]. It is inherently asymmetric and is characterized by phase inversion in the pulses triggered by the presence of a logical “one” in the previous bit slot. Duobinary spectrum has DC content while modified duobinary does not have any DC content. MDRZ has opposite phase in adjacent “1” s and due to this fact SPM in single channel, XPM and IFWM in WDM transmission systems can be reduced [169-172]. In this format, the phases of two groups of ‘ones’ that wrap an isolated ‘zero’ are flipped, leading to reduced ghost pulse generation caused by IFWM. While the discrete frequency tones of RZ signal spectrum are effectively suppressed by both DRZ and MDRZ, the latter provides the advantage of smaller timing jitter and amplitude distortion. Moreover, when compared to RZ, both DRZ and MDRZ signals provide smooth operation even at relatively higher average channel powers.

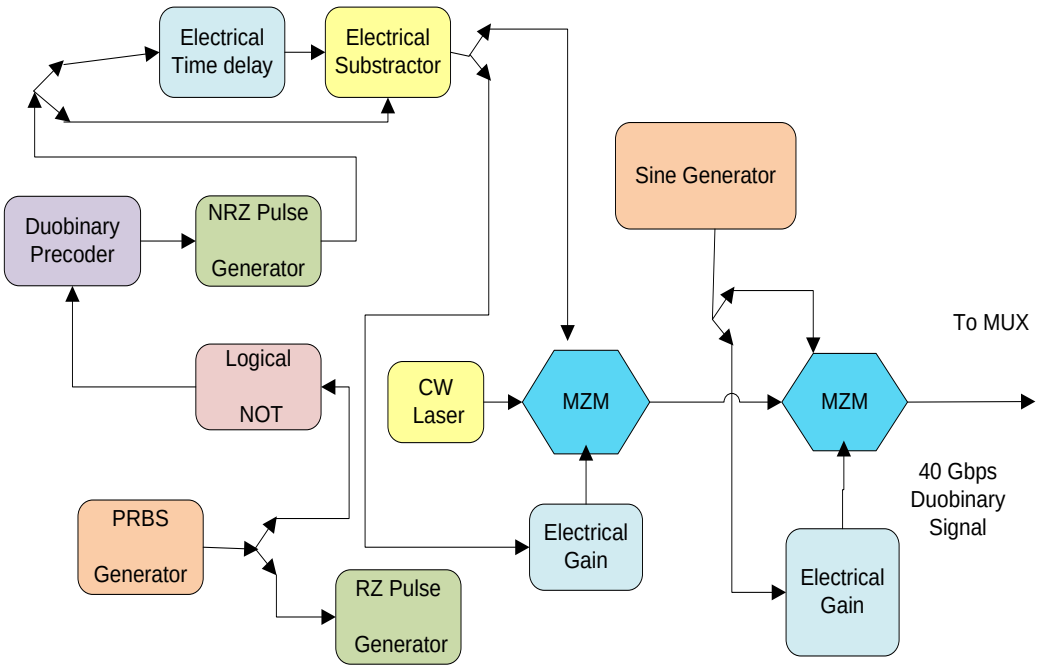

Fig. 3.11: Block diagram of Modified Duobinary transmitter

Fig. 3.11 outlines the design of the 40 Gbps MDRZ transmitter. It requires two optical modulators to obtain this signal; one to generate NRZ duo-binary signal and the other to carve the NRZ data to RZ signal. It is similar to DRZ transmitter as the first step is to generate a NRZ duobinary signal, but here a delay-and subtract circuit is used instead of the delay-and-add circuit. The output of this block signals the first MZM, whose output is concatenated with a second modulator which is driven by a sinusoidal electrical signal with 40 GHz frequency and phase −90°.

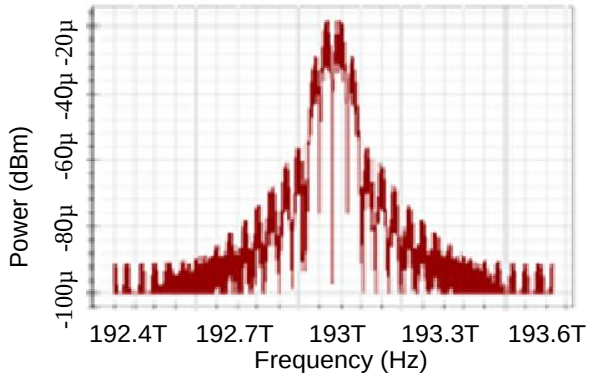

Fig. 3.12: Spectrum of MDRZ signal

In duobinary signal case, we change the phase of bits '1's only after a bit '0' appears, but in the MDRZ case we alternate the phase between 0 and π for the bits '1'. That is, while keeping the phase of all the "zero" bits constant, a 180° phase variation is introduced between all the consecutive "ones" which leads to suppression of carrier of the duobinary signal as shown in Fig. 3.12.

3.3. Simulations for Various Modulation Formats

In order to study the feasibility and performance of the DWDM system, both simulation and experimental methods could be used. However, due to its economic advantage, simulation method is used very often as simulation does not require any physical devices and equipment. Once the simulation model is built, it is very easy to change the system parameters and the time needed to check a specific setup is usually much smaller comparing to an experimental investigation. Secondly, in a simulation, the only limitation is the computing power of the computer such as CPU speed and memory size. Simulations can be performed for a complex system while it is very difficult to fulfill in a real experiment, which requires many devices and equipment.

3.3.1. General Considerations for numerical simulation of optical fiber transmission systems

Modeling of an optical fiber system is quite different from than the modeling of other types of communication systems, such as wireless system, due to its high bit rate, low bit error rate and its transmission media, which needs special consideration. High bit rate means that the simulation bandwidth has to be very large and the number of bits that can be simulated at one time will be small due to the limitation of the computing hardware. Low bit error rate means a BER lower than 10^{-9} and we have to run a very long simulation in order to see even a single error bit transmitted. Among all the devices and subsystems of an optical transmission system, the optical fiber is usually the main source of the system penalty and its modeling is the most important part of the whole model.

As explained in chapter 2, analytical calculation can also be used to model the fiber transmission. As there is no close form solution to the nonlinear transmission equation that governs the waveform evolution along the fiber, linear addition model is applied. However, compared to the analytical methods, the numerical integration of the propagation equation is generally more accurate and takes into account all the linear and non-linear effects automatically [45-47]. There are generally two categories of numerical methods which can be used to solve the equation, one of them is the finite difference method and the other is the pseudo-spectral methods, and pseudo-spectral methods is faster

by up to an order of magnitude to achieve the same accuracy. Among the second category, SSFM is used most extensively to solve the pulse propagation problem in nonlinear dispersive media as it is fast and easy to implement and thus is used in this work as the algorithm for the fiber model.

The complexity of optical communication systems employing DWDM requires a comprehensive computer aided modeling platform in order to optimize design, experimental costs and evaluate the performance of the implemented networks. A numerical modeling or simulation program for a system should include the models of all the components that constitute that specific system. As a system level simulation, the model for each individual component should be kept as simple as possible when the accuracy requirements allow. It is not necessary to use their detailed models because it will not significantly increase the overall accuracy of the simulation but it would increase complexity dramatically and results in a much lower efficiency. Integrated computer-based tools or packages for optical link design can simulate or imitate both electrical (e.g. FEC encoders) and optical (lasers, optical amplifiers etc.) components**.** This large library of components offers the designers a wide exploration of optical systems and avoids error from guesswork or back-of-the-envelope computations and is time efficient. In this work, we have used the OptiSytem 10.0 simulator that gives us an environment identical to the physical realization of a fiber-optic transmission system**.**

3.3.2. OptiSystem

OptiSystem 10.0 is an advanced optical communication system design simulation package to simulate and analyze an optical link and is extensively used in research and development activities [144-146]. In the present thesis, it has been used to design and simulate optical communication systems to evaluate their performance considering the appropriate system component parameters. This tool supports modeling with an acceptable accuracy and ease of use on both Windows and UNIX platforms. It represents an optical communication system as an interconnected set of blocks, with each block representing a component or subsystem in the communication system. As physical signals are passed between components in a realistic communication system, “signal” data is passed between component models in the OptiSystem simulation.

It provides multiple simulation engines that provide complementary simulation techniques. This enables the greatest flexibility in modeling and simulating systems ranging from short-distance data communication links, to ultra-long-haul DWDM telecom systems, to large metro networks with feedback paths and EDFA transients due to adding and dropping of channels. Optisytem’s data post-

processing and display facilities provide an intuitive and flexible measurement graphical interface that acts as a lab-like set of virtual instruments. Interactive and post-processing functionality (e.g. graph superimposition, correlation graphs, interactive cursor read-out data, peak search, eye-diagram measurements, BER/Q evaluation) allow one to simulate the project once and perform further analysis of results later (saving time during the design process).

3.4. Simulation Set-Up for CSRZ format

In order to compensate for the accumulated dispersion three different schemes of dispersion compensation viz., pre-, post-, and symmetrical compensation have been attempted in the present thesis. In pre-compensating case, DCF is used as a pre-compensating component for the accumulated dispersion of the transmission fiber. The gain G of the amplifier following the DCF is balancing the fiber loss of the DCF and can be determined by:

$$G = \alpha_{DCF} L_{DCF} \quad \ldots (3.1)$$

where α_{DCF} is the attenuation coefficient of the dispersion compensating fiber, L_{DCF} is the length of the DCF. For the gain of the amplifier subsequent to the transmission fiber a similar equation holds, where α_{TF} is the attenuation coefficient of the transmission fiber.

$$G = \alpha_{TF} L_{TF} \quad \ldots (3.2)$$

The linear dispersive compensation length, L_{DCF}, should be so chosen to compensate the dispersion of the transmission fiber via:

$$L_{DCF} = \frac{L_{TF} D_{TF}}{-D_{DCF}} \quad \ldots (3.3)$$

where L_{TF} is the length of the transmission fiber, D_{TF} is the dispersion of the transmission fiber, D_{DCF} is the dispersion of the DCF. In post-compensating case, the DCF post compensates the dispersion of the transmission fiber. In the symmetrical compensation case, fiber placement follows the sequence of transmission fiber, DCF and transmission fiber [33]. The proposed 32 channel DWDM system consists of transmitter section, fiber and optical receivers as shown in Fig. 3.13 with the central frequency of the first channel as 193.1 THz. The simulation parameters used are given in Table 3.1.

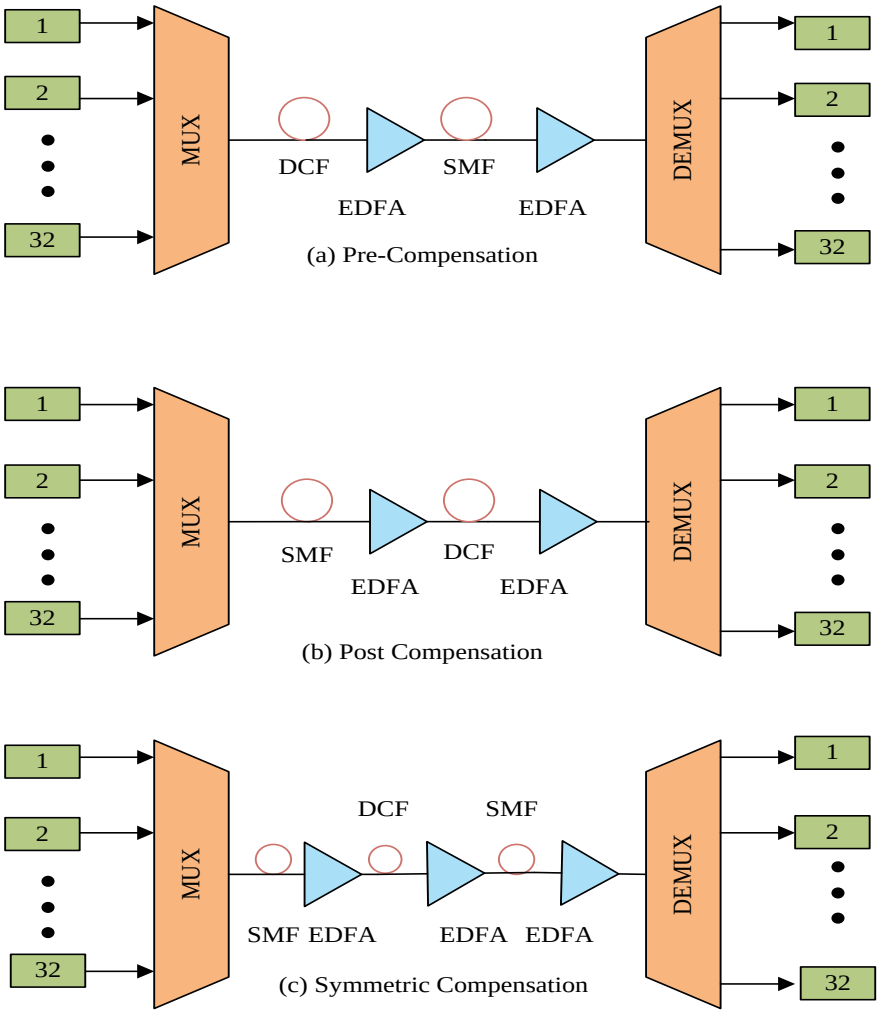

Fig. 3.13: Schematic of simulation setups: (a) pre-compensation scheme, (b) post-compensation scheme and (c) symmetrical-compensation scheme

The design of transmission link has been done using periodic dispersion management technique wherein fibers with normal and anomalous GVD are combined to form a dispersion map such that the GVD is high locally all along the link length, but keeping an overall low average value [13]. The parameters of DCF and SMF are chosen such that the first-order dispersion is compensated exactly (D = 0) i.e. $D_{SMF}\, L_{SMF} = D_{DCF}\, L_{DCF}$ where D means the first-order dispersion parameter [ps/nm/km] of the corresponding fiber and L stands for the total SMF or DCF length per span.

Table 3.1: Simulation parameters

Bit rate	40 Gbps
Sequence length	64
Samples/bit	256

DWDM channel spacing	50 GHz
Central frequency of the 1st channel	193.1 THz
Capacity	32-channel 40-Gbps
Distance	30 Km X N Spans
Input Power	-10 dBm

A. Transmitter section

The WDM transmitter consists of a pseudo random bit sequence (PRBS) generator, CW lasers, data modulators, filters and the optical multiplexer. The PRBS generator generates bit sequences at the rate of 40 Gbps with 2^7 –1 bits. The emission frequencies of CW laser are equally spaced and are in the range of 193.1–194.65 THz with the frequency spacing of 50 GHz between the adjacent channels. Extinction ratio of MZM is set at 30 dB. To each output port of each CW laser a CSRZ transmitter as designed in Fig. 3.6 has been connected. Optical signals from 32 such data modulators are fed to the 32 input ports of an optical multiplexer. To ensure separation between the channels in the frequency domain (linear cross-talk suppression), before multiplexing, each channel is optically filtered with narrow transmission optical filter [27]. Here, a second order Gaussian filter with a bandwidth equal to 50 GHz has been considered. The channel spacing and operating wavelengths are as defined by ITU-T standards.

B. Fiber section

The combined optical signal is fed into the SMF. The model in OptiSystem takes into account the unidirectional signal flow, stimulated and spontaneous Raman scattering, Kerr-nonlinearity and dispersion. The fiber parameters have been specified in the Table 3.2. The gain of the EDFA placed after each fiber is set to compensate the losses of the preceding fiber. The noise figure of the amplifiers is constant and set to 6 dB. Scalar model of both the fiber has been used to avoid PMD. The signal is then launched over N spans of SMF of 30 km each. The proposed DWDM system has been simulated for pre, post and symmetrical dispersion compensation scheme. In pre-compensation scheme, as shown in Fig. 3.13(a), to compensate for the dispersion and the nonlinearities, DCF fiber of 5 km is used prior to the SSMF fiber of 25 km length. Also, two in-line-EDFA with gain 2.5 dB and 5.5 dB, respectively, have been used in the link. The post-compensation scheme has been shown in Fig. 3.13 (b) where DCF fiber of 5 km is used after the SSMF fiber of 25 km length to combat the accumulated dispersion. In symmetrical-compensation scheme, as shown in Fig. 3.1(c), DCF fiber of 5 km is used in the middle

of the SSMF fiber of 25 km length. Here, three in-line EDFA's with gain 2.75 dB, 2.5 dB and 2.75 dB have been used.

Table 3.2: Fiber parameters

Fiber Type	Attenuation (dB/Km)	Dispersion (ps/km-nm)	Dispersion Slope	Mode Effective Area	Non linear refractive index
SMF	0.22	17	0.08	80	2.6×10^{-20}
DCF	0.5	-85	-0.45	30	2.6×10^{-20}

C. Receiver section

In the receiver the signal is de-multiplexed, detected by PIN detector, passed through the filter and 3R regenerator. Optical de-multiplexer used has 32 output ports Bessel band pass filters with filter parameters: 3 dB cut off frequency = 65 GHz, order of the filter = 4, depth = 100 dB have been used to separate out the channels at the respective wavelengths. The filter parameters have been optimized to give the best result. The optical signal from each port is then passed through PIN photodiode whose reference frequency ranges from 193.1–194.65 THz respectively, responsivity [A/W] =1 and dark current = 0.1 nA. An electrical low pass Bessel filter follows the PIN photodiode whose cut-off frequency is determined by the modulation used and is optimized at 40 GHz with order 3. Thereafter, 3R regenerator is used to regenerate an electrical signal connected directly to the BER analyzer which is used as a visualizer to generate graphs and results such as eye diagram, BER, Q value, eye opening etc.

3.4.1. Investigation and Discussions of CSRZ format

The performance of CSRZ modulation format has been compared for pre, post and symmetrical dispersion compensation schemes for 1.28 Tbps DWDM system in terms of received maximum Q value and eye opening. For system analysis, the results of the first channel have been considered as it corresponds to the worst-case scenario. In this simulation, a 30 Km span is designed by appropriately choosing SMF and DCF fibers to compensate GVD. Then transmission spans have been cascaded in series to realize lengths in multiples of 30 Km. Fig. 3.14 (a)–(d) shows the graphical representation of Q value as a function of signal input power for spans 1 to 4 for pre, post and symmetrical-compensation schemes.

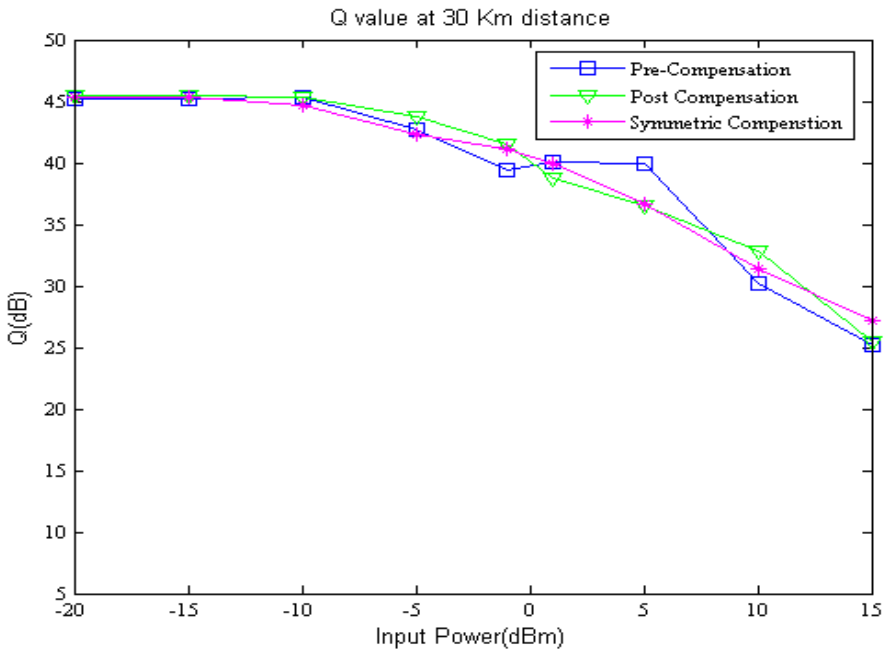

Fig. 3.14(a)

For a high data rate WDM system it is desirable that the input power should be as low as possible to limit non-linear effects. Keeping this in mind, the input power has been varied from -20 dBm to 15 dBm. Though generally it is not desirable to operate at power level greater than 5 dBm, the designed system works well even at 10 dBm but at 15 dBm power Q values falls below the minimum required 15.6 dB but only for the 4th Span. Also, it can be seen that as the signal input power increases Q value is initially maintained for all the dispersion compensation schemes till -10 dBm and then it starts to decrease. This can be understood from the fact that for low powers the DWDM system has very less non-linear effects coming into play. However, at higher powers, the pulses tend to overlap each other due to more dominance of non-linear effects like XPM and FWM caused by optical Kerr's effect and thus reduces the Q value. This observation is in close agreement with the reported results [153, 156].

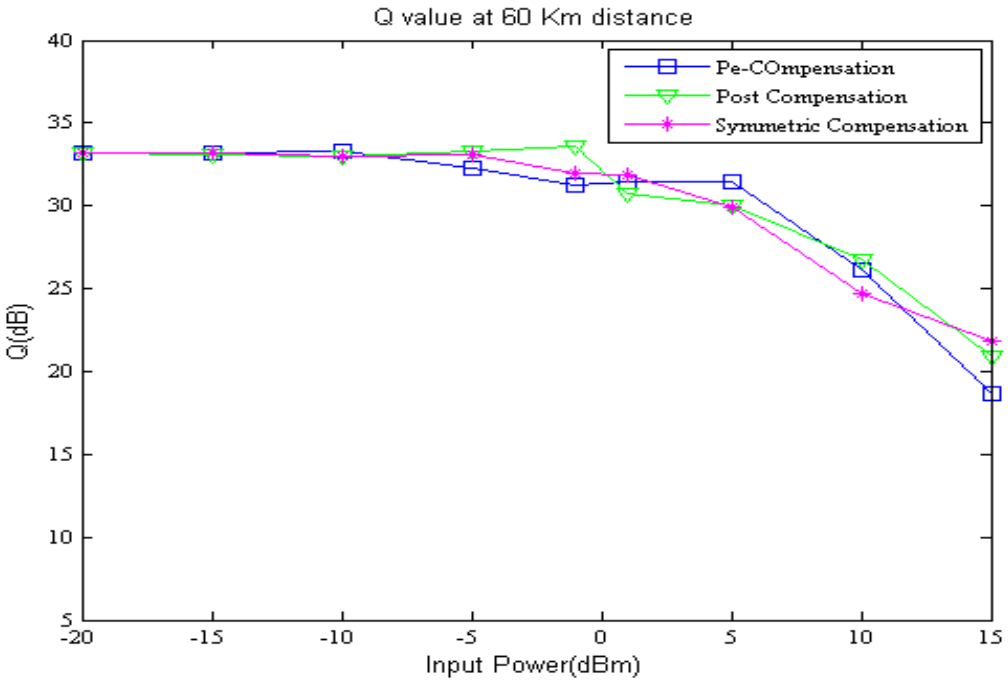

Fig. 3.14(b)

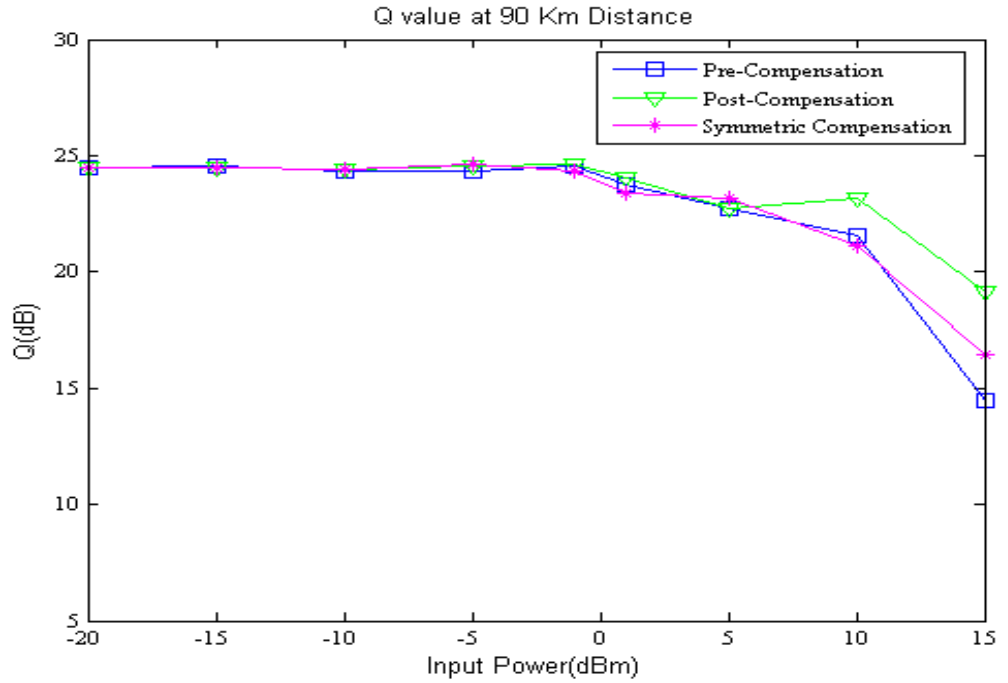

Fig. 3.14(c)

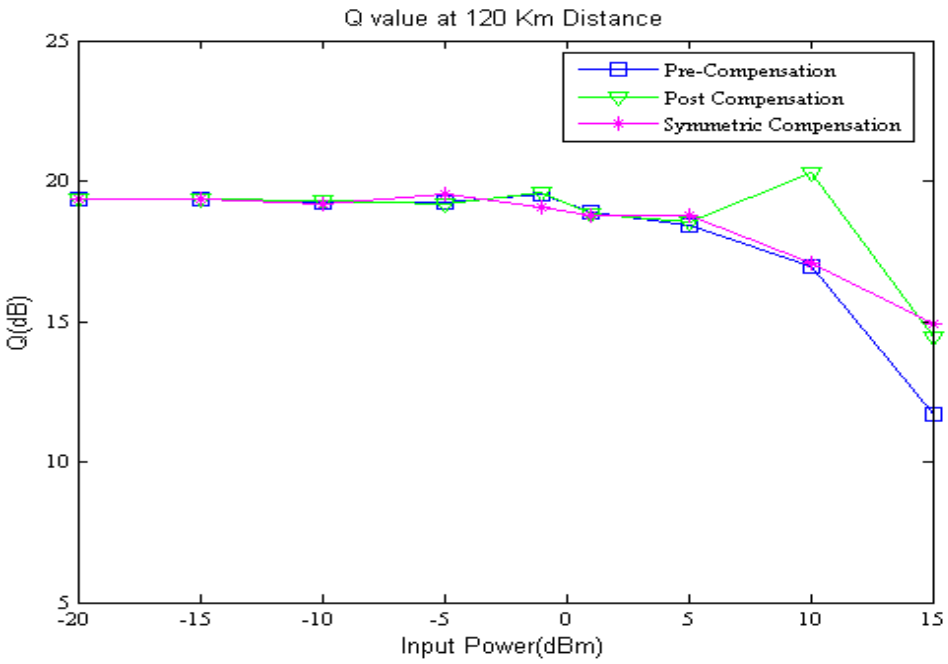

Fig. 3.14(d)

Fig. 3.14: Q value as a function of signal input power for a) span 1 (30 Km) (b) span 2 (60 Km) (c) span 3 (90 km) and (d) span 4 (120 km) for various dispersion compensation schemes

It is found that as the input signal power increases, Q value is initially maintained for all the three schemes up to –10 dBm and beyond this it starts decreasing due to the dominance of non-linear optical Kerr's effects. Further, it is observed that the worst performance is shown by pre-compensation scheme. However, post and symmetric compensation schemes follow each other closely with post giving better results even at 15 dBm of input power.

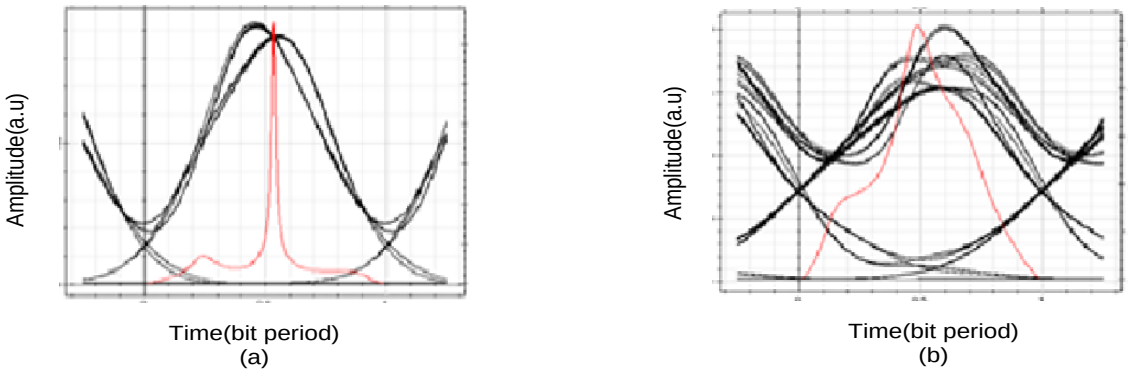

Fig. 3.15: Eye diagrams of CSRZ modulation format at Pin= -10 dBm for post compensation scheme at a distance of (a) 30 Km (b) 120 Km

The best Q value obtained is 45.46 dB at input power of -20 dBm using post-compensation scheme at a distance of 30 Km while Q falls to 19.35 dB at a distance of 120 km. Since the performance of post-compensation scheme is the best hence we have further analysed this scheme to predict the eye diagrams at the receiver as shown in Fig. 3.15. The shape of the eye as well as the eye opening decreases with the distance.

It is thus established that post compensation scheme shows a better performance in terms of Q value and eye opening as compared to pre and symmetrical dispersion compensation schemes. The CSRZ format although robust against GVD and SPM effect due to narrow spectral width, but still DWDM transmission causes more degradation owing to inter-channel XPM and FWM due to spectral broadening. The wave frequencies interacting through FWM lead to the generation of sum and difference frequencies, which further interact among each other leading to increased bandwidth. To accommodate the expanded pulse bandwidth, the used filter bandwidth has been chosen three times so that the higher order FWM products are aliased CSRZ format results in the expansion of optical spectra and reduction in the Q value at large distances. In addition, carrier suppression reduces the efficiency of four wave-mixing in WDM systems**.** Thus, it is inferred that CSRZ format shows a better suitability for DWDM systems over the conventional NRZ / RZ.

3.5. Simulation Set-Up for Duobinary Format (DRZ)

Duobinary format has shown the most promising results for the deployment of 40 Gbps technology on the existing 10 Gbps WDM transmission. The main advantage of DRZ format is their high dispersion tolerance and narrowband optical filtering. In this work, a 32 channel 40 Gbps Duobinary modulated DWDM transmission system is designed and simulated for long haul applications. Till now, this format has been studied for WDM systems with 50 GHz channel separation [173], but with lesser number of channels or at a lower data rate [174]. Here, 32 DRZ transmitters are multiplexed over the fiber to study the influence of pre, post and symmetrical dispersion compensation schemes under two cases (i) perfect dispersion compensation (D = 0) (ii) residual dispersion (D ≠ 0). The residual dispersion scheme is further divided into two cases (i) under compensation and (ii) overcompensation depending on the compensation ratio (CR).

The link is optimized and results are concluded on the basis of Q value and eye opening for multiple transmission spans for varying signal input powers. The proposed 32 channel DWDM system consists

of a DRZ transmitter, fiber and photodetector receiver as shown in Fig. 3.13 with the central frequency of the first channel as 193.1 THz. The simulation parameters are specified in Table 3.3.

Table 3.3: Simulation parameters

Bit rate	40 Gbps
Sequence length	64
Samples/bit	256
DWDM channel spacing	50 GHz
Central frequency of the 1st channel	193.1 THz
Capacity	32-channel 40-Gbps
Distance	60 Km X N Spans
Input Power	-1 dBm

A. Transmitter section

The WDM transmitter consists of a PRBS generator, CW lasers, data modulators, filters and the optical multiplexer. The PRBS generator generates bit sequences at the rate of 40 Gb/s with $2^7 - 1$ bits. The emission frequencies of CW lasers are equally spaced and are in the range of 193.1–194.65 THz with 50 GHz channel separation. The extinction ratio of MZM's is set at 30 dB. Each CW laser is driven by a DRZ transmitter as shown in Fig. 3.9. The modulated optical signal is fed to the 32 input ports of an optical multiplexer. To avoid crosstalk between the adjacent channels, before multiplexing, each channel is optically filtered with a second order Gaussian filter having a bandwidth of 50 GHz.

B. Fiber section

The combined optical signal is then fed into the SMF. The fiber model in OptiSytem takes into account the unidirectional signal flow, stimulated and spontaneous Raman scattering, Kerr-nonlinearity and dispersion. Scalar model of both the fibers has been considered to negate the PMD. The fiber parameters used are given in Table 3.2. EDFA's with noise figure of 4 dB are placed after each fiber such that their gain compensates for the losses in the preceding fiber. The signal is then launched over N spans of 60 km each. Fig. 3.13(a) shows the schematic of pre-compensation scheme where a DCF of 10 km is used before the SMF of 50 km length to compensate for the dispersion and the nonlinearities. The gain of the EDFA's used in the link is 5 dB and 11 dB, respectively. The post-compensation scheme is shown in Fig. 3.13(b) where to combat the accumulated dispersion a DCF of 10 km is used after a 50 km SMF. In symmetrical-compensation scheme, a 10 km DCF is used in between the SMF of 50 km as shown

in Fig. 3.13(c). Here, three in-line-EDFA's with a gain of 5.5 dB, 5 dB and 5.5 dB, respectively are used

C. Receiver section

The receiver consists of the de-multiplexer, PIN detector, filters and 3R regenerator. To the 32 output ports of the optical de-multiplexer, Bessel band pass filters with parameters: 3 dB cut off frequency = 47 GHz, order = 4, depth = 100 dB have been connected to separate out the individual channel. The filter parameters have been optimized to give the best result. This optical signal is then passed through PIN photodiode whose reference frequency is in the range from 193.1–194.65 THz respectively, responsivity [A/W] =1 and dark current = 0.1 nA. An electrical low pass Bessel filter follows the PIN photodiode whose cut-off frequency is determined by the modulation used and is optimized at 90 GHz with order 3. Thereafter, a 3R regenerator is connected to the BER analyzer which generates graphs and results such as eye diagrams, BER, Q value, eye opening etc.

3.5.1. Results and Discussions for DRZ format

The system analysis has been done under two cases: zero and residual dispersion in the link. For perfect compensation, the parameters of DCF and SMF are chosen such that the first-order dispersion is compensated exactly (D = 0) i.e. $D_{SMF}\, L_{SMF} = D_{DCF}\, L_{DCF}$. However, for. maintaining some residual dispersion ($D \neq 0$) in the link, the CR has been varied from 95 % to 105 % to find the optimum value of compensation length for pre, post and symmetrical schemes [175]. In this case the optimized DCF length was 9.98 Km (less than 10 Km) which implies undercompensation case.

For system analysis, the results of the 16th channel have been considered as it corresponds to the worst-case scenario. Fig. 3.16 (a) - (g) and Fig. 3.17 (a) - (g) depict the graphical representation of Q value for perfect compensation and under compensation cases, respectively as a function of transmission distance for power varying from 10 dBm to -15 dBm for all the three schemes. For a high data rate WDM system it is desirable that the input power should be as low as possible to limit non-linear effects. Keeping this in mind, the input power has been varied from -15 dBm to 10 dBm.

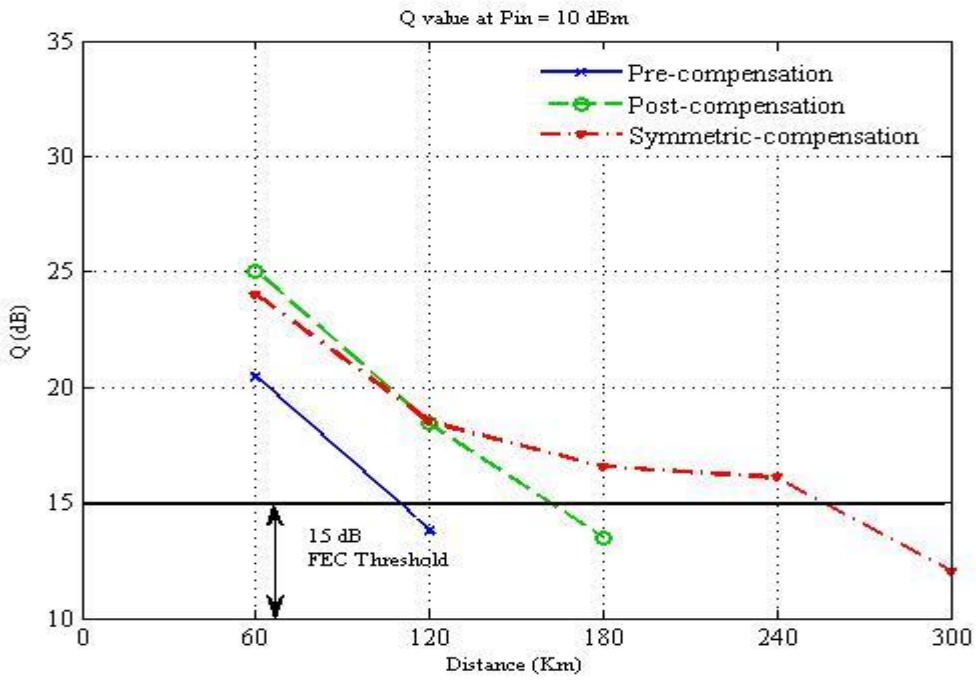

Fig: 3.16(a)

Transmission performance over different distances reveals that, in perfect compensation case the duobinary format shows the best performance in pre-compensation scheme whereas with under compensation, symmetric configuration outperforms the pre and post scheme. It can be clearly seen that for the same power level using under-compensation the transmission distance nearly doubles for all the three schemes though the starting value of Q is lesser.

Though generally we do not operate at power level greater than 5 dBm per channel, the designed system works well even at 10 dBm. Also, it can be seen that as the signal input power increases, Q value is initially maintained for all the dispersion compensation schemes and then it starts decreasing. This is evident from the fact that for low power values, the non-linear effects coming into picture are very insignificant. However, as the power increases, the pulses tend to spread out overlapping with each other as the non-linear effects like FWM and XPM start dominating reducing the Q value. This is in close agreement with the reported results [176].

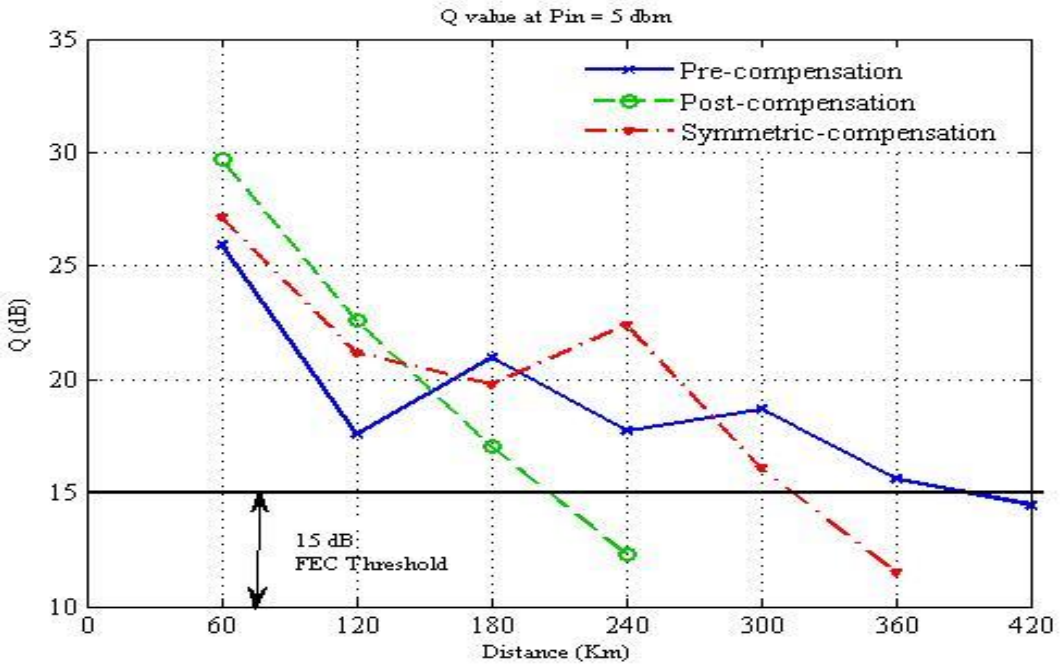

Fig: 3.16(b)

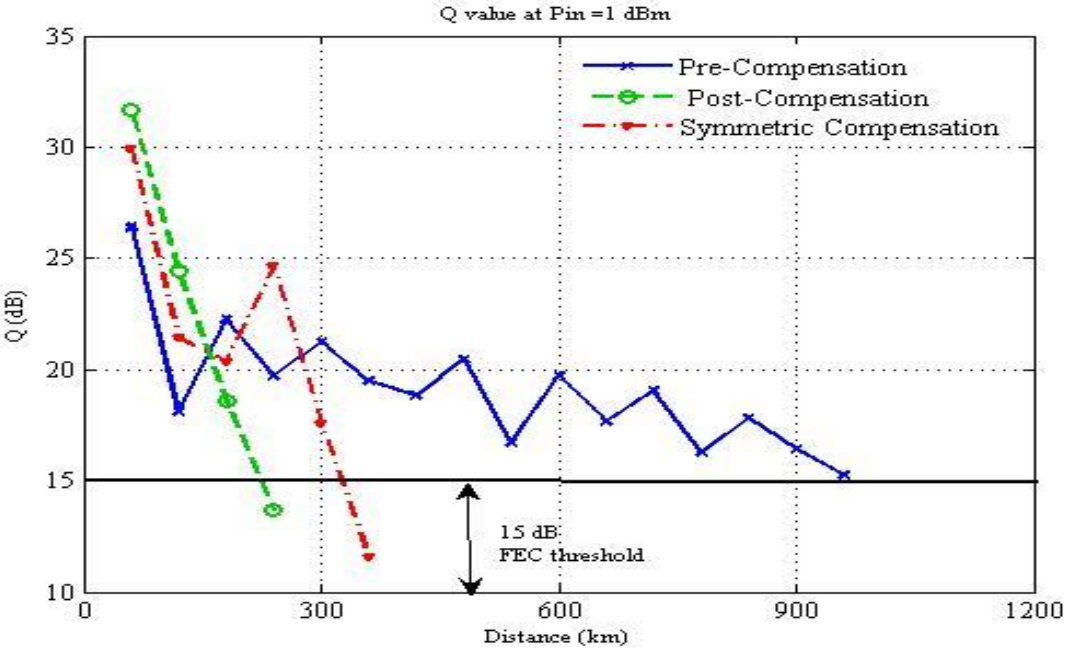

Fig: 3.16(c)

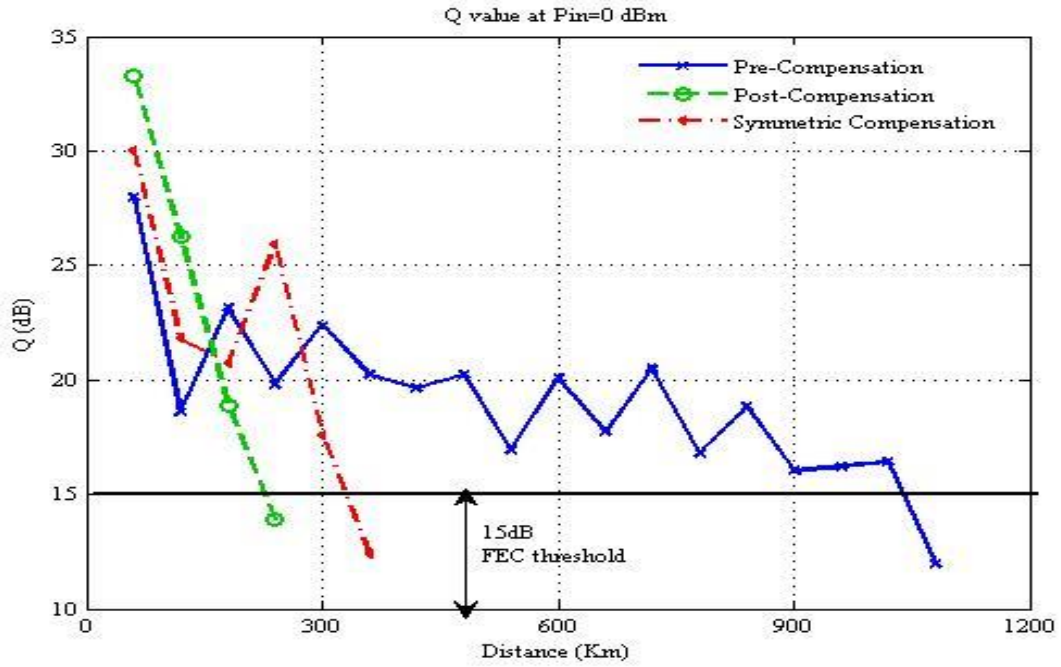

Fig: 3.16(d)

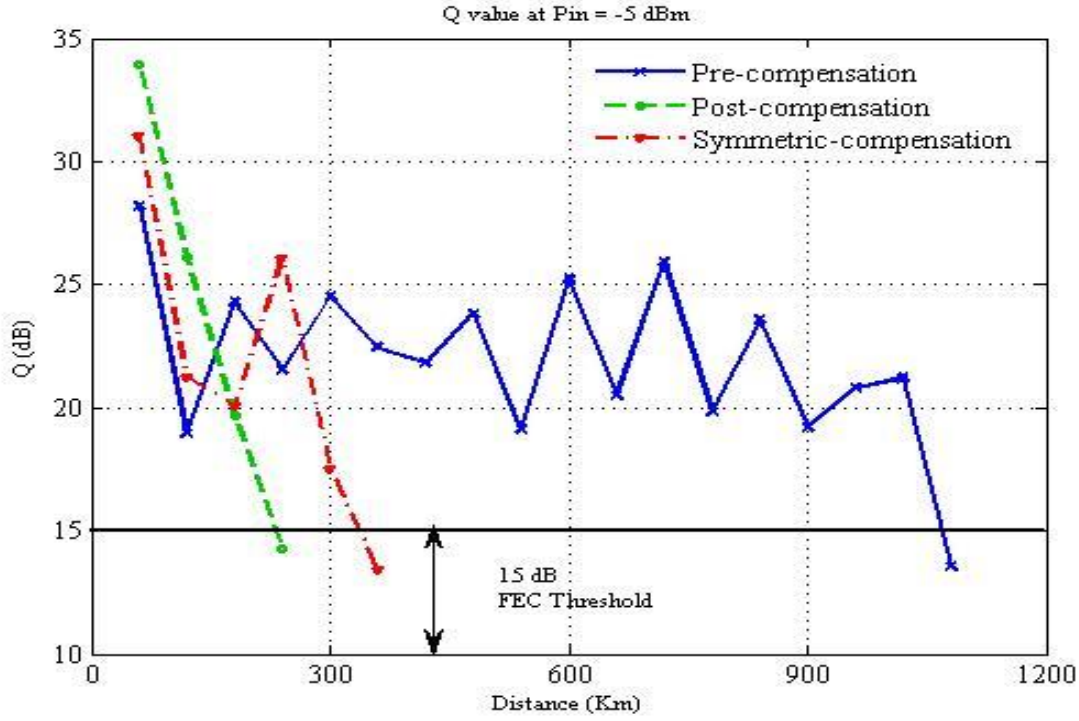

Fig: 3.16(e)

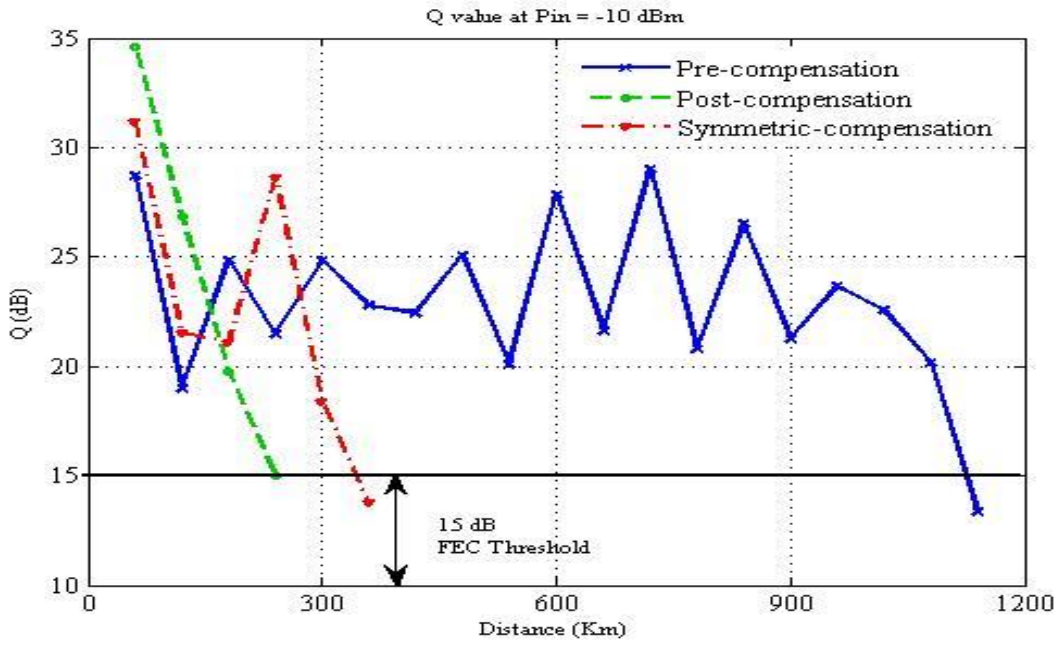

Fig: 3.16(f)

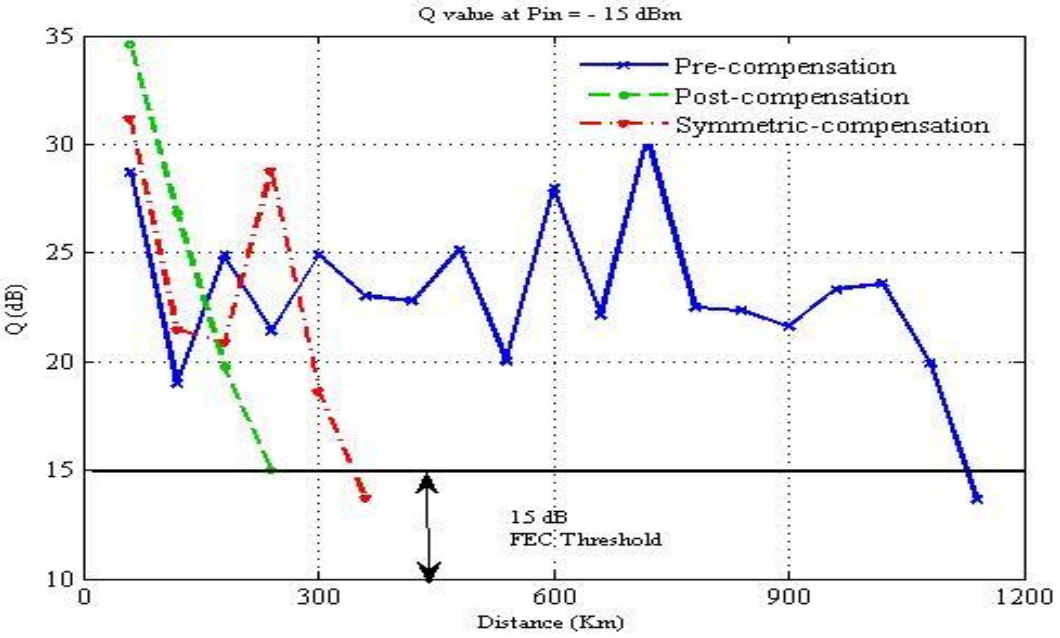

Fig: 3.16(g)

Fig. 3.16: Q value as a function of transmission distance for perfect compensation (D=0) with different dispersion compensation schemes: (a) Pin = 10 dBm, (b) Pin = 5 dBm, (c) Pin = 1 dBm, (d) Pin = 0 dBm, (e) Pin = -5 dBm, (f) Pin = -10 dBm, (g) Pin = -15 dBm,

For perfect compensation, though in post and symmetric schemes Q value falls below the minimum required 15 dB in 3 or 4 spans only, but for pre scheme the Q value is maintained above the threshold up to 18 spans i.e. 1080 km for -10 dBm and -15 dBm as shown in Fig. 3.16 (f)-(g). At a high power level of 10 dBm symmetric scheme performs better than pre or post schemes traversing a distance of 240 Km as shown in Fig 3.16 (a). The best Q value obtained is 34.44 dB at input power of -15 dBm at 60 km using post-compensation. Though the Q value for pre scheme is slightly less 28.72 dB for the same distance but it maintains itself over a considerably large distance, falling to 13.63 dB at 1140 km.

For undercompensation case, post and symmetric schemes behave in a nearly similar fashion for power levels from 10 dBm to -5 dBm with symmetrical performing moderately better till 2100 Km as shown in Fig. 3.17 (a)-(d). This is an improvement over the results reported in [177]. It is seen in Fig. 3.17(e) that for transmission distances greater than 3500 km the Q value drops below the threshold value of 15 dB due to the impact of intra-channel FWM and ASE noise of EDFA's. The most interesting results are observed at low power levels of -10 dBm and -15 dBm where the symmetric scheme achieves a distance of 8000 km and 12000 km, respectively as shown in Fig. 3.17 (f)-(g). At these powers even pre scheme shows good performance till 2500 km and post till 4000 Km.

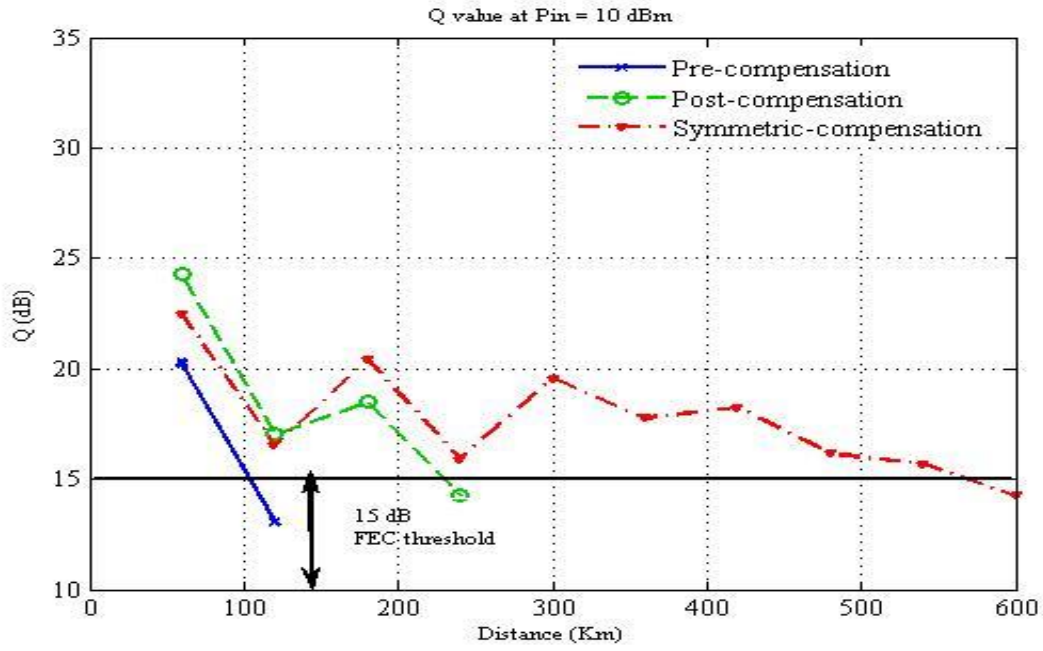

Fig. 3.17(a)

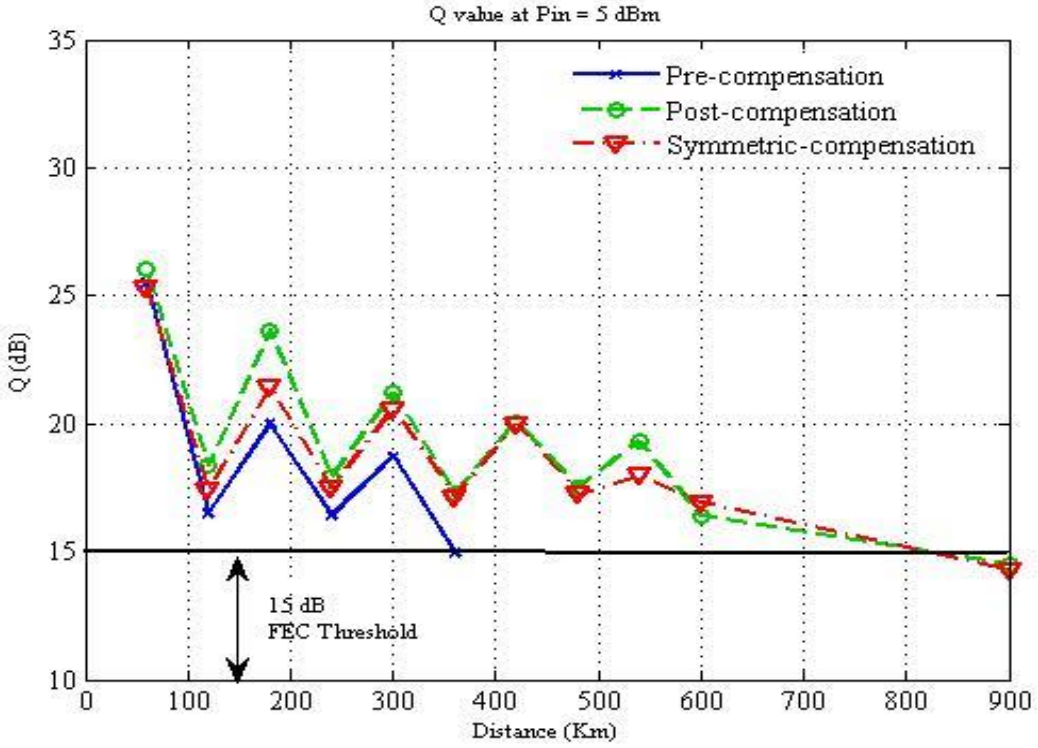

Fig. 3.17(b)

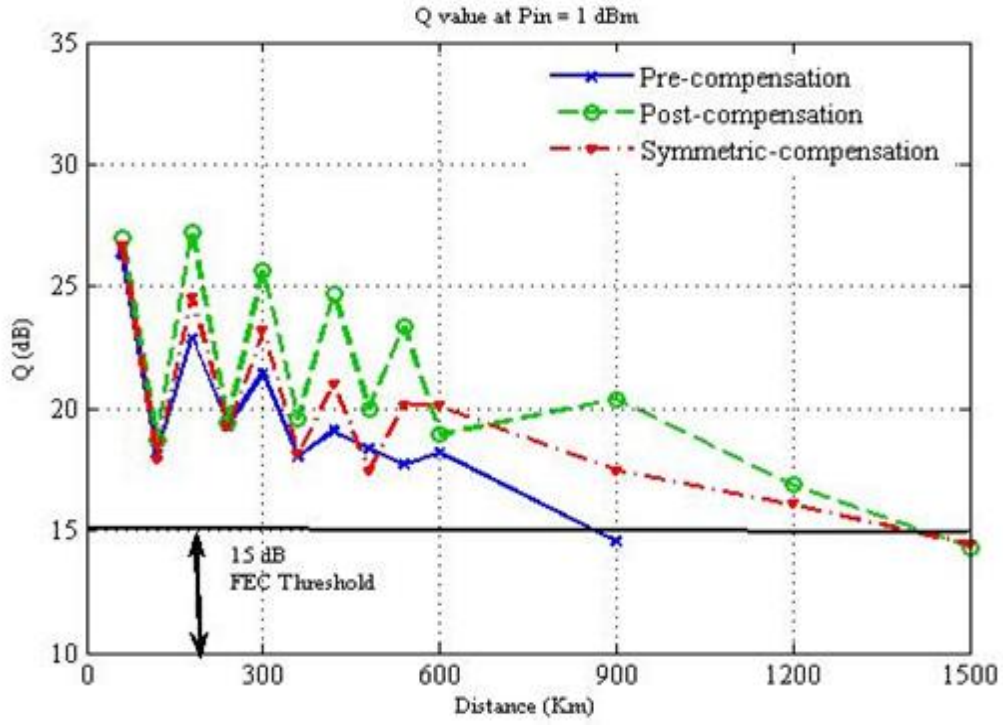

Fig. 3.17(c)

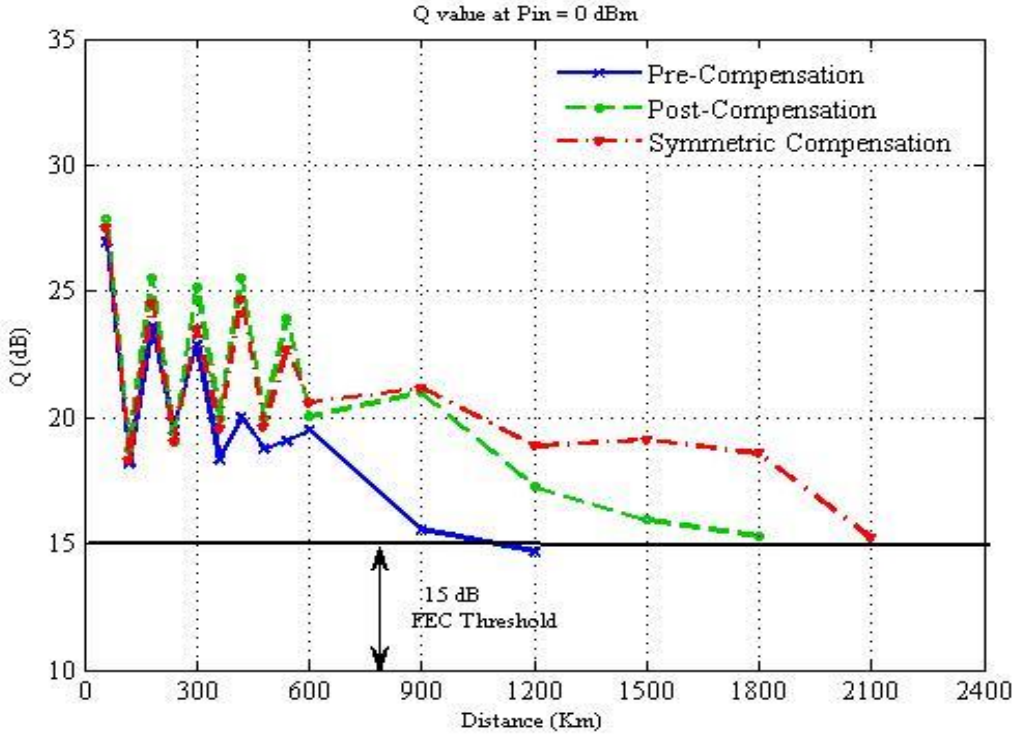

Fig. 3.17(d)

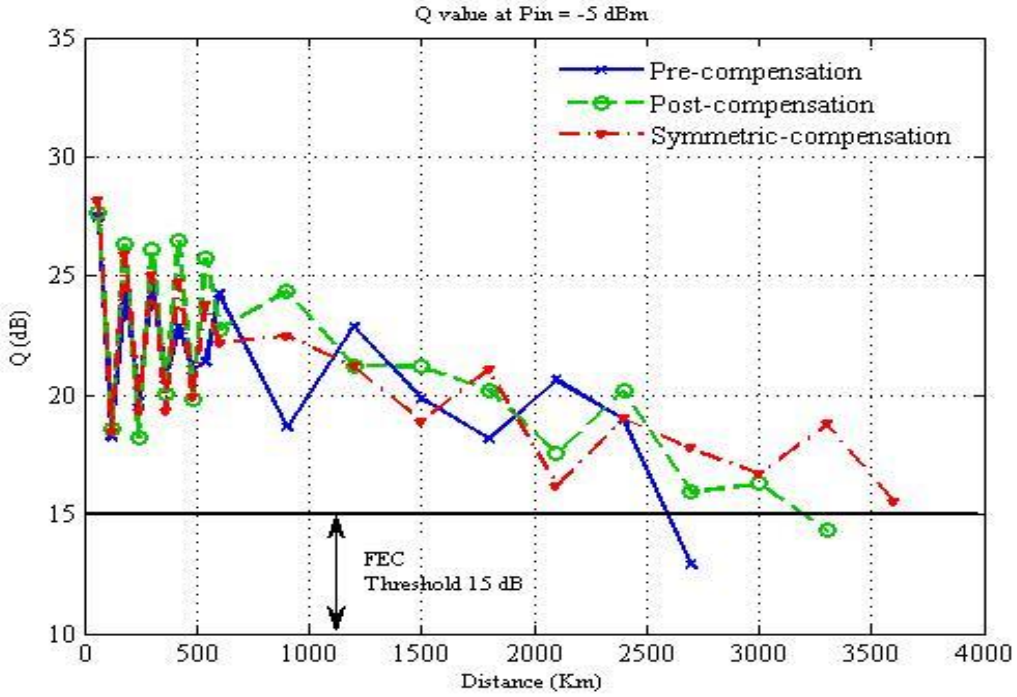

Fig. 3.17(e)

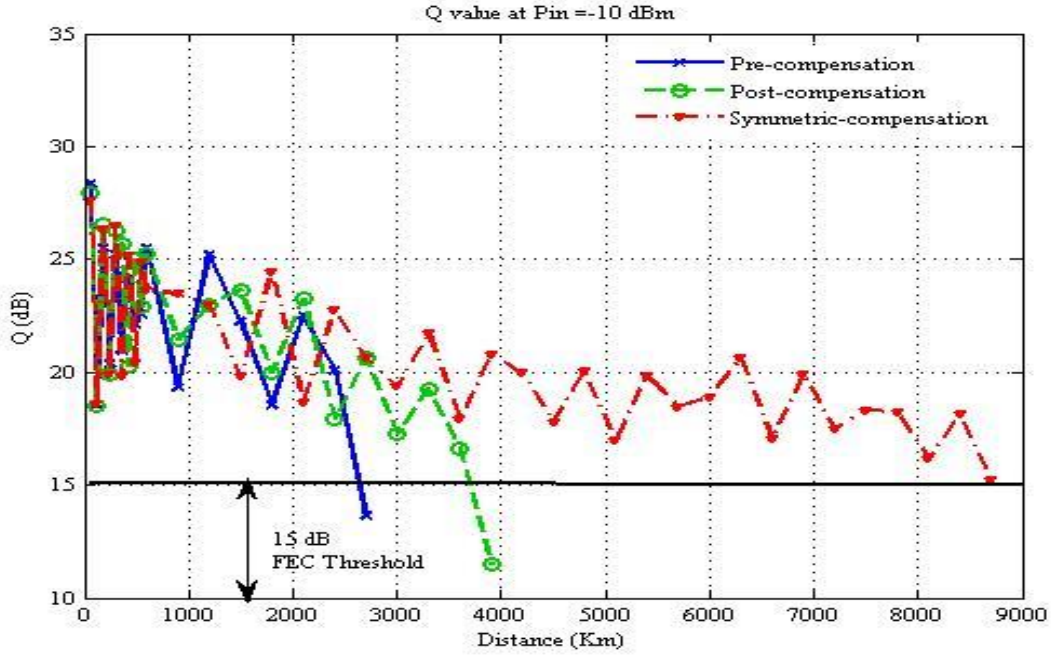

Fig. 3.17(f)

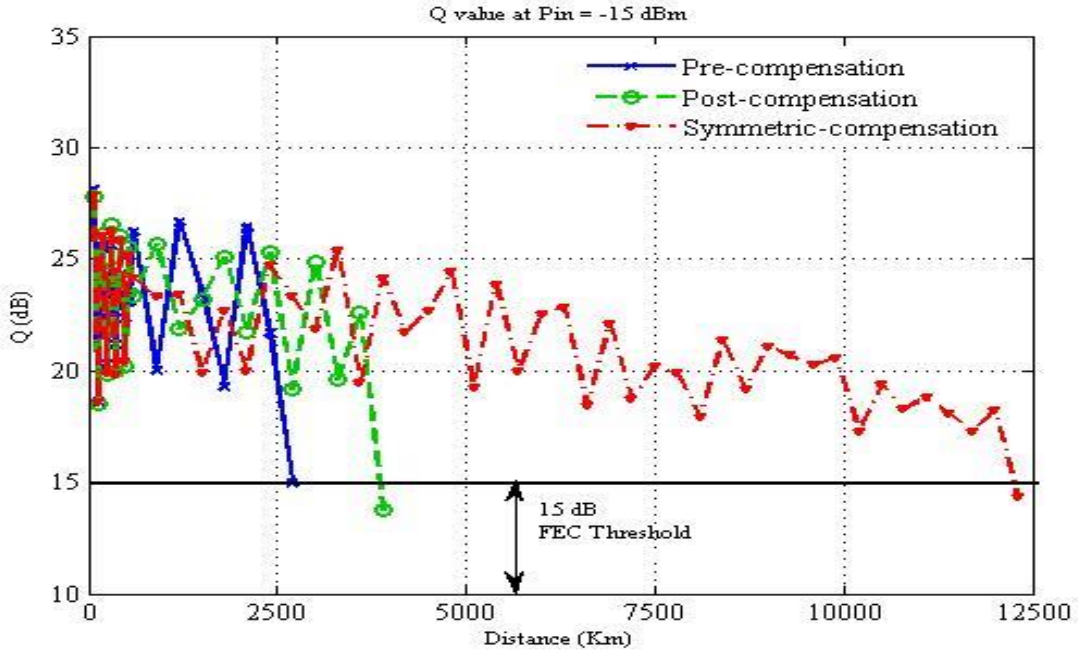

Fig. 3.17 (g)

Fig 3. 17. Q value as a function of transmission distance for under compensation ($D \neq 0$) with different dispersion compensation schemes: (a) Pin =10 dBm, (b) Pin = 5 dBm, (c) Pin = 1 dBm, (d) Pin = 0 dBm, (e) Pin = -5 dBm, (f) Pin = -10 dBm, (g) Pin = -15 dBm.

This work presents a simulation setup to analyze a 32 channel x 40 Gbps DWDM system for long haul transmission distance using DRZ modulation format. The designed system has been investigated to evaluate its performance for pre, post and symmetrical dispersion compensation schemes for various input signal power. It is found that as the signal input power increases Q value starts decreasing due to the dominance of non-linear optical Kerr's effects like cross phase XPM and FWM. It is concluded that the symmetrical compensation scheme shows a superior performance in terms of Q value and eye opening as compared to pre and post schemes for under-compensation while the pre-scheme shows a better performance with perfect compensation. DRZ format being robust against the fiber nonlinearities and optical Kerr's effect can be used for long haul transmission distance with the undercompensation method. The maximum transmission distance achieved is 9000 Km at -10 dBm input power and is 12000 km at -15 dBm power using symmetrical scheme with under-compensation.

3.6. Simulation Set-up for Modified Duo-binary Return-to-Zero (MDRZ) Format

MDRZ format has a much narrower optical bandwidth over the DRZ leading to greater dispersion tolerance and higher fiber non linearity tolerance [177, 178]. This format has been examined till now for DWDM systems [179], but involving lesser number of channels (typically 8 or 16) or at data rate lesser than 40 Gbps [180]. Here, a simulation study is performed to test the proposed 40 Gbps MDRZ modulated system and compare its transmission performance under typical physical impairments with the conventional duobinary transmission. These formats are also investigated to analyze the influence of various dispersion management methods such as pre, post and symmetric schemes. These schemes are studied with both perfect dispersion compensation and residual dispersion as discussed previously and results are concluded by varying the input signal power, on the basis of received Q value and eye opening information for various transmission spans. Here, the link was optimized for best performance at a DCF length of 10.044 Km which implies over-compensation of dispersion. The study also explores the potency of the integration of unequal channel spacing for suppression of FWM in such optical link.

The simulation results are derived by solving the NLSE analytically using the SSFM. The parameters used in simulation are highlighted in Table 3.4. The proposed DWDM link consists of 32 data modulated MDRZ transmitters, a fiber section and 32 optical receivers as shown in Fig. 3.13.

A. Transmitter section

The DWDM transmitter setup comprises of a PRBS generators, DRZ and MDRZ modulators for the respective cases, CW lasers, filters and the optical multiplexer and demultiplexer. The bit sequence is generated by the PRBS generator at 40 Gbps data rate with 2^9 –1 bits. The CW lasers emit equally spaced frequencies between 193.1–194.65 THz with 50 GHz channel spacing. MZM's with extinction ratio of 30 dB are used. CW laser is driven by a data modulator shown in Fig 3.9 and Fig 3.11 for DRZ and MDRZ respectively to generate the modulated optical signal which acts as the input for the 32 input ports of an optical multiplexer. Crosstalk between the adjacent channels is avoided by optical filtering each channel using a second order Gaussian filter with a bandwidth of 56 GHz in the multiplexer.

Table 3.4: Simulation parameters

Bit rate	40 Gbps
Sequence length	128
Samples/bit	64
DWDM channel spacing	50 GHz
Central frequency of the 1st channel	193.1 THz
Capacity	32-channel 40 Gbps
Distance	60 Km X N Spans
Input Power	-1 dBm

B. Fiber section

The multiplexed optical signal is then launched over the SMF. Table 3.5 enlists the fiber parameters used. The fiber model considers attenuation, Kerr non-linearities, unidirectional signal flow, dispersion effects and both stimulated as well as spontaneous Raman scattering. To suppress the deleterious effects of dispersion over the link we have considered the three possible placement strategies of DCF in the link (i) before the SMF called as pre-compensation scheme (ii) after the SMF referred as post compensation scheme and (iii) symmetrical compensation scheme in which DCF is set between split SMF's as shown in Fig. 3.13. All the configurations have been explored and the best one is used in analysis of results. The length of the DCF is set such that the dispersion accumulated in SMF is cancelled out. Negation of PMD is done by considering the scalar model of both the fibers. Fig. 3.13(a) outlines the pre-compensation scheme where dispersion and the nonlinearities are compensated by using 10 km DCF before the 50 Km SMF. The gain of EDFA's is set to overcome the attenuation encountered as signal propagates over both the fibers and is 5 dB and 10 dB, respectively. Fig. 3.13 (b) shows the model used for post-compensation scheme wherein a 10 km DCF is used after a 50 km SMF to combat the accumulated dispersion. Symmetrical-compensation scheme uses a 10 Km DCF between

the SMF of 50 Km as shown in Fig. 3.13(c). It uses three in-line-EDFA's each with 5 dB gain, to compensate for losses and a noise figure of 4 dB. The combined signal is then launched over N spans of 60 km each.

Table 3.5: Fiber parameters

Fiber	Attenuation (dB/Km)	Dispersion (ps/km- nm)	Dispersion Slope (ps/km-nm^2)	Mode Effective Area	Non linear refractive index (n_2)
SMF	0.2	17	0.08	80	2.6×10^{-20}
DCF	0.5	-85	-0.45	30	2.6×10^{-20}

C. Receiver section

The complete receiver realization involves the de-multiplexer, PIN detector, filters and 3R regenerator. At each of the 32 output ports of the optical de-multiplexer 2nd order Gaussian band pass filters having 3 dB cut off frequency as 40 GHz, and depth of 100 dB are used to filter out the individual channels. The filter parameters also have been optimized and various orders and cut-off frequencies were explored to arrive at the best possible value practically. This filtered optical signal passes through individual PIN photodiodes with responsitivity [A/W] of 1 and dark current of 0.1 nA, corresponding to incoming reference frequency range i.e. 193.1–194.65 THz respectively. The electrical signal from PIN photodiode then passes through a 4th order electrical low pass Bessel filter whose cut-off frequency depends on the modulation format used and is optimized at 32 GHz. Thereafter, a 3R regenerator is connected to the BER analyzer which generates graphs and results such as eye diagrams, BER, Q value, eye opening etc.

3.6.1. Performance Investigation and Analysis

The performance of both DRZ and MDRZ formats was first investigated for all the three schemes i.e. pre, post and symmetrical dispersion compensation in terms of the received maximum Q value and eye opening. For system analysis, the results of the 1st channel were studied to correlate and infer the results of other adjacent channels. For both DRZ and MDRZ formats, the optimum performance was observed for the case of symmetrical dispersion compensation case which is in close agreement to the results reported in literature [181], and hence this scheme was used throughout this case. After finalizing on the symmetric scheme, we ran the simulations for two cases 1) Perfect compensation of GVD and, 2) Residual Dispersion compensation of GVD.

For perfect dispersion compensation case, the parameters of DCF and SMF are chosen with an objective to compensate the first-order dispersion exactly. However, to maintain a residual dispersion-per-span (RDSP) [21, 27] in each map, we varied the CR between 95% to 105% to find the optimum DCF length. This enables us to visualize the effects of both under compensation and over-compensation which further mitigates the influence of FWM and XPM. The optimum length of DCF was found to be 10.044 km which corresponds to the case of over compensation. It was readily seen that the performance of the link was improved substantially for MDRZ format by using over-compensation over both perfect and undercompensated case. Thus, overcompensation method has been used to design the proposed 32 channel long haul DWDM link. The present study also considers different power levels and varied combinations of the channel spacing to visualize the impact of non -linearity on the overall performance of the system

Fig. 3.18 (a) - (d) outline the performance of both DRZ and MDRZ format graphically for the over compensated case in terms of the Q value as a function of transmission distance. To support high data rate DWDM system, the input launch power must as low as possible to prevent the excitation of non-linear effects. Hence, the input power is varied from – 5 dBm to 10 dBm. It is clearly seen from Fig. 3.18 (a) that that at low launch power of -5 dBm DRZ scheme performs better than MDRZ in terms of satisfactory performance distance which is 1200 km for DRZ as compared to just 700 km for MDRZ after which the Q value drops below 15 dB threshold.

It is observed that Q value for MDRZ is greater for a shorter distance but with a relatively higher slope of attenuation degradation with length. This may be attributed due to the absence of high power carrier component in the MDRZ format. However, as the signal propagates, the accumulated scattering induced non-linearity adds up and degrades the performance and Q value. Obviously channel impairments owing to non-linearity become more challenging for a multi-channel high power DWDM system design. This led to the evaluation of the performance of such systems for various power levels. Similar analysis made for 0 dBm of launch power is presented in Fig. 3.18 (b) which shows nearly same qualitative behavior with a quantitative difference. DRZ here achieves a distance of 2700 km while MDRZ manages around 2000 km which again is an improvement over the -5 dBm case.

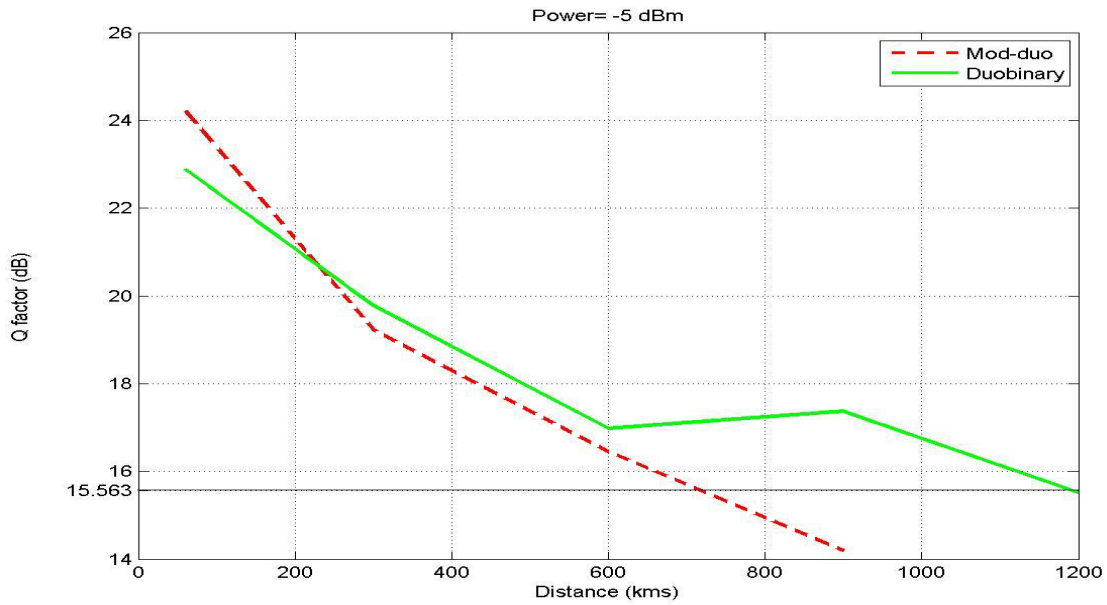

Fig. 3.18 (a)

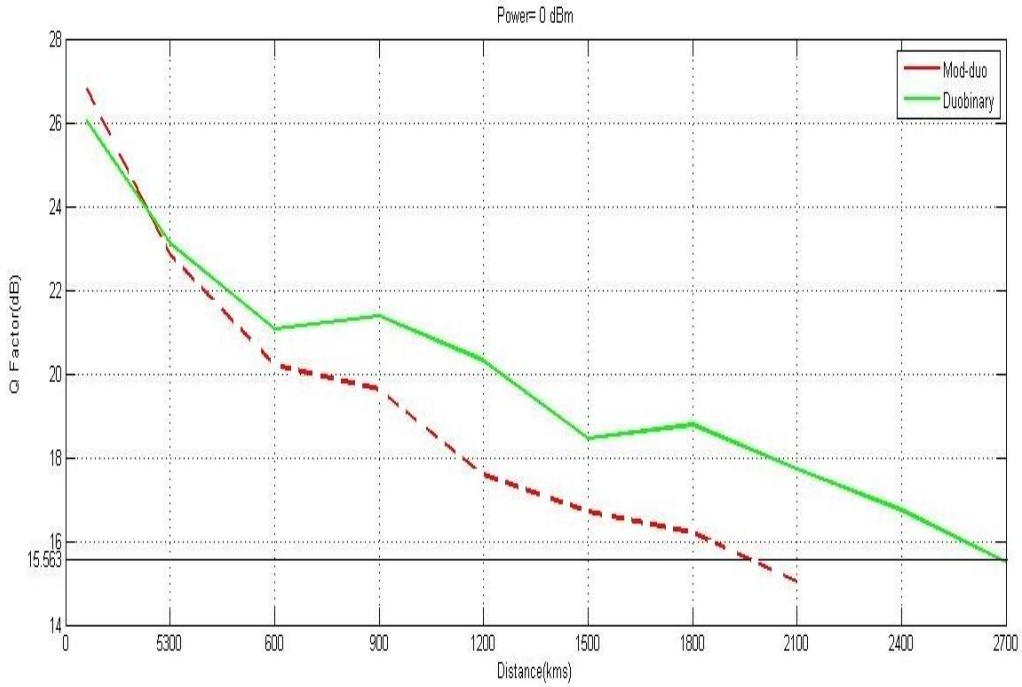

Fig. 3.18 (b)

As the launch power was further increased it is seen that, the DRZ format does not shows significant improvement in the maximum achievable distance but MDRZ still performs better up to 2700 km. Another important inference can be made when we further increase the launch power to 5 dBm as shown in Fig. 3.18(c) where MDRZ format performs better than DRZ accomplishing a total distance of 2100 km while for DRZ the distance decreases to 1600 Km.

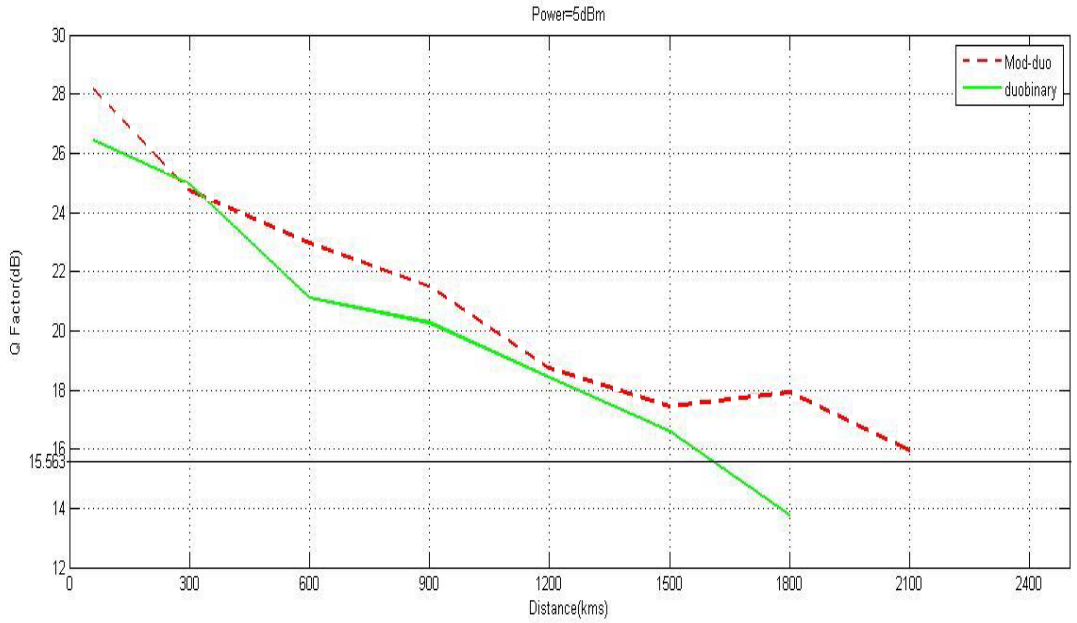

Fig. 3.18 (c)

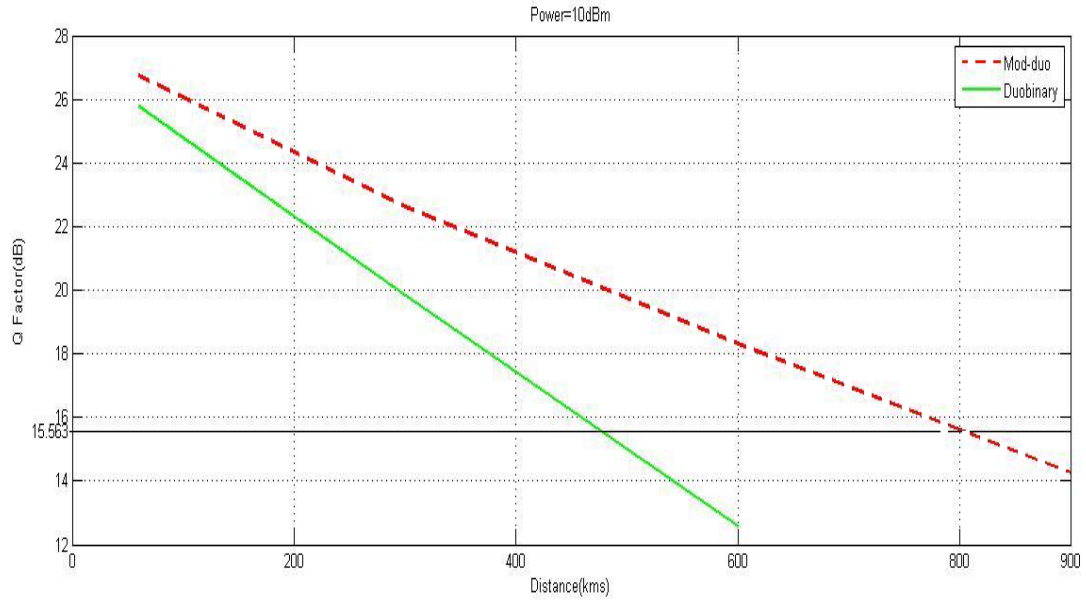

Fig. 3.18 (d)

Fig. 3.18: Q value as a function of transmission distance for (a) Pin = - 5 dBm (b) Pin = 0 dBm (c) Pin = 5 dBm (d) Pin =10 dBm

Though the distance has decreased for both the formats at higher launch power due to the evolution of non-linearities, but even at this power satisfactory performance is achieved with MDRZ format up to

2000 km. Though most of the designed systems don't work satisfactorily at a power level higher greater than 5 dBm, but the proposed system works smoothly even at 10 dBm power with MDRZ format consistently performing better than DRZ as shown in Fig. 3.18 (d). While for DRZ, Q falls off at around 500 Km, MDRZ manages transmission over 500 Km. This observation reinstates the affirmation that both DRZ and MDRZ formats are suitable for systems operating at high power levels, with MDRZ showing good performance even at 10 dBm. Thus we can infer that for high-speed optical transmission systems, duobinary coding significantly increases system dispersion tolerance while at the same time reducing the sensitivity to non-linear effects while providing higher spectral efficiency.

Owing to the superiority of the MDRZ format over DRZ, this format was analyzed for unequal channel spacing, for 16 and 32 channels to observe the impact of FWM cross products on such systems using reported algorithm [182]. The study has also been extended for equal channel separation of 100 GHz for 32 channels under perfect compensation scheme requiring a total bandwidth of 3.1 THz. For the unequally spaced case, a minimum channel spacing of 50 GHz is considered and the channel separations are, respectively, 125, 100, 75 and 50 GHz and vice versa resulting in the total unequal bandwidth of 2.675 THz. Fig. 3.19 (a) and Fig. 3.19 (b) shows the comparison of equal vs. unequal channel spacing for 16 channels and 32 channels, respectively.

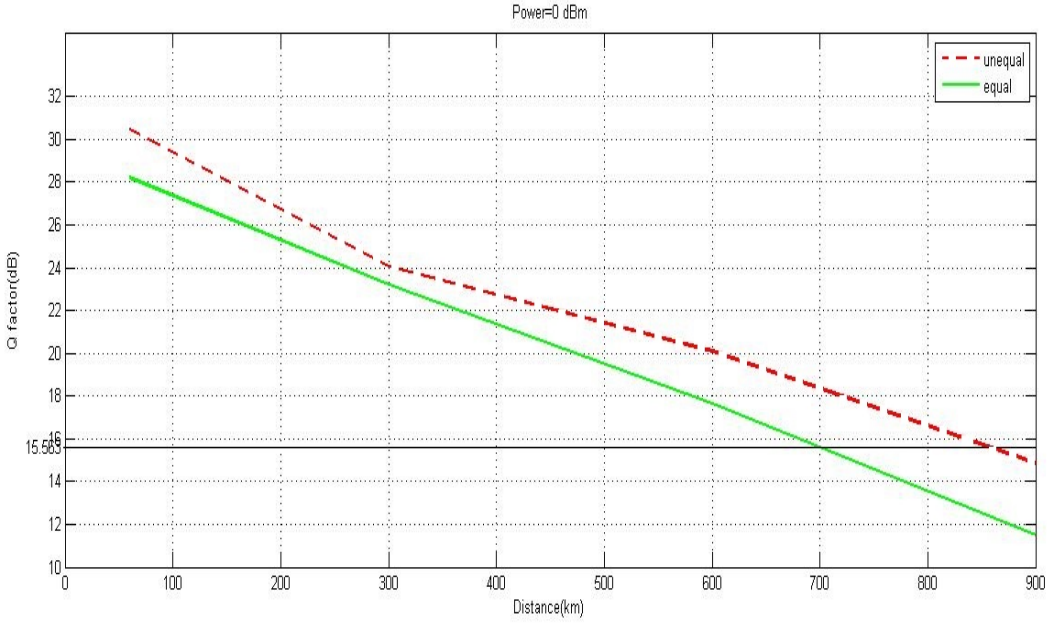

Fig. 3.19(a)

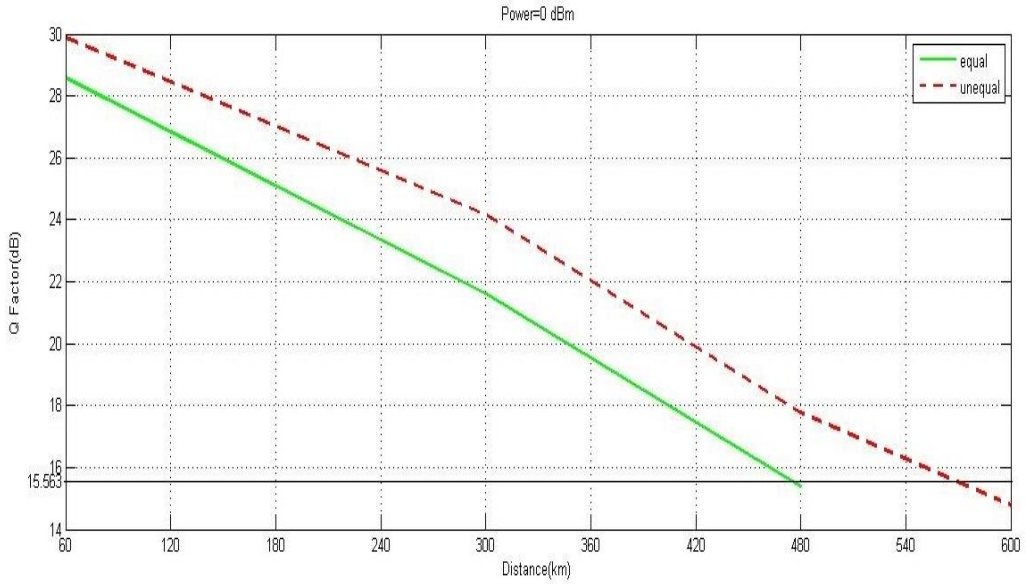

Fig. 3.19(b)

Fig. 3.19: Comparison of MDRZ format with equal and unequal channel spacing for (a) 16 channel (b) 32 channel case.

It is inferred that in both cases the unequal channel spaced network performs better than the equal one. The maximum distance for 32 unequally spaced channels at 0 dBm launch power is around 600 km as compared to 450 Km for the equal channel case. Moreover, there is an added advantage of bandwidth saving when using unequal channel separation which saves around for ~ 225 GHz for the 16 channel case, and approximately ~ 425 GHz for 32 channel case which is considerable bandwidth saving.

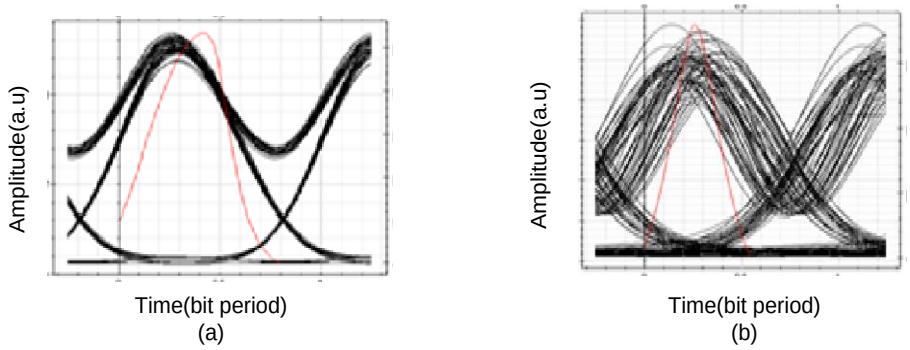

Fig. 3.20. Comparison of eye diagrams for MDRZ format at 5 dBm launch power after (a) 60 Km and (b) 1800 Km obtained from BER analyzer

The received eye diagrams of the first channel for MDRZ format is shown in Fig. 3.20 for a launch power of 5 dBm. Fig. 3.20 (a) depicts the wide eye at a distance of 60 km while Fig. 3.20 (b) shows the eye diagram after signal propagates through 30 spans i.e. 1800 Km. The eye has become considerably distorted as a result of the FWM crosstalk arising due to the interference between the transmitted channels and the FWM products generated at the channel frequency. Thus, it is concluded that for DWDM systems MDRZ format performs better as compared to the conventional NRZ/RZ owing to its higher tolerance to inherent noise, inter-channel cross-talk, FWM spurious products along with improved receiver sensitivity at higher power.

This work demonstrates the design of a 32 channel DRZ and MDRZ modulated optical link operating with 50 GHz channel separation up to 2700 km using over compensation technique. The simulated design has been investigated to evaluate optimum long haul distance by using different dispersion compensation schemes for varying input signal power. The simulation predicts that the symmetrical compensation scheme is a superior choice compared to pre and post schemes. It is also inferred that over compensation of the residual dispersion per span makes DRZ and MDRZ superior for long haul applications. MDRZ scheme performs substantially better than DRZ at higher launch powers by suppressing the discrete frequency tones.

3.7. Summary

This chapter presented the various intensity modulated formats such as NRZ, RZ, CSRZ, DB and MDB. The transmitter design of each format was discussed and simulation set up for 32 channel DWDM system has been explored in detail. The proposed design strategy for non-linear effect mitigation with superior dispersion management realizes an efficient DWDM system. The performance analysis is presented via graphs and conclusions for each modulation format are discussed in detail to understand the applicability of each scheme. It is clearly seen that in order to design an efficient optical network having maximum capacity it is important to take into account all the contributing facts, such as channel data rate, transmission distance, signal optical power, amplifier noise figure, channel wavelength spacing, optical amplifier spacing, fiber dispersion and nonlinear parameter, dispersion management strategy, receiver bandwidth and so on. In the next chapter phase modulated formats are investigated in detail.

Chapter 4

Link Optimization through Phase Modulation

In high speed DWDM optical transmission systems, appropriate modulation formats having good spectrum efficiency reduce non-linear transmission impairments effectively. There has been a considerable research on the impact of nonlinear effects on signal degradation to limit the speed and length of the DWDM links [183,184,185]. In such multichannel systems, XPM effect for OOK and DPSK format has been studied theoretically [27], numerically [186] and experimentally [187]. Due to random temporal waveform alignments of WDM channels, large variations of XPM degradation have been predicted for OOK and DPSK signals [27,187]. Raman crosstalk dynamics in OOK soliton WDM systems demonstrated the combined effect of delayed Raman response and bit pattern randomness on pulse propagation in optical fiber communication systems [188-190]. The propagation was described by a perturbed stochastic nonlinear Schrödinger equation and extensive numerical simulations were performed with the model to analyze the dynamics of the frequency moments, BER, and the mutual distribution of pulse position. In another study DPSK modulation was considered and stability of WDM DPSK transmission against Raman crosstalk effects under the influence of inter-pulse Raman crosstalk [185] was quantitatively explained. These approaches involve non-deterministic channel dynamics and thus become a very complex problem to visualize and model the system for its performance analysis.

Recently, several multi-bit per symbol optical modulation schemes have been proposed as a competitive method to achieve higher spectral efficiency with relaxed dispersion management and improved PMD tolerance [191, 192]. Using multilevel signaling it is possible to increase the data rate per channel, and thus improve the bandwidth efficiency. Multilevel modulation formats such as DQPSK double the transmission rate by transmitting more information in the phase of the optical carrier signal [193-195]. However, the corresponding DQPSK receiver requires more complex and costly components including delay interferometers and balanced detection photodiode receivers [196]. The above studies along with other reported literatures [32, 38, 43, 44, 48, 78, 197, 198] show the applicability of DPSK and DQPSK in optical communications for long haul optical link design.

Phase shift keying (PSK) is a digital modulation format in which information is carried by the phase of the signal. In electrical communication systems it is well established that phase modulation provides

better performance and thus it may also be tested for an optical encoding system. In the early days, the optical phase of the available sources was not stable enough to realize phase modulation schemes. However, in the recent years, with the rapid improvement in coherent sources with active optical phase locking capability, PSK scheme became feasible in practical optical systems. Phase modulation formats are an attractive alternative over the intensity modulation formats, as they provide better spectral efficiency and are highly tolerant to CD and channel non-linearities which facilitate a longer operating distance [199].

In the present chapter, the focus is to study the performance of DPSK and DQPSK modulation format for DWDM system. Both these formats have shown very promising results for the deployment of 40 Gbps technology over the existing 10 Gbps DWDM transmission infrastructures [200, 201]. Though these schemes require complex trans-receiver architecture as compared to the IMDD method, but they provide a significant improvement in the receiver sensitivity. In this chapter, first the suitability of DPSK modulation format for a 1.28 Tbps long haul DWDM optical link is investigated by proposing a design model on the basis of simulation study of a 32 channel transmission system. Further, a DQPSK based 32 channels 40 Gbps link is designed in Optisystem and its performance was compared to DPSK format. In order to realize a better physical intuition about the performance of such an optical link, a Matlab Simulink model based on the discussed mathematical model (Chapter 2) has been developed in the next phase to analyze the performance of a single channel DQPSK link. This block based Simulink model involving the linear and non-linear characteristics turns out be very time consuming and complex even for a single channel case and becomes much tedious in case of a multi-channel long haul system and thus we attempt a professional software platform to study and analyze a practical multi-channel optical link. However, to gain an intuitive understanding of high speed propagation, such a modeled system is quite helpful in developing a realistic practical long haul optical link. The following sections present the functional architectures of the DPSK and DQPSK transceiver used in simulation study.

4.1. Differential Phase Shift Keying (DPSK)

The use of DPSK in optical systems operating at moderate bit rates involving heterodyne detection were extensively studied in the early 1990s but could not be commercialized due to the requirement of phase matching and complex receiver design. The high capacity potential of such schemes motivated the researchers to innovate and implement suitable circuits for DPSK implementation [202]. This design relaxes the strict requirement on the laser source line width for an increased bit rate. Further,

DPSK design has been improved incorporating its various variants to exploit their spectrum distribution to enable long-haul, high capacity optical communication systems [203]. It has been observed that variants of DPSK like RZ-DPSK and CSRZ-DPSK exhibit a superior transmission performance than standard DPSK owing to its reduced SPM effect. The constant amplitude modulation in this scheme mitigates the non-linear impairments by reducing the pattern-dependent nonlinear effects such as XPM by making the amount of XPM-induced nonlinear polarization rotation constant and deterministic. Although, the tolerance of DPSK and CSRZ formats to fiber nonlinearities is similar, but the improved sensitivity of the former results in a superior system performance.

The main advantage of using DPSK compared to intensity modulation is a 3-dB receiver sensitivity improvement [197,198] and the lower OSNR requirement. It may be noted that in case of OOK modulation scheme, the constellation length is E_s, however for DPSK this increases to $\sqrt{2}E_s$ translating to a ~ 3-dB advantage in OSNR tolerance. In DPSK, information is encoded by impressing phase shifts onto an optical carrier wave. Instead of using the absolute phase of the optical signal to carry the information as in PSK format, DPSK signal uses the previous bit as its own phase reference. DPSK encodes information on the binary phase change between adjacent bits: a 1-bit is encoded onto a π phase change, whereas a 0-bit is represented by the absence of a phase change. In this format, the serial data is converted into a differentially encoded pattern using suitable inverse-XOR functions. The phase difference of the DPSK signal is described as:

$$\Delta\phi = \phi_k - \phi_{k-1} \quad \ldots (4.1)$$

where *k* and *k-1* stand for the k^{th} and $k\text{-}1^{th}$ bits. By using this differential method, all patterns can be correctly demodulated when the phase difference is stable. The next subsection describes the design models of the transmitter and receiver block of DPSK used in the simulation study.

4.1.1. DPSK Precoder

As DPSK modulation is based on differential detection, it requires pre-coding of the transmitted sequence in order to facilitate a reliable recovery of the data at the receiver [204]. The pre-coder for DPSK is similar to the pre-coder required for duobinary modulation. Fig. 4.1 shows an optical DPSK system with a precoder scheme on the bottom left.

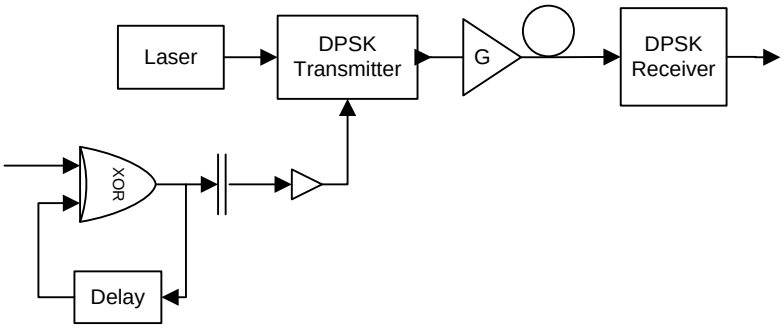

Fig. 4.1: Generalized schematic diagram of a DPSK transmitter

The precoder contains a XOR gate with a one-bit delay feedback loop form its output. The precoding function could be expressed as:

$$b_k = a_k \oplus b_{k-1} \quad \ldots (4.2)$$

where $a_k \in \{0, 1\}$ is the original transmitted binary data sequence. $b_k \in \{0, 1\}$ is the precoded binary sequence and $\oplus$ is logic XOR gate. After a DC block and an amplifier, sequence is shifted to $c_k \in \{+1, -1\}$, which is used to drive DPSK modulator. A binary 1 is encoded if the present input bit and the past encoded bit are of opposite logic and a binary 0 is encoded if the logic is similar. Table 4.1 illustrates how digital signals are converted at different stages of a DPSK transmission system. A reference bit is needed to initial the differential encoding process. This reference bit could be set to logic "0" or "1". In this case, it is set to be logic "0" at the time instant K = - 1.

Table 4.1: Different digital signals at different stage for DPSK modulation

Time instant K	-1	0	1	2	3	4	5	6
Transmitted data a_k		0	1	1	0	1	0	0
Diff. encoded data b_k	0	0	1	0	0	1	1	1
MZM drive signal c_k	-1	-1	+1	-1	-1	+1	+1	+1
MZM drive voltage $\pm V_\pi$	$-V_\pi$	$-V_\pi$	$+V_\pi$	$-V_\pi$	$-V_\pi$	$+V_\pi$	$+V_\pi$	$+V_\pi$
MZM electric field $\pm E$	$+E$	$+E$	$-E$	$+E$	$+E$	$-E$	$-E$	$-E$
Transmitted phase ϕ	0	0	π	0	0	π	π	π
Phase difference $\lvert\phi\rvert$		0	π	π	0	π	0	0

4.1.2. Modulator Architecture

As DPSK modulation carries the information in the optical phase, the most straightforward modulator configuration is based on a phase modulator. An (ideal) phase modulator changes only the phase of the

optical signal, which results in constant amplitude. However, as the electro-optical bandwidth of a practical phase modulators is limited, the 180^o phase transition is not instantaneous, which introduces chirp between symbol transitions. In the presence of chromatic dispersion and/or nonlinear impairments, this chirp limits transmission tolerances. The practical DPSK transmitter design is, therefore based on a MZM. DPSK (or more correctly NRZ-DPSK) can be generated using a single MZM. The MZM must be biased at a null, and the electrical NRZ drive signal amplitude is amplified to $2V_\pi$ [46- 48]. The output phase actually varies between 0 and π for successive intensity peaks in the MZM transmission curve. Thus, by biasing the MZM at a null, and using a high-power RF driver amplifier with $V_{p-p} \sim 2V_\pi$ we can modulate the output phase between 0 and π, producing an optical PSK signal. When the electrical data signal is differentially encoded prior to the MZM driver amplifier, the MZM optical output becomes DPSK. Employing an intensity modulator (instead of a pure phase modulator) to generate optical DPSK has the advantage that exact π phase shifts are produced. However, some residual intensity modulation is present in the signal but does not cause any problem in decoding of the DPSK signal, as it occurs between the bits. Note that DPSK can also be generated with RZ pulses by employing an RZ pulse carver in addition to the DPSK modulator. In this case, the transmitter output is a periodic RZ pulse train, with the phase of each pulse modulated between 0 and π according to the data. Thus, there are actually two forms of DPSK: so-called NRZ-DPSK and RZ-DPSK and are discussed next.

4.1.2.1. NRZ-DPSK

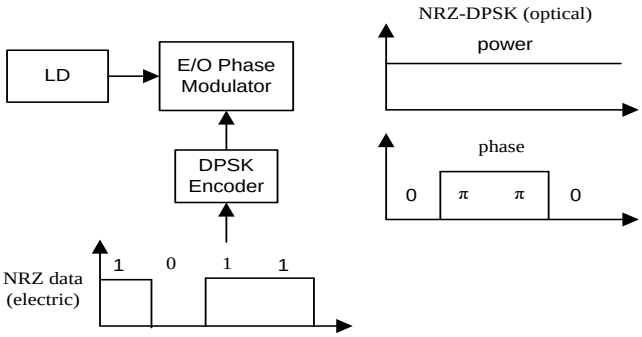

Fig. 4.2: Block diagram of NRZ-DPSK transmitter

Fig. 4.2 shows the block diagram of a typical NRZ-DPSK transmitter. Like duobinary, the data signal is first differentially encoded at the transmitter, which avoids error propagation that may occur by differential decoding at the receiver. This DPSK encoded electrical signal is then used to drive an

electro-optic phase modulator to generate a DPSK optical signal. A digital "1" is represented by a π phase change between the consecutive data bits in the optical carrier, while there is no phase change between the consecutive data bits in the optical carrier for a digital "0". A very important characteristic of NRZ-DPSK is that its signal optical power is always constant. However, the optical field shifts between "1" and "-1" (or the phase shifts between "0" and "π") and the average optical field is zero. As a consequence, there is no carrier component in its optical spectrum unlike in case of NRZ-OOK which has a strong carrier component.

Intuitively, because of its constant optical power the performance of NRZ-DPSK should not be affected by optical power related nonlinear effects such as SPM and XPM. However, when chromatic dispersion is considered, this conclusion is not entirely true. Phase modulations can be converted into intensity modulation through GVD, and then SPM and XPM may contribute to wave form distortion to some extent [205]. In a long distance DPSK system with optical amplifiers, nonlinear phase noise is usually the limiting factor for phase-shift-keying optical signals. Several papers have proven that PSK or DPSK optical coding is vulnerable to nonlinear phase noise, a phenomenon called Gorden-molleneur effect [206,207]. ASE noise generated by optical amplifiers is converted into phase noise through the Kerr effect nonlinearity in the transmission fiber and disturbs the signal optical phase to cause waveform distortions.

4.1.2.2. RZ-DPSK

In order to improve system tolerance to nonlinear distortion and to achieve a longer transmission distance, return-to-zero DPSK (RZ-DPSK) is a preferred solution. Similar to NRZ-DPSK modulation format, the binary data encoded as either a "0" or a "π" phase shift between adjacent bits having a narrower optical pulse width. In order to generate the RZ-DPSK optical signal, one more intensity modulator has to be used compared to the generation of NRZ-DPSK. The block diagram for RZ-DPSK transmitter is shown in Fig. 4.3.

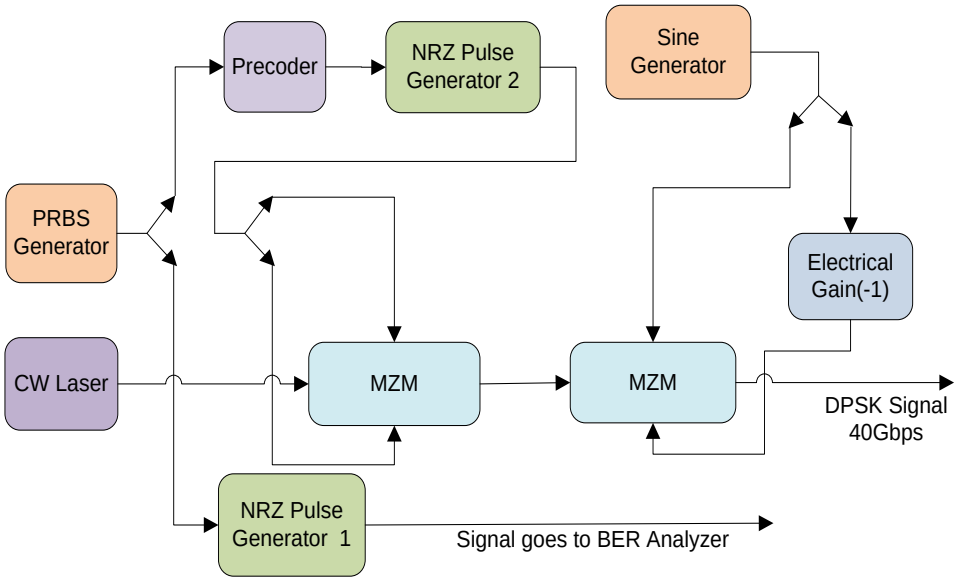

Fig. 4.3: Block Diagram of DPSK Transmitter

The phase modulated signal is generated by first encoding the NRZ signal using a precoder that drives an electro-optic phase modulator which generates a conventional NRZ-DPSK optical signal. Then this NRZ-DPSK optical signal is modulated by a clock signal through an electro-optic intensity modulator which is driven by a sinusoidal electrical signal with half the data rate. To generate the DPSK signal, the MZM is biased at the trough point and is driven with a binary electrical driving signal that has amplitude of $2V_{\pi}$, instead of V_{π}. Thus, the driving signal moves between two adjacent crest points that differ in their phase by π. Sometimes RZ-DPSK is also referred to as intensity modulated DPSK (IM-DPSK) because of its additional bit-synchronized intensity modulation. In this modulation format, the signal optical power is no longer constant; this will probably introduce the sensitivity to power-related nonlinearity like SPM. The narrow optical pulse exhibits in form of wider spectrum for RZ-DPSK as compared to the conventional NRZ-DPSK. Intuitively, this wide optical spectrum would make the system more susceptible to chromatic dispersion and thus requires a suitable dispersion compensation scheme. These encoded pulses have to be effectively demodulated at the receiver. In the next subsection simulation model for DPSK receiver is being discussed.

4.1.3. DPSK Decoder

A critical element in any DPSK system is the demodulator, which converts phase modulation into intensity modulation for detection at the receiver by photodiode. The demodulation of PSK signals requires knowledge of the carrier phase to recover the information bits. If the channel induces phase

rotations or distortions, a technique is needed for estimating the phase of the carrier at reception. This is accomplished by a synchronous optical carrier that is recovered at the receiver so that absolute phase information can be correctly extracted without ambiguity. This is referred as coherent detection which offers high receiver sensitivity but needs costly and complex components including optical phase locked loops and phase matching devices [208-210]. Under the assumption that the channel-induced phase rotations are slower than the symbol rate (i.e., the effects of the channel can be considered constant over at least two symbols), demodulation can be simplified by use of differential encoding of the information. The carrier then need not be regenerated, and one can instead use non-coherent self-homodyne (interferometric) detection schemes.

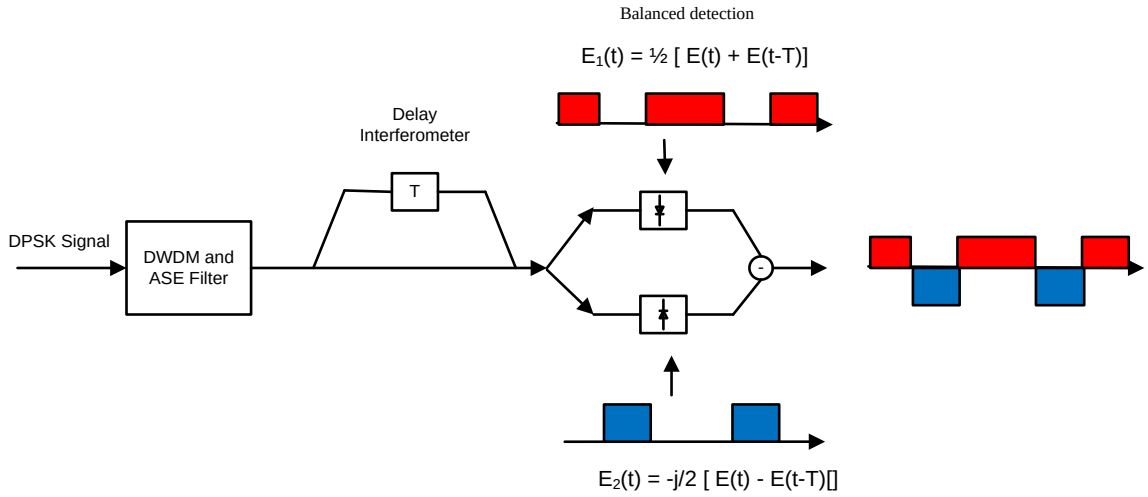

Fig. 4.4. Schematic of a DPSK receiver

In a generic DPSK receiver as shown in Fig. 4.4, the differential phase modulation is converted into amplitude modulation using a Mach-Zehnder delay-line interferometer (MZDI) which correlates each bit with its neighbor and make the phase-to-intensity conversion. It demodulates the differential phase between each data bit and its successor, which implements the differential de-coding of DPSK modulation. It splits up the signal in two copies, delays one copy by a single bit period ΔT and then recombines that with the other arm to create optical interference. The transfer function of the MZDI is defined through,

$$u_{\pm}(t) = r(t) \pm \exp(j\Delta\phi)\, r(t - \Delta T) \qquad \ldots (4.3)$$

where $u_{\pm}(t)$ is the constructive and destructive component, respectively. $r(t)$ is the input signal and $\Delta\phi$ the phase difference between both interferometer arms. The phase difference ($\Delta\phi$) is ideally equal to 0 or $\pm\,\pi$. This can be understood by noting that for this phase shift and an unmodulated input signal, destructive interference occurs at one of the outputs and constructive interference at the other output. Hence, the output ports of the MZDI are referred to as the constructive and destructive port, respectively. For constructive port, when the two consecutive bits are in-phase, they are added constructively in the MZI and results in a high signal level; otherwise, if there is a π phase difference between the two bits, they cancel each other in the MZI and results in a low signal level. For destructive port, it is vice-versa.

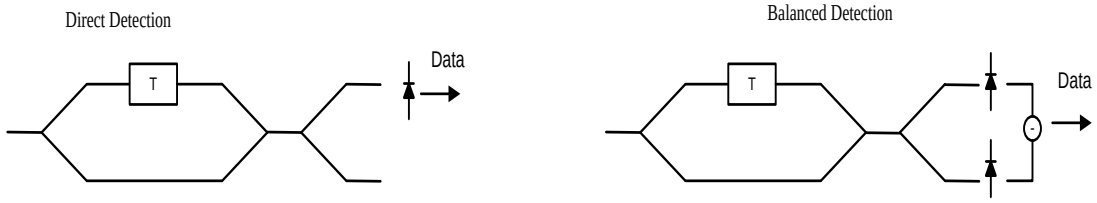

Fig. 4.5: DPSK receiver configurations: (a) Direct detection (b) Balanced detection

Both the constructive and destructive output port of an MZDI carries the full information of the DPSK signal. Therefore, detecting either only the constructive or destructive output is sufficient. This is known as single-ended detection as shown in Fig 4.5(a). But in order to obtain the ~ 3-dB OSNR improvement of DPSK over OOK modulation, both MZDI output ports have to be detected simultaneously. This is known as balanced detection, which uses two photodiodes followed by a differential amplifier as shown in Fig. 4.5(b) and the same has been used in our simulation study. The transfer function of a DPSK receiver using MZDI and balanced detection is now defined by the following equation where $u(t)$ is the output after balanced detection:

$$u(t) = |u_{+}(t)|^2 - |u_{-}(t)|^2$$

$$= \left|\frac{1}{2}r(t) + \exp(j\Delta\phi)\frac{1}{2}r(t-\Delta T)\right|^2 - \left|\frac{1}{2}r(t) - \exp(j\Delta\phi)\frac{1}{2}r(t-\Delta T)\right|^2 \quad \ldots(4.4)$$

Using this MZDI detection scheme, DPSK receiver architecture has been designed for the present simulation study and is presented in Fig. 4.6.

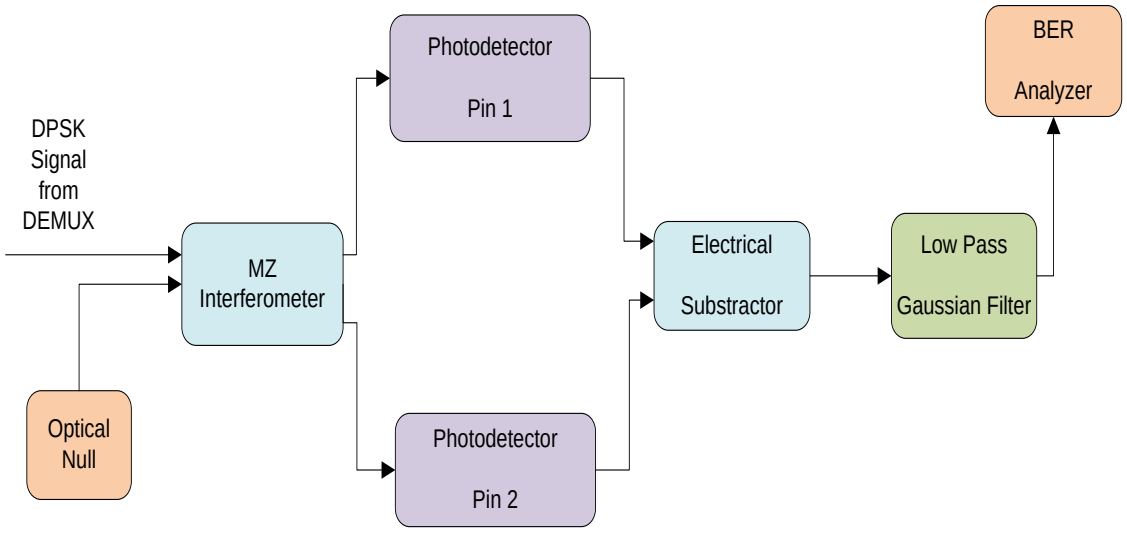

Fig. 4.6: Block Diagram of DPSK Receiver

It consists of a MZDI and a dual photodiode balanced receiver interfaced appropriately with the incoming optical bit sequences. The DPSK signal is detected differentially as the receiver has no phase reference, and hence the phase of the preceding symbol is used as the phase reference. Due to this, a precoder discussed previously is usually utilized at the transmitter side which is similar in structure to the duobinary pre-coder. This encoding in the initial bit sequence allows the demodulation of the transmitted signal at the receiver by using a MZDI and balanced photodiodes. Then the two photocurrents are combined (logical subtract) to double the signal level. At a certain input optical signal level, this means a 1.5 dB increase in the receiver Q. In a DPSK system, since signal amplitude swings from “1” to “-1”, in the ideal case, when a balanced photo-detection and a matched optical filter are used, its receiver sensitivity is 3 dB better than a conventional OOK system, where the signal swings only from “0” to “1” [57]. However, this advantage in performance must be weighed against the increased complexity and cost of the MZDI with balanced detection.

4.2. Differential Quadrature Phase Shift Keying (DQPSK)

A significant number of multi-level modulation formats have been proposed incorporating modulation in either amplitude, phase or polarization [211,212]. In order to minimize the OSNR requirements and maximize nonlinear tolerance for long-haul transmission systems, modulation formats with phase and/or polarization encoding appear to be the most acceptable. So many bandwidth efficient multi-level schemes have been explored for their suitability in optical communications. Among these, QPSK

modulation format having four-phase-levels seems to be a promising one and is an extension of the binary PSK signal. In PSK format we transmit one bit per symbol and hence the symbol rate equals the bit rate, but for the QPSK format, it is more efficient because it transmits two bits per symbol and hence the symbol rate is half the bit rate. The merit is that the effects of dispersion are considerably less for this modulation format [213, 214].

As mentioned in the discussion about DPSK format, the phase synchronization required for the coherent detection is difficult to achieve at the optical frequencies. It requires addition of optical frequency locked loops at each receiver in a WDM system, and is cumbersome. Therefore, a differential scheme called DQPSK is commonly used. It provides a suitable alternative as it, like QPSK, transmits 2 bits per symbol and hence the symbol rate is half the bit rate. QPSK and DQPSK differ by the encoding on the transmission end and the detection/decoding on the receiver end. In DQPSK, the symbol information is encoded as the phase change from one symbol period to the next rather than as an absolute phase (QPSK). In this case, the receiver has to detect phase changes and not the absolute value of the phase, which avoids the need for a synchronized local carrier and reduces the cost and complexity of the system.

So multilevel DQPSK format has received considerable attention recently [50, 68, 69, 71, 81] and is gradually becoming a research focus owing to its good tolerance capability against dispersion, better spectrum utilization and greater suppression of nonlinear effects [215, 216]. In DQPSK scheme, two bits are transmitted for each symbol, inserting a phase reference of "л/2" in between the phase of "0"and "1" which doubles spectrum utilization. Thus, for the same bit-rate DQPSK has half the symbol rate, resulting in increased tolerance to dispersion and nonlinearities and thereby lowering the component cost. Moreover, its much narrower spectrum allows a closer channel spacing which leads to reduced cost, relaxed dispersion management, and improved performance with suitable dispersion maps. The compressed spectrum is beneficial for achieving high spectral efficiencies in DWDM systems, as well as for increased tolerance to CD and PMD present in the optical channel. Evidently in DQPSK the number of constellation points is doubled and the distance between the constellation points is halved as compared to DPSK case and thus it supports double bit rate for the same symbol rate. However, the halved constellation distance requires, at least, a 3-dB higher OSNR for the same BER. Thus, usually DQPSK is used at half the symbol rate of binary modulation to obtain the same total bit rate with lower OSNR penalty in comparison to DPSK modulation.

4.2.1. DQPSK Precoder

Due to the differential nature of decoding in DQPSK, a precoding function is required to provide a direct mapping of the data from the input to the output [217] taking care that the received data streams are identical to the original transmitted data streams. The precoder for the DQPSK transmitter operates at a clock rate which is half of total transmission data rate. Since the DQPSK signal is composed by the two orthogonal patterns, both I and Q patterns should be known. Fig. 4.7 shows a schematic of an optical DQPSK precoder to be implemented in the simulation study.

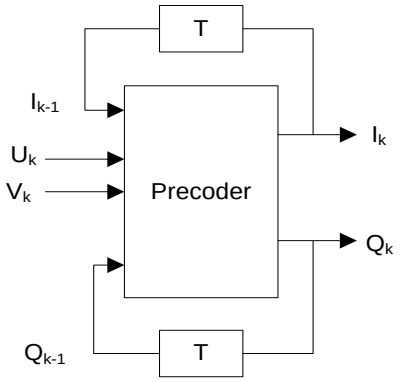

Fig. 4.7: Schematic of an optical DQPSK precoder

Table 4.2 : The transmitted and received data bit streams at different stages for an optical DQPSK system

Time Instant k	-1	0	1	2	3	4	5	6	7
Binary Data U_k		1	0	0	1	1	1	0	1
Binary Data V_k		0	0	1	1	0	1	1	0
Precoded Data I_k	0	1	0	1	1	0	0	1	0
Precoded Data Q_k	0	0	1	1	1	1	1	1	1
I/P Voltage to MZM (I)	$-V_\pi$	$+V_\pi$	$-V_\pi$	$+V_\pi$	$+V_\pi$	$-V_\pi$	$-V_\pi$	$+V_\pi$	$-V_\pi$
I/P Voltage to MZM (Q)	$-V_\pi$	$-V_\pi$	$+V_\pi$	$+V_\pi$	$+V_\pi$	$+V_\pi$	$+V_\pi$	$+V_\pi$	$+V_\pi$
O/P Electrical Field E_0	$+1+j$	$-1+j$	$+1-j$	$-1-j$	$-1-j$	$+1-j$	$+1-j$	$-1-j$	$+1-j$
Transmitted Phase Φ	$\pi/4$	$3\pi/4$	$7\pi/4$	$5\pi/4$	$5\pi/4$	$7\pi/4$	$7\pi/4$	$5\pi/4$	$7\pi/4$
Phase Difference $\Delta\Phi$		$\pi/2$	π	$3\pi/2$	0	$\pi/2$	0	$3\pi/2$	$\pi/2$
Received Data u_k		1	0	0	1	1	1	0	1
Received Data v_k		0	0	1	1	0	1	1	0

With the use of a precoder before the optical encoder, the original input data signals U_k and V_k are mapped to the phase changes ($\Delta\Phi_k$). The phase change corresponds to the phase difference between the current phase Φ_k and the previous phase Φ_{k-1}. This phase difference contains the transmitted

information that can be extracted at the receiver by the DQPSK decoder. The functional operation of DQPSK pre-coder is described in terms of logic functions [45, 60] as below:

$$I_k = V_k \oplus \overline{I_{k-1}Q_{k-1}} + U_k \oplus (I_{k-1}\overline{Q_{k-1}}) \quad \ldots (4.5)$$

$$Q_k = U_k \oplus \overline{I_{k-1}Q_{k-1}} + V_k \oplus (\overline{I_{k-1}}\, Q_{k-1}) \quad \ldots (4.6)$$

where U_k and V_k are original input binary data streams, I_k and Q_k are precoded data streams after precoder, I_{k-1} and Q_{k-1} are one bit delay version of pre-coder outputs I_k, and Q_k. The two precoded signals I_k and Q_k are used to drive MZM to produce optical DQPSK signals**.** The transmitted and received data bit streams at different stages for an optical DQPSK system are also shown in Table 4.2.

4.2.2. Modulator Structure

Compared with a QPSK system, though the configuration of a DQPSK system is less complex, but needs larger size and consumes more power of the optical transceivers and thus poses a challenge to the designers [218]. The block level architecture of a DQPSK I-Q transmitter is realized using OptiSystem model and is depicted in Fig. 4.8.

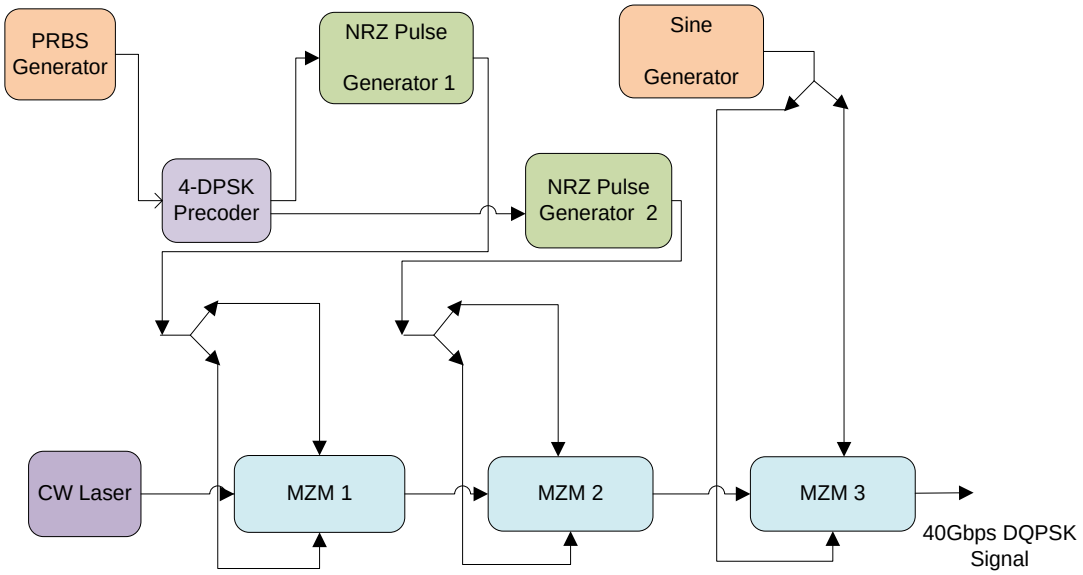

Fig. 4.8: Block Diagram of DQPSK Transmitter

A 40 Gbps signal is produced by a PRBS generator. To ensure that the received signal is detected accurately during demodulation by using two set of interferometers and balanced receivers, a precoding

component is needed to avoid iterative decoding, incorrect transmission and lower the complexity of the hardware. This DPSK precoder generates two encoded I and Q signals which modulate the first and second MZM for four level phase modulation. The last modulator generates the RZ signal of different duty cycles. The output phase difference of DQPSK is π/2, and the modulation method is inseparably related to the precoding. Using this transmitter structure, we take advantage of the near perfect π phase shifts produced by MZMs, independent of drive signal overshoot and ringing. Second, this transmitter structure requires only binary electronic drive signals, which are much easier to generate at high speeds than multilevel drive waveforms.

4.2.3. Demodulator Structure

Like at the transmitter, one also strives to work with binary electrical signals at the DQPSK receiver due to implementation benefits in high-speed electronics. The DQPSK demodulator is a key component for converting the optical phase modulation into intensity modulation. The conventional "self-homodyne" DQPSK receiver includes two MZDI for demodulation of each quadrature, followed by balanced detection [219, 220] as shown in Fig. 4.9.

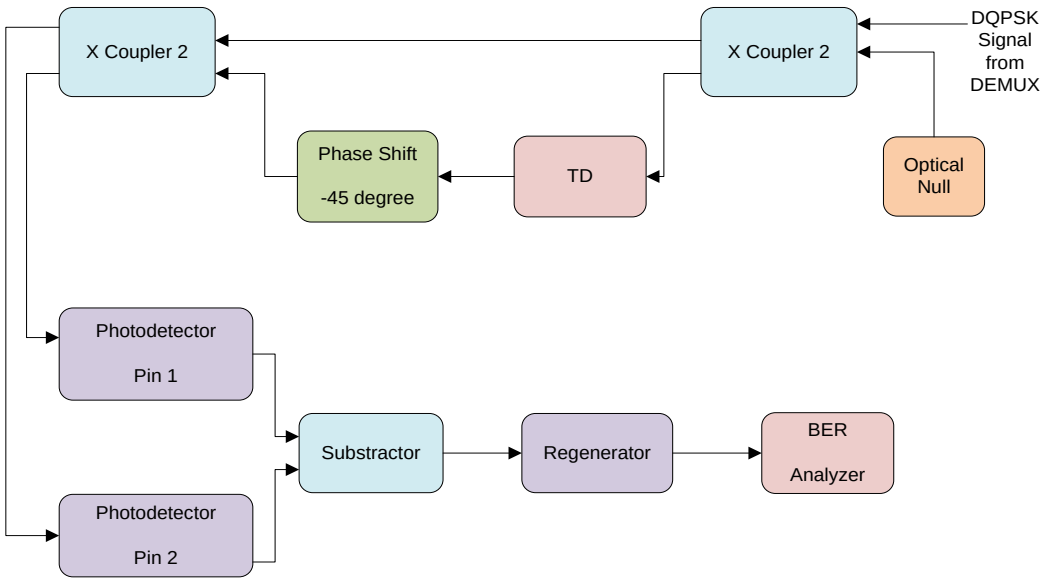

Fig. 4.9: Block Diagram of DQPSK Receiver

To simultaneously receive the two transmitted data streams, the decoder needs two MZDI to match the phases of the I and Q branch in order to achieve the required delay in the two arms, thus realizing the coherency and cancellation of the optical signals. Two balanced detectors are also needed in the

receiver as in DPSK demodulator, enabling the upper and lower branches to implement the required phase separation of $\pi/4$ and $-\pi/4$. The DQPSK signal is thus first split into two equal parts, and is used in balanced receivers with differently biased delay interferometers to simultaneously demodulate the two binary data streams contained in the DQPSK signal. MZDI delay is kept equal to the symbol duration for DQPSK demodulation, which is twice the bit duration. In DQPSK transmission, information is encoded into optical phase shifts in both quadratures of the optical carrier, thus doubling spectral efficiency compared to binary modulation formats [221].

4.3. Numerical Simulation Model and System Description

The simulation of signals in an optical fiber transmission system system involves modeling of the generation, propagation and reception of the transmitted signal. The trade-off of any simulation is between accuracy and time. Usually it requires a large amount of time and resources, to research, develop, test and improve the complex models required to implement an optical system simulator. Due to the availibity of commercial optical system simulators, with sophesticated simulation algorithms, easy-to-use graphical user interfaces, and reasonable prices, it was decided to use Optisystem 10.0 simulator to evaluate the transmission performances of various phase modulation formats. It is a well-accepted standard simulator and contains simulation modules for active and passive photonic components, different fiber types, different built in digital signal processing modules, time domain and frequency domain analyzers, electrical signal sources, filters and other related sub-systems. This simulator can also be interfaced with other programming languages such as Matlab® to enable the users to define and implement the custom modules and integrate them with Optisystem.

To begin with a single channel optical link employing DPSK and DQPSK formats at 40 Gbps has been designed for an optimum performance. Then, the channel numbers were gradually increased to 32 with a channel spacing of 50 GHz to achieve an overall capacity of 1.28 Tb/s. The simulation analysis has been performed in the C-band (1530 nm – 1565 nm) for different types of fiber to evaluate the system performance for the attempted modulation formats. The proposed 32 channel DWDM system schematic is depicted in Fig. 4.10 with the central frequency of the first channel as 193.1 THz. In literature, these formats have been investigated with 50 GHz channel spacing, but with a lesser number of channels or at a lower transmission data rate. In this work, both the formats are studied under different dispersion compensation arrangements. Pre, post and symmetric compensation arrangements have been analyzed to investigate the non-linear mitigation performance in this proposed design. In pre-compensation scheme a DCF of 10 km is used before the SMF of 50 km length to compensate for

the dispersion and the non-linearities. The gain of the EDFA's used in the link is 5 dB and 11 dB, respectively. In the post-compensation scheme to combat the accumulated dispersion a DCF of 10 km is used after a 50 km SMF. In symmetrical-compensation scheme, a 10 km DCF is used in between the SMF of 50 km as shown in Fig. 4.10. Here, three in-line-EDFA's with a gains of 5.5 dB, 5 dB and 5.5 dB, respectively are used. It was observed that post compensation scheme provides an optimum performance for both DPSK and DQPSK formats in agreement with the results in the literature [217] and hence this scheme has been used in the present analysis. The results are analyzed on the basis of Q value and eye opening for multiple transmission spans stretching up to 1600 km in a specific case.

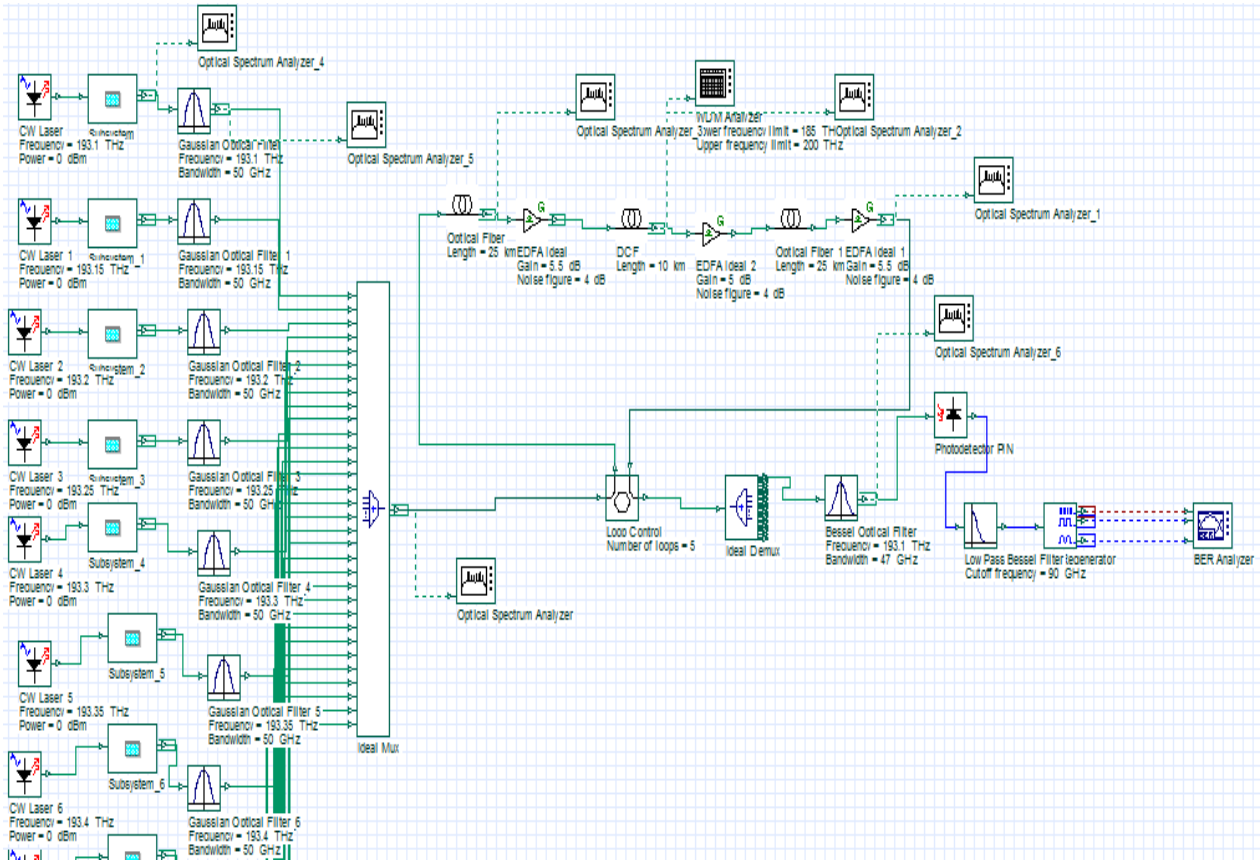

Fig. 4.10. Schematic of simulation setup

The input power has been varied and the signal is launched over N spans of 60 Km each. The WDM transmitter consists of a PRBS generator, CW lasers, data modulators, filters and the optical multiplexer. The emission frequencies of CW lasers are equally spaced and are in the range of 193.1–194.65 THz with 50 GHz channel separation. The extinction ratio of MZM's is set at 30 dB. Each CW laser is driven by a data modulator shown in Fig. 4.3 and Fig. 4.7 for DPSK and DQPSK respectively. The modulated optical signal acts as the input for the 32 input ports of an optical multiplexer

In DWDM systems, the mutual interaction between the signals and also between signals and the accumulated ASE noise leads to the inevitable linear and nonlinear crosstalk impairments. Hence, for an accurate comparison between the two modulation formats, optimization of optical and electrical filters at both the transmitter and receiver side is indispensable [222]. Keeping this in mind, we have evaluated the filter performance on the basis of receiver sensitivity in terms of the received Q value. Optical filters of both multiplexer and de-multiplexer were modeled by using the transfer function of 'elevated cosine' type with the center at the signal carrier frequency. We optimized the type and order of both the multiplexer and the de-multiplexer filter as filter characteristics play a significant role in link design. In Table 4.3, a comparison of the number of loops traversed with different types and order of filters is presented by changing the multiplexer filter order while keeping the de-multiplexer filter order fixed as 2.

Table 4.3: Multiplexer Filter optimization

Filter Order	No of loops	Q value With Bessel Filter	Q value with Gaussian Filter	Q value with Rectangular
3	1	23.56	24.29	18.85
	5	23.17	21.74	18.48
	10	21.4	19.02	17.81
	15	19.99	16.84	17.06
	20	17.71	15.41	15.66
	25	16.49	14.2	14.32
4	1	23.36	24.04	18.85
	5	22.82	21.93	18.48
	10	21.84	18.72	17.8
	15	19.61	16.95	17.06
	20	17.92	15.31	15.43

The table clearly shows that though the starting Q value of both Bessel and Gaussian filters is same, we can get a longer transmission reach with the Bessel filter and thus we have used it in our design. For the rectangular case the initial Q value is too small, so the link designed will not be very stable. We also evaluated the optimum optical and electrical filter bandwidth required for efficient signal transmission and results point out that for smaller channel spacing, larger electrical bandwidth is required. Keeping this in mind, in order to avoid crosstalk between the adjacent channels, before multiplexing, each channel is optically filtered using a third order Gaussian filter with a bandwidth of 50 GHz for DPSK and a fourth order Bessel filter with a bandwidth of 50 GHz for DQPSK format.

The combined optical signal is fed to the SMF taking into consideration of unidirectional signal flow, stimulated Raman scattering, Kerr-nonlinearity and dispersion. A scalar model of both the fibers segments has been considered to negate the effect of PMD. An SMF with attenuation (α) of 0.22 dB/km, D of 17 ps/km-nm and dispersion slope (S) of 0.08 ps/nm^2/km at 1550 nm, nonlinear refractive index (n_2) of 2.6×10^{-20} m^2/W, and core effective area of the fiber (A_{eff}) as 80 μm^2 has been considered. The DCF segment used in each span has α of 0.5 dB/km, D of -85 ps/km-nm, S is -0.45 ps/nm^2/km at 1550 nm, $n_2 = 2.6\times 10^{-20}$ m^2/W and $A_{eff} = 30$ μm^2.

The receiver consists of the de-multiplexer, demodulators, filters and 3R regenerator. The output at 32 port de-multiplexer has been simulated to evaluate the required filter parameters. The design shows an optimized performance with a third order Gaussian filter of bandwidth 50 GHz for the DPSK case, and a second order Bessel band pass filter with a 3 dB bandwidth of 50 GHz for the DQPSK case. The receiver modules discussed in Fig 4.6 and Fig 4.8 are used for DPSK and DQPSK respectively. Thereafter, a 3R regenerator is connected to the BER analyzer which generates graphs and results such as eye diagram**s,** BER, Q value and eye opening.

4.4. Results and Discussions

The performance at receiver is degraded owing to power penalty caused by various limitations of system components and channel degradations. The spontaneous emission accumulated noise in EDFA puts the minimum required amplifier noise figure F_n to be 3 dB even in the ideal case. Hence, to observe the performance of the designed optical system under ASE imposed limitations, we have considered the value of F_n as 4 dB for a fully compensated GVD case. DCF and SMF fibers meet the specifications mentioned in previous section. The signal is then launched over N spans of 60 km each comprising of 50 km of SMF and 10 km of DCF, respectively.

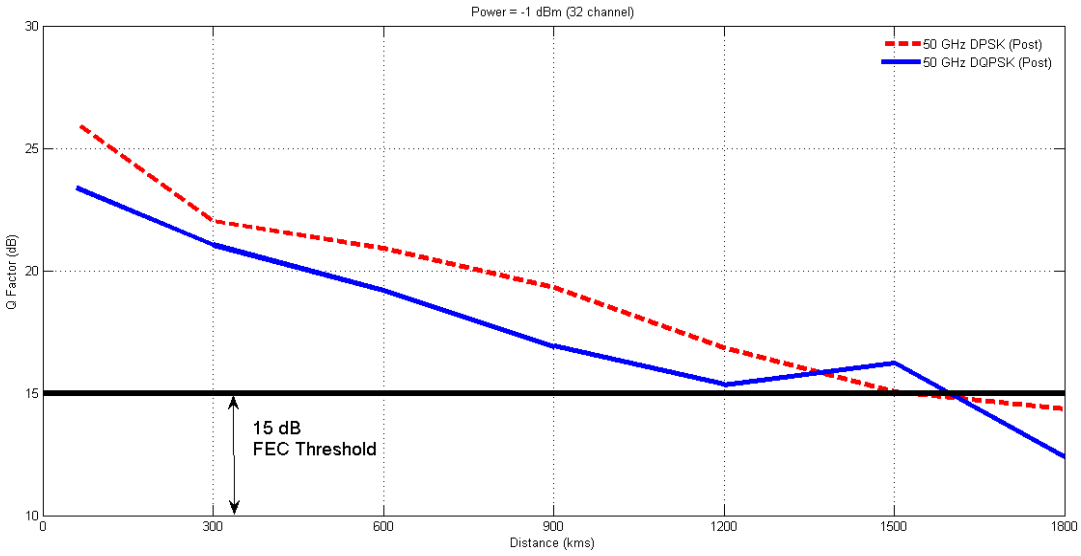

Fig. 4.11(a)

Degradations due to nonlinear effects are kept manageable by ensuring low values of the launched power into SMF viz., - 1 dBm ,0 dBm and 1 dBm. Fig. 4.11 outlines the safe operating distance for both these formats w.r.t the Q value with varying launch power. It is observed from Fig. 4.10 (a) that at a launch power of -1 dBm, DPSK scheme performs better than DQPSK till 1500 km, after which the Q value drops below the 15 dB threshold, however DQPSK still provides an acceptable Q value up to a transmission distance of 1700 km. As we increase the launch power to 0 dBm, both the schemes show comparable performance to yield a safe operating distance of 1400 km as shown in Fig. 4.10 (b). Further enhancing the input power to 1 dBm, it is seen that DQPSK consistently performs better than DPSK to provide a safe transmission distance of 1200 km as compared to 900 km for that of DPSK as shown in Fig. 4.11(c). Thus, it is inferred that for higher powers DQPSK performs better than DPSK because of its narrower spectrum and relatively higher tolerance to non linearities. Non-linear effects accumulate in such high speed multi-channel optical link and add up with GVD induced delay to manipulate the spectrum of the data transmitted. The next subsection presents a simple OptiSytem link model to implement different combinations of dispersion compensation to evaluate the link performance.

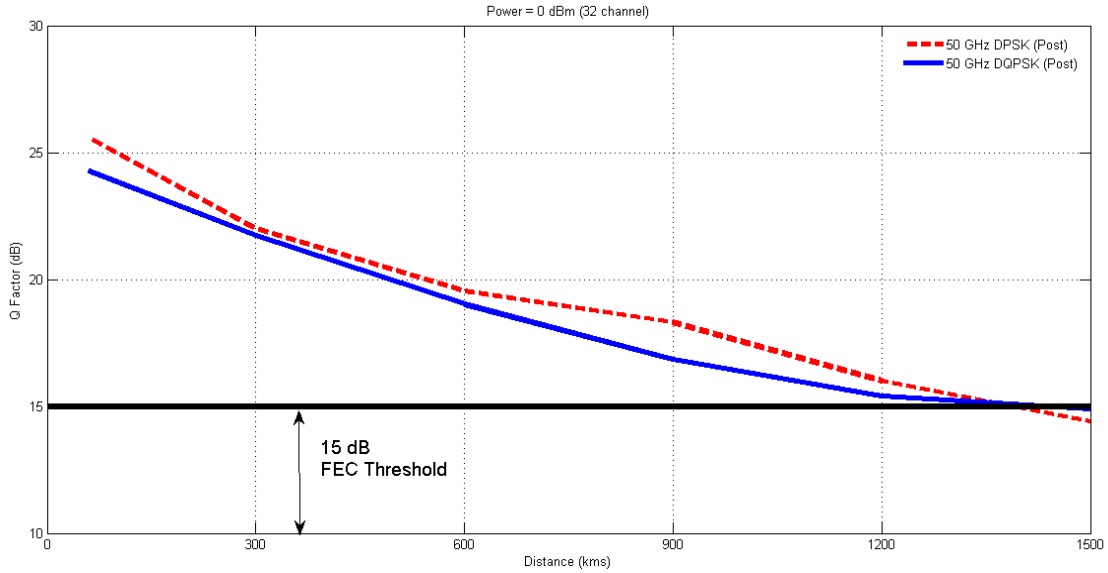

Fig. 4.11 (b)

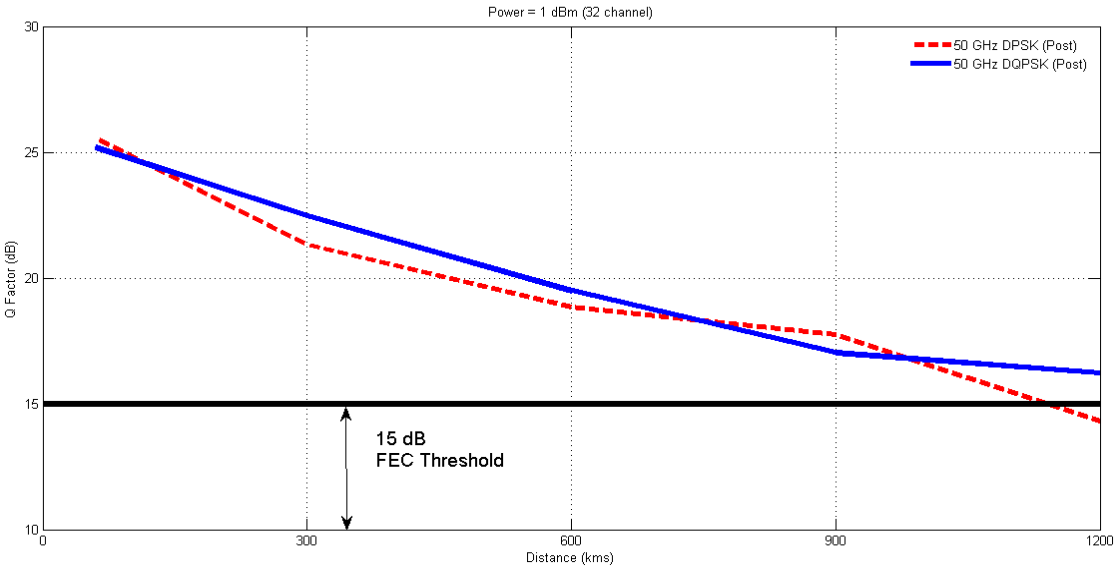

Fig. 4.11 (c)

Fig. 4.11: Q value as a function of transmission distance for (a) Pin = -1 dBm (b) Pin = 0 dBm (c) Pin = 1 dBm

4.4.1. GVD limited system

Group velocity dispersion induced impairments limit the system performance by introducing ISI at high data rates. The analysis for GVD induced degradation has been made by employing the simulation

setup as shown in Fig. 4.10 with SMF length as 10 Km. Here, the CR has been varied from 95% to 105% to find the optimum value of DCF length to maintain a RDSP in each map. This enables us to visualize the effects of both under compensation and over-compensation which further mitigates the influence of FWM and XPM for both DPSK and DQPSK systems. Based on the optimizations after the simulation run, the DCF length is chosen to be 9.94 km and 9.989 km for DPSK and DQPSK respectively, which corresponds to the case of under-compensation of the RDSP. ASE noise has been neglected by setting the EDFA noise figure to 0 dB. This setup allows us to investigate the proposed system performance under GVD induced degradations, ignoring PMD effects also. In the simulation to avoid nonlinear effects, low values of launch power are considered viz. -10 dBm, -5 dBm and -1 dBm and variation of Q vs. the operating length is examined as shown in Fig. 4.12.

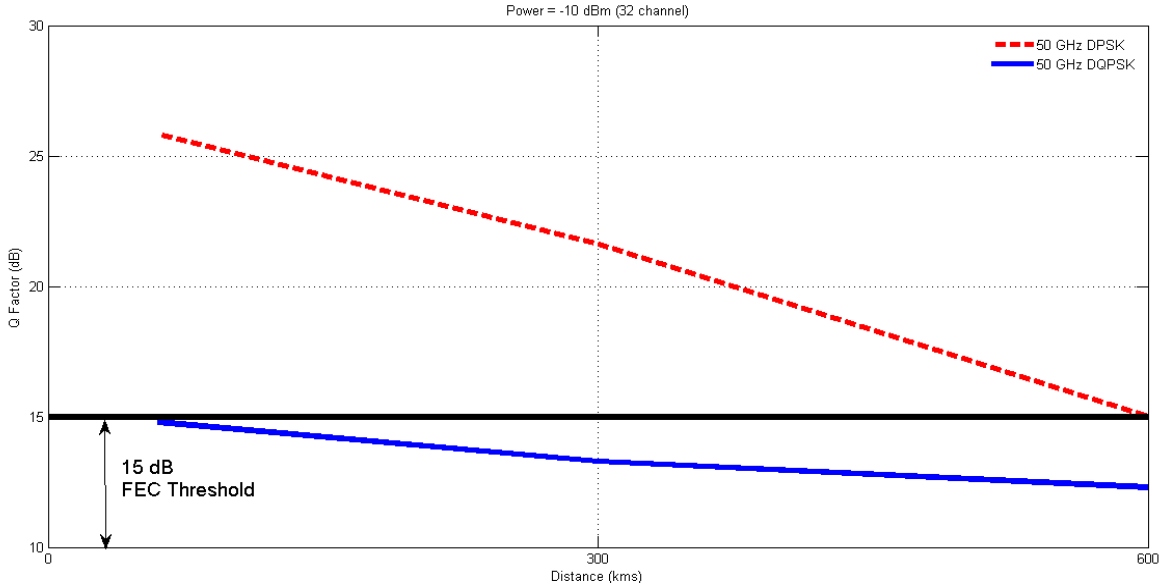

Fig. 4.12 (a)

Fig. 4.12 (a) reveals that for very low power levels of -10 dBm, the DPSK modulated system manages to run for 10 spans i.e. a distance of 600 km while the DQPSK based network remains below the threshold even after the first span i.e. 60 Km. However, as the launched power is increased to -5 dBm, for the initial spans DPSK shows a much better Q value of 27 dB while for DQPSK the Q value is around 19 dB as shown in Fig. 4.12(b). Both the schemes start to follow each other beyond 600 Km and achieve a safe operating distance of 1000 Km before degrading below the 15 dB FEC threshold.

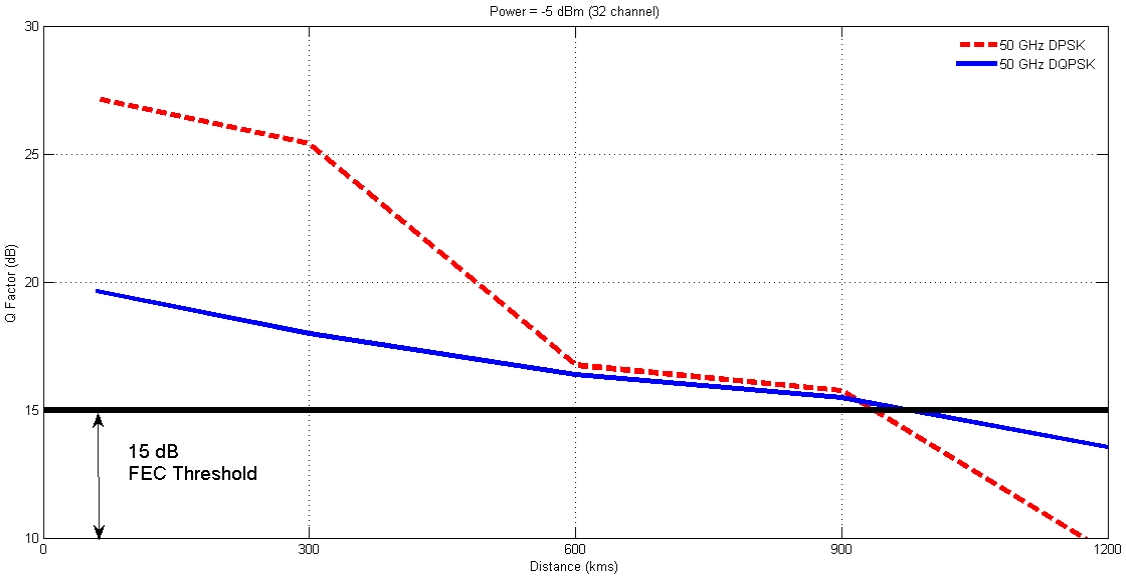

Fig. 4.12(b)

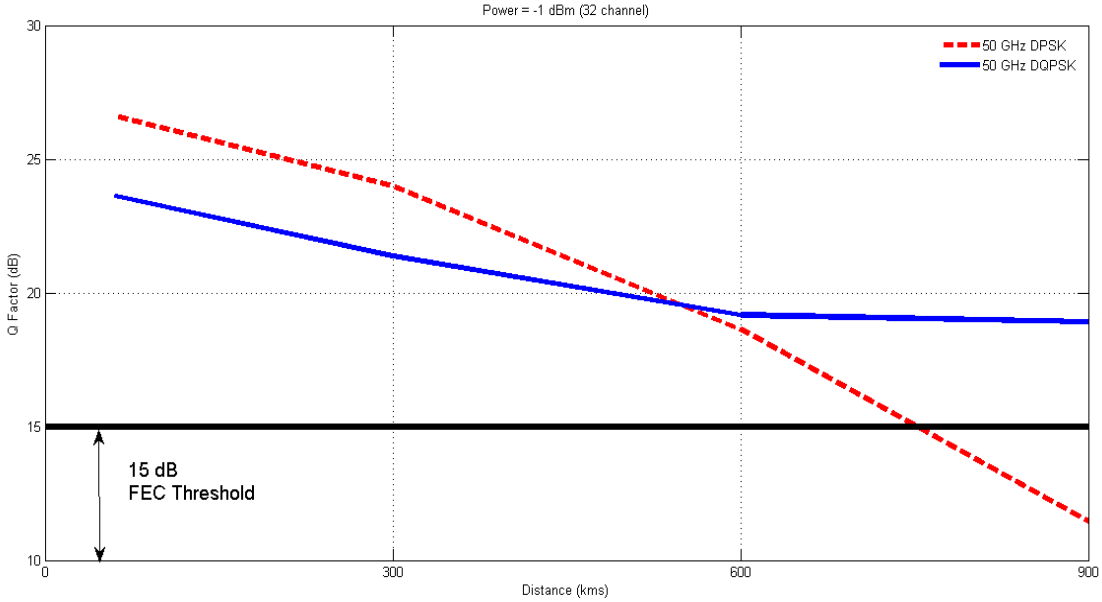

Fig. 4.12(c)

Fig. 4.12: Q value as a function of transmission distance for (a) Pin = -10 dBm (b) Pin = -5 dBm (c) Pin = -1 dBm

Further, as the power is increased to -1 dBm, DQPSK performance degrades slowly with distance to provide a larger operating length of 900 Km as depicted in Fig. 4.12 (c). It is observed from the analysis that the DQPSK modulation format is more suitable for higher values of power as it offers generous

system margin due to its high spectral efficiency and relatively good tolerance to fiber degradations making it desirable for long haul transmission using under compensation method.

4.4.2 XPM limited system

XPM effect becomes more dominant with higher values of launch power. Hence, the XPM-induced signal degradation has been evaluated using the simulation set up of Fig. 4.9 for three different power levels viz., 0 dBm, 1 dBm and 5 dBm to observe its influence on system performance. An SMF segment of 50 km and a 10 km DCF is used to avoid GVD induced degradations and EDFA is assumed to have a noise figure of 0 dB to neglect ASE noise. The curves for the estimated Q values vs. transmission distance with different launch powers are presented in Fig. 4.13. A closer analysis of Fig. 4.13(a) reveals that at 0 dBm launch power initially DPSK performs better than DQPSK modulated system, but for distances over 1200 Km, the latter is more efficient.

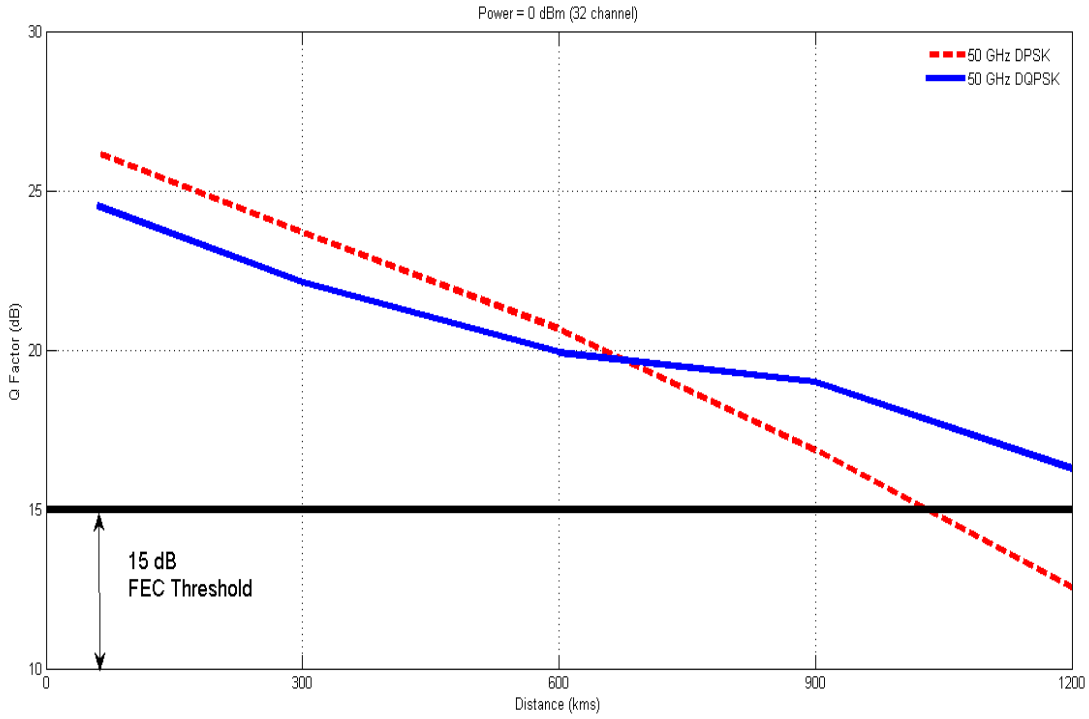

Fig. 4.13(a)

For the 1dBm launch power case as in Fig. 4.13 (b), DQPSK outperforms DPSK from the first span and maintains superiority up to 1500 Km. Another interesting observation is seen in Fig. 4.13(c) for a 5 dBm launch power wherein the DQPSK based setup substantially outperforms DPSK system. While the DPSK modulated link declines below the limiting FEC value at around 600 km but the DQPSK

modulated system operates fairly well up to 1000 km which is approximately the double of the distance managed by the former.

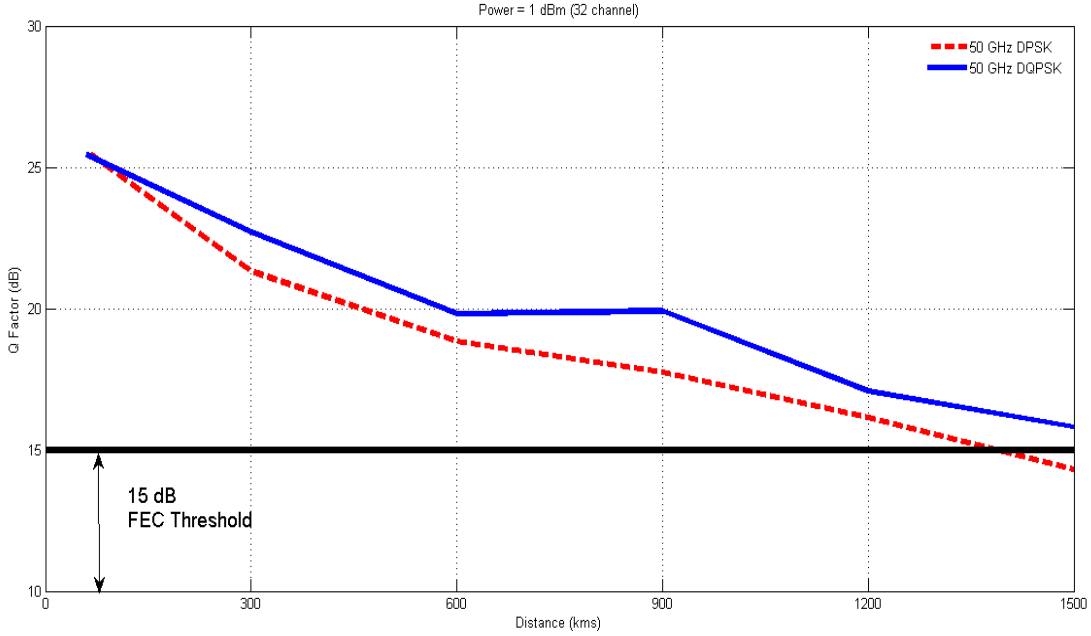

Fig. 4.13(b)

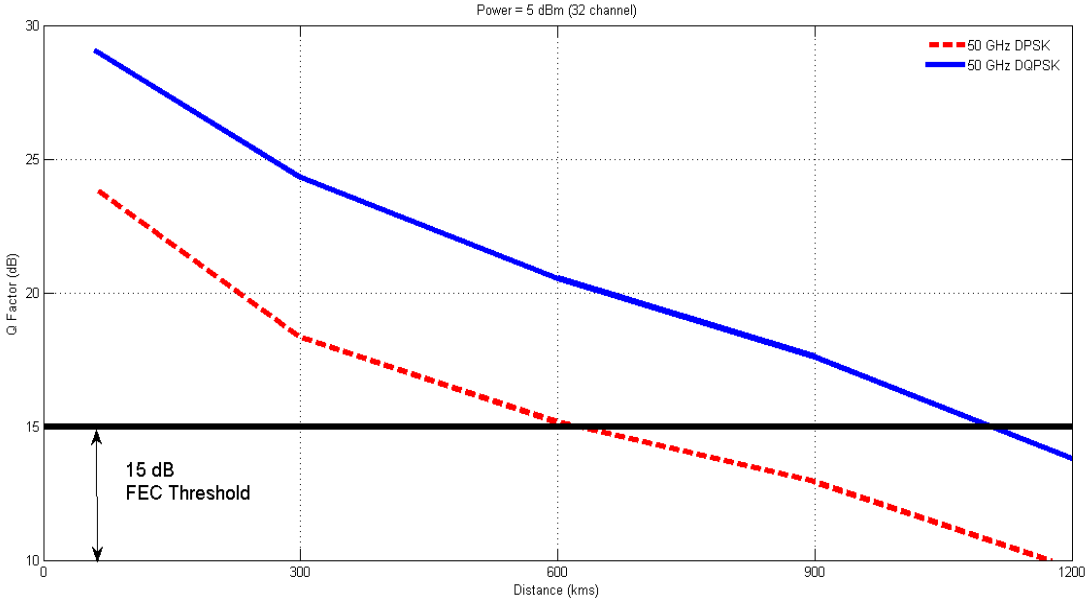

Fig. 4.13(c)

Fig. 4.13: Q value as a function of transmission distance for (a) Pin = 0 dBm (b) Pin = 1 dBm (c) Pin = 5 dBm

This observation reinstates our assertion of the fact that DQPSK scheme is the right choice when we need to design a high power DWDM system due to its higher tolerance to dispersion, and greater ability to suppress nonlinear effects

4.5. Conclusion of Optisystem Simulation

This chapter presents a simulation setup to analyze a 32 channel 40 Gbps DWDM system for long haul transmission using DPSK and DQPSK modulation format. The proposed system has been investigated to evaluate its performance with pre, post and symmetrical dispersion compensation schemes. The link has been analyzed for full compensation and under compensation of dispersion to see the effect of ASE, GVD and XPM. It is found that as the signal input power increases, Q value starts diminishing due to the dominance of non-linear optical Kerr's effects like XPM and FWM. The analysis concludes that the post compensation scheme is a superior choice over the pre and symmetrical schemes.

For low values of launch power, DPSK is the preferred choice with perfect compensation. However, the DQPSK modulated optical link outperforms the DPSK link at higher launch powers due to its high spectral efficiency enabling it to tolerate the dispersion induced degradations. It is also inferred that by maintaining a residual dispersion per span, the DPSK and DQPSK based system can achieve significant safe operating distance up to 1000 km and 1600 Km respectively. The DQPSK scheme provides a longer safe operating distance with a compromise of a complex and costlier transmitter and receiver design. The analysis reports that the decision of choosing between DPSK or DQPSK depends on a trade-off between the spectral efficiency and the tolerance to nonlinear impairments and thus provides an insight for a practical DWDM system design.

4.6. DQPSK optical Simulink Model

In order to investigate the performance of DWDM systems in the presence of fiber non-linearities various analytical models using the solution of NLSE have been proposed [223]. Modeling and theoretical analysis of DWDM system provides interesting intuitions and understanding, but becomes quite tedious and time consuming complex problem. This involves expert knowledge in areas of physical EM and spectral optical dispersion in confined media and related linear and non-linear optical signal processing capabilities. Unfortunately, system specifications such as the total transmission distance, the number of WDM channels, the channel spacing, the allowable power per channel, the amplifier spacing, etc., cannot be easily modeled to develop a mathematical expression for the signal

transmission in real optical communication link. Alternatively, numerical simulation of such systems can be used to simplify this problem and then to approach some suitable experimental and realistic cases to evaluate the fitting parameters to make the simulation as accurate as possible. This approach thus offers better insight in system design and allows fixing the optimized system parameters [224,225]. Therefore, computer simulation plays an important role in the design, optimization and evaluation of system performances in the presence of linear and nonlinear impairments occurring in practical long haul optical links.

Simulink [226] is a graphical programming environment for modeling and simulation analysis of communications systems. The flexible nature of the simulation platform offered by Simulink allows a simulation ease for understanding practical modern optical communication systems. It provides the flexibility to incorporate the various photonic components as either user-defined or fixed which can also be enhanced or removed from the model as per the design requirements [227,228]. Here, we have used Matlab/Simulink model to study the effects of nonlinear distortion on the transmission capacity of DWDM based optical communication links. The simulation model considers the different optical components used in link design with their behavior as represented initially by theoretical interpretation in Chapter 2. The included transmitter topology, MZM module and, the propagation model for optical fibers enables to realize an operational experimental WDM configuration.

Basically, a DWDM system comprises of a transmitter module, multiplexer, fiber loop sections consisting of filters and in-line amplifiers, de-multiplexer component, and a receiver block. The proposed model describes the detailed operation and need of every component used and its representation in Simulink blocksets for a single channel long haul link. The evaluation of the system performance and its tolerance effects of design parameters is studied in terms of BER and eye diagram analysis. This designed model can be extended to more than one channel to realize WDM system. The next section describes the approach followed for system design through simulation, the various models developed in Simulink as counter part of the DQPSK based transmitter and receiver as well as the fiber model and the various assumptions applied. The next section discusses the designed sub-blocks and findings of the analysis.

4.6.1. Simulation Approach

The complete schematic has been developed in three main steps, in correspondence with the major components of an optical link i.e. transmitter, fiber and receiver model [229]. Fig. 4.14 shows the developed schematic model of DQPSK based single channel optical transmission link.

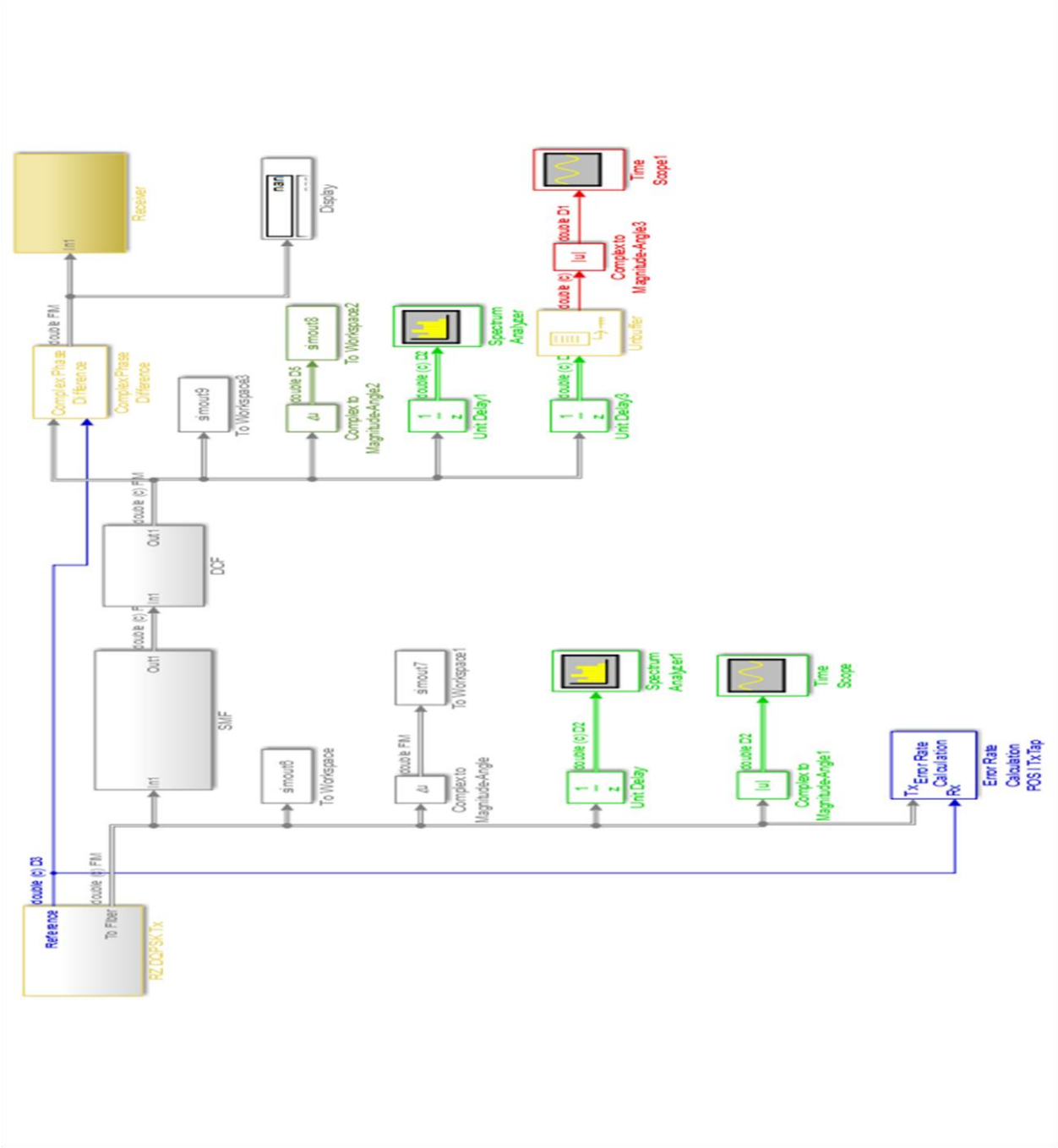

Fig. 4.14**:** Simulink block schematic of single channel DQPSK Link

The link is initially simulated only for a point to point transmission link operating at 10 Gbps to visualize the basic transmission characteristics of DQPSK format. The designed model has been further

investigated by adding or altering few new blocks to optimize the system performance as per the need. Simulation initialization begins by defining and declaring the variables such as bit-rate, fiber length, simulation time, number of transmitted di-bits for the RZ-DQPSK optical link. These values are properly defined in a Matlab m-file which needs to be run prior to simulation. The time for the simulation was set to 10^{-10} seconds.

4.6.2. Assumptions

Simulink DSP blockset and Simulink Communications blockset are used to effectively model fiber optic systems. In the present transmitter design, chirping effects from the DFB laser are assumed to be absent and an ideal signal generator is used corresponding to the fixed wavelength of light wave. Further an X-cut $LiNbO_3$ MZIM is used with negligible insertion losses, coupling losses and recombination losses. The model assumes that the optical intensity characteristic of the MZIM is ideal, translating to a large extinction ratio. The minimum output power, P_{min}, of the MZIM is modeled to be close to zero at the minimum transmission point.

We used Matlab subsidiary program Simulink to develop the models whose block sets support data types of discrete sources/ values, hence a method to convert the continuous waveforms to corresponding discrete values is a prime requirement. As Matlab processes and stores data in discrete form, the input waveform and other signals need to be sampled at a certain interval T, to ensure synchronization and enable correct processing and minimize sampling errors. Nyquist sampling time is used in the sample time fields of blocks, wherever required to maintain the integrity of the signals. Nyquist theorem states that the sampling interval must be at least twice the highest frequency in the system ($f_{sampling} \geq 2B$) and hence the sampling time for the simulation has been set accordingly as $T_{sampling} = \frac{1}{2B}\ s = 2.59\ x\ 10^{-15}\ s.$

4.6.3. Transmitter Model

The transmitter for the generation of DQPSK modulated signal is developed first. An important feature of the DQPSK modulation format is that it provides double the bandwidth and better spectral efficiency over OOK. Moreover, non-coherent detection further reduces the overall cost of the system design. DQPSK uses four-symbol states {0, π/2, π or 3π/2), compared to two possible symbol phases (0 or π) as in DPSK. To encode the desired di-bit combination we vary the phase difference, $\Delta\phi_{mod}$, between the two adjacent symbols systematically. The transmitter block model in Simulink includes digital

pulse shaping and sampling circuits and various pulse conditioning and modulating circuits. The Simulink model of complete transmitter block and its various sub-components are depicted in Fig. 4.15 and are briefly discussed in next sub-section.

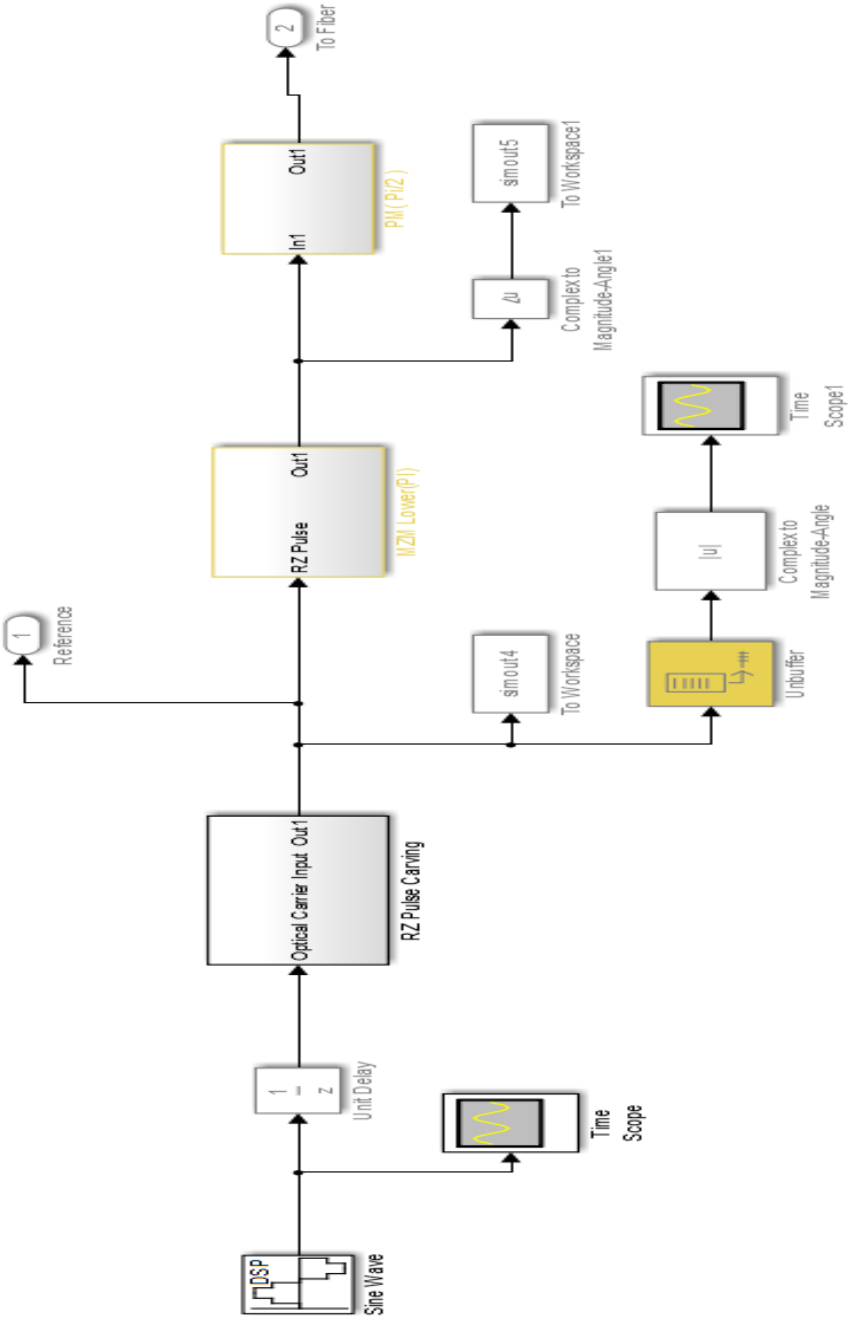

Fig. 4.15: Transmitter Model

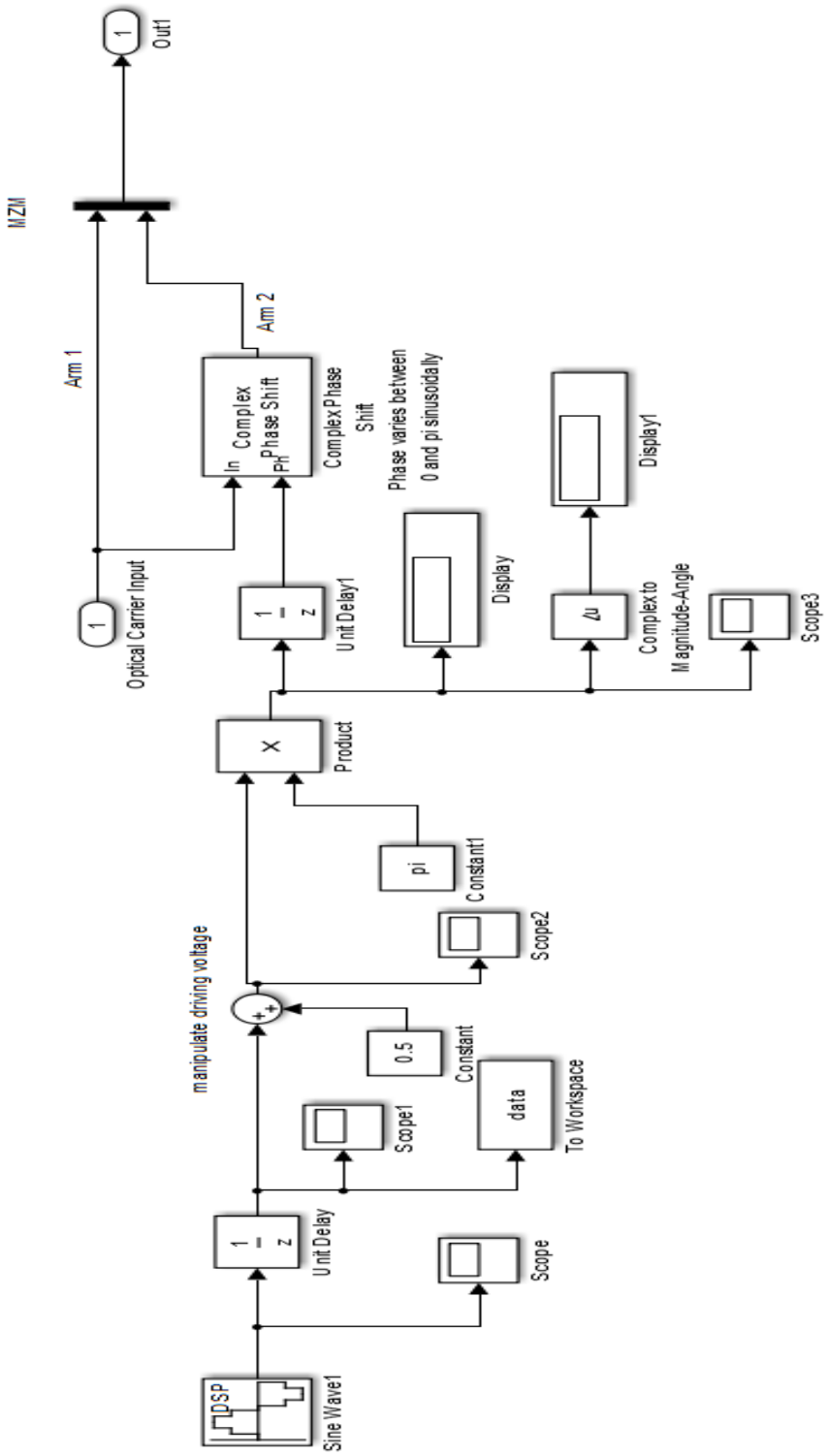

Fig. 4.16 (a): RZ pulse carving Block inside transmitter

The transmitter design is realized in three stages consisting of; a RZ pulse carving MZIM (to generate the desired RZ pulse shape), an MZIM (to generate 0 or π phase shift) which is coupled with a Phase modulator (PM) to induce appropriate phase shifts (0 or π/2) in the optical carrier. This design allows

to achieve the four phase states of the optical carrier as needed in DQPSK modulation format, {0, π/2, π or 3π/2}. Random binary generators operating at 10 Gbps drive both the MZIM and PM.

The driving signal of MZIM is generated by a 10 GHz signal as shown in Fig. 4.16(a) to set the input to the 'Complex Phase Shift' block 'Ph' to be a value between 0 and pi. The phase of the optical carrier at the 'In' port is shifted by the amount of 'Ph' by this block and is then added to an unaffected optical carrier which simulates the Y recombiner of the MZIM in Simulink environment. The second MZIM (as designed in Fig. 4.16 (b)) and the PM (Fig. 4.16 (c)) perform the phase modulation on this received signal from the output of Fig. 4.16(a).

The second MZIM acts as a phase shifter when biased at the minimum transmission point offering two possible states 0 or π. Usually a PM which provides a π phase difference is used, but its performance deteriorates at high data rate and it becomes costly if phase correction circuits are also interfaced [15]. So a MZIM based design is proposed with Simulink blocks and shows a satisfactory performance up to 40 Gbps. The optical carrier splits at the input of the MZIM, resulting in an output of two optical pulses beating together, if some phase change is there in the lower arm. As the pulse transmission is modeled only through the lower MZIM arm, so either a 0 or π phase difference is experienced by the carrier depending on the digital driving voltage signal value. A random NRZ bit pattern is generated by the 'Bernoulli Binary' block whose value is multiplied by pi to get a value of either {0, π}. This is sampled via unit delay block every bit period i.e. at 100 ps for 10 Gbps operation and results in a phase shift of 0 or π of the RZ-pulse carved optical carrier.

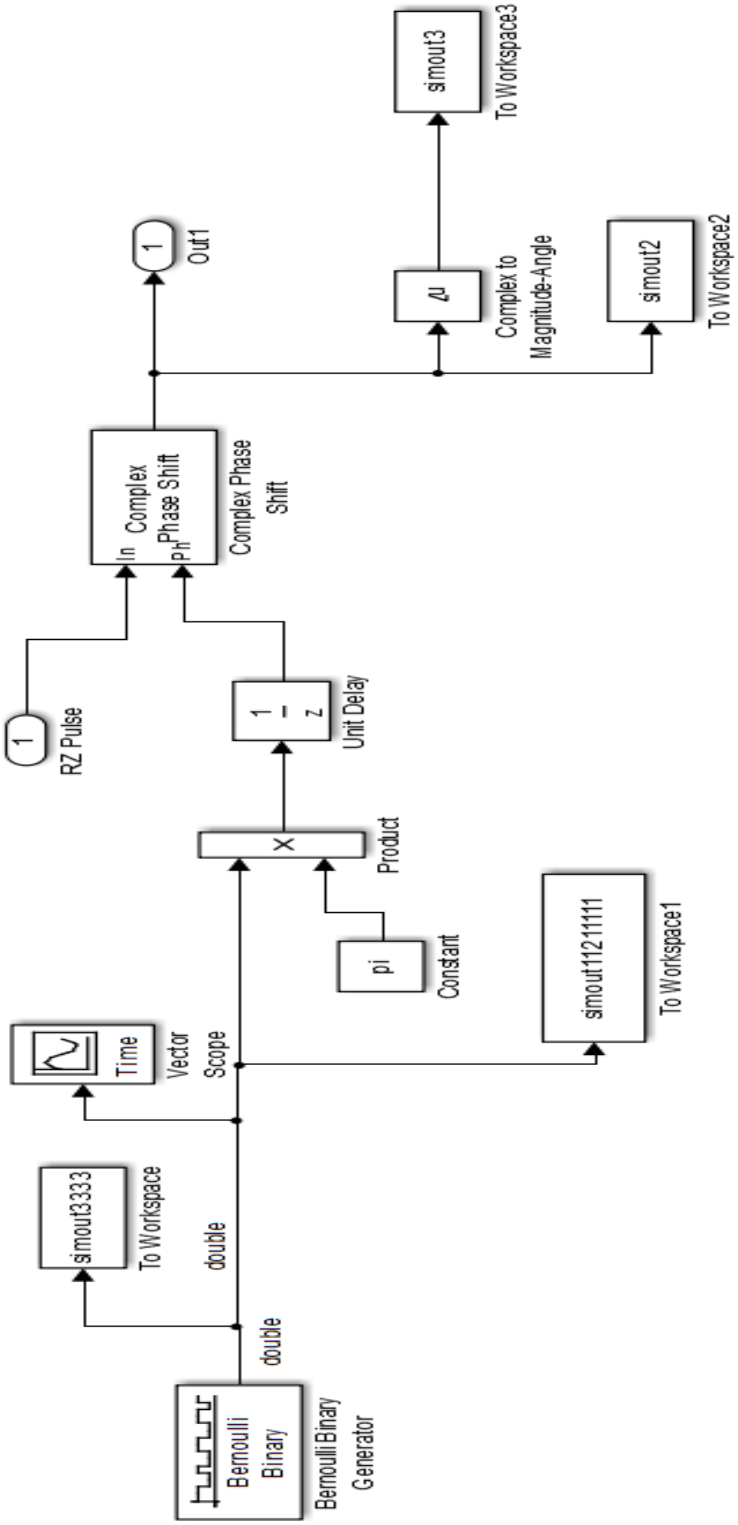

Fig. 4.16 (b): MZM Lower (Pi) Subsystem in Transmitter Model

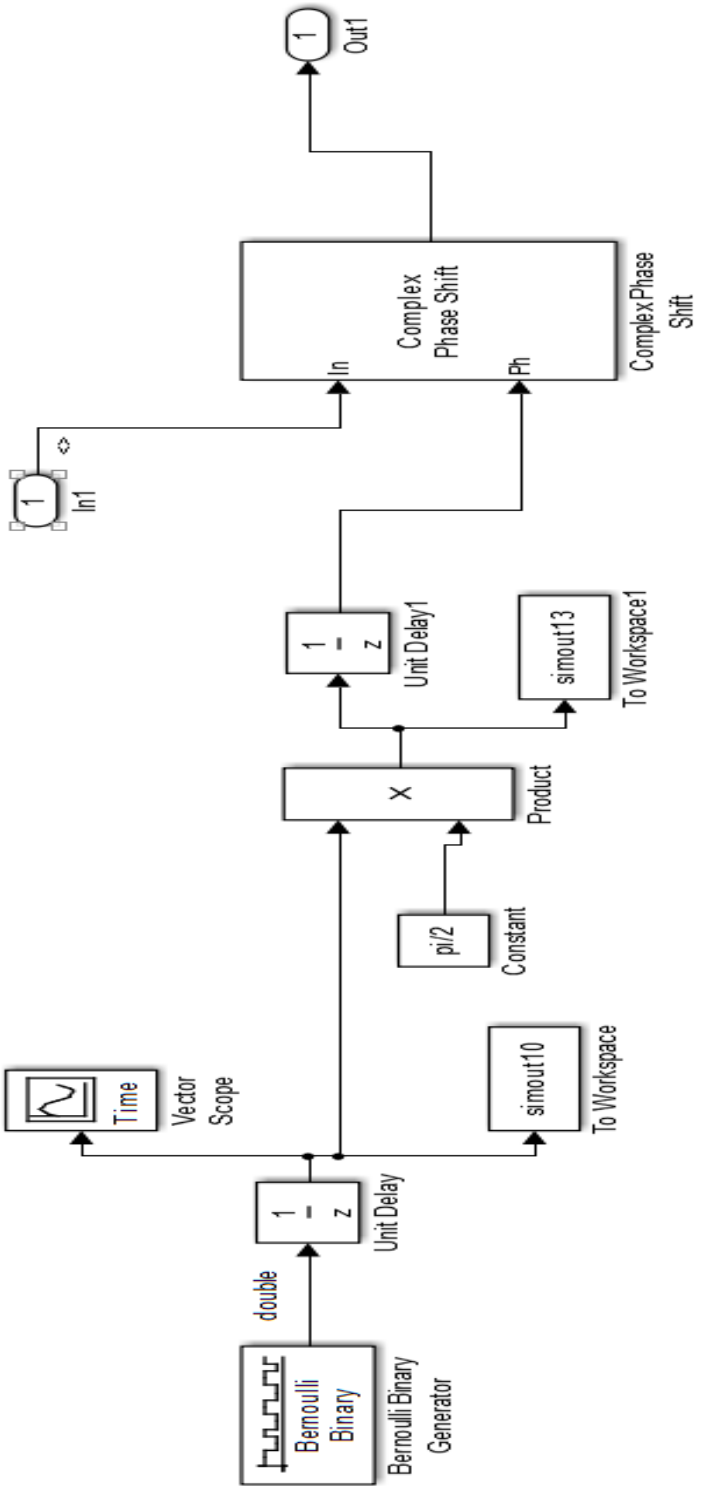

Fig. 4.16 (c): PM (pi/2) Subsystem in Transmitter Model

The Phase Modulator (PM) shown in Fig.4.17 (c) operates on a similar principle, but the multiplier to the random NRZ bit-stream is $\pi/2$ rather than π. This bit stream is made different from that driving the MZIM by usage of an additional 'unit delay block' at the output of the Bernoulli Binary generator. It

causes the original bit stream to be delayed by one-bit interval, thereby ensuring that 'uncorrelated' data drives both the MZIM and PM and enables to achieve during simulation run-time all the four possible states of the signal constellation.

4.6.4. Linear Fiber Propagation Model

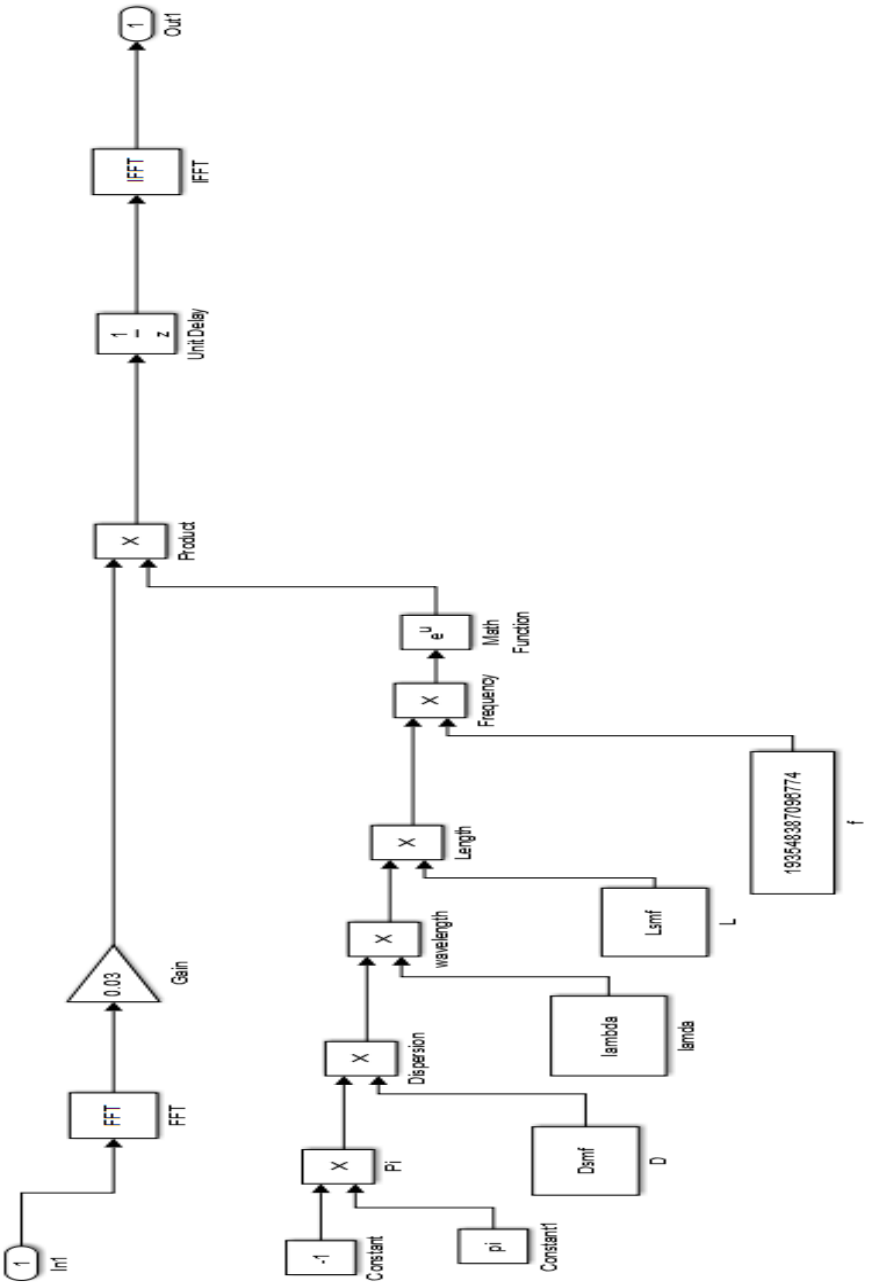

Fig. 4.17**:** Single Mode Optical Fiber (SMF) Block

In high speed optical link design suitable dispersion management strategies have attempted to achieve performance improvement and hence a Simulink based model is proposed mainly to consider the dispersion effects and explore the methods to combat it by incorporation of DCF. This model is based on the assumption that we can treat SMF as a bandpass filter having a flat amplitude response in the passband [16]. To simulate fiber propagation in real sense, we have considered the attenuation effects as an extension of model. The mathematical background has been discussed in detail in Chapter 2 and hence here, we present only the transfer function of the fiber as:

$$H(f) = e^{-j\pi D(\lambda)\frac{\lambda^2}{c}f^2} = e^{-j\pi D(\lambda)\lambda L f} \quad \ldots (4.7)$$

As it is more convenient to operate in frequency domain, rather than performing the tedious, time domain convolution, the output of the fiber $\widehat{X}_{out}(f)$ for a given input signal $\widehat{X}_{in}(f)$ is given by Eq.(4.8) and can be implemented by the Simulink block given in Fig. 4.17.

$$\widehat{X}out(f) = H(f)\widehat{X}in(f) \quad \ldots (4.8)$$

Thus, by performing the FFT operation on the input signal which is multiplied by H(f), and then taking the IFFT allows to represent fiber propagation accurately with some additional chromatic dispersion, thus linearizing the model. The simulation assumes $D(\lambda)_{SMF}$ = +17 ps/nm.km at 1550 nm wavelength, L = 80 Km for the standard SMF fiber with no optical amplifiers and a DCF of 16 Km with a corresponding, $D(\lambda)_{DCF}$ = -85 ps/km-nm to effectively cancel the accumulated dispersive effects. Corning fiber SMF-28 with a specified attenuation of 0.2 dB/km is used, implying a total 16 dB attenuation of power after 80 km which is considered in a Simulink gain block of 0.03 at the top of the model. A similar DCF model has been realized with parameters set to combat dispersion along the link.

4.6.5. Receiver Model

The DQPSK receiver model attempts, within Simulink capabilities, to simulate efficient decoding of the DQPSK modulated signal. The demodulation and detection stage can be considered as 'non coherent' scheme due to the differential nature of the modulation process, resulting in the absence of a local oscillator (LO) and no extra photonic hardware requirement as in conventional detectors, making this method quite captivating for researchers. The receiver configuration is shown below in Fig. 4.18 and efficiently demodulates the signal transmitted along the 96 km dispersion compensated fiber span.

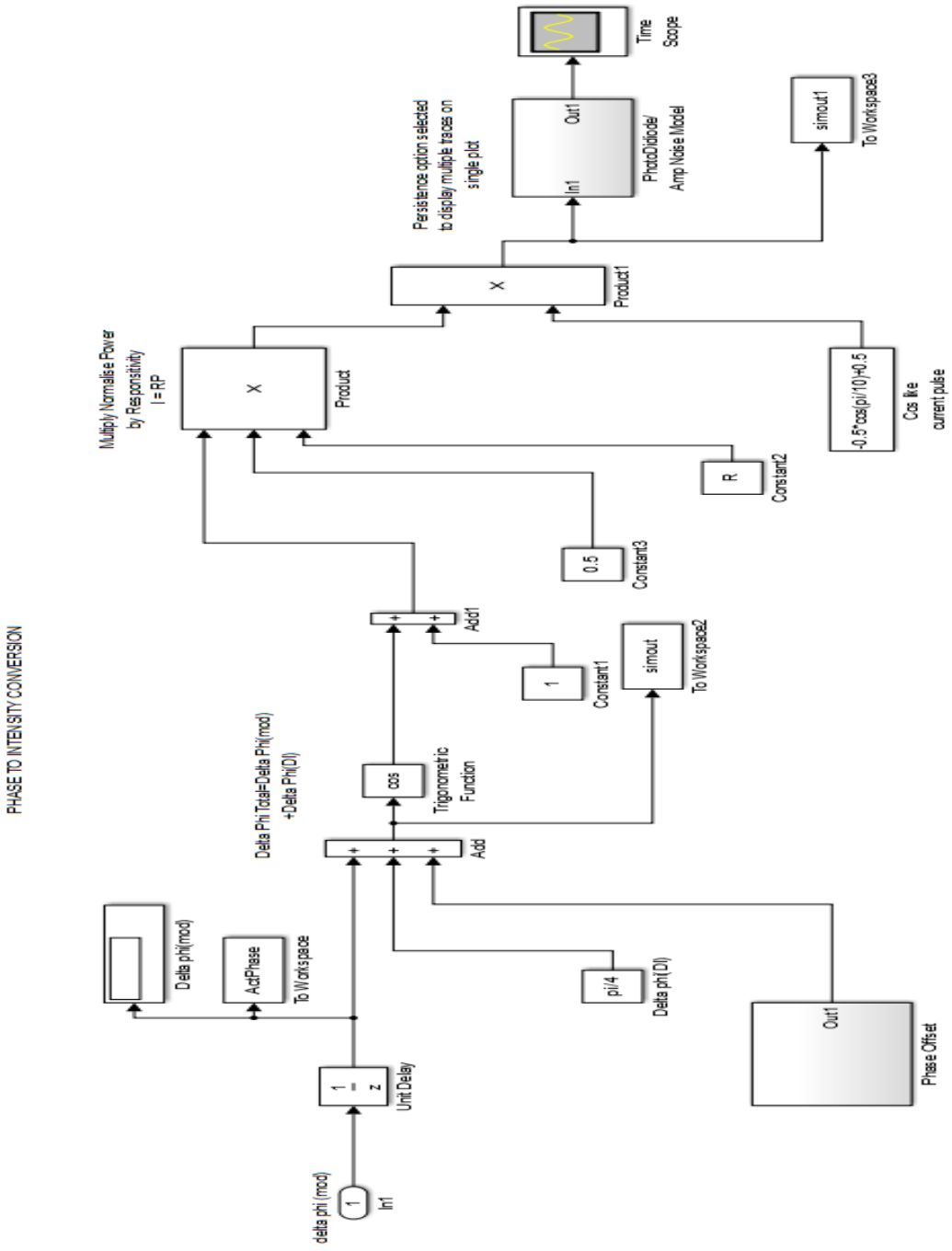

Fig. 4.18: Receiver model including noise sources

The ‘Complex Phase Difference’ block at the input of Receiver block as seen in Fig. 4.14, deduces the phase shift between the received symbol whose phase is encoded and the reference signal produced directly by the transmitter prior to modulation. Due to the periodic nature of the optical carrier the output of this block varies continuously, so to rule out this problem, the ‘Phase difference’ is sampled every 100 ps for 10 Gbps operation. This sampling is performed by the first unit delay block of Fig.

4.19 and the optical phase difference between the adjacent symbols is extracted to perform the phase to intensity conversion operation of the MZDI, allowing the information coded in phase to be converted into detectable intensity information.

As only the real component of the received signal is considered, we add an extra +π/4 phase shift to the phase difference $\Delta\phi_{mod}$ of the signal received. From the phase information received, the corresponding output intensity of the MZDI is determined as

$$I = 0.5\cos(\Delta\emptyset_{mod} + \Delta\emptyset_{DI} + \delta\emptyset_{DI} \quad \ldots (4.9)$$

$$\text{where, } \delta\emptyset_{DI} = \frac{+\pi}{4}$$

The last term, $\delta\emptyset_{DI}$ is the phase offset originated from the MZDI and results in addition of extra phase noise to the system, to reduce the eye opening at the receiver. This effect arises due to the thermal instability of the heaters, inducing the required +π/4 phase shift, and thus resulting in random values about this bias point. This phase offset noise has been modeled in Simulink by assuming a maximum possible value of $\delta\emptyset_{DI}$ and using a random 'Gaussian White noise generator' with small variance as depicted in Fig. 4.19. Once we have the intensity equivalent of the phase difference, the need to convert received optical signal to electrical by the single-ended photodiode arises. A photodetector (PD) detects the received modulated signal of the transmitted optical power P*(t)* to generate a primary photocurrent given by:

$$I_{sig} = \frac{\eta q P}{hf} \quad \ldots (4.10)$$

which clearly points out the need to multiply the power, which is obtained from the MZDI, by the photodiode Responsivity,$\Re(= \eta q/hf)$ which has a typical value of 0.5A/W.

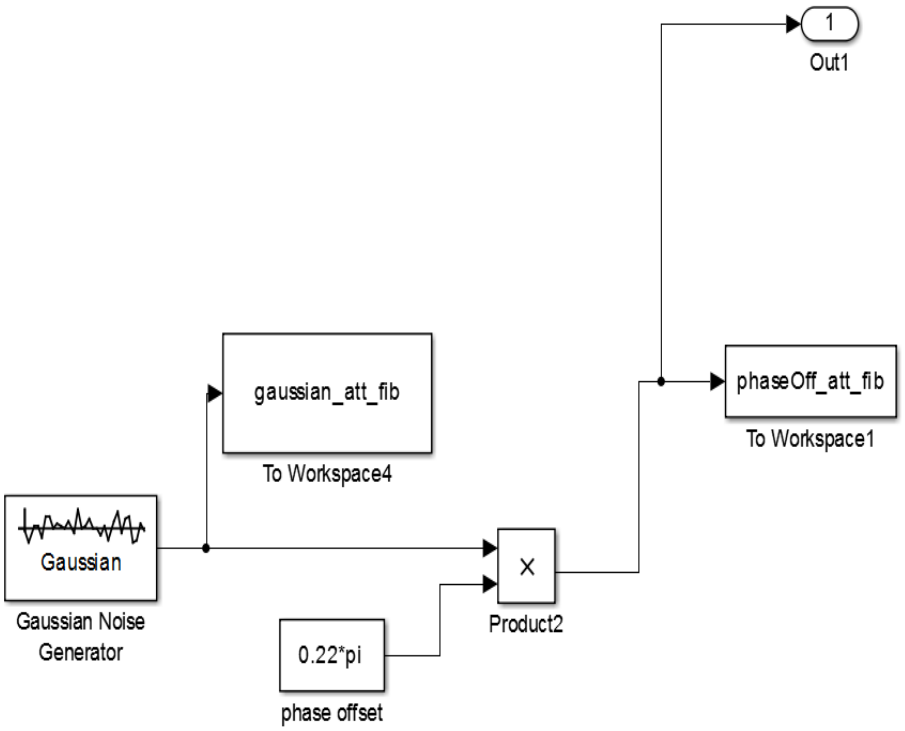

Fig. 4.19: Phase Offset Subsystem in Receiver Model

For analysis of the eye diagram generated by the received 'real' bits, the eye diagram pattern is approximated by the I pulse variable in our simulations. As the MZDI characteristic is cos-like, we treat the current waveforms forming the eye-diagram to show cos-like behaviour. The I pulse variable is expressed as:

$$Ipulse = -0.5\cos(t)+0.5 \quad ; \quad 0 \le t \le 2\pi; \qquad \ldots(4.11)$$

As the received optical signal is generally quite weak so we use an electronic amplification circuitry, after the photodiode, to ensure an optimum SNR. As the prime aim is to model the optical components used in real experiments in the best possible way, the effects of three noise sources is considered: the quantum shot noises i_{sh} , the PD dark current noise i_{dk} and the thermal (Johnson) noise i_{th}. The major contribution from the PIN photodiode based receiver noise is calculated and superimposed over the ideal photodiode signal current. The total current generated by the photodiode when optical power falls on it is given by:

$$i_{total} = i_{sig} + \sqrt{\langle {I_{noise}}^2 \rangle} \ldots\ldots, \text{where} \quad \langle {I_{noise}}^2 \rangle = \langle {I_{sh}}^2 \rangle + \langle {I_{th}}^2 \rangle + \langle {I_{dk}}^2 \rangle \qquad \ldots (4.12)$$

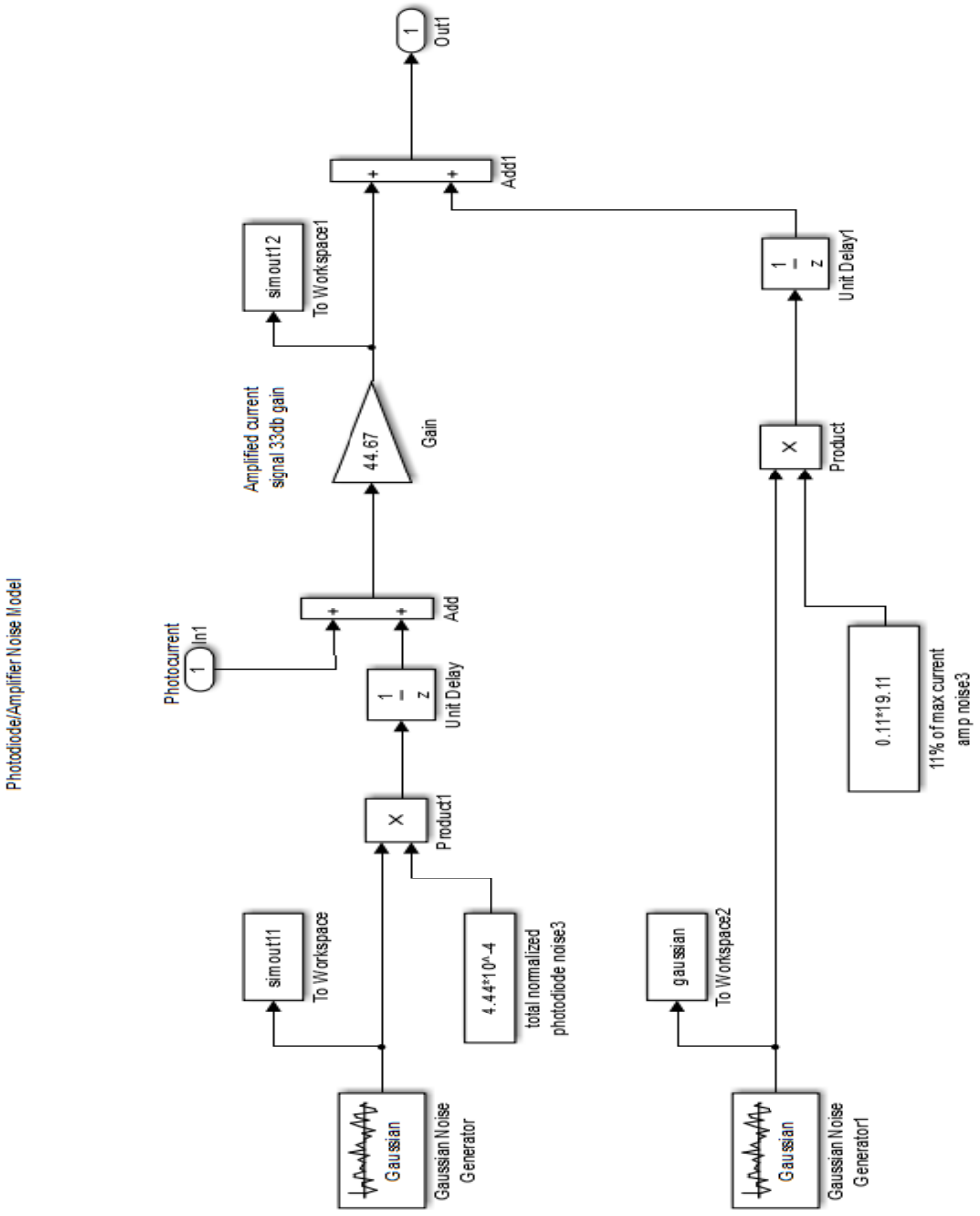

Fig. 4.20. Photodiode/Amplifier Noise Subsystem in Receiver Model

The amplification of the photodiode current is a critical requirement to ensure correct retrieval of data. The gain related to an amplifier is implemented with NF of 0.5 dB, translating to an 11% amplifier noise addition to the current waveform. The gain of this is set to 33 dB which translates to a power gain

of 44.67. The addition of the photodiode noise to the photocurrent, the amplifier gain and addition of amplifier noise models developed in Simulink are presented in Fig. 4.20.

4.6.6. Simulation Results

The simulation begins once the initialization file is run and the variables are loaded into the Matlab workspace. All the Simulink models have been connected properly and all the subsystems are working when simulated individually. The simulator displays the following window scopes in real time:

- MZIM and PM NRZ electrical random data driving signal;
- Optical power spectrum of single channel post transmitter and at receiver inputs;
- Single photodiode electrical current eye diagram scope at the receiver with no Photo diode/amp noise; and
- Single photodiode electrical current eye diagram scope post transmitter, and at the receiver super imposed by all noise sources.

Other time scopes in the simulator system can be manually opened during simulation run-time. The importance of certain data representation is left to users and can be disabled if required. However, the scopes selected to be displayed present a good overview of the current system design and allow, in particular, BER estimation directly from the eye diagram traces. Perfect signal propagation is seen in the Transmitter Block as visualized on the time scope of the transmitter subsystem in Fig. 4.21.

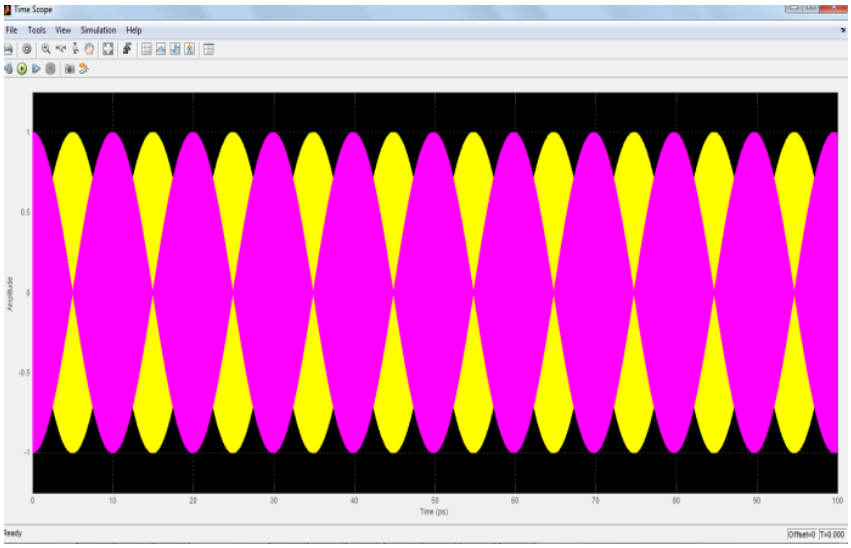

Fig. 4.21: Time scope of transmitter subsystem

The eye diagram obtained is outlined in Fig. 4.22 which shows a snapshot of the simulation on run and depicts the intermittent values on various signal scopes. The eye diagram is not very clear which points out certain discrepancies to be resolved in this model.

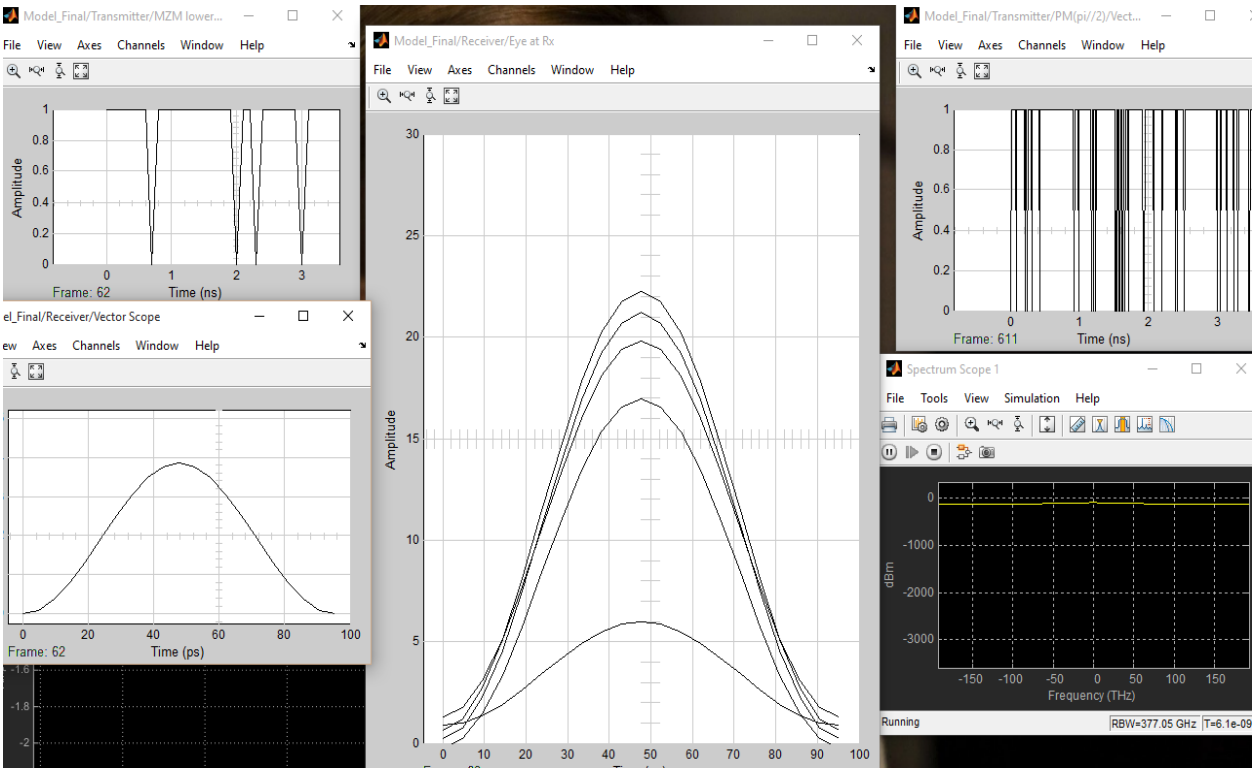

Fig. 4.22: Eye diagram at various time instants

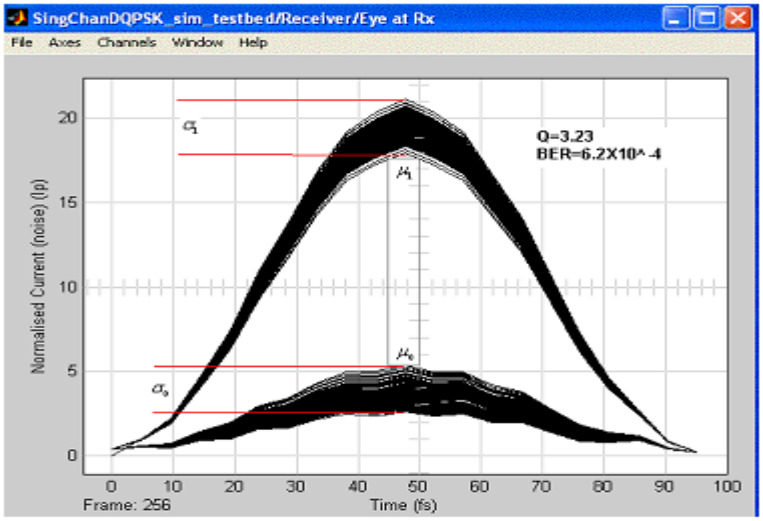

Fig. 4.23: Electrical current eye diagram generated at Rx with SMF link, No DCF inserted with PD and amp noise added.

For the case of no dispersion management we have calculated a BER of 6.2 x 10^{-4} as shown in Fig. 4.23. We thus now include the DCF fiber module in series with the SMF fiber and look at the positive effects of exact phase difference detection and improved BER. Since the dispersion factor of the DCF is approximated to exactly equalize all dispersion effects of the SSMF we expected an error-free eye

diagram at the receiver. We obtain the following eye diagram traces as shown in Fig. 4.24 and derive the Q-factor and its corresponding BER.

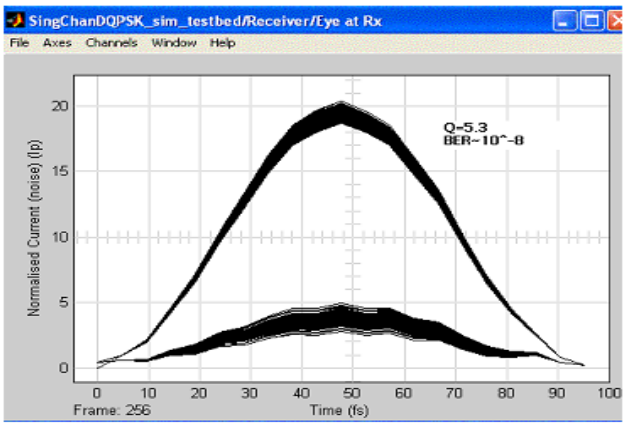

Fig. 4.24: Electrical current eye diagram generated at Rx with SMF & DCF inserted with PD and amp noise added

The BER of 10^{-12} achieved for 10 Gb/s single channel DQPSK dispersion compensated transmission system is considered error-free for single photodiode detection schemes. As mentioned earlier our intentions are to compare our simulated results with those published and experimentally conducted. In some published works, BER values extend to as low as 10^{-5} regions for single PD detection [223]. In practice, it is more common to use balanced detection receiver configurations they have shown to offer a 3 dB power improvement. If balanced detection is implemented, the BER would be expected to be 10^{-15}.

4.6.7. Conclusion of Simulink Modeling

The designed Simulink model demonstrates a 10 Gbps single channel DQPSK modulated optical link. In this model, corresponding Simulink blocks for the transmitter, fiber channel comprising of repeater loops, dispersion compensation and the receiver and other related sub-components are developed. The flexible nature of Simulink and its wide range of pre-designed block sets allow several important features for implementation of optically amplified transmission systems. Due to the good linkage developed between all parts of the optical fiber systems, the optimization of various block components is achieved. This simulator has, as required, simulated the most complex modulation format of the family of optical modulation techniques proposed in literature of digital optical communications. The nature in which the simulator has been designed in Simulink allows for future development of the DPSK and other optical modulation formats, e.g. multi-level M-ary schemes. The flexible nature of

Simulink allows the system to be customized to handle different fiber types, and can with simple alteration of the transmitter and receiver even implement the DPSK modulation format. Presently, this has been designed for DQPSK transmission; however certain components from this simulator may be used to generate new simulators suitable for alternative modulation formats.

This model provides a better physical intuition to visualize the transmission characteristics of DQPSK signaling in a realistic optical link and thus the proposed design considers a single channel link. The present model becomes quite complex to analyze and interpret for a DWDM system due to their multiple linear and non-linear distortions and unpredictable spread in spectrum. Even upgrading the data rate from 10 Gbps to 40 Gbps caused the simulations to crash intermittently due to high computational complexity and time consuming iterations. So to get an intuitive understanding of such a complex DWDM scenario together with numerous signal interactions and their interplay, for a 32 channel DQPSK link operating at 40 Gbps, a professional platform Optisystem is used. This 32 channel DQPSK link is the compared with the corresponding 40 Gbps 32 channel DPSK link to get an insight into the performance of phase modulated formats.

Chapter 5

DQPSK Modulated Ultra DWDM System

The amount of traffic carried on backbone networks has been growing exponentially over the past two decades. Internet traffic, driven by multitude of new users and bandwidth–hungry applications, is rapidly surpassing all other forms of voice and data transfer within today's communication networks. The required network bandwidth increases between 40% and 60% per year due to the rapid emergence of new communication services: social networking, 4K video, data traffic of smart phones and tablets, and cloud services. Enabled by such multifarious and the ever increasing traffic, which is mainly composed by high bandwidth data traffic, the optical fiber infrastructure is undergoing an evolution process in order to meet the array of wide variety of applications [137, 230]. The explosion of these services has led to the necessity of implementing new technologies in optical transport networks which increase their capacity.

5.1. Challenges Involved

Optical networks have rapidly evolved in a way that enables re-configurability characteristics and capability of handling high speed DWDM traffic. As the demand for such data traffic grows, suitable capacity enhancement strategies are achieved by, first, laying down more optical fiber links, second, by increasing higher bit rate per channel (10 Gb/s toward 40 Gb/s, even 100 Gb/s), and third, by applying more efficient use of the available fiber links [2, 231, 232] as described in the literature survey presented in Chapter 1. The first method requires a lot of infrastructural layout and is extremely costly. The second method is limited by the speed of commercially available electric devices, which is limited to 40 Gbps nowadays. The third method based on employing advanced multilevel modulation formats having better spectral efficiency, provides a cost-effective solution to achieve desired capacity. Transmission structures with phase modulation and differential coding and interferometer based reception for phase difference extraction are being used for 40 Gbps systems as discussed in Chapter 4. Usually, the application of advanced multilevel modulation formats in closely packed channels enhances the spectral efficiency of such fiber optic communication channels from 0.4 (b/s/Hz) to 1.6 (b/s/Hz) and beyond.

To enable the deployment of 40 and 100 Gbps services in optical terrestrial networks, high data rate channels must be loaded on an already existing WDM infrastructure designed for 10 Gbps OOK channels while reducing the channel separation down to 25 GHz. Photonic networks based on DWDM technologies require wavelength conversion to accommodate and route the channel wavelengths in various light paths. Such a configuration requires low crosstalk and small guard bands, especially for multiband transmission. However, wide guard bands around the pump wavelength are normally required to suppress the signal quality degradation caused by the parametric crosstalk among the WDM signals in the conversion process, especially if the channel spacing is narrow. The modulation format employed in the upgraded channels must thus feature both high spectral efficiency and good tolerance to narrow optical filtering. So the designer has to be extremely flexible in selecting a number of properties such as the type of modulation, efficiency, bit rate and the channel spacing needed for a long haul optical link. Therefore, all these factors must be studied in detail simultaneously to realize a higher spectral efficiency and greater total throughput in a long haul communication link [233]. So in this chapter 25 GHz-spaced DWDM transmission is being investigated intensively to support increase in traffic demand [234], by best utilization of the bandwidth resources.

5.2. Background work

Optical fibers have a unique feature of low threshold for nonlinear effects. When large number of signals simultaneously co-propagate in optical fiber, due to high power confinement nonlinear effects come into picture. In presence of optical amplifiers, these nonlinearities are greatly enhanced. The nonlinear effect SRS causes power transfer from one channel to another while XPM and SPM cause phase modulation of DWDM channels. The modulation of power and phase in one channel due to nonlinear effects in adjacent channels is considered as crosstalk in the present research work. Phase modulation of signals due to SPM and XPM gets converted to intensity modulation through dispersion and thus results in waveform distortions. Depending on fiber chromatic dispersion and its management, XPM induced nonlinear phase shift may become very detrimental for WDM signals [235,236]. In DWDM transmission systems, XPM induces a broadening of the signal spectrum and so wider optical filter bandwidth is required at the receiver. This degrades the system performance, because more spontaneous emission noise enters the receiver and becomes more critical at 25 GHz channel separation.

In reference [27, 237], authors extensively compare intensity and phase modulation formats with respect to chromatic dispersion, PMD, WDM crosstalk, optical amplifier noise, narrowband optical filtering and fiber nonlinearity. Phase modulation formats offer higher spectral efficiency and OSNR tolerance at the cost of transceiver's complexity. In [238], authors investigate different types of formats, such as CSRZ, DB, RZ-DPSK, NRZ-DPSK applied in WDM-PONs for link distances from up to 50 km and rates 1.25 Gbps, 2.5 Gbps and 10 Gbps. The study given in [239] shows a detailed performance comparison of various types of DB and PSBT formats for 40 Gbps and mixed 10/40 Gbps long-haul WDM transmission systems based on SMF and LEAF. Both DB and PSBT formats are more robust to intra-channel Kerr nonlinear effects than NRZ and offers an acceptable compromise between robustness to OSNR degradation and chromatic dispersion immunity. On the other hand, DB is a little bit less resistant to differential group delay than NRZ. DPQSK is primarily limited by XPM and is more suitable for transmission based on SMF.

Authors in [240] evaluate the performance of 42.7 Gbps DWDM systems for formats such as NRZ-OOK, DB, NRZ-DBPSK and RZ-DQPSK. Results from simulations show that RZ-DQPSK combined with Least Effective Area Fiber (LEAF) for 50 GHz channel spacing and spectral efficiency of 0.8 bit/s/Hz can provide approximately 50% improvement in terms of transmission distance over implementations based on other fiber and modulation formats. In [241], DPSK and DQPSK formats with NRZ, 33% RZ and CSRZ are investigated in 160 Gbps channels. Chromatic dispersion, higher-order chromatic dispersion, nonlinearity and OSNR are considered as well. Simulation results show that RZ-DQPSK offers the longest reach, NRZ-DQPSK offers the highest dispersion tolerance and RZ-DPSK enables the highest nonlinearity tolerance.

Other advanced solutions have recently been designed such as PDM-QPSK. PDM has been widely denoted either by polarization multiplexing, polarization division multiplexing, dual polarization or orthogonal polarization [242]. PDM-QPSK combined with coherent detection [243] and advanced DSP offers a very promising modulation format designed primarily for 100 Gbps optical channels. Authors in reference [244], investigate the performance of 100 Gbps PDM-QPSK channels for 8 Tbps transmission over a dispersion managed link based on low dispersion fibers. Experiment in reference [245] compares the system performance of 80 Gbps × 112 Gbps long-haul PDM-QPSK DWDM transmission over large-area fiber and SMF spans. Other modulation formats for 100 Gbps and higher rates are recently under research, e.g. the Dual Polarization Multi-Band OFDM (DP-MB-OFDM) format. Authors in reference [246] show that DP-MB-OFDM and PDM-QPSK offer nearly the same

performance at 100 Gbps after transmission over a 10 km × 100 km fiber line. Another promising modulation format for transmission rates of 100 Gbps [247] is the combination of polarization division multiplexing with Quadrature Amplitude Modulation (QAM) formats. Experiment in reference [248] shows the suitability of 256 Gbps PM-16 QAM and 128 Gbps PM-QPSK modulated signals in long-haul and submarine systems with span lengths over 100 km.

Stupendous advances in optical communication has enabled the researchers to combine DWDM, optical time-division multiplexing (OTDM) and optical code-division multiple access (OCDMA) systems. Moreover, coherent fiber optic systems involving homodyne or heterodyne detection schemes have also been extensively explored [249]. The high receiver sensitivity offered by these systems motivated a huge surge in their demand but were not commercialized due to costly and complex components and challenges in the proper design of optical PLLs. More recently [20,251] coherent optical systems are re-emerging as an active domain of research due to relaxation in line width requirements and development of sub-megahertz line width lasers. High-speed DSP techniques have enabled the implementation of critical operations like phase locking, frequency synchronization and polarization control in the electronic domain. These developments led to the realization of stable coherent receivers but are costly and still have scope for further improvements. So in this work the design of a 25 GHZ spaced UDWDM optical link is targeted using a simple transmitter and receiver architecture. A crucial decision while doing so is to choose the modulation format to be used which is discussed in the next section.

5.3. Optical DQPSK in UDWDM system

Some formats are better suited than others when it comes to tight WDM channel packing, quantified by their spectral efficiency. Apart from SE-dependent nonlinearity considerations, there are two concern impairments arising from dense channel spacing: crosstalk and filter narrowing. An optical channel can be affected by two different types of crosstalk [233]: linear or inter-channel crosstalk (undesirable power of adjacent DWDM channels in the desired band generating interferences at square-law detection) and homodyne or intra-channel crosstalk (also known as Multipath Interference or MPI) [252], which describes the coherent interference of a signal with residual signals at the same wavelength due to imperfect, reflective fiber connectors, double-Rayleigh backscattering, or due to from imperfect drop capabilities of Optical Add Drop Multiplexers. The former is quite easy to avoid with optimal filtering of the desired band, but the latter is hardly removed by optical filters. In general,

phase modulated signals are more tolerant to linear and homodyne crosstalk than intensity modulations. In analogy to linear crosstalk, undesirable power in-band with the signal gives rise to signal-MPI beat noise at square-law detection becoming amplitude jitter in the eye diagram, so that the eye penalty in DQPSK is lower than in OOK signals due to the fact that information is encoded in the optical phase. Strictly, the impact of crosstalk on system performance depends on the number of interferers, the OSNR delivered, the modulation format and the signal's waveform (in particular the signal extinction ratio, and the phase coherence of the interfering signals) [253-255].

After the phase and the amplitude, the state of polarization is considered as the third dimension for encoding data on optical signals. Polarization-multiplexing is an efficient way for transmitting two entirely independent signals simultaneously over the same bandwidth, using the two orthogonal polarizations of light. Nowadays, polarization-multiplexing is widely believed to be an indispensable part of any high SE optical transmission system. A SMF in reality has a split of the fundamental mode into degenerate modes orthogonal polarized, constituting the x and y components of the E field vector. These orthogonal modes can be used to simultaneously carry two independent channels, thus doubling the information throughput. The reasoning is that when a monochromatic radiation having a certain polarization has imposed on it a change of SOP (state of polarization) to the orthogonal SOP (antipodal position), this orthogonality survives the propagation process, and the received states of polarization remain orthogonal. There are two posible ways of carrying out Polarization Division Multiplexing; the first is to employ a co-channel arrangement, in which two channels having the same carrier frequency are orthogonally polarized [256] and the second is to apply polarization interleave multiplexing, in which each channel is orthogonally polarized to the neighboring channels [257, 258]. We have used the first arrangement in our simulations to increase the capacity of the optical link.

So keeping all the above discussed parameters in consideration an interesting approach to increase capacity is to use a large number of closely spaced channels. The optical bandwidth of the used amplifiers and the frequency separation between adjacent channels, are the two factors which limit the number of channels supported on such a link. Incorporation of multilevel modulation formats in DWDM system has led to the exploration of the 25 GHz channel grid, popularly known as UDWDM systems, a new research frontier. Transmission on the 25 GHz grid has been reported previously for long-haul and submarine applications [259]. It demands several wavelengths spaced by a few GHz to be launched over several Kms of an optical fiber, resulting in substantial nonlinear crosstalk which deteroirates the system performance. Although the spectral density and the total transmission capacity

of a 25 GHz grid may not be up to the mark to that provided by a 100 Gbps system operating on the 50 GHz grid, but a system with lower data rate operating on the 25 GHz plan offers a feasible alternative.

Strong optical pre-filtering is a critical need to ensure low crosstalk during transmission of high speed data over the narrow channel spacing, whereas, excessive filtering leads to ISI, making the determination of a suitable modulation format tolerant to tight optical filtering a vital factor. Among the proposed modulation formats that meet these requirements, DQPSK has been investigated using a standard incoherent receiver. It's compression in frequency offers higher SE compared to DPSK primarily at 40 Gbps, as well as increased tolerance to CD and PMD due to its longer symbol length and, doubles the bit rate for a given bandwidth. As a multi-level modulation format, DQPSK encodes 2 bits/symbol practically achieving a SE of 1 b/s/Hz and is compatible with 50 GHz/25 GHz DWDM spacing grid [255]. In this chapter, the challenges in supporting spectrally efficient 40 Gbps DQPSK modulation format are addressed by examining an UDWDM link, in terms of distance achievable for a target BER of 10^{-9} using Optisystem 10.0. Till now, various schemes have been proposed in literature to transmit DQPSK modulated signals over long haul distance, but most of them use lesser number of channels [260] or, operate at a lower bit-rate [261] or use complex signal processing either at the transmitter or the receiver end using coherent detection [243, 262]. We discuss here, the generation, transmission and detection of alternate-polarized DQPSK signal to support transmission at 25 GHz channel spacing by a simple method. The theory and transceiver structures required for DQPSK modulation have already been discussed in detail in the previous chapter. The same modulator and demodulator structure with the addition of alternate polarization for each subsequent channel is used in this chapter to realize a cost–effective UDWDM system.

5.4. Numerical Simulation Model and System Description

The major issues critical for the design of current and future UDWDM systems are the relationship between transmitted signal modulation format, bit rate, optical channel spacing and parameters of multiplexer and de-multiplexer filter [121,190]. Rigorous study and efficient modeling of non-linear effects, has resulted in various approaches, each focusing on the features and requirements of the system being analyzed. In DWDM environment, nonlinear propagation phenomena leads to either intra-channel effects, which manifest themselves as non linear inter-symbol interference, or inter-channel effects, such as XPM and FWM, and in a complex network scenario, these distortions are random and are customarily treated as noise. The primary objective of analytical models of fiber

propagation is to characterize this noise accurately in terms of its statistical properties. Such models provide a better insight by prediction of nonlinear noise power and spectrum, estimation of system capacity considering the nonlinear noise and, also the non-linear impact can be eliminated by selecting proper system parameters [26,29]. Investigation of the performance of DWDM systems incorporating the effect of fiber nonlinearities uses primarily, numerical simulations, based on the solution of the NLSE, as it allows visualizing the effect of each transmission impairment individually, while making the computation of the collective effect of the simultaneous presence of various impairments also feasible.The detailed XPM model built upon coupled NLSE has been discussed in Chapter 2 and we use it here to analyze the effect of XPM as signal propagates over the optical fiber.

This chapter presents a simulative model to implement and analyze alternative polarized DQPSK modulated UDWDM system in order to evaluate its resilience to XPM and fiber nonlinearity. To consider the various detrimental effects, a semi-analytical model is adopted in which signal propagation along the link is evaluated using simulation.

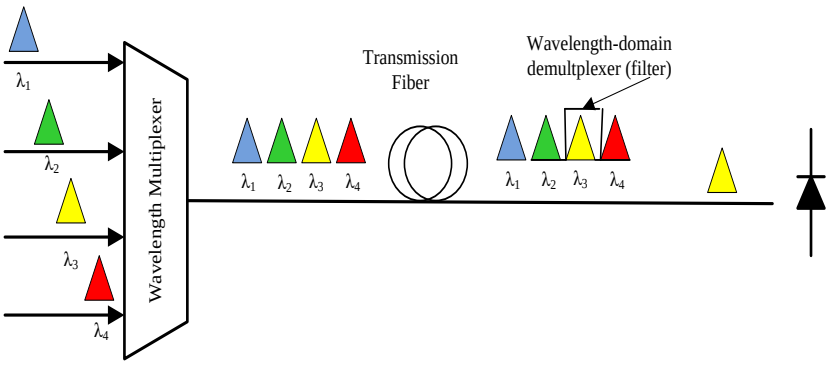

Fig. 5.1: Generailized 4 channel UDWDM system

Firstly, a DQPSK modulated 4 channel 25 GHz spaced network as shown in Fig. 5.1 is designed and gradually the number of channels is increased to 8, 16 and then 32. Next, the performance of this 32 channel 25 GHz spaced system is compared with that of an 50 GHz spaced link at different power levels to provide a comparative analysis of the maximum distance achievable, on the basis of Q value and eye opening for multiple transmission spans by varying the input power of a signal. The study explores the effect of changing the number of channels, channel spacing and its influence on both the received BER and XPM.

A multi-segmented, optically amplified UDWDM system model is assumed to arrive at the generalized forms of fiber non linearity-induced distortions. We consider chromatic dispersion as a lumped distortion at the end of each span which is compensated by dispersion compensation element, assuming no PM-IM conversion is involved. Only XPM and loss are considered to be distributed over the length of the fiber. The degree of XPM impairment is influenced by various parameters, such as nonlinear fiber coefficient γ, walk-off between the two adjacent channels, individual channel power and the modulation format used [263]. Signal launch power is kept low enough to ensure that the system is not susceptible to SPM induced nonlinearities. Deployment of appropriate DCFs in the fiber link curtails the degradation due to GVD.

Phase modulated systems are very sensitive to fiber non-linearities as the imposed phase shift directly affects the received signal. The major source of intensity fluctuations is the ASE noise from optical amplifiers which results in nonlinear phase noise in long haul multi span systems. This model relies on the fact that a certain number of bits pass through the adjacent DQPSK channel due to dispersion making the XPM induced phase shift to be bit pattern dependent. A frequency difference of $\Delta\nu$ between the channels corresponds to a typical Δt, time difference given as $LD\lambda^2\Delta\upsilon/c$,where D is the dispersion parameter, λ is the optical wavelength, L the fiber length, and c is the speed of light. The number of walk-of bits that pass from a particular point of the DQPSK signal over the entire fiber length is defined as N_W, and equals to $\Delta t.B$ with B being the bit rate. This accounts for determining the standard deviation of the DQPSK phase shift at the receiver side. In a fully dispersion compensated system, both DCF and SMF have the same N_W, but vary in the signal power level and the direction of passing.

The nonlinear phase shift $\Delta\varphi_{XPM}$ is equal to $2\gamma P\Delta z$. For simpler calculations, it is assumed that power level in DCF is too small to allow any considerable nonlinear phase shift and the major distortions occur in SMF. Moreover, it is assumed that the signal shape is not altered over the fiber length as major nonlinear crosstalk occurs in the initial fiber segment where the power is comparatively higher [264, 265]. Considering ones and zeros to be equi-probable, a distribution of phase shifts corresponding to a system with specific parameters is built and standard deviation of phase, σ_{NL}, is calculated as it is shows the degree to which the phase modulated signal disperses and thus is a parameter for quality assessment. The total phase shift is found by integrating the differential phase shifts along the fiber length, as the power term depends both on the position and bit stream. The maximum possible phase shift corresponds to the case when all N_W bits are one and the minimum phase shift occurs when all N_W bits

are zero, and phase shifts get distributed between these two limits. Thus, a bit stream of *bi (i=1, 2,3...., N_W)* will result in:

$$\Delta\emptyset_{XPM} = \sum_{i=1}^{N_w} b_i \Delta\emptyset_i \quad \ldots (5.1)$$

where $\Delta\emptyset_i$ is the phase shift caused by *ith* bit given by:

$$\Delta\emptyset_i = \frac{2\gamma}{\alpha}\left[exp\left(\frac{-\alpha L(i-1)}{N_w}\right) - exp\left(\frac{\alpha i L}{N_w}\right)\right] G_1 P_{in} \quad \ldots (5.2)$$

The BER is calculated from the standard deviation of the phase using:

$$BER_{QPSK} = \frac{1}{2} erfc\left(\frac{\pi}{4\sqrt{2}\sigma_{NL}}\right) \quad \ldots (5.3)$$

In a multiple span system, any sample point on the DQPSK signal coincides with the same set of bits, and experiences similar nonlinear phase shift in each span. Hence, we multiply σ_{NL} by the number of spans to consider the effective phase shift for the entire system [32]. For error free communication, the threshold of optical communication system corresponds to a BER of less than or equal to 10^{-9}, translating to a Q-factor of greater than or equal to 6 or 15 dB. This is considered as a reference and the performances for different cases are evaluated based on Q-factor using Optisystem.10.0.

5.4.1. Transmitter Design

The proposed 32 channels link consists of a transmitter section, fiber module and an optical receiver as shown in Fig. 5.2 with the central frequency of the first channel as 193.1 THz. The signal is launched with alternate polarization into the respective channels. The 40 Gbps DQPSK signals with 50% duty cycle are generated by conventional DQPSK transmitter called an I-Q modulator which consists of a PRBS generator, DPSK precoder, NRZ pulse generators and three MZM's concatenated together in order to achieve phase stability as shown in Fig 4.8. The input power is varied and the signal is launched over N spans of 60 Km each. The system has been configured for both 25 GHz and 50 GHz channel spacing and a comparative assessment is presented in terms of BER and Q-factor. The emission frequencies of CW lasers are equally spaced for both 25 and 50 GHz channel separation, and the optical channels have alternate polarization. A 128-bit sequence with 32 samples per second modulates each

channel. MZM's with the extinction ratio set to 30 dB are used. The modulated optical signal is then fed to the 32 input ports of an optical multiplexer.

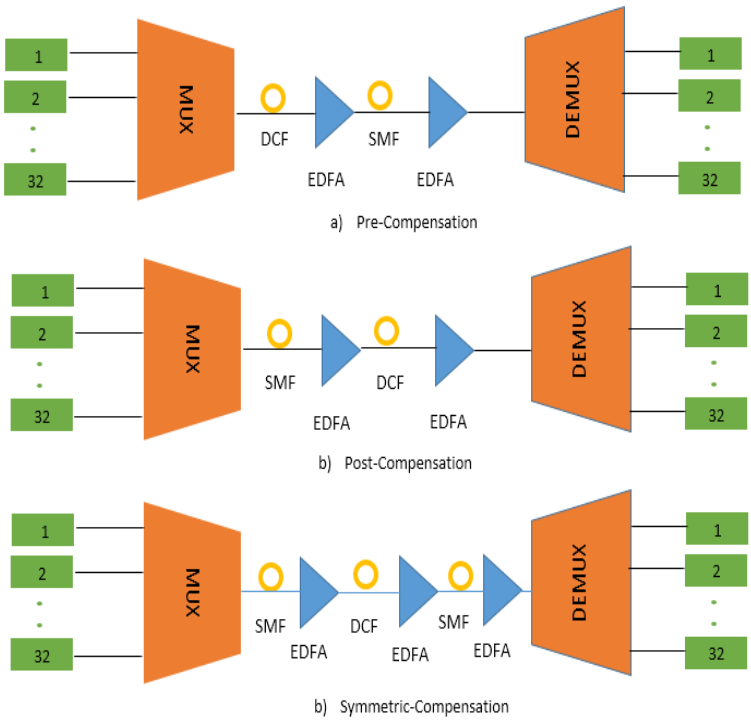

Fig. 5.2: Schematic of simulation setups:
(a) pre-compensation scheme, (b) post-compensation scheme and (c) symmetrical-compensation scheme

Crosstalk between the adjacent channels is avoided by tight optical filtering before multiplexing. As XPM appears only in multi-wavelength systems thus, the key optical components in DWDM systems are those performing the function of combining (multiplexing) different wavelength channels and splitting (de-multiplexing) them. Combining different wavelengths is a relatively simple task and can be achieved with a component such as star coupler or an arrayed waveguide grating (AWG). The operational data-rate and the bandwidth of each channel have to be taken care off while choosing optimal filters. De-multiplexing, however, requires optical filters with sharp wavelength cut-offs; it is a much more challenging problem when practical systems are considered. It becomes a real challenge in UDWDM systems with very low channel spacing. So it is important to determine how to choose optimal transmitting filters. Very little has been reported on this subject [121, 222]. Several observations regarding filtering are drawn upon using optical spectrum as a first guideline. However, due to the fact that practical optical fiber systems are non-linear systems, makes it difficult to offer

clear statements about optimal filters. Nevertheless, simulations regarding electrical and optical filter structures and parameters (eg. filter order, amplitude, and or phase response, filter bandwidth) were carried out to gain some insight.

Butterworth and Bessel filters of various orders were examined. These filters represent a wide range of properties. The Butterworth filter is known for its magnitude response that is maximally flat in the pass band and monotonic overall; on the other hand, it presents a poor-time delay performance, giving rise to effects such as overshoot and ringing, when driven by pulse signals. The Bessel filter is known for its maximally flat group delay response; the price paid for almost constant delay is signal attenuation and less steepness in the transition region between pass band and stop band. In short, Butterworth filters present good frequency-domain performance preserving signal amplitude. On the other hand, Bessel filters provide excellent time-domain performance that minimizes waveform distortion. For Butterworth filter, the optimal filtering bandwidth depends on the filter roll-off. Filters with fast roll-off tend to have wider bandwidths. Furthermore, low-order filters present better performance than high-order filters. For Bessel filters, the optimal filtering bandwidth dependence on filter order is not as much evident as in the case of Butterworth filters.

Overall, simulations have shown that Bessel filters have a slight better performance than Butterworth filters as they allow signals to span longer distances due to their superior attenuation characteristics and hence have been used as demux filters in our simulations. We optimized the type and order of both the multiplexer and the de-multiplexer filter as filter characteristics play a significant role in link design and evaluated the filter performance on the basis of receiver sensitivity in terms of the received Q value. Optical filters for both multiplexer and de-multiplexer is modelled by using the transfer function of 'elevated cosine' type with the center at the signal carrier frequency. Each channel is filtered optically with a fourth order Bessel filter with a bandwidth of 25 GHz for 25 GHz channel separation and a bandwidth of 50 GHz for the other case.

The combined optical signal is then fed into the SMF. CD is compensated by using a single-periodic amplification scheme at the span input (pre-compensation) as Fig. 5.2(a), at the span output (post-compensation) as in Fig. 5.2(b) and along the span (inline-compensation) as in Fig. 5.2(c) by sections of DCF. It was observed that post compensation scheme provides an optimum performance for DQPSK formats in agreement with the results in the literature [234] and hence this scheme has been used in the present analysis. In each section, EDFA having a noise figure of 4 dB is used to compensate the power

loss of the link ignoring the corruption due to ASE noise. The fiber model in OptiSytem takes into account the unidirectional signal flow, stimulated and spontaneous Raman scattering, Kerr-nonlinearity and dispersion. An SMF with α of 0.22 dB/km, D of 17 ps/km-nm and dispersion slope (S) of 0.08 ps/nm^2/km at 1550 nm, nonlinear refractive index (n_2) of 2.6×10^{-20} m^2/W, and A_{eff} as 80 μm^2 has been considered. The DCF segment used in each span has α of 0.5 dB/km, D of -85 ps/km-nm, S is -0.45 ps/nm^2/km at 1550 nm, $n_2 = 2.6\times 10^{-20}$ m^2/W and $A_{eff} = 30$ μm^2.

5.4.2. Receiver Design

There are two different approaches to demodulate the DQPSK signal, the first one is to receive the DQPSK format with differential direct detection receivers which requires efficient dispersion compensation and tight filtering as used in this thesis. The second approach uses coherent receivers combined with EDC exploiting DSP capabilities for practical implementation [233]. As the phase information is preserved in the coherent systems, coherent systems offer more options such as PM-QPSK (polarization-multiplexed quadrature phase-shift keying), PS-QPSK (polarization-switched quadrature phase-shift keying), PM-16 QAM (Polarization-Multiplexed Quadrature Amplitude Modulation) and DP-QPSK (Dual-Polarization quadrature phase shift keying) [266]. But moving to these higher order modulation techniques needs a compromise on the optical reach as the amount of optical power is less for each bit in modulation symbol. Also coherent optical systems require much more complex electro-optics than direct-detection schemes which simply translates into increased cost. Moreover, such systems require complex DSP based algorithms leading to computation complexity as well. Most of the work using coherent reception has been reported for single wavelength 40 Gbps and 100 Gbps deployments [250]. Single channel setups are easier to simulate but coherent QPSK-UDWDM systems are still unexplored to a great extent. Though coherent UDWDM offers high sensitivity and better co-existence with current PON deployments, the potential high cost and device complexity has limited its attractiveness to operators [243, 267].

The main aim of the present analysis is to explore the integration of DQPSK modulation in UDWDM network. In this work, we have attempted to achieve long haul transmission with 32 DQPSK transmitters without using complex setup of polarization controllers, polarization splitters, electronic signal processing and strict phase matching requirements and got appreciable results using a much simpler setup. The DQPSK signals are decoded optically using a simple optical delay and add interferometer structure as shown in Fig. 4.9. This design is basically based on direct detection

technique, avoiding the complex design of a DSP based coherent receiver. The MZI performs the correlation of each received bit with that of its neighbor and performs the corresponding phase-to-intensity conversion. Though the present design compromises a little bit with the phase coherency requirement, but offers an acceptable insight of the performance of the proposed lightwave system.

In the receiver side the signal is first filtered by a 3rd Order Bessel optical bandpass filter with a 3-dB bandwidth of 23 GHz for 25 GHz channel separation case and a 2nd order Bessel optical bandpass filter with a 3-dB bandwidth of 50 GHz for 50 GHz channel separation case, at the receiver side. This removes the ASE noise power outside the signal bandwidth. Two asymmetrical MZI and two balanced photodiodes detect this filtered optical signal, which now is filtered electrically by a fifth-order Bessel filter with a 3-dB bandwidth of 40 GHz. The impact of FWM is weak compared to the SPM and XPM due to the chromatic dispersion of the SMF [34] and is thus neglected. Thereafter, a 3R regenerator connected to the BER analyzer is used which generates graphs and results such as eye diagrams, BER, Q value, etc.

5.5. Simulation Results

First a four channel DQPSK modulated 25 GHz spaced system is designed and its performance is evaluated at 0 dBm power level. We choose the DCF and SMF parameters to compensate the first-order dispersion exactly (D = 0) i.e. $D_{SMF}L_{SMF} = D_{DCF}L_{DCF}$. Then the number of channels was gradually increased to 8, 16 and then to 32. Table 5.1 presents a comparative assessment of Q factor observed vs. maximum distance traversed by the optical signal for different channel spacing configurations. The dependency presented in the table indicates an increase in the level of crosstalk with transmission by using a greater number of adjacent channels. Though the starting Q value is nearly in the same range of all four cases, but the transmission distance is around 1800 Km for 4 channels as compared to 900 Km for a 32 channel case, clearly indicating the increase in XPM induced crosstalk.

Table 5.1: Q- factor for different number of channels

No. Of Spans	Q Factor (4 channel)	Q Factor (8 channel)	Q Factor (16 channel)	Q Factor (32 channel)
1	13.56	13.43	13.67	12.64
5	12.4	12.38	11.67	10.44
10	9.85	10.16	10.97	9.26
15	8.32	8.2	8.64	7.27
20	6.47	5.19	6.04	5.56
25	6.2	5.34	5.85	NA

30	6.51	NA	NA	NA
35	5.21	NA	NA	NA

Note: NA (Not acceptable as below 6 which is the reference value)

Next the proposed 32 channels UDWDM system is simulated for the ideal situation i.e. in the absence of non linearities by setting the non-linear coefficient, γ to zero at a fixed power level of 0 dBm. The performance gain is obvious and clearly visible in Fig. 5.3 where it is compared with a system that considers non-linearities. Since the main aim of the paper is to study the effect of nonlinear impairments in a UDWDM system, we included the nonlinear limitation in all further studies.

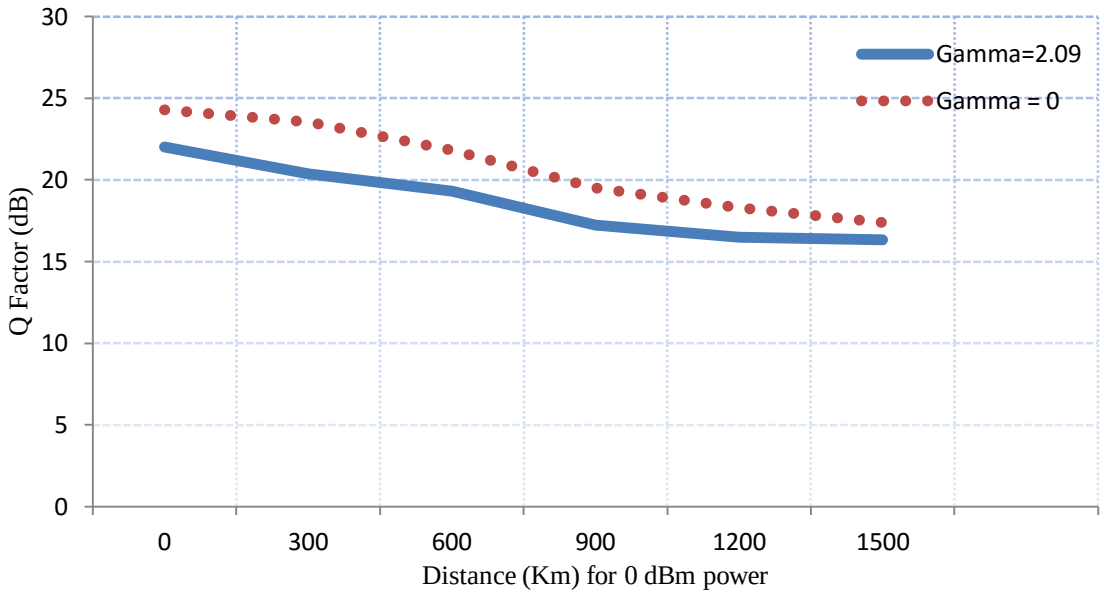

Fig. 5.3. System performance comparison in the absence and presence of non-linearities.

The 32 channel system has been further analyzed for various input power levels. Fig. 5.4(a) - (c) outline the performance of both 50 GHz and 25 GHz spaced DQPSK system graphically in terms of the Q value as a function of transmission distance. It was observed that eye-opening penalty increases for very strong transmitted power, highlighting the SPM induced phase modulation to intensity modulation conversion through fiber dispersion. By increasing the power, SPM grows and depletes the signals. Thus, power increases up to the point where non-linearity dominates over chromatic dispersion impling that signal degradation starts to occur. On the other hand, for low input powers an improvement is observed in the system performance. So for a high data rate WDM system, it is desirable that the input power should be as low as possible to limit non-linear effects hence we vary the input power between - 5 dBm to 5 dBm. Fig. 5.4 (a) reveals that for very low power levels of

-5 dBm, the 25 GHz DQPSK modulated system manages to run for 10 spans i.e. a distance of 600 km, while the 50 GHz system attains a transmission distance 900 km. The initial Q value after the first span is 20 dB for 50 GHz case, while it is 18 dB for 25 GHz. The curves overlap between 500 to 700 Km indicating similar performance in both the cases.

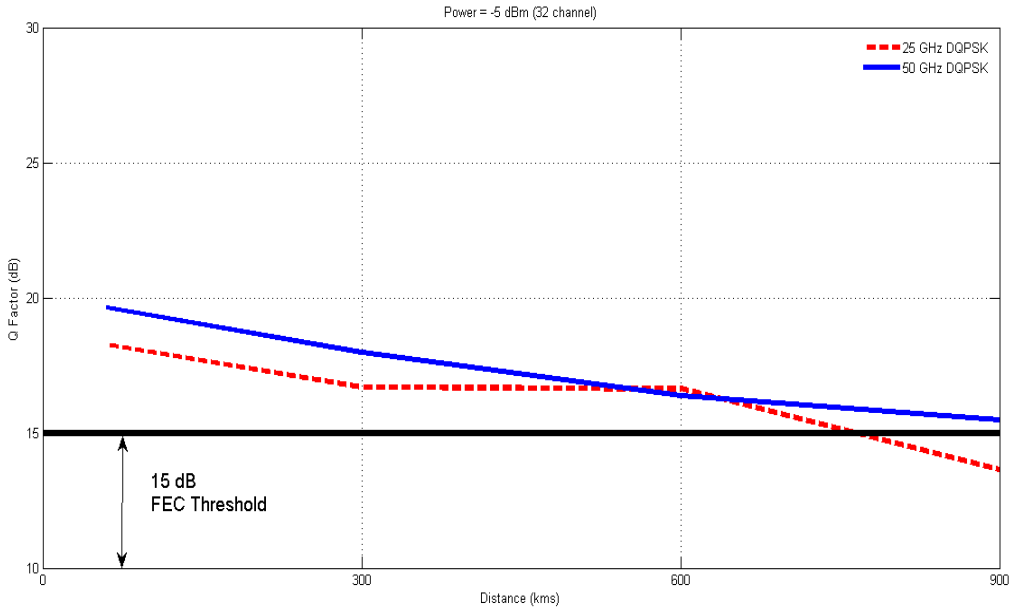

Fig. 5.4(a)

As the power increases to -1 dB, the safe operating distance increases in both cases, being close to 1200 km for 50 GHz case and around 1000 km for the latter. Another point to be noted is that tough the Q value for 25 GHz separation remains below the former, but the initial Q values also increase close to 24 dB as compared to 18 dB for -5 dBm power level. CD produces a variation of the instantaneous frequency in a modulated optical signal [25]. This variation of the instantaneous frequency results in pulse broadening which generates ISI. Obviously, after propagating some distance in the fiber, a point is reached where the accumulating pulse spread is too great for the receiver to recover the signal pulses within the equipment BER specifications.

Performance at 0 dBm power follows closely the case of -1 dBm as highlighted in Fig. 5.4 (b) for both cases. We achieve a safe operating distance of 1500 Km for 50 GHz case and upto 1200 km for 25 GHz spacing, before the Q-value degrades below 15 dB threshold. So, we can infer that the DQPSK modulation format is more suitable for higher values of power as it offers generous system margin due to its high spectral efficiency and relatively good tolerance to fiber degradations making it desirable

for long haul transmission. The tolerance of a modulation format to CD with and without filtering is fixed by the spectrum and the waveform launched to the fiber. In a simulation scenario without optical filters these factors are exclusive of the specific modulation employed in the lightpath. In contrast, in the scenario with filtering the waveform and the spectrum are determined by the set "modulation & filters". The narrower the signal spectrum, the higher the tolerance to the CD_{acum}. Filtering process reduces the bandwidth of the signals, so the difference between the group delays of the different spectral components will be smaller.

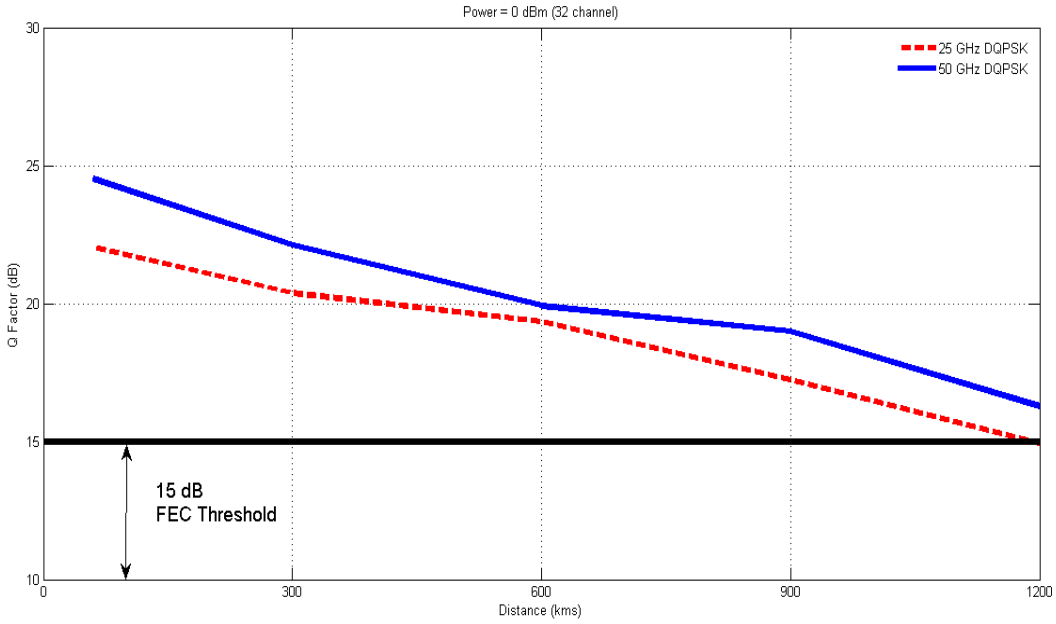

Fig. 5.4 (b)

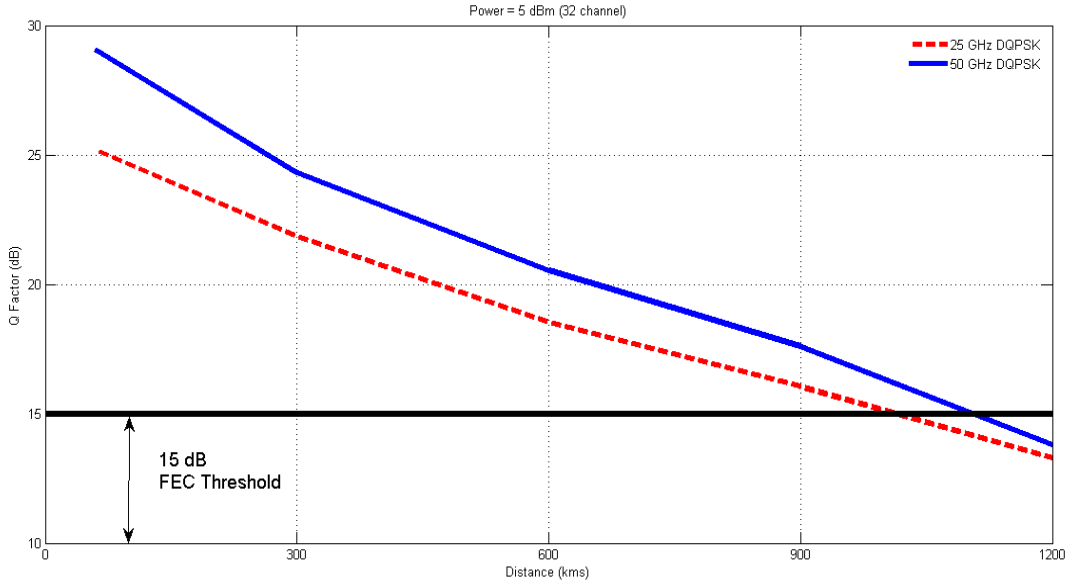

Fig. 5.4(c)

Fig. 5.4. Q value as a function of transmission distance for (a) Pin = -5 dBm (b) Pin = 0 dBm (c) Pin = 5 dBm

At 1 dBm launch power initially the Q value increases up to 26 dB and it performs well for distances over 1200 Km, but the curves do not follow each other closely. For the 5 dBm launch power case as in Fig. 5.4 (c), 50 GHz system outperforms the 25 GHz one from the first span with as starting Q value close to 30 dB as compared to 26 dB for 25 GHz case and maintains its superiority up to 1100 Km, while the 25 GHz system falls below the threshold at 1000 Km only. In both the cases, a maximum transmission distance of 1000 Km is is attained.

A significant decrease in observed in XPM effect when the input signal with a finite small rise and fall time is considered. Thus, signal shape is an important parameter regarding the XPM impact. A possible explanation is that assuming finite rise and fall times is equivalent to a strong attenuation of the secondary lobes of the signal spectrum. Thus, pulses with steep leading and trailing edges broaden more rapidly with fiber propagation. When raised cosine signals with different roll-off factors are used, the pulse widths as well as steepness of their edges are also changed. Therefore, the length of fiber where interference takes place is smaller for pulse shapes with relatively broad leading and trailing edges, according to the definition of the walk-off length. As a result, XPM induced interferences reduces, consistent to results reported in literature.

Regarding cross-phase modulation effects, it was observed that it scales almost inversely proportional with channel spacings. It was also seen that the magnitude of the XPM induced interference is smaller for pulse shapes with relatively broad leading and trailing edges; for raised cosine shaped input signals, roll-off factors greater than 0.5 should be considered. Also, the average input power should be kept under 8-10 dBm, otherwise the combined effect of XPM and SPM induce strong penalties. In all simulations, the superposition takes place in a very short time. When the channel spacing is narrower XPM-induced interference is much more severe; also, the impact of pulse shapes is not so important as compared to spacing's greater or equal to 0.5 nm

XPM induced coupling among light waves is indeed polarizaton dependent. When the pump and probe waves have orthogonal polarizations the impact of XPM inducednon-lnear phase shifts is lower than the case of parallel polarization. It was also verified that XPM interfence was mostly generated near the beginning of fiber. Since the dispersion parameter of the simulated fiber is kept constant, the intensity fluctuations measured at the end of fiber are essentially determined by the phase shift induced in the beginning of fiber. These simulated results are in agreement with theoritical results [144-145].

The numerical results show that DQPSK could achieve after optimizing the simulation parameters a maximum reach of 1500 km for at least 10^{-9} BER, in the optical path in a 40 Gbps transmission system with 25 GHz channel spacing. Larger channel spacing significantly decreases the inter-channel interference. In case of DQPSK, a channel spacing of 50 GHz could achieve up to 40 % reach improvement. RZ-DQPSK improves the system performance at the cost of the transmitter's complexity. The performance of 50 GHz system no doubt is better as compared to 25 GHz case, but even for the latter the Q value maintains above the FEC threshold for upto 1000 km which is an interesting observation. In work [266] experimental and numerical investigations of the transmission reach of PS-QPSK and PM-QPSK are reported for three different fiber span lengths i.e. 83, 111 and 136 km which is lesser as compared to the present investigation and moreover it operates with only 9 channels on a 50 GHz grid. In work [268] the performance of 42.8-Gb/s and 112-Gb/s intradyne coherent PM-QPSK system is studied with inline DCF to acheive a distance reach of 1000-km which is comparable to our results but with a higher cost and complex design. This reinstates that using DQPSK over UDWDM offers three key functionalities: (i) better wavelength selectivity removes the requirement of expensive ultra-dense filter technology; (ii) high receiver sensitivity enables a system with better splitting ratios and longer reach; (iii) usage of digital signal processing relaxes the implementation of equalization of transmission impairments as well as FEC.

5.6. Conclusion

The work successfully demonstrates the transmission of 32 DQPSK modulated channels up to 1500 km in the presence of various simulated fiber nonlinearities. The OptiSystem trans-receiver model is developed to estimate the comparative transmission performance parameters of the proposed UWDM systems operating at 25 GHz and 50 GHz channel spacing at various input power levels. The simulation study of the results shows that DQPSK modulation is better in terms of crosstalk mitigation during the transmission of signals. It also outperforms at higher launch powers due to its better spectral efficiency, enabling it to tolerate the dispersion induced degradations.

The observations of the present analysis are useful for an experimentalist to visualize the various complexities involved in such high speed links. However, the scope still remains open to choose the preferable fiber to transmit DQPSK modulated signals with varying duty cycle. As very few UDWDM system experiments have been conducted till now, so the fundamental limiting factors and their remedies in such systems are not clearly defined, especially when transmitting at a data rate higher than 40 Gb/s. Thus, it is inferred that at these data rates severe chromatic dispersion and polarization-mode dispersion limitations need to be addressed before dealing with optical non linearity-induced penalties. QPSK has a better PMD tolerance compared to BPSK. But it is still sensitive to the polarization limitation. One way to overcome this problem is to use coherent detection for each of the subcarriers. This method requires four very stable receiver lasers as the local oscillators, which is obviously a very expensive solution. Such an integration of coherent technology based on PM-QPSK, PS-QPSK, PM-16 QAM and DP-QPSK with UDWDM can be explored as a part of future work as usage of DSP relaxes the equalization of transmission impairments as well as implementation of forward error correction.

Chapter 6

Conclusions and Future Scope

This thesis reports the theoretical study and analysis of the optical channel characteristics to model, design and simulate the optimum conditions for a long haul optical communication link to achieve an optimized propagation length. The analytical model and numerical simulation analysis of such fiber transmission channel allows the designer to choose the design plan and select a suitable solution under the given operating constraints for various modulation formats. The main focus of the thesis is to deal with the analysis of linear and non-linear phase impairments arising during pulse propagation through the fiber medium and their influence in the design of long-haul fiber optic communication systems. This chapter summarizes the findings and contributions of the present investigation and also points out some of the possible extensions of the proposed research as a future work.

The growing bandwidth demand has resulted in a tremendous interest in increasing the transport capacity and transmission distance of DWDM system with simultaneous reduction in cost per transported information bit. Obviously, with the progress of optical communication systems, and the constraints brought by DWDM transmission, new ways of encoding the binary data over the optical carrier have been proposed. In this thesis we examined the challenges of such modulation schemes at various stages of implementation. In general, the choice of optimum optical modulation format depends on many factors such as fiber types, channel data rate, wavelength spacing and so on. Optimal modulation formats permit service providers to innovate their existing light wave network without overall upgrade and utilize most of the existing systems; thus saving the expenses.

6.1. Contributions of the Thesis

The general objective of the thesis is to study and analyze different spectrally efficient modulation formats in a simulation environment for an optimized optical transmission link. In this research, both intensity and phase modulated systems have been covered to analyze the transmission characteristics of high speed WDM systems. When choosing a modulation scheme, the trend is to consider on the basis of spectral efficiency and power efficiency in attain high data rate at a low cost, while maintaining the ease of implementation. The most important technical issue is to increase the spectral efficiency of a particular modulation scheme while maintaining OSNR tolerance. The sustained increasing demands

of capacity have pushed higher channel bit rates, high optical powers per channel and narrower spacing between channels to allow increased channel count. These factors exacerbate non-linear cross talk between channels due to the non-linear properties of the optical fiber. Thus the impact of fiber non-linearities due to Kerr non-linearity (SPM, XPM and FWM) are assessed by means of numerical simulations and modeling for the various modulation formats under investigation. Thus, characteristics of several modulation formats and their tolerance to linear and nonlinear impairments is simulated to infer valuable results and conclusions suitable for the high-speed light wave systems.

The premise for exploring these signals was that as they achieve spectral compression and carrier compression, enhanced immunity to non-linearities and chromatic dispersion should be achieved. All signaling methods are investigated through theoretical considerations and computer simulations. The initial focus was to design a single channel optical link with different modulation schemes under consideration. Further, we gradually increased the number of channels, bit rates and system complexity using different type of optical fibers, components and amplifiers to evaluate the performance of the system. A detailed analysis has been attempted to investigate the optical linear and nonlinear effects for optimal system performance. The system performance was monitored by means of eye-diagram, BER and Q estimation using the Optisystem 10.0 platform and Simulink.

Chapter 1 summarizes briefly the development of lightwave communication systems and the importance of optical modulation formats in optical channel performance characterization and performance enhancement. The chapter also describes the motivation for the current work and set the objective of the thesis.

Chapter 2 discusses the basics of optical fiber communication systems and focuses on the important factors that limit the performance of high speed DWDM systems. The theory behind the operation of the various components used in optical communication system and their corresponding mathematical modeling has also been discussed. This chapter presents a brief overview of the need of simulation, and a description of the models used for different system components including laser, external modulator, fiber and optical detector. The mathematical models for fiber non-linearities corresponding to SPM, XPM and FWM are also discussed. The described mathematical model is used in Chapter 4, to develop and analyze a Simulink model of a fiber optic link based on DQPSK forma**t**. The chapter also emphasizes a generic model used in system simulations for the performance assessment under various linear and non-linear impairments induced in optical fiber in high speed data transmission.

Chapter 3 presents the waveform generation and detection schemes and emphasizes on the major characteristics of intensity modulation formats applicable to optical transmission. The theoretical foundations regarding RZ, CSRZ, Duobinary and modified Duobinary were presented with their equivalent models. Computer simulations were then used to characterize the designed optical system to evaluate the system performance of different modulation formats for 32 channels each operating at 40 Gbps in a DWDM system having 50 GHz channel spacing. The dispersion tolerance in case of CSRZ modulation is improved due its reduced spectral width compared to RZ modulation. Moreover, as carrier suppression reduces the efficiency of FWM in DWDM systems, hence CSRZ offers a better tolerance to fiber nonlinearity and robustness against transmission impairments. The other intensity modulation formats considered are DRZ and MDRZ which ameliorate the effects of fiber dispersion, as well as reduce adjacent channel crosstalk. Duobinary systems also enjoy a cost advantage over other advanced modulation formats, such as RZ and DPSK, since it requires less dispersion compensation with transmitters and receivers that are comparable in cost to those used in NRZ systems. Waveform distortion due to fiber chromatic dispersion in high-speed optical transmission systems is a serious problem and MDRZ modulation is an effective way to avoid such distortion resulting in an increased dispersion tolerance compared to binary NRZ modulation format. MDRZ format has a much narrower optical bandwidth over the DRZ and therefore provides a better dispersion tolerance and higher fiber non linearity tolerance.

Chapter 4 explores many aspects for the applicability of phase modulation to optical communications by offering solutions to overcome its higher cost and complexity to enjoy benefits of phase modulation in terms of non-linear resilience and noise sensitivity. The discussed DPSK and DQPSK modulated systems have inherent 3-dB better receiver sensitivity with the use of balanced receiver, which make them very attractive choice in this research context. The transmitters and receiver architectures for DPSK and DQPSK are presented, and 32 channel DWDM system is designed and analyzed by numerical simulations at 40 Gbps. The simulation study establishes that DPSK has a better resilience to XPM and FWM, as compared with intensity modulation formats due to its nearly constant power envelope. It is also observed that DPSK suffers less crosstalk compared to OOK format due to the fact that in the former case only differential phase of the signal is affected. Further it was found that with the decrease in duty cycle of the pulse, crosstalk suffered by the signal decreases because in RZ-pulse, the ‘1’ bit occupy only a fraction of the time slot. Nevertheless, as a binary signal, 40 Gbps DPSK has a large bandwidth which makes its tolerance to the aggressive filtering effect resulting from the cascaded

of several 50 GHz filters a real issue. The advantage of DPSK is obtained at the expense of increased complexity and cost in the transmitter and receiver structure and is useful in submarine appl.

In the second part of Chapter 4, DQPSK format is investigated which transmits two bits per symbol which results in reduced spectral occupancy and bandwidth requirements for the transmitter and receiver components. Another advantage of DQPSK is the extended chromatic dispersion and PMD tolerances. The high spectral efficiency of DQPSK can be even doubled by using polarization multiplexing. In this research work, analytical expressions have been derived for nonlinearity induced crosstalk for DQPSK format. Initially, a Matlab Simulink model is designed for a single channel DQPSK link i.e. transmitter, fiber and receiver modules using Simulink block set by modeling of the generation, propagation and reception of the transmitted signal. The model was time consuming and it becomes difficult to extend the computation for a 2 channel case due to mathematical complexity. Due to the availibity of commercial optical system simulator with sophesticated simulation algorithms and easy-to-use graphical user interfaces, it seems reasonable to use Optisystem to simulate and comapare the performance of DPSK and DQPSK. Thus to get an intuitive understanding of such a complex DWDM scenario having numerous signal interactions and their interplay a 32 channel DQPSK link operating at 40 Gbps was developed. The performance of this system has been evaluated and the same is compared with the corresponding DPSK for varying input powers. In the deployment of high spectral-efficient WDM transmission systems, narrow optical filtering effects on such modulation formats are of key importance because these signals pass through various narrow optical filters at different stages. In this regard, design of MZDI in DQPSK decoder becomes very significant since choice of optimal FSR helps us to relieve some degradation due to strong optical filtering. This approach enables us to realize high bit rate spectrally efficient DWDM DQPSK transmission systems.

In order to achieve even higher capacities, either the channel bit rates are increased, or the channel spacing is reduced. Obviously both the strategies face limitations in the presence of pulse distortions and need a suitable strategy to mitigate those. Considering the spectral advantages of DPQSK especially at narrow channel spacing we have attempted this format in **Chapter 5** to design a UDWDM system. The proposed system has 32 channels spaced at 25 GHz and operates under varying input power levels. The channels were launched with orthogonal polarization to study the BER performance for an optimum distance. A systematic study regarding the impact of filters was carried out. For Butterworth filters, the best filtering is obtained for low–order, slow roll-off filters; for Bessel filters best performance is achieved for high order filters. In practical implementations trade-offs between

filter complexity, cost and performance must be weighted according to system specifications. Simulation results were presented based on the impact of chromatic dispersion on system performance. The bandwidth saving of DQPSK over both OOK and DPSK suggests that DQPSK can improve efficiency of DWDM systems.

For DRZ format at an input power of -5 dBm the maximum distance achieved is 3500 Km and at -10 dBm upto 9000 Km is reported. For MDRZ format, at 5 dBm input power the maximum distance achieved is 2100 Km. For DQPSK format at 1 dBm input power the maximum distance achieved is 1500 Km. For UDWDM case, even at 5 dBm input power the maximum distance achieved is 1100 Km. So among the investigated modulation schemes, optical duobinary format turns out to be one of the leading choices, since it has high tolerance to CD, better non-linear tolerance and can go through narrowband optical filtering to place channels more closely to improve spectral efficiency. Furthermore, it is easy to implement and the overall system setup is simpler compared to other competing formats. The DPSK and DQPSK formats require modifications at the transmitter and receiver to increase the system cost and complexity but are strong candidates for high data-rate spectrally efficient DWDM systems due to inherent 3-dB better receiver sensitivity by using balanced detection. DPSK is much more tolerant to nonlinear optical impairments compared to DQPSK, since its constellation points are further apart in terms of phase. Consequently, the choice between using DPSK or DQPSK in a specific system depends on a trade-off between SE and the tolerance to nonlinear impairments (which translates into reach).

This learning helps the designer to study superior techniques and explore their suitability. However, there exists a reasonable compromise between efficiency and reliability. High level modulation techniques (M-PSK) are always preferred for high data rate. But as the error rate increments with increasing M; it results in signal distortions at the expense of high data rate; thus lower level should be preferred in that case for long distance communication and vice versa. QPSK shows best BER performance with double data rate but optical power requirement is high too. The other available methods i.e. Volterra method, Regular Perturbation method and Digital Backward Propagation represent only the waveform affected by nonlinearity and dispersion and cannot be used for general performance evaluation. The simulations in this work, however, give a good understanding of different nonlinear effects and their influence over different parameters of DWDM system for performance evaluation.

From the theoretical and simulation studies, a few important conclusions were achieved. A unified and integrated approach to analyze the potential of intensity and phase modulated formats was developed. The theoretical foundations and simulation framework was presented in this thesis. A mathematical model for optical link was developed and studied analytically using Matlab Simulink. The impact of chromatic dispersion on system performance is evaluated for different modulation schemes and analysis of crosstalk performance for different parameters like input signal power, wavelength separation and bit rate of the system is presented. Guidelines were established on how to choose optical transmitting filters. The study and the analysis carried in the present thesis suggests suitable system bounds for a typical DWDM system to work under practical operating conditions and helps to develop theoretical understanding of such systems. The present study attempts to simulate and analyze long haul transmission link with various modulation formats to evaluate the performance of each format under various transmission impairments. These results will play a good role in fast–evolving areas of advanced communication system and design of efficient DWDM system.

6.2. Scope for future prospects

A tremendous growth in the required hardware with the increase of the modulation order is considered as one of the major drawbacks for direct-detection receivers, since increasing the number of components means a dramatic increase in the cost and the footprint of the receiver. A second problem of direct detection receivers for high data-rate signals lies in their incapability of compensating linear transmission impairments due to reduction in the symbol duration, which leads to a significant vulnerability to linear transmission impairments such as CD, PMD or the phase ripples. The last problem is their inability to efficiently detect polarization multiplexed signals and the need for an automatic polarization controller at the receiver side to track the changes in the polarization state. Recently, the combination of coherent detection with DSP has been proposed to overcome all of the above mentioned imperfections of direct detection [267, 268]. This interest in optical coherent receivers has been triggered by the recent advances in DSP speeds [269] and the high sampling rates of state of the art analog-to-digital converters (ADC) [270, 271]. Due to their ability to translate the information in the amplitude, phase and polarization state of the detected signal to the electrical domain, digital coherent receivers prove to be able to solve most of the problems of direct detection such as polarizations de-multiplexing, besides CD and DGD compensation. Furthermore, unlike direct-detection receivers, a coherent receiver has a generic structure that can be used to detect any modulation format. So the investigation of coherent receivers will be taken up as future study.

These modulation formats discussed in this research work can be used with other recent technologies like EDC, forward error correction and receiver designs utilizing adaptive electronic post-processing and equalization to realize high spectral-efficient and cost effective DWDM transmission networks. At 10 Gbps data rates, electronic signal processing is already being used ranging from simple feed-forward equalizer (FFE) schemes to Maximum Likelihood Sequence Estimation (MLSE) and at the transmitters, while controlled signal pre-distortion is becoming available at 10 Gbps [272-276]. In future, further experimental and numerical analysis can be performed for investigating end-to-end over-all system performance for advanced modulation formats in the conjunction with some of the above mentioned technologies. Similarly, we can investigate multi-level signals beyond two bits per symbol and other promising schemes like OFDM. The research outcomes obtained in this thesis mainly result from the computer-aided simulation. Therefore, in future, to better verify the results, more efforts will be made in the experimental investigation.

The most critical factor driving the architecture of long-haul DWDM networks is the cost per bit transmitted per kilometer traversed or cost/bit/km. While each successive generation of DWDM technology has increased bandwidth, transmitting successively higher rates over long distances while decreasing cost has often proved challenging. Now that 100G services crisscross the globe, these capacities must grow beyond their current levels, driven by DWDM wavelengths that deliver higher rates, lower costs, and exceptional optical performance.

Bibliography

[1] G P. Agrawal, Fiber Optic Communication Systems, Third edition, 2002.

[2] G. Keiser, Optical Fiber Communications, Third edition, 2000.

[3] J. M. Senior, Optical Fiber Communications Principles and Practice, Second Edition, 1992.

[4] G.P. Agrawal, Nonlinear Fiber Optics, fourth ed., Academic Press, New York, 2001.

[5] A. R. Chraplyvy and R.W Tkach, "What is the actual capacity of single-mode fibers in amplified lightwave systems?", IEEE Photonics Technology Letters, Vol. 5, No. 6, pp. 666-668, 1993.

[6] M.S. Borella, J. P. Jue, D. Banerjee, B. Ramamurthy and B. Mukherjee, "Optical Components for WDM Lightwave Networks", Proceedings of the IEEE, Vol. 85, No. 8, August 1997.

[7] A. R. Chraplyvy, "Limitations on lightwave communications imposed by optical fiber nonlinearities," Journal of Lightwave Technology, Vol. 8, No. 10, pp. 1548-1557, Oct. 1990.

[8] G.692 ITU-T Recommendation, "Optical Interfaces for Multichannel Systems with Optical Amplifiers", International Telecommunication Union, Geneva, Switzerland, 1998.

[9] G. Charlet, "Progress in Optical Modulation Formats for High-Bit Rate WDM Transmissions", IEEE Journal of Selected Topics in Quantum Electronics, Vol. 12, No. 4, July/August 2006.

[10] A. Gumaste and T. Antony, "DWDM Network Designs and Engineering Solutions," Cisco Press, 2002.

[11] R. Sabella, "Tutorial: Key elements for WDM Transport Networks", Photonic Network Communications, Vol. 2, No. 1, pp. 7-14, 2000.

[12] Y. Aoki, K. Tajima, and I. Mito, "Input power limits of single-mode optical fibers due to stimulated Brillouin scattering in optical communication systems," Journal of Lightwave Technology, Vol. 6, No. 5, pp. 710-719, 1988.

[13] A. R. Chraplyvy, "Impact of Nonlinearities on Lightwave Systems," Optics and Photonics News, Vol. 5, pp. 16-21, May 1994.

[14] R. H. Stolen and A. Ashkin, "Optical Kerr effect in glass waveguide," Applied Physics Letters, Vol. 22, pp. 294-296, 1973.

[15] Y. R. Zhou, A. Lord and E. S. R. Sikora, "Ultra-long-haul WDM transmission Systems", BT Technology Journal, Vol. 20, No. 4, pp. 61–70, 2002.

[16] G. P. Ryan, "Dense Wavelength Division Multiplexing", ATG"s Communications & Networking Technology Guide Series, 1997.

[17] G. E. Keiser, “A Review of WDM Technology and Applications”, Optical Fiber Technology, Vol. 5, No. 1, pp. 3 – 39, 1999.

[18] P. Serena, A. Bononi, and A. Orlandini,” Fundamental laws of parametric gain in periodic dispersion-managed optical links”, Journal of Optical Society of America, Vol. 24, No. 4, pp. 773–787, 2007.

[19] M. Suzuki and N. Edagawa, “Dispersion-Managed High-Capacity Ultra-Long-Haul Transmission” Journal of Lightwave Technology, Vol. 21, No. 4, April 2003.

[20] L. N. Binh, Digital Optical Communications, CRC press 2009.

[21] N. S. Bergano, C. R. Davidson, M. A. Mills, P. C. Corbett, R. Menges, J. L. Zyskind, J. W. Sulhoff, A. K. Srivastava, and C. Wolf, "Long-Haul WDM Transmission Using 10 Gb/s Channels: A 160 Gb/s (16x10 Gb/s) 6,000 km Demonstration," Optical Amplifiers and Their Applications, M. Zervas, A. Willner, and S. Sasaki, eds., Vol. 16 , OSA Trends in Optics and Photonics Series, paper SN14, Optical Society of America, 1997.

[22] A. K. Srivastava, J. W. Sulhoff, L. Zhang, C. Wolf, Y. Sun, A. A. Abramov, T. A. Strasser, J. R. Pedrazzani, R.P. Espindola and A.M. Vengsarkar., “L-Band 64 ×10 Gb/s DWDM Transmission over 500 km DSF with 50 GHz Channel Spacing,” ECOC ’98, pp.73-75, 1998.

[23] N. S. Bergano, C. R. Davidson, M. A. Mills, P. C. Corbett, S. G. Evangelides, B. Pedersen, R. Menges, J. L. Zyskind, J. W. Sulhoff, A. K. Srivastava, C. Wolf, and J. Judkins, "Long-Haul WDM Transmission Using Optimum Channel Modulation: A 160 Gb/s (32×5Gb/s) 9,300 km Demonstration," Optical Fiber Communications Conference, OSA Technical Digest Series, paper PD16, 1997.

[24] S. Zhang, “Advanced Optical Modulation Formats in High-speed Lightwave System”, Thesis (M.S.), Department of Electrical Engineering and Computer Science and the Faculty of the Graduate School of the University of Kansas, 2004.

[25] Y. J Wen, J. Mo, and Y. Wang, “Advanced Data Modulation Techniques for WDM Transmission”, IEEE Communications Magazine, pp. 58-65, August 2006.

[26] L. N. Binh, “MATLAB Simulink Simulation Platform for Photonic Transmission Systems”, International Journal of Communications, Network and System Sciences, Vol. 2, pp. 91-168, May 2009.

[27] P. J. Winzer and R. Essiambre, “Advanced Optical Modulation Formats”, IEEE Invited paper, Vol. 94, No. 5, pp. 952-985, May 2006.

[28] A.G. Perez, J.A.A Lucio, O.G.I. Manzano, M. T. Duran and H.G. Martin, “Efficient Modulation Formats for High Bit-Rate Fiber Transmission”, Acta Universitaria, mayo-agosto, Vol. 16, No. 002, Universidad de Guanajuato, Mexico, pp. 17-26, 2006.

[29] L. N. Binh and D. Wong, “DWDM Optically Amplified Transmission Systems-Simulink Models and Test-Bed: PART III DPSK Modulation Format”, Monash University, Department of Electrical and Computer Systems Engineering, Technical Report, 2005.

[30] A. Kanaev, G. Luther and V. Kovanis, "Nonlinear dynamics of modulation formats for 40 Gb/s transmission on standard single-mode fiber and dispersion-managed fiber", Proceedings of Lasers and Electro-Optics Society (LEOS), Vol. 1, pp. 315-316, November, 2002.

[31] X. Li, F. Zhang, X. Zhang, D. Zhang, Z. Chen and A. Xu, "Free spectral range optimization of return-to-zero differential phase-shift keyed demodulation in 40 Gbit/s nonlinear transmission,” Optics Express, Vol. 16, No. 3, pp. 2056-2061, February 2008.

[32] B. Konrad, K. Petermann, J. Berger, R. Ludwig, C. Weinert, H. Weber and B. Schmauss," “Impact of Fiber Chromatic Dispersion in High-Speed TDM Transmission Systems," IEEE Journal of Lightwave Technology, Vol. 20, No. 12, pp. 2129-2135, December 2002.

[33] C. Kurtzke, "Suppression of Fiber Nonlinearities by Appropriate Dispersion Management," IEEE Photonics Technology Letters, Vol. 5, No. 10, pp. 1250-1252, October 1993.

[34] D. Boivin, G.-K. Chang, J. Barr and M. Hanna," Reduction of Gordon-Mollenauer phase noise in dispersion-managed systems using in-line spectral inversion," Journal of the Optical Society of America B, Vol. 23, No. 10, pp. 2019-2023, October 2006.

[35] R. Essiambre, P. Winzer, X. Wang, W. Lee, C. White and E. Burows," Electronic predistortion and fiber nonlinearity,” IEEE Photonics Technology Letters, Vol. 18, No. 17, pp. 1804-1806, September 2006.

[36] L. Dou, Z. Tao, W. Yan, T. Tanimura, T. Hoshida and J. Rasmussen, "A Low Complexity Pre-Distortion Method for Intra-Channel Nonlinearity, “Optical Fiber Communications Conference, paper. OThF5, 2011.

[37] S. Ferber, R. Ludwig, C. Boerner, A. Wietfeld, B. Schmauss, J. Berger, C. Schubert, G. Unterboersch and H. Weber, "Comparison of DPSK and OOK modulation format in 160 Gbit/s transmission system,” IEEE Electronics Letters, Vol. 39, No. 20, pp. 1458-1459, October 2003.

[38] C. Behrens, R. Killey, S. Savory, M. Chen and P. Bayvel, "Reducing the Impact of Intrachannel Nonlinearities by Pulse-Width Optimisation in Multi-level Phase-Shift-Keyed Transmission, "European Conference on Optical Communication, paper. 10.4.1, September 2009.

[39] J. Li, Z. Tao, H. Zhang, W. Yan, T. Hoshida and J. Rasmussen, “Spectrally Efficient Quadrature Duobinary Coherent Systems with Symbol-Rate Digital Signal Processing," IEEE Journal of Lightwave Technology, Vol. 29, No. 8, pp. 1098-1104, April 2011.

[40] K. Inoue, "Fiber Four-Wave Mixing Suppression Using Two Incoherent Polarized Lights,” IEEE Journal of Lightwave Technology, Vol. 11, No. 12, pp. 2116-2122, December 1993.

[41] D. van den Borne, S. Jansen, S. Calabro, N. Hecker-Denschlag, G. Khoe and H. de Waardt, “Reduction of Nonlinear Penalties Through Polarization Interleaving in 2 x 10 Gb/s Polarization-Multiplexed Transmission,” IEEE Photonics Technology Letters, Vol. 17, No. 6, pp. 1337-1339, June 2005.

[42] T. Mizuochi, K. Ishida, T. Kobayashi, J. Abe, K. Kinjo, K. Motorhome and K. Kasahara," A Comparative Study of DPSK and OOK WDM Transmission Over Transoceanic Distances and Their Performance Degradations Due to Nonlinear Phase Noise," IEEE Journal of Lightwave Technology, Vol. 21, No. 9, pp. 19331943, September 2003.

[43] X. Liu, X. Wei, R. Slusher, C. McKinstrie, "Improving transmission performance in differential phase-shift keyed systems by use of lumped nonlinear phase-shift compensation," Optics Letters, Vol. 27, No. 18, pp. 1616-1618, September 2002.

[44] C. Xu, X. Liu, "Post nonlinearity compensation with data-driven phase modulators in phase-shift keying transmission," Optics Letters, Vol. 22, No. 3, pp. 779783, March 2004.

[45] S. Watanabe, T. Chikama, G. Ishikawa, T. Terahara and H. Kuwahara, “Compensation of Pulse Shape Distortion Due to Chromatic Dispersion and Kerr Effect by Optical Phase Conjugation,” IEEE Photonics Technology Letters, Vol. 5, No. 10, pp. 12411243, October, 1993.

[46] K. Petermann, Optical Communication Theory and Techniques, 2005.

[47] O. Kuzucu, Y. Okawachi, R. Salem, M. Foster, A. Turner-Foster, M. Lipson, and A. Gaeta,” Spectral Phase Conjugation via Temporal Imaging,” Optics Express, Vol. 17, No. 22, pp. 20605-20614, October 2009.

[48] K. Ho and J. Kahn,” Electronic Compensation Technique to Mitigate Nonlinear Phase Noise,” IEEE Journal of Lightwave Technology, Vol. 22, No. 3, pp. 779-783, March 2004.

[49] I. P. Kaminow and Tingye Li,” Optical Fiber Telecommunications IV-A,” Fourth Edition, 2002.

[50] R. Hui and Sen Zhang, “Advanced Optical Modulation Formats and Their Comparison in Fiber-Optic Systems”, A Technical Report to Sprint, by Lightwave Communication Systems Laboratory, The University of Kansas, 2004.

[51] M. Harris, “Advanced Modulation Formats for High-Bit-Rate Optical Networks”, Dissertation, School of Electrical and computer Engineering, Georgia Institute of Technology, August 2008.

[52] S. Ramachandran,” Optical and Fiber Communications Reports, Fiber Based Dispersion Compensation”, Vol. 5, 2007.

[53] Agilent Technologies, “From Loss Test to Fiber Certification Fiber Characterization Today Part I: Chromatic Dispersion”, White Paper, April. 2003.

[54] I. Tomkos, D. Chowdhury, J. Conradi, D. Culverhouse, K. Ennser, C. Giroux, B. Hallock, T. Kennedy, A. Kruse, S. Kumar, N. Lascar, I. Roudas, M. Sharma, R.S. Vodhanel, and C. C. Wang, “Demonstration of Negative Dispersion Fibers for DWDM Metropolitan Area Networks” IEEE Journal on Selected Topics in Quantum Electronics, Vol. 7, No. 3, May/June 2001.

[55] R. Ramaswami and K.N. Sivarajan, “Optical Networks: A practical Perspective”, San Francisco, Morgan Kaufmann, 1998.

[56] B. Ramamurthy, D. Datta, H. Feng, J. P. Heritage, and B. Mukherjee, “Impact of Transmission Impairments on the Teletraffic Performance of Wavelength-Routed Optical Networks”, Journal of Lightwave Technology, Vol. 17, No. 10, October 1999.

[57] C.D. Cantrell, “Transparent optical metropolitan-area networks”, LEOS 2003, 16th Annual Meeting, Vol. 2, pp. 608-609, 2003.

[58] B. Wedding, A. Chiarotto, W. Kuebart and H. Bülow, “Fast adaptive control for electronic equalization of PMD”, OFC, Los Angeles, USA, paper TuP4, 2001.

[59] J. D. Downie, I. Tomkos, N. Antoniades, and A. Boskovic, “Effects of Filter Concatenation for Directly Modulated Transmission Lasers at 2.5 and 10 Gb/s”, Journal of Lightwave Technology, Vol. 20, No. 2, February 2002.

[60] V. T. Cartaxo, “Cross-Phase Modulation in Intensity Modulation-Direct Detection WDM Systems with Multiple Optical Amplifiers and Dispersion Compensators”, Journal of Lightwave Technology, Vol. 17, No. 2, pp. 178-190, 1999.

[61] S. Pachnicke and E. Voges, “Analytical assessment of the Q-factor due to cross-phase modulation (XPM) in multispan WDM transmission systems”, Proc. SPIE, Vol. 5247, Orlando, FL, pp. 61-70 Sep. 2003.

[62] W. Zeiler, F. Di Pasquale, P. Bayvel, and J. E. Midwinter, “Modeling of four-wave mixing and gain peaking in amplified WDM optical communication systems and networks,” Journal of Lightwave Technology, Vol. 14, No. 9, pp. 1933-1996, Sep. 1996.

[63] K. Inoue, K. Nakanishi, K. Oda, "Crosstalk and Power Penalty Due to Fiber Four-Wave Mixing in Multi-Channels Transmissions", Journal of Lightwave Technology, Vol. 12, No. 8, pp. 1423-1439, Aug 1994.

[64] J. P. Hamaide, "Linear and Nonlinear Effects in Lightwave Transmission: Dispersion Management in Terrestrial and Submarine Systems," Optical Fiber Communications Conference, Anaheim, tutorial paper, 2002.

[65] J. M. Kahn and K. P. Ho, "Spectral efficiency limits in DWDM systems", 31st European Conference on Optical Communication (ECOC 2005), Glasgow, Vol. 4, pp. 843–846, September 2005.

[66] K. Petermann and S. Randel, "Strategies for spectrally efficient optical fiber communication systems with direct detection", International Conference on Transparent Optical Networks (ICTON 2003), Warsaw, Poland, Vol. 2, pp. 58 – 63, 2003.

[67] H. Louchet, K. Petermann, A. Robinson, and R. Epworth, "On the spectral information distribution in optical fibers", IEEE Lasers and Electro-Optics Society Annual Meeting (LEOS 2004), Puerto Rico, Vol. 1, pp. 17 – 18, 2004.

[68] N. Kikuchi, "Amplitude and phase modulated 8-ary and 16-ary multilevel signaling technologies for high-speed optical fiber communication", SPIE Proceedings, Vol. 6021, pp. 17 – 18, 2005.

[69] S. Bigo, G. Charlet, and E. Corbel, "What has hybrid phase/intensity encoding brought to 40 Gbit/s ultralong-haul systems?",30th European Conference on Optical Communication, Sweden, pp. 872 – 875, 2004.

[70] M. Jeruchim. "Techniques for Estimating the Bit Error Rate in the Simulation of Digital Communication Systems", IEEE Journal on Selected Areas in Communications, Vol. 2, No.1, pp. 153–170, Jan 1984.

[71] K. Shanmugam and P. Balaban," A Modified Monte-Carlo Simulation Technique for the Evaluation of Error Rate in Digital Communication Systems ", IEEE Transactions on Communication, Vol. 28, No.11, pp. 1916–1924, Nov. 1980.

[72] M. W. Chbat, and Denis Penninckx, "High-Spectral-Efficiency Transmission Systems," OFC'00, Vol. 1, pp. 134-136, 2000.

[73] T. Kataoka, Y. Miyamota, K. Hagimoto, and K. Noguchi, "20 Gbps long distance transmission using a 270 photon/bit optical preamplifier receiver", IEEE Electronic Letters, Vol. 30, No. 9, pp. 715 – 716, April 1994.

[74] M. Daikoku, N. Yoshikane, and I. Morita, “Performance comparison of modulation formats for 40 Gbit/s DWDM transmission systems”, Optical Fiber Communications Conference), Anaheim, USA, paper. OFN2, March 2005.

[75] A. Hodzic, B. Konrad, and K. Petermann, “Alternative Modulation Formats in N×40 Gb/s WDM Standard Fiber RZ-Transmission Systems”, Journal of Lightwave Technology, Vol. 20, No. 4, pp. 598–607, April 2002.

[76] G. Bosco, R. Gaudino, and P. Poggiolini, “An Exact Analysis of RZ Versus NRZ Sensitivity in ASE Noise Limited Optical Systems,” European Conference on Optical Communications, Vol. 4, pp. 526-527, Amsterdam, 2001.

[77] M. Pfennigbauer, M. Pauer, P. J. Winzer, and M. M. Strasser, ‘Performance Optimization of Optically Preamplified Receivers for Return-to-Zero and Non Return-to-Zero Coding’, International Journal of Electronics in Communication., Vol. 56, pp. 261–267, 2002.

[78] M. I. Hayee and A. E. Willner, “NRZ vs RZ in 10–40 Gb/s dispersion-managed WDM transmission systems,” IEEE Photonic. Technology Letter, Vol. 11, pp. 991-993, 1999.

[79] A. Hodzic, “Investigations of high bit rate optical transmission systems employing a channel data rate of 40 Gb/s”, Ph.D. thesis, Technische Universität Berlin, Berlin, Germany, 2004.

[80] O. Leclerc, B. Lavigne, E. Balmefrezol, P. Brindel, L. Pierre, D. Rouvillain, and F. Seguineau, “Optical regeneration at 40 Gb/s and beyond,” Journal of Lightwave Technology., Vol. 21, No. 11, pp. 2779–2790, Nov. 2003.

[81] L.N. Binh, "An introduction to optical planar waveguides and optical fibers", Department of Electrical and Computer systems engineering; Monash University, 1997, pp. 20-21.

[82] J. Ryan, “Fiber considerations for metropolitan networks,” Alcatel Telecommunication Rev., pp. 52-55, 1st quarter, 2002

[83] J. Hecht, “City of Light: The Story of Fiber Optics”, 2nd ed. USA: Oxford University Press, 2004.

[84] G. Cattani, “Technological pre-adaptation, speciation and emergence of new technologies: How corning invented and developed fiber optics," Vol. 15, No. 2, pp. 28-318, Feb. 2006.

[85] O. V. Sinkin, R. Holzlohner, J. Zweck and C. R. Menyuk, "Optimization of the Split-Step Fourier Method in Modeling Optical-Fiber Communications Systems", IEEE Journal of Lightwave Technology, Vol. 21, No.1, pp. 61-68, 2003.

[86] M. Premaratne, “Split-Step Spline Method for Modeling Optical Fiber Communications Systems”, IEEE Photonics Technology Letters, Vol. 16, No. 5, pp. 1304-1306, May 2004.

[87] J. C. Palais, "Fiber Optic Communications": Prentice Hall, 1984.

[88] B. Xu, “Study of fiber nonlinear effects on fiber optic communication systems," Ph.D. dissertation, Department of Electrical and Computer Engineering, University of Virginia, 2003.

[89] J. H. Winters, R. D. Gitlin, and S. Kasturia, “Reducing the effects of transmission impairments in digital fiber optic systems”, IEEE Communications Magazine, Vol. 31, pp. 68-76, 1993.

[90] A. F. Elrefaie, "Chromatic Dispersion limitations in coherent lightwave transmission systems’," IEEE Journal of Lightwave Technology, Vol. 6, 1988.

[91] R. J. Nuyts, Y. K. Park, and P. Gallion, “Performance improvement of 10 Gb/s standard fiber transmission system by using the SPM effect in the dispersion compensating fiber,” IEEE Photonic Technology Letters, Vol. 8, No. 10, pp. 1406–1408, Oct. 1996.

[92] I. D. H. Batshon and B. Vasic, “An improved technique for suppression of intrachannel four-wave mixing in 40 gb/s optical transmission systems," IEEE Photonics Letters, Vol. 19, No. 2, pp. 67-69, Jan. 2007.

[93] H. Bulow, “PMD mitigation techniques and their effectiveness in installed fiber”, IEEE/OSA Optical Fiber Communication Conference, Vol. 3, pp. 110-112, 2000.

[94] Y. Painchaud, É. Pelletier and M. Guy, “Dispersion compensation devices: applications for present and future networks**”,** ECOC 04, Paper. We2.4.1, 2004.

[95] J. Marti, D. Pastor, M. Tortola, J. Capmany and A. Montero, “On the use of tapered linearly chirped gratings as dispersion-induced distortion equalizers in SCM systems,” Journal of Lightwave Technology, Vol. 15**,** pp. 179, 1997.

[96] P. Kristensen, “Design of dispersion compensating fiber”, ECOC 04, Paper. We3.3.1,2004.

[97] T. L. Koch and R. C. Alferness,” Dispersion Compensation by Active Predistorted Signal Synthesis”, Journal of Lightwave Technology, Vol. LT-3, No. 4, August 1985.

[98] E. Mateo, L. Zhu, and G. Li. Impact of XPM and FWM on the Digital Implementation of Impairment Compensation for WDM Transmission Using Backward Propagation. Optics Express, Vol. 16, No. 20, pp. 16124-16137, 2008.

[99] M. Taghavi, G. Papen, and P. Siegel, “On the multiuser capacity of WDM in a non-linear optical fiber: Coherent communication," IEEE Transactions on Information Theory, Vol. 52, No. 11, pp. 5008-5022, Nov. 2006.

[100] X. Gu and L. C. Blank, “10 Gbit/s unrepeated optical transmission over 100 km of standard fiber,” IEEE Electronics Letters, Vol. 29, No. 9, pp. 2209–2211, Dec. 1993.

[101] S.J. Savory, G. Gavioli, R.I. Killey, and P. Bayvel, "Electronic compensation of chromatic dispersion using a digital coherent receiver", Optics Express, Vol. 15, No. 5, pp. 2120-2126, 2007.

[102] G. Charlet and S. Bigo, "Upgrading WDM Submarine Systems to 40-Gbit/s Channel Bitrate," Proc. IEEE, Vol. 94, No. 5, pp. 935-951, 2006.

[103] M. J. N. Sibley, Optical components and systems, 2nd ed: J. Wiley, 1995.

[104] Michel C. Jeruchim, Philip Balaban, K. Sam Shanmugan," Simulation of Communication Systems: Modeling, Methodology and Techniques", Kluwer Academic Publishers, New York, USA, 2nd edition, 2000.

[105] S. W. Golomb. Shift Register Sequences. Holden-Day, Inc, San Francisco, USA, 1967.

[106] K. P. Ho and and J. M. Kahn., "Spectrum of externally modulated optical signals," IEEE Journal of Lightwave Technology, Vol. 22, No. 2, pp. 658–663, 2004.

[107] J. Proakis, Digital Communications, 4th ed. McGraw-Hill Science/Engineering/Math, Aug. 2000.

[108] Y. Matsui, D. Mahgerefteh, X. Zheng, C. Liao, Z. F. Fan, K. McCallion, and P. Tayebati, "Chirp-managed directly modulated laser (CML)," IEEE Photonic Technology Letters, Vol. 18, No. 2, pp. 385–388, 2006.

[109] R.S. Tucker & D. J Pope, "Large Signal Circuit Model for Simulation of Injection-Laser Modulation Dynamics", IEEE Journal of Quantum Electronics, Vol. QE-19, July 1983.

[110] S.A. Javaro and S.M. Kang, "Transforming Tucker's Linearized Laser Rate Equations to a Form that has a Single Solution Regime", Journal of Lightwave Technology, Vol. 13, No 9, September 1995.

[111] L. Bjerkan and A. Royset, "Measurement of Laser Parameters for Simulation of High Speed Fibre Optic Systems", Journal of Lightwave Technology, Vol. 14, No. 5, May 1996.

[112] G. P. Agrawal, Lightwave Technology: Components and Devices. JohnWiley & Sons, Inc, New Jersey, USA, 2005.

[113] Z. Tao, W. Yan, L. Liu, L. Li, S. Oda, T. Hoshida, and J. Rasmussen," Simple Fiber Model for Determination of XPM Effects," IEEE Journal of Lightwave Technology, Vol. 29, No. 7, pp. 974-986, April 2011.

[114] G. L. Li and P. K. L. Yu, "Optical Intensity Modulators for Digital and Analog Applications", IEEE Journal of Lightwave Technology, Vol. 21, No. 9, pp. 2010 – 2030, September 2003.

[115] J. T. Gallo, "Optical Modulators for fiber systems," IEEE GaAs Digest, pp. 145-148, 2003.

[116] N. S. Bergano, F. W. Kerfoot, and C. R. Davidson, “Margin measurements in optical amplifier systems,” IEEE Photonics Technology Letters, Vol. 5, pp. 304-306, 1993.

[117] P. A. Humblet and M. Azizoglu, “On the bit error rate of lightwave systems with optical amplifiers,” IEEE Journal of Lightwave Technology, Vol. 9, No. 11, pp. 1576–1582, Nov. 1991.

[118] J. Burgemeier, A. Cords, R. Marz, C. Schaffer, and B. Stummer, “A black box model of EDFA’s operating in WDM systems” IEEE Journal of Lightwave Technology, Vol.16, No.7, pp.1271–1275, July 1998.

[119] M. Pfennigbauer, M.M. Strasser , M. Pauer and P.J. Winzer, “Dependence of optically preamplified receiver sensitivity on optical and electrical filter bandwidths: Measurement and simulation,” IEEE Photonic Technology. Letter, Vol. 14, No. 6, pp. 831–833, June 2002.

[120] W. F. G. Jones and J. Nijhof, “Economic benefits of all-optical cross connects and multi-haul DWDM systems for European national networks," Optical Fiber Communication Conference, UK, paper. WH2, 2004.

[121] P. J. Winzer, “Optimum filter bandwidths for optically pre-amplified NRZ receivers,” IEEE Photonics Technology Letters, Vol. 19, No. 9, pp. 1263–1273, Sep. 2001.

[122] G. Jacobsen and P. Wildhagen, “A General and Rigorous WDM Receiver Model Targeting 10–40-Gb/s Channel Bit Rates”, Journal of Lightwave Technology, Vol. 19, No. 7, pp. 966-976, July 2001

[123] G. Foschini, L. Greenstein, and G. Vannucci, “Non coherent detection of coherent lightwave signals corrupted by phase noise,” IEEE Transactions on Communications, Vol. 36, pp. 306–314, Mar. 1988

[124] G. Jacobsen, “Multichannel system design using optical preamplifiers and accounting for the effects of phase noise, amplifier noise and receiver noise,” Journal of Lightwave Technology, Vol. 10, pp. 367–377, Mar. 1992.

[125] G. Jacobsen, K. Bertilsson and Z. Xiaopin, “WDM transmission system performance: Influence of non-Gaussian detected ASE noise and a periodic DEMUX characteristic, Journal of Lightwave Technology, Vol. 16, pp. 1804–1812, Oct. 1998.

[126] A. J. Price and N. L. Mercier, “Reduced bandwidth optical intensity modulation with improved chromatic dispersion tolerance”, IEEE Electronic Letters, Vol. 31, No. 1, pp. 58–59, January 1995.

[127] G. Goeger, M. Wrage and W. Fischler, "Cross-Phase Modulation in Multispan WDM systems with Arbitrary Modulation Formats", IEEE Photonics Technology Letters, Vol. 16, No.8, pp. 1858-1860, 2004.

[128] J. Wang and K. Petermann, "Small Signal Analysis for Dispersive Optical Fiber Communication Systems", Journal of Lightwave Technology, Vol 10, pp. 99-100, 1992.

[129] M. Shtaif, "Impact of cross phase modulation in WDM systems," Proceedings of the Optical Fiber Communication Conference, Baltimore, Paper ThM1 (invited) 2000.

[130] M. Eiselt, M. Shtaif, and L. D. Garrett, "Contribution of timing jitter and amplitude distortion to XPM system penalty in WDM systems", IEEE Photonics Technology Letters, Vol. 11, No. 6, June 1999.

[131] A. Bertaina and S. Biga, "Impact of residual dispersion on SPM-related power margins in 10 Gbit/s-based systems using standard SMF," Proceedings of 24th European Conference onOptical Communications (ECOC), Vol. 1, pp. 681–682, 1998.

[132] T. Wuth, K. Kaiser and W. Rosenkranz, "Impact of self-phase modulation on bandwidth efficient modulation formats," Optical Fiber Communication Conference (OFC), Anaheim, CA, Paper MM6, 2001.

[133] N. Yoshikane, I. Morita and N. Edagawa, "Improvement of dispersion tolerance by SPM-based all-optical reshaping in receiver," IEEE Photonic Technology Letters, Vol. 15, No. 1, pp. 111–113, Jan 2003.

[134] A. E. Elrefaie, "'Chromatic Dispersion limitations in coherent lightwave transmission systems," IEEE Journal of Lightwave Technology, Vol. 6, No.5, pp.704-709,1988.

[135] S. Al-Mamun and M. S. Islam, "Effect of chromatic dispersion on four-wave mixing in optical WDM transmission system", 6th IEEE International Conference on Industrial and Information Systems, Sri Lanka, pp. 425-428, 2011.

[136] T. Tokle, "Optimized Dispersion Management and Modulation Formats for High Speed Optical Communication Systems", Ph.D. thesis, Research Center COM, Technical University of Denmark, 2004.

[137] W. Rosenkranz, "High Capacity Optical Communication Networks- Approaches for Efficient Utilization of Fiber Bandwidth", First Joint Symposium on Opto & Microelectronic Devices and Circuits (SODC 2000), Nanjing, China, pp. 106 – 107, April 2000.

[138] E. B. Desurvire, "Capacity Demand and Technology Challenges for Lightwave Systems in the Next Two Decades," IEEE Journal of Lightwave Technology, Vol. 24, p. 4697, 2006.

[139] K. Fukuchi, “Wideband and Ultra-Dense WDM Transmission Technologies Toward over 10-Tb/s Capacity,” OFC’02, paper ThX5, 2002.

[140] D. Penninckx, “Dispersion-tolerant modulation techniques for optical communications”, 24th European Conference on Optical Communication (ECOC 1998), Madrid, Spain, Vol. 1, pp. 509 – 510, September 1998.

[141] J. M. Kahn and K.-P. Ho, “Spectral Efficiency Limits and Modulation/Detection Techniques for DWDM Systems,” IEEE Journal on Selected Topics in Quantum Electronics, Vol. 10, No. 2, pp. 259, 2004.

[142] M. Birks and B. Mikkelson, “40 Gbit/s upgrades on existing 10 Gbit/s transport infrastructure”, Proceedings of SPIE, Vol. 6012, 60120D, 2005.

[143] S. V. Kartalopoulos, "Introduction to DWDM technology: Data in a rainbow", J Wiley, 2001

[144] O.V. Shtyrina, M.P. Fedoruk and S.K. Turitsyn, "Study of new modulation data-transmission formats for dispersion-controlled high-bit-rate fibre optic communication lines", Journal of Quantum Electronics, (IOP Science), Vol.37, No. 9, pp 885 - 890, 2007.

[145] A. Sheetal, A. K. Sharma and R.S. Kaler, “Simulation of high capacity 40 Gb/s long haul DWDM system using different modulation formats and dispersion compensation schemes in the presence of Kerr's effect”, Optik ((Elsevier), Vol.121, pp. 739-749, 2010.

[146] OptiSystem Application Notes and Examples (2010), Optiwave, Ottawa, ON, Canada.

[147] E. L. Wooten, K. M. Kissa, A. Yi-Yan, E. J. Murphy, D. A. Lafaw, P. F. Hallemeier, D. Maack, D. V. Attanasio, D. J. Fritz, G.J. McBrien and D.E. Bossi, “A Review of Lithium Niobate Modulators for Fiber-Optic Communications Systems,” IEEE Journal of Selected Topics in Quantum Electronics, Vol. 6, pp. 69-82, 2000.

[148] K. Sato, S. Kuwahara, Y. Miyamoto, and N. Shimizu, “40 Gb/s direct modulation of distributed feedback laser for very-short reach optical links,” IEEE Electronic Letters, Vol. 38, No. 15, pp. 816–817, 2002.

[149] R. Hui, M. O’ Sullivan, A. Robinson, and M. Taylor, “Modulation instability and its impact in multi-span optical amplified IMDD systems: theory and experiments”, IEEE Journal of Lightwave Technology, Vol. 15, No. 7, pp. 1071–1082, July 1997.

[150] Mahapatra and E. J. Murphy, “Electro-optic modulators,” Optical Fiber Telecommunications IV, I. Kaminow and T. Li, Eds. New York: Academic, pp. 258–294, 2002.

[151] T. Matsuda, A. Naka and S. Saito, “Comparison between NRZ and RZ signal formats for in-line amplifier transmission in the zero-dispersion regime,” IEEE Journal of Lightwave Technology, Vol. 16, pp. 340-348, 1998.

[152] M. I. Hayee, A. E. Willner,” NRZ Versus RZ in 10–40-Gb/s dispersion managed WDM transmission systems”, IEEE Photonics Technology Letters, Vol. 11, pp. 991–93, 1999.

[153] G. Bosco, A. Carena, V. Curri, R. Gaudino and P.Poggiolini, “ On the use of NRZ, RZ, and CSRZ Modulation at 40 Gb/s with narrow DWDM channel spacing,” IEEE Journal of Lightwave Technology, Vol. 20, No.9, 2002.

[154] A. Hodzik, B. Konrad and K. Petemann,” Alternative modulation formats in N X 40 Gb/s WDM standard fiber RZ-transmission systems”, IEEE Journal of Lightwave Technology, Vol. 20, No .4, pp. 598-607, 2002.

[155] T. Hoshida, O. Vassilieva, K. Yamada, S. Choudhary, R. Pecqueur and H. Kuwahara, "Optimal 40 Gb/s modulation. formats for spectrally efficient long-haul DWDM systems", IEEE Journal of Lightwave Technology, Vol. 20, No.12, pp. 1989-1996, 2002.

[156] B. Patnaik and P.K. Sahu, "Ultra high capacity 1.28 Tbps DWDM system design and simulation using optimized modulation format", Optik (Elsevier), Vol. 124, No. 14, pp. 1567-1573, 2013.

[157] M. Shtaif and A. H. Gnauck, “The relationship between optical duobinary modulation and spectral efficiency in WDM systems,” IEEE Photonics Technology Letters, Vol. 11, No. 6, pp. 712–714, Jun. 1999.

[158] I. Lyubomirsky, and B. Pitchumani, “Impact of optical filtering on duobinary transmission,” IEEE Photonics Technology Letters, Vol. 16, pp. 1969-1971, 2004.

[159] S. Walkin and J. Conradi, “On the relationship between chromatic dispersion and transmitter filter response in duobinary optical communication systems,” IEEE Photonics Technology Letters, Vol. 9, No. 7, pp. 1005–1007, Jul. 1997.

[160] K. Yonenaga, S. Kuwano, S. Norimatsu, and N. Shibata, “Optical duobinary transmission system with no receiver sensitivity degradation”, IEEE Electronic Letters, Vol. 31, No. 4, pp. 302 – 304, Feb. 1995.

[161] A. Royset and D. R. Hjelme, “Novel dispersion tolerant optical duobinary transmitter using phase modulator and Bragg grating filter,” ECOC, Madrid, Spain, 1998, pp. 225–226.

[162] G. Charlet, S. Lanne, L. Pierre, C. Simonneau, P. Tran, H. Mardoyan, P. Brindel, M. Gorlier, J.-C. Antona, M. Molina, P. Sillard, J. Godin, W. Idler, and S. Bigo, Cost-optimized 6.3 Tbit/s-

capacity terrestrial link over 17 x 100 km using phase-shaped binary transmission in a conventional all-EDFA SMF-based system," OFC, Atlanta, pp. PD25-1, 2003.

[163] Y. Miydmoto, K. Yonenaga, A. Hirano, H. Toba, K. Murata and H. Miydzawa, "100GHz-spaced 8 x 43Gbit/s DWDM unrepeatered transmission over 163 km using duobinary-carrier-suppressed return-to-zero format", IEEE Electronics Letters, Vol. 37, No. 23, pp. 1395-1396, 2001.

[164] S. K. Ibrahim, S. Bhandare, and R. Noé, "Performance of 20 Gbit/s Quaternary Intensity Modulation Based on Binary or Duobinary Modulation in Two Quadratures with Unequal Amplitudes", IEEE Journal of Selected Topics in Quantum Electronics, Vol. 12, no. 4, pp. 596 – 602, 2006.

[165] T. Ono, Y. Yano, and K. Fukuchi, "Demonstration of high-dispersion tolerance of 20 Gbit/s optical duobinary signal generated by a low-pass filtering method", Optical Fiber Communications Conference, Dallas, paper. ThH1, pp. 268 – 269, February 1997.

[166] T. Ono, Y. Yano, K. Fukuchi, T. Ito, H. Yamazaki, M. Yamaguchi, and K. Emura, "Characteristics of Optical Duobinary Signals in Terabit/s Capacity, High-Spectral Efficiency WDM Systems", IEEE Journal of Lightwave Technology, Vol. 16, No. 5, pp. 788 -797, May 1998.

[167] K. Yonenaga and S. Kuwano, "Dispersion-Tolerant Optical Transmission System Using Duobinary Transmitter and Binary Receiver", IEEE Journal of Lightwave Technology, Vol. 15, No. 8, pp. 1530 – 1537, August 1997.

[168] D. Penninckx, M. Chbat , L. Pierre and J. P. Thiery, "The Phase-shaped Binary Transmission (PSBT): A new technique to transmit far beyond the chromatic dispersion limit," European Conference on Optical Communication (ECOC'96), Vol. 2, Oslo, pp. 173–176.

[169] H. Bissesur, G. Charlet, W. Idler, C. Simonneau, S. Borne, L. Pierre, R. Dischler, C. De Barros and P. Tran, "3.2 Tb/s (80x40 Gb/s) C-band transmission over 3100 km with 0.8 bit/s/Hz efficiency," European Conference on Optical Communication (ECOC'01), Amsterdam, paper. PD.M.1.11, 2001.

[170] L. Moller, C. Xie, X. Wei, X. Liu, C. Stook, J. Wood, P. Bravetti, P. Bergamini, and C. Gualandi, "A Novel 10-Gb/s Duobinary Receiver with Improved Back-to-Back Performance and Large Chromatic Dispersion Tolerance," Photonics Technology Letters., Vol. 16, pp. 1152-1154, 2004.

[171] B. K. A. ElRazak, M. B. Saleh, M.H. Aly, "Duobinary Modulation Format and Unequal Channel Spacing Integration to Suppress Four-Wave Mixing Crosstalk in WDM systems", IEEE Saudi International Electronics, Communications and Photonics Conference, Riyadh, pp. 1-5, 2011

[172] G. Charlet, J.-C. Antona, S. Lanne, P. Tran, W. Idler, M. Gorlier, S. Borne, A. Klekamp, C. Simonneau, L. Pierre, Y. Frignac, M. Molina, F. Beaumont, J.- P. Hamaide, and S. Bigo, "6.4Tb/s (159×42.7Gb/s) Capacity over 21×100 km using Bandwidth-limited Phase-Shaped Binary Transmission", 28th European Conference on Optical Communication (ECOC 2002), Copenhagen, Denmark, paper. PD4.1, September 2002.

[173] W. Kaiser, T. Wuth, M. Wichers, and W. Rosenkranz, "Reduced Complexity Optical Duobinary 10-Gb/s Transmitter Setup Resulting in an Increased Transmission Distance", IEEE Photonics Technology Letters, Vol. 13, No. 8, pp. 884 – 886, August 2001.

[174] A. J. Price, L. Pierre, R. Uhel, and V. Havard, "210 km Repeaterless 10 Gb/s Transmission Experiment Through Non Dispersion-Shifted Fiber Using Partial Response Scheme", IEEE Photonics Technology Letters, Vol. 7, No. 10, pp. 1219 – 1221, October 1995.

[175] H. Kim and C. X. Yu, "Optical Duobinary Transmission System Featuring Improved Receiver Sensitivity and Reduced Optical Bandwidth", IEEE Photonics Technology Letters, Vol. 14, No. 8, pp. 1205 – 1207, August 2002.

[176] H. Kim, C. X. Yu, and D. T. Neilson, "Demonstration of Optical Duobinary Transmission System Using Phase Modulator and Optical Filter", IEEE Photonics Technology Letters, Vol. 14, No. 7, pp. 1010 – 1012, July 2002.

[177] D. Sikdar, S. Chaubey,V. Tiwari and V K Chaubey, "Simulation and Performance Analysis of Duobinary 40 Gbps Optical Link", Journal of Modern Optics (Taylor & Francis), Vol. 59, No. 10. , pp. 903–911, 2012.

[178] G. Bosco, A. Carena, V. Curri, R. Gaudino, and P. Poggiolini, "Quantum limit of direct-detection receivers using duobinary transmission," IEEE Photonics Technology Letters., Vol. 15, pp. 102–104, 2003.

[179] L. Moller, C. Xie, R. Ryf, X. Liu, and X. Wei, "10 Gb/s duobinary receiver with a record sensitivity of 88 photons per bit," OFC, paper. PDP30. 2004.

[180] J.-P. Elbers, H. Wernz, H. Griesser, C. Glingener, A. Faerbert, S. Langenbach, N. Stojanovic, C. Dorschky, T. Kupfer, and C. Schulien, "Measurement of the dispersion tolerance of optical duobinary with an MLSE receiver at 10.7 Gb/s", Optical Fiber Communications Conference, Anaheim, USA, paper. OThJ4, 2005

[181] L. Xu, T. Wang, A. Chowdhury, J. Yu and G. Chang," Spectral efficient transmission of 40 Gbps per channel over 50 GHz spaced DWDM systems using optical carrier suppression,

separation and optical duobinary modulation, OFC and National Fiber Optic Engineers Conference, Anaheim, paper NTuC2, 2006.

[182] I. Lyubomirsky and C.C. Chien, "Optical duobinary spectral efficiency versus transmission performance: Is there a tradeoff?" Conf. Lasers Electro-Optics/Quantum Electron. Laser Science Conf. (CLEO/QELS), Baltimore, MD, pp. JThE72, 2005.

[183] K. Po Ho, "Spectral density of cross phase modulation induced phase noise," Optics Communications., Vol. 169, pp. 63-68, 1999.

[184] Y. Yadin, M. Shtaif and M. Orenstein, "Nonlinear phase noise in phase-modulated WDM fiber optic communications," IEEE Photonic Technology Letters, Vol. 16, pp. 1307–1309, 2004.

[185] Q.M. Nguyen and A. Peleg, "Deterministic Raman crosstalk effects in amplified wavelength division multiplexing transmission," Optics Communications, Vol. 283, No. 18, pp. 3500-3511, 2010.

[186] S. L Jansen, I. Morita, Van Den Borne, G. D. Khoe, H. de Waardt, and P. M. Krummrich, "Experimental study of XPM in 10-Gb/s NRZ pre-compensated transmission systems," Proceedings of Optical Fiber Communications conference (OFC 2007), CA, pp. OThS6, 2007.

[187] R. S. Luis, A. Teixeira and P. Monteiro, "XPM Degradation of Dispersion-Precompensated Intensity Modulation Direct-Detection Systems Without Inline Dispersion Compensation," IEEE Photonic Technology Letters, Vol. 20, pp. 736-738, 2008.

[188] A. Peleg, "Log normal distribution of pulse amplitudes due to Raman cross talk in wavelength division multiplexing soliton transmission," Optics Letters, Vol. 29, Issue 17, pp. 1980-1982, 2004.

[189] R. S Luis and A.V.T Cartaxo, "Analytical characterization of SPM impact on XPM–induced degradation in dispersion-compensated system," Journal of Lightwave Technology, Vol. 23, No. 3, pp. 1503-1512, 2005.

[190] A. Peleg, "Intermittent dynamics, strong correlations, and bit-error-rate in multichannel optical fiber communication systems," Physics Letters A 360, pp. 533-538, 2007.

[191] A. Gnauck, "40-Gb/s RZ-Differential Phase Shift Keyed Transmission", Optical Fiber Communications Conference (OFC 2003), Atlanta, USA, paper ThE1, March 2003.

[192] W. Atia and R. S. Bondurant, "Demonstration of return-to-zero signaling in both OOK and DPSK formats to improve receiver sensitivity in an optically preamplified receiver," Proc. LEOS, pp. 226–227, 1999.

[193] B. Zhu, “3.08 Tbit/s (77 x 42.7 Gbit/s) WDM transmission over 1200 km fibre with 100 km repeater spacing using dual C- and L-band hybrid Raman/erbium-doped inline amplifiers”, Electronic Letters, Vol. 37, 2001.

[194] A. H. Gnauck and P. J. Winzer,” Phase-Shift-Keyed Transmission”, Optical Fiber Communication Conference, paper. TuF4, Los Angeles, 2004.

[195] K. P. Ho, “Phase-Modulated Optical Communication Systems”, Springer, 2005, ISBN 0-387-24392-5.

[196] X. Wei, "Numerical Simulation of the SPM penalty in a 10Gb/s RZ-DPSK system", IEEE Photonics Technology Letters, Vol. 15, 2003.

[197] A. H. Gnauck and P. J. Winzer, “Optical Phase-Shift-Keyed Transmission”, IEEE Journal of Lightwave Technology, Vol. 23, No. 1, pp. 115 – 130, January 2005.

[198] H. Kim, “Differential Phase Shift Keying for 10-Gb/s and 40-Gb/s Systems”, IEEE Lasers and Electro-Optics Society Annual Meeting (LEOS 2004), Puerto Rico, paper ThC1, pp. 13 - 14, 2004.

[199] B. Linlin, L. Jianming, L. Li, Z. Xuecheng, “Comprehensive Assessment of New Modulation Techniques in 40 Gb/s Optical Communication Systems,” IOP Publishing, 3rd International Photonics & Opto Electronics Meetings, Journal of Physics: Conference Series 276, pp. 012054, 2011.

[200] H. Bissessur, G. Charlet, E. Gohin, C. Simonneau, L. Pierre, and W. Idler, “1.6 Tb/s (40_40 Gb/s) DPSK transmission with direct detection,” ECOC, Denmark, Paper 8.1.2, 2002.

[201] D. Penninckx, H. Bissessur, P. Brindel, E. Gohin, and F. Bakhti, “Optical differential phase shift keying (DPSK) direct detection considered as a duobinary signal,” 27th European Conference on Optical Communication, ECOC 2001, Vol. 3, pp. 456–457, 2001.

[202] H. Kim, “Robustness to Laser Frequency Offset in Direct-Detection DPSK and DQPSK systems"," IEEE Journal of Lightwave Technology, Vol. 21, 2000.

[203] A. H. Gnauck and P. J. Winzer, "Tutorial: Phase shift keyed transmission," Optical Fiber Communication Conference, Technical Digest (CD) (Optical Society of America), paper TuF5, 2004.

[204] E. A. Swanson, J. C. Livas, and R. S. Bondurant, “High Sensitivity Optically Pre-amplified Direct Detection DPSK Receiver with Active Delay-Line Stabilization”, IEEE Photonics Technology Letters, Vol. 6, No. 2, pp. 263–265, February 1994.

[205] P. J. Winzer and H. Kim, “Degradations in balanced DPSK receivers,” IEEE Photonic Technology Lett., Vol. 15, No. 9, pp. 1282–1284, Sep. 2003.

[206] G. Bosco and P. Poggiolini, “The Impact of Receiver Imperfections on the Performance of Optical Direct-Detection DPSK”, IEEE Journal of Lightwave Technology, Vol. 23, No. 2, pp. 842 – 848, February 2005

[207] A. H. Gnauck, S. Chandrasekhar, J. Leuthold, and L. Stulz, “Demonstration of 42.7 Gb/s DPSK Receiver with 45 Photons/Bit Sensitivity”, IEEE Photonics Technology Letters, Vol. 15, No. 1, pp. 99 – 101, January 2003.

[208] I. Lyubomirsky, and C.-C. Chien, “DPSK Demodulator Based on Optical Discriminator Filter,” IEEE Photonics Technology Letters, Vol. 17, pp. 492-494, 2005.

[209] D. Penninckx, H. Bissessur, P. Brindel, E. Gohin, and F. Bakhti, “Optical differential phase shift keying (DPSK) direct detection considered as a duobinary signal,” Proc. ECOC., Amsterdam, pp. 456–457, 2001.

[210] E. Ciaramella, G. Contestabile, and A. D’Errico, “A novel scheme to detect optical DPSK signals,” IEEE Photonics Technology Letter, Vol. 16, No. 9, pp. 2138–2140, Sep. 2004.

[211] S. K. Ibrahim, Study of Multilevel Modulation Formats for High Speed Digital Optical Communication Systems, Ph.D. thesis, University of Paderborn, Germany, 2007.

[212] R. A. Griffin and A. C. Carter, “Optical differential quadrature phase shift key (oDQPSK) for high capacity optical transmission,” OFC, Anaheim, CA, 2002.

[213] J. M. Gené, M. Soler, R. I. Killey, and J. Prat, “Investigation of 10-Gb/s Optical DQPSK Systems in Presence of Chromatic Dispersion, Fiber Nonlinearities, and Phase Noise”, IEEE Photonics Technology Letters, Vol. 16, No. 3, pp. 924 – 926, March 2004.

[214] A. H. Gnauck, P. J. Winzer, C. Dorrer, and S. Chandrasekhar, “Linear and nonlinear performance of 42.7-Gb/s single-polarization RZ-DQPSK format,” IEEE Photonic Technology Letter, Vol. 18, No. 7, pp. 883–885, April 2006.

[215] D. van den Borne, S. L. Jansen, E. Gottwald, E. D. Schmidt, G. D. Khoe, and H. de Waardt, “DQPSK modulation for robust optical transmission,” Paper OMQ1, OFC, San Diego, 2008.

[216] C. Wree, “RZ-DQPSK format with high spectral efficiency and high robustness towards fiber nonlinearities"," University of Kiel, 2002.

[217] D. van den Borne, S. L. Jansen, E. Gottwald, P. M. Krummrich, P. Leisching, G. D. Khoe, and H. de Waardt, “A robust modulation format for 42.8-Gbit/s long-haul transmission: RZ-DPSK or RZ-DQPSK?”, 7th ITG Fachtagung on Photonic Networks, Germany, pp. 51 – 56, April 2006.

[218] C. Wree, J. Leibrich, J. Eick, and W. Rosenkranz, “Experimental investigation of receiver sensitivity of RZ-DQPSK modulation format using balanced detection”, Optical Fiber Communications Conference, Atlanta, USA, Vol. 2, pp. 456 – 457, March 2003.

[219] I. Lyubomirsky, C.-C. Chien and Y.-H. Wang, “Optical DQPSK Receiver with Enhanced Dispersion Tolerance,” IEEE Photonic Technology Letter, Vol. 20, pp. 511-513, 2008.

[220] K.-P. Ho and H.-W. Cuei, “Generation of Arbitrary Quadrature Signals Using One Dual-Drive Modulator”, IEEE Journal of Lightwave Technology, Vol. 23, No. 2, pp. 764 – 770, February 2005.

[221] G. Bosco, and P. Poggiolini, “On the Joint Effect of Receiver Impairments on Direct-Detection DQPSK Systems,” IEEE Journal of Lightwave Technology, Vol. 24, pp. 1323-1333, 2006.

[222] X. Zhou, J. Yu, T. Wang, and G. Zhang, “Impact of Strong Optical Filtering on DQPSK Modulation Formats”, ECOC, paper Po94, 2007.

[223] A. Carera, " A time domain optical transmission system simulation package accounting for Nonlinear and Polarization-related effects in fiber," IEEE Journal of Selected Areas in Communications, Vol. 15, 1997.

[224] L. N. Binh, D. Lam, K.Y. Chi, "Monash Optical Communications Systems Simulator,” ECSE Monash University, Melbourne Australia 1997.

[225] J. Armstrong, "Simulink Optical Simulator”, Electrical and Computer Systems Engineering, Clayton, Australia: Monash, pp. 62, 2003.

[226] MATLAB, "MATLAB 2012, Release 14".

[227] L. N. Binh, and Li, C.H., "EDFA Simulink Simulator," Monash University, Melbourne Australia 2004.

[228] L. N. Binh, A. Chua and G. Alagaratnam," MOCSS2004: Monash Optical Communication System Simulator for Optically Amplified DWDM Advanced Modulation Format", Technical Report, MECSE-2-2005, 2005.

[229] G.H. Ahmed and O. Ali,” Design and conception of optical links simulator for telecommunication applications under Simulink environment”, 5th WSEAS International Conference on Applied Electromagnetics, Wireless and Optical Communications, Tenerife, Spain, December 14-16, 2007.

[230] B. Milivojevic, "Study of Optical Differential Phase Shift Keying Transmission Techniques at 40 Gbit/s and beyond", Ph.D. thesis, University of Paderborn, EIM-E, Paderborn, Germany, 2005.

[231] G. Kramer, A. Ashikhmin, A. J. van Wijngaarden, and X. Wei, “Spectral Efficiency of Coded Phase-Shift Keying for Fiber-Optic Communication”, IEEE Journal of Lightwave Technology, Vol. 21, No. 10, pp. 2438 – 2445, October 2003.

[232] M. Wu, W.Y Way, “Fiber Nonlinearity Limitations in Ultra-Dense WDM Systems”, Journal of Lightwave Technology, Vol. 22, No.6, pp. 1483-1498, 2004.

[233] V. Tavassoli, "High Capacity Phase/Amplitude Modulated Optical Communication Systems and Nonlinear Inter-Channel Impairments", Phd Thesis, University of Victoria, 2012.

[234] S. Chandrasekhar and X. Liu, “Impact of Channel Plan and Dispersion Map on Hybrid DWDM Transmission of 42.7 Gb/s DQPSK and 10.7 Gb/s OOK on 50-GHz Grid”, IEEE Photonics Technology Letters, Vol. 19, No. 22, 1801–1803, 2007.

[235] M. Jaworski, “Performance Evaluation of Multilevel Optical Modulation Formats,” IEEE 7th International Conference on Transparent Optical Networks**,** Spain, pp. 389-392, 2005.

[236] D. Wang, J. Zhang, G. Gao, X. Cheng, S. Chen, Y. Zhao and W. Gu, "Pulse broadening factor as a criterion to assess nonlinear penalty of 40-Gbit/s RZ-DQPSK signals in dynamic transparent optical networks", Optical Fiber Technology, Vol. 17, pp. 305–309, 2011.

[237] C. R Silveira, D.M. Pataca, M.A. Romero and M. L Rocha, "A Cost-Benefit Analysis on Modulation Formats for 40-Gb/s Optical Communication Systems", Fiber and Integrated Optics, Vol. 30, No. 2, pp. 87-101, 2011.

[238] L. Lia, J. Zhang, D. Duana and A. Yin, "Analysis modulation formats of DQPSK in WDM-PON system", Optik (Elsevier), Vol. 123, pp. 2050-2055, 2013.

[239] A. Tan and E. Pincemin, “Performance comparison of duobinary and DQPSK modulation formats for mixed 10/40-Gbit/s WDM transmission on SMF and LEAF fibers”, Journal of Lightwave Technology, Vol. 27, No.4, (2009) 396-408.

[240] S. Ghoniemy, K.F. George and L. MacEachern, “Performance evaluation and enhancements of 42.7 Gb/s DWDM transmission system using different modulation formats”, Ninth Annual Communication Networks and Services Research Conf., pp. 189–194, 2011.

[241] D. Wang, D. Lu, C. Lou, L. Huo and W. Yu, “Performance comparison of phase modulated formats in 160 Gb/s transmission system”, IEEE Communications and Photonics Conference, ACP, Asia, pp. 1- 6, 2011

[242] E. Lach and W. Idler, “Modulation formats for 100G and beyond”, in Optical Fiber Technology, Vol. 17, pp. 377–386, 2011.

[243] E. Ip, A. Lau, D. Barros and J. Kahn, “Coherent detection in optical fibers system”, Optics Express, Vol. 16, No. 2, pp. 753–791, 2008.

[244] J. Renaudier, O. Bertran-Pardo, G. Charlet, M. Salsi, H. Mardoyan, P. Tran and S. Bigo, “8 Tb/s long haul transmission over low dispersion fibers using 100 Gb/s PDM-QPSK channels paired with coherent detection”, Bell Labs Technical Journal, Vol. 14, No. 4, pp. 27–45, 2010.

[245] B. Zhu, D. W. Peckham, X. Jiang, and R. Lingle Jr, “System performance of long-haul 112-Gb/s PDM-QPSK DWDM transmission over large-area fiber and SSMF spans”, 39th European Conference on Optical Communication (ECOC), 2013.

[246] J. Karaki, E. Pincemin, D. Grot, T. Guiliossou, Y. Jaouen, R. le Bidan and T. le Gall, “Dual-polarization multi-band OFDM versus single–carrier DP-QPSK for 100 Gbps long-haul WDM transmission over legacy infrastructure”, 38th European Conference on Optical Communications (ECOC), 2012.

[247] T. J. Xia, G. A. Wellbrock, M. Huang, S. Zhang, Y. Huang, D. Chang, S. Burtsev, W. Pelouch, E. Zak, H. de Pedro, W. Szeto and H. Fevrier, “Transmission of 400G PM-16QAM channels over long-haul distance with commercial all-distributed raman amplification system and aged standard SMF in field”, OFC Conference and Exhibition, 2014.

[248] X. Zhou, L. E. Nelson, P. Magill, R. Isaac, B. Zhu, D. W. Peckham, P. I. Borel and K. Carlson, “High spectral efficiency 400 Gb/s transmission using PDM time-domain hybrid 32–64 QAM and training-assisted carrier recovery”, Journal of Lightwave Technology, Vol. 31, No. 7, pp. 999–1005, 2013.

[249] N Eduardo S. Rosa, Victor E. S. Parahyba, Júlio C. M. Diniz, Vitor B. Ribeiro, Júlio C. R. and F. Oliveira, "Nonlinear Effects Compensation in Optical Coherent PDM-QPSK Systems", Vol. 12, No. 2, pp. 707-717, 2013.

[250] C. Xie, “WDM coherent PDM-QPSK systems with and without inline optical dispersion compensation”, Optics Express, Vol. 17, No. 6, pp. 4815, 2009.

[251] T. Tokle, C.R. Davidson, M. Nissov, J.X. Cai, D. Foursa and A. Pilipetski," 6500 km transmission of RZ-DQPSK WDM signals, IEEE Electronics Letters, Vol. 40, No. 7, pp. 444–445, 2004.

[252] J D. Reis, D. M. Neves and A. L. Teixeira”, Analysis of Nonlinearities on Coherent Ultra dense WDM-PONs Using Volterra Series”, Journal of Lightwave Technology, Vol. 30, pp. 234-241, 2012.

[253] V. Tiwari, D Sikdar and V.K Chaubey,"Performance optimization of the RZ-DQPSK modulation scheme for dispersion compensated optical link," Optik (Elsevier), Vol. 124, pp. 2593-2596, 2013.

[254] S. L. Jansen, D. Borne, P.M. Krummrich, G.D Khoe and H. Waardt, "Experimental Co-mparison of Optical Phase Conjugation and DCF Aided DWDM 2 x 10.7 Gbps DQPSK Transmission", 31st European Conference on Optical Communication, Scotland, Vol. 4, paper Th 2.2.3, 2005.

[255] H. Toda, T. Yamashita, K. Kitayama and T. Kuri," DWDM Demultiplexing with 25-GHz Channel Spacing for 60-GHz Band Radio-On-Fiber Systems", 28th European Conference on Optical Communication, Copenhagen, Vol. 3, paper 8.2.4, 2002.

[256] D. van-den Borne, S. L. Jansen, E. Gottwald, P. M. Krummrich, G. D. Khoe and H. de Waardt, "1.6-b/s/Hz Spectrally Efficient Transmission Over 1700 km of SSMF Using 40 x 85.6-Gb/s PolMux-RZ-DQPSK," IEEE Journal of Lightwave Technology, Vol. 25, pp. 222, 2007.

[257] S. Bhandare, D. Sandel, B. Milivojevic, A. Hidayat, A. Fauzi, H. Zhang, S. K. Ibrahim, F. Wüst, and R. Noé, "5.94-Tb/s 1.49-b/s/Hz (40×2×2×40 Gb/s) RZ-DQPSK Polarization-Division Multiplex C-Band Transmission Over 324 km", IEEE Photonic Technology Letters, Vol. 17, No. 4, pp. 914 – 916, April 2005.

[258] B. Milivojevic, A. F. Abas, A. Hidayat, S. Bhandare, D. Sandel, R. Noé, M. Guy and M. Lapointe, "1.6-b/s/Hz 160-Gb/s 230-km RZ-DQPSK Polarization Multiplex Transmission with Tunable Dispersion Compensation", IEEE Photonics Technology Letters, Vol. 17, No. 2, pp. 495–497, February 2005.

[259] C. Wree, N. Hecker-Denschlag, E. Gottwald, P. Krummrich, J. Leibrich, E.-D. Schmidt, B. Lankl, and W. Rosenkranz, "High Spectral Efficiency 1.6-b/s/Hz Transmission (8×40 Gb/s with a 25-GHz Grid) Over 200-km SSMF Using RZ-DQPSK and Polarization Multiplexing", IEEE Photonics Technology Letters, Vol. 15, No. 9, pp. 1303 – 1305, September 2003.

[260] P. S. Cho, V. S. Grigoryan, Y. A. Godin, A. Salamon, and Y. Achiam, "Transmission of 25-Gb/s RZ-DQPSK Signals with 25-GHz Channel Spacing Over 1000 km of SMF-28 Fiber", IEEE Photonics Technology Letters, Vol. 15, No. 3, pp. 473 – 475, March 2003.

[261] E. Yamada," 106 channels 10 Gbit/s, 640 km DWDM transmission with 25 GHz spacing with super-continuum multi-carrier source", IEEE Electronic Letters, Vol. 37, 2001.

[262] D. van den Borne, S. L. Jansen, E. Gottwald, P. M. Krummrich, G. D. Khoe, and H. de Waardt, "1.6-b/s/Hz Spectrally Efficient 40×85.6-Gb/s Transmission Over 1,700 km of SSMF Using POLMUX-RZ-DQPSK", OFC 2006, Anaheim, paper. PDP34, March 2006.

[263] C. Wree, J. Leibrich, J. Eick, W. Rosenkranz and D. Mohr, “Experimental Investigation of receiver sensitivity of RZ-DQPSK modulation format using balanced detection”, OFC Conference, 2003.

[264] P. Serena, A. Orlandini, and A. Bononi,” Parametric-gain approach to the analysis of single-channel DPSK/DQPSK systems with nonlinear phase noise,” Journal of Lightwave Technology, Vol. 24, No. 5, pp. 2026–2037, May 2006.

[265] V. Tavassoli and T. E. Darcie,” An analytical method for performance evaluation of a DQPSK channel in presence of OOK signal”, Proceedings of the SPIE, Vol.7386, Photonics North 73861C, 2009.

[266] M. Sjödin, B J. Puttnam, P. Johannisson, S Shinada, N. Wada, P. A. Andrekson and M. Karlsson, "Transmission of PM-QPSK and PS-QPSK with different fiber span lengths", Optics Express, Vol. 20, No. 7, pp. 7544, 2012.

[267] H. Rohde, E. Gottwald, A. Teixeira, J. D. Reis, A. Shahpari, K. Pulverer and J S. Wey,” Coherent Ultra Dense WDM Technology for Next Generation Optical Metro and Access Networks”, IEEE, Journal of Lightwave Technology, Vol. 32, No. 10, pp. 2041-2052, 2014.

[268] J. Zheng, F. Lu, M. Xu, M. Zhu, Md I. Khalil, X. Bao, D. Guidotti, J. Liu, N. Zhu and Gee-Kung Chang,” A dual-polarization coherent communication system with simplified optical receiver for UDWDM-PON architecture, Optics Express, Vol. 22, No. 26, pp. 31735, 2014.

[269] Li. L, C. Jin-ling and Zhang Ji-Jun,” Research of 100 Gbit/s DP-QPSK Based on DSP in WDM-PON System”, International Journal of Signal Processing, Image Processing and Pattern Recognition”, Vol. 8, No.3, pp.121-130, 2015.

[270] R. Agalliu, and M. Lucki,” Benefits and Limits of Modulation Formats for Optical Communications”, Optics and Optoelectronics Vol. 12, No.2, pp. 160-167, June 2014.

[271] P. Zhang, L. Liren, J. Huilin, K. Xizheng, F. De-jun, W. Huang, D. Jia, and J. Ma, “Comparison of dispersion compensation for DQPSK modulated formats in 100 Gbps DWDM optical communication system”, Proceedings of the SPIE, Vol.8906, International Symposium on Photo-electronic Detection and Imaging, Laser Communication Technologies and Systems, pp. 89061E, 2013.

[272] V. Tiwari, D Sikdar, M. N. Jyothi, G. Dixit and V.K Chaubey," Investigation of optimum pulse shape for 112 Gbps DP-DQPSK in DWDM transmission", Optik (Elsevier), Vol. 124, pp. 5567-5572, 2013.

[273] Y. Gao, F. Zhang, J. Li, L. Liu, Z. Chen, L. Zhu, L. Li and A. Xu," Experimental Demonstration of Nonlinear Electrical Equalizer to Mitigate Intra-Channel Nonlinearities in Coherent QPSK Systems, European Conference on Optical Communication, paper. 9.4.7, September 2009.

[274] D. Millar, S. Makovejs, C. Behrens, S. Hellerbrand, R. Killey, P. Bayvel and S. Savory, "Mitigation of Fiber Nonlinearity Using a Digital Coherent Receiver," IEEE Journal of Selected Topics in Quantum Electronics, Vol. 16, No. 5, pp. 1217-1226, September/October 2010.

[275] C. Lin, R. Asif, M. Holtmannspoetter, and B. Schmauss, "Nonlinear mitigation using carrier phase estimation and digital backward propagation in coherent QAM transmission," Optics Express", Vol. 20, pp. B405-B412, 2012.

[276] R. Agalliu and M. Lucki, "System Performance and Limits of Optical Modulation Formats in DWDM systems", Elektronika and Elektrotechnika, Vol. 22, No. 2, pp. 123-129, 2016.

List of Publications

Total number of Journal Publications: ***3***

Total number of Conference publications: ***3***

Journals:

1. Performance Evaluation and Nonlinear Mitigation through DQPSK Modulation in 32 × 40 Gbps Long-Haul DWDM Systems, **Lucky Sharan**, Vaibhav M. Agrawal and V. K. Chaubey, Journal of Optical Communications, Vol. 38, No. 3, pp. 297-307, August 2017, Published Online: July 2016, ISSN: 2191-6322, DOI: https://doi.org/10.1515/joc-2015-0060 **(SCI indexed).**

2. Link Optimization of a 32 x 40 Gbps Ultra DWDM System using Alternate Polarized DQPSK Modulation Format , **Lucky Sharan,** Vaibhav Madangopal Agrawal, Vinod Kumar Chaubey, Journal of Microwaves, Optoelectronics and Electromagnetic Applications, Vol. 15, No. 4, pp. 349-364, December 2016, DOI: http://dx.doi.org/10.1590/2179-10742016v15i4715, **(SCIEO and Scopus Indexed)**

3. Investigation of Modified Duobinary Modulated 40 Gbps 32 Channel DWDM Optical Link for Improved Non-Linear Performance**, Lucky Sharan,** Akshay G. Shanbhag ,V K Chaubey, Vol. 3, No.1, pp. 1256562, November 2016, Cogent Engineering–Taylor and Francis Online : http://dx.doi.org/10.1080/23311916.2016.1256562 **(Emerging Sources Citation Index (ESCI) Indexed)**

Conferences:

1.Simulink models for performance analysis of high speed DQPSK modulated optical link, **Lucky Sharan**, Rupanshi, and V. K. Chaubey, **2nd International Conference on Communication Systems (ICCS 2015),** AIP Conference Proceedings 1715, 020041 (2016); doi: 10.1063/1.4942723 **(Scopus indexed)**

2. Design and Simulation of CSRZ Modulated 40 Gbps DWDM System in Presence of Kerr Non Linearity, **Lucky Sharan**, V K Chaubey, **IEEE 9th International Conference on Wireless and Optical Networks (WOCN 2012)** Next Generation Internet, Indore from 20-22nd September 2012, Sponsored by IEEE**. (Scopus indexed)**

3. Design and Simulation of Long-Haul 32 x 40 Gb/s Duobinary DWDM Link in the Presence of Non-Linearity with Under-compensated Dispersion, **Lucky Sharan**, V K Chaubey**, IEEE 3rd International Conference on Photonics 2012 (ICP 2012)** held at Penang, MALAYSIA from 1st - 3rd October'2012, Sponsored by IEEE Photonics Society, Malaysia Chapter. **(Scopus indexed**

Brief Biography of the Candidate

Lucky Sharan received her M.E. (Communication Systems) degree from the Birla Institute of Technology and Science, Pilani, India in 2009 and is pursuing her Ph.D. degree in the area of High Speed Optical Networks. Currently she is working as lecturer in the Department of Electrical and Electronics Engineering, BITS-Pilani. Her main area of interest includes optical communications and networks. She is actively involved in the design, analysis, development and simulation studies in the area of optical communication systems and networks. The main research focus is in two dimensions, one in the design, modeling and optimization of the performance of optical network at the physical layer and control plane by exploring different types of online and distributed routing protocols, algorithms suitable to circuit switched or packet switched networks. The other main focus is to design, analyze and optimize the high-speed single and multi-channel optical communication subsystems/systems for long-haul links by mitigating the linear and non-linear impairment. She has published three journal and three conference papers in her research domain. She has been actively involved in teaching and has taught courses like Electrical Science, Communication Systems, Analog Electronics and has a total of 7 years of teaching experience.

Brief Biography of the Supervisor

Prof. Vinod Kumar Chaubey received his master's degree with specialization in Electronics & Radio Physics and PhD Degree in the field of Fiber optics communication from BHU, Varanasi, India in 1985 and 1992 respectively. Dr. Chaubey joined BITS, Pilani in 1994 and presently working as Professor in the Department of Electrical & Electronics Engineering. Dr. Chaubey has more than 24 years of teaching, research and administrative experience at BITS Pilani. He has published more than 48 research journal papers and also more than 50 conference papers in the area of Optical Communication & Networks, Optoelectronic Devices circuits and Systems and also guided/guiding several Ph.D. students. He is a Fellow and life member of IETE and senior member of IEEE.